frontiers | Research Topics

Case reports in pulmonary medicine

Edited by
Rodrigo Torres-Castro and Suzana Erico Tanni

Published in
Frontiers in Medicine

ISSN 1664-8714
ISBN 978-2-8325-3944-6
DOI 10.3389/978-2-8325-3944-6

About Frontiers

Frontiers is more than just an open access publisher of scholarly articles: it is a pioneering approach to the world of academia, radically improving the way scholarly research is managed. The grand vision of Frontiers is a world where all people have an equal opportunity to seek, share and generate knowledge. Frontiers provides immediate and permanent online open access to all its publications, but this alone is not enough to realize our grand goals.

Frontiers journal series

The Frontiers journal series is a multi-tier and interdisciplinary set of open-access, online journals, promising a paradigm shift from the current review, selection and dissemination processes in academic publishing. All Frontiers journals are driven by researchers for researchers; therefore, they constitute a service to the scholarly community. At the same time, the *Frontiers journal series* operates on a revolutionary invention, the tiered publishing system, initially addressing specific communities of scholars, and gradually climbing up to broader public understanding, thus serving the interests of the lay society, too.

Dedication to quality

Each Frontiers article is a landmark of the highest quality, thanks to genuinely collaborative interactions between authors and review editors, who include some of the world's best academicians. Research must be certified by peers before entering a stream of knowledge that may eventually reach the public - and shape society; therefore, Frontiers only applies the most rigorous and unbiased reviews. Frontiers revolutionizes research publishing by freely delivering the most outstanding research, evaluated with no bias from both the academic and social point of view. By applying the most advanced information technologies, Frontiers is catapulting scholarly publishing into a new generation.

What are Frontiers Research Topics?

Frontiers Research Topics are very popular trademarks of the *Frontiers journals series*: they are collections of at least ten articles, all centered on a particular subject. With their unique mix of varied contributions from Original Research to Review Articles, Frontiers Research Topics unify the most influential researchers, the latest key findings and historical advances in a hot research area.

Find out more on how to host your own Frontiers Research Topic or contribute to one as an author by contacting the Frontiers editorial office: frontiersin.org/about/contact

Case reports in pulmonary medicine

Topic editors

Rodrigo Torres-Castro — University of Chile, Chile

Suzana Erico Tanni — Sao Paulo State University, Brazil

Citation

Torres-Castro, R., Tanni, S. E., eds. (2023). *Case reports in pulmonary medicine*. Lausanne: Frontiers Media SA. doi: 10.3389/978-2-8325-3944-6

Table of contents

frontiers | Frontiers in Medicine

TYPE Editorial
PUBLISHED 01 November 2023
DOI 10.3389/fmed.2023.1279945

OPEN ACCESS

EDITED AND REVIEWED BY
Dawei Yang,
Fudan University, China

*CORRESPONDENCE
Rodrigo Torres-Castro
klgorodrigotorres@gmail.com

RECEIVED 18 August 2023
ACCEPTED 23 October 2023
PUBLISHED 01 November 2023

CITATION
Torres-Castro R and Tanni S (2023) Editorial: Case reports in pulmonary medicine.
Front. Med. 10:1279945.
doi: 10.3389/fmed.2023.1279945

Editorial: Case reports in pulmonary medicine

Rodrigo Torres-Castro[1]* and Suzanna Tanni[2]

[1]Department of Physical Therapy, Faculty of Medicine, University of Chile, Santiago, Chile, [2]Pulmonology Division of Internal Medicine Department, Botucatu Medical School, São Paulo State University (UNESP), Botucatu, São Paulo, Brazil

KEYWORDS

respiratory medicine, clinical case, pulmonary medicine, report, unique case study

Editorial on the Research Topic
Case reports in pulmonary medicine

Case reports are vital components of scientific literature, providing essential insights into rare or unique medical conditions, diagnostic dilemmas, and therapeutic challenges (1). There has been a growing trend in the publication of clinical case reports over the years. In the year 2000, ~42,000 case reports were published in PubMed-indexed journals. However, this number surged significantly to 89,125 by the year 2020, signifying a remarkable growth rate of close to 110%. This increase highlights the escalating importance and impact of these reports in contributing to the advancement of medical knowledge and enhancing clinical practice.

Clinical case reports correspond to articles with the lowest level of evidence on the hierarchy of various research study types (2). However, this type of publication have historically played a vital role in identifying emerging or uncommon diseases, assessing the positive and adverse outcomes of interventions, and enriching medical education (1). They provide a platform for clinicians to share unusual clusters of symptoms or presentations that might indicate the presence of a new disease or variant. The swift dissemination of such medical information can facilitate prompt public health responses, as demonstrated during outbreaks of infectious respiratory diseases like the recent COVID-19.

Medical literature is often dominated by observational studies involving larger patient cohorts, leaving rare and unusual cases underrepresented. Case reports fill this gap by presenting detailed accounts of such unique situations that can be useful for other clinicians (3). Within the domain of respiratory medicine, where unique conditions such as rare lung diseases, unconventional infections, and atypical manifestations prevail, case reports form the bedrock upon which comprehension of these puzzling illnesses is built.

The diverse range of respiratory diseases often presents diagnostic challenges due to overlapping clinical features. Case reports detailing unique diagnostic dilemmas and the strategies used to resolve them offer valuable learning opportunities for healthcare professionals (4). By sharing their experiences, clinicians can contribute to the collective knowledge, leading to improved diagnostic accuracy and timely initiation of appropriate treatment.

Case reports can provide early evidence of the effectiveness of novel therapies or management strategies for different conditions (3). In instances where patients experience suboptimal responses to common and standard treatments, alternative approaches tested in individual cases can be reported (4). While not conclusive evidence, these reports can prompt further research and eventually lead to the development of more effective treatments

(4). On the other hand, these reports act as preliminary evidence, encouraging researchers to investigate potential causal links or mechanisms behind the observed outcomes. Such investigations can guide the design of more rigorous studies, eventually leading to evidence-based medical practices.

For example, in this Research Topic, we present unusual cases that can provide valuable insights for clinicians facing similar challenges in their practice. One of the cases reported highlights a refractory pneumothorax secondary to human immunodeficiency virus -associated *Pneumocystis jiroveceii* pneumonia, which exhibited a positive response to endobronchial Watanabe spigot and blood coagulation factor XIII supplementation (Koyama et al.). In the same way, others atipical respiratory infection are exposed in this Research Topic. Sun et al. described a chronic respiratory condition due to *Fusobacterium nucleatum* in pleural effusion associated with squamous cell carcinoma. Similarly, Yuan et al. presented a case with *Actinomyces graevenitzii*, Zhang et al. illustrated an abnormal *Streptococcus pneumoniae* thoracic image presentation, Peng et al. showed a hypervirulent *Klebsiella pneumonia*, and Liu and Gao described an infection with *Chlamydia psittaci* in severe pneumonia cases. All these cases had a positive clinical resolution after identification of the pathogen by molecular sequencing. Unfortunately, molecular diagnostics by next-generation sequencing is not a procedure accessible at the most respiratory centers in the world. In this context, these published cases are important to propose management of rare infection cases in respiratory field.

Another intriguing cases involved abnormalities in the thoracic anatomy. A post-COVID-19 tracheal stenosis with fibrotic bridges, leading to significant respiratory distress (Zuccatosta et al.). The absence of cartilaginous support involvement allowed for successful bronchoscopic treatment, resulting in complete and permanent resolution of the stenosis (Zuccatosta et al.). Other rare conditions are described in the biliobronchial fistula after cholecystectomy surgery case (Batalin Júnior et al.), a Kartagener síndrome with DNAH9 mutation case (Feng et al.), an anomalous systemic arterial supply to the left lower lung lobe (Wu et al.), an epithelioid hemangioendothelioma in main bronchus (Gong et al.), and tracheal lobular capillary hemangioma (Tao et al.). These reports offer important clinical knowledge and potential solutions for managing complex respiratory conditions.

Finally, this type of evidence serve as powerful teaching tools, especially in medical education (1). They provide real-world examples of clinical decision-making, the importance of thorough patient histories, and the significance of physical examinations (4). Aspiring medical professionals can learn from the experiences shared in case reports, enabling them to make more informed decisions when faced with similar clinical scenarios.

Despite representing the lowest level of evidence, clinical case reports continue to be among the most significant sources of knowledge in the biomedical field. They offer valuable insights into unusual disease presentations and the benefits of employing unconventional approaches in treatment (2). Moreover, case reports enable readers to explore novel concepts and foster innovative perspectives for their everyday clinical practice (2).

Author contributions

RT-C: Writing – original draft, Writing – review & editing. ST: Writing – original draft, Writing – review & editing.

Funding

The author(s) declare that no financial support was received for the research, authorship, and/or publication of this article.

Conflict of interest

The authors declare that the research was conducted in the absence of any commercial or financial relationships that could be construed as a potential conflict of interest.

Publisher's note

References

1. Riley DS, Barber MS, Kienle GS, Aronson JK, von Schoen-Angerer T, Tugwell P, et al. CARE guidelines for case reports: explanation and elaboration document. *J Clin Epidemiol.* (2017) 89: 218–35. doi: 10.1016/j.jclinepi.2017.04.026

2. Pineda-Leguízamo R, Miranda-Novales G, Villasís-Keever MÁ, Pineda-Leguízamo R, Miranda-Novales G, Villasís-Keever MÁ. La importancia de los reportes de casos clínicos en la investigación. *Rev Alerg México.* (2018) 65: 92–8. doi: 10.29262/ram.v65i1.348

3. Agha R, Rosin RD. Time for a new approach to case reports. *Int J Surg Case Rep.* (2010) 1:1. doi: 10.1016/j.ijscr.2010.04.001

4. Nayak B. The significance of case reports in biomedical publication. *Indian J Ophthalmol.* (2010) 58:363. doi: 10.4103/0301-4738.67038

frontiers | Frontiers in Medicine

CASE REPORT
published: 31 May 2022
doi: 10.3389/fmed.2022.875311

Case Report: Massive Hemoptysis From a Spontaneously Regression Inflammatory Bronchial Polyp

Yuichiro Iwamoto[1,2]*, *Haruka Takenouchi*[2], *Katsumasa Koyama*[2], *Ryo Shirai*[2], *Hideaki Kaneto*[1] and *Koichi Tomoda*[2]

[1] Department of Diabetes, Endocrinology and Metabolism, Kawasaki Medical School, Kurashiki, Japan, [2] Department of General Internal Medicine 1, Kawasaki Medical School, Okayama, Japan

Background: Bronchial inflammatory polyps are usually treated by surgical operation or with steroids and/or antibiotics, and it is quite rare that such polys spontaneously disappear without any treatment. This report shows a rare case with a bronchial inflammatory polyp which caused massive hemoptysis but spontaneously disappeared without any treatment.

Case Presentation: A 66-year-old man with type 2 diabetes mellitus and a history of cough and asthma suddenly developed massive hemoptysis while smoking and was brought to an emergency room in our institution. In bronchoscopy on admission, a polypoidal elevated lesion was observed in the left upper lobe bifurcation. Pulsatile hemorrhage from a polypoidal elevated lesion was observed upon stimulation of passage of the bronchoscope. Bronchoscopy performed 25 days after discharge showed no evidence of active bleeding and a tendency toward reduction of the elevated lesion. In bronchoscopy performed 106 days after the initial hospitalization, the bronchial inflammatory polyp completely disappeared.

Conclusions: We should bear in mind the possibility of spontaneous disappearance of bronchial inflammatory polyps causing some serious symptoms such as massive hemoptysis and repeated bloody sputum. Finally, we should select the best therapy for bronchial inflammatory polys based on each patient's background and conditions in clinical practice.

Keywords: bronchial inflammatory polyp, lung hemorrhage, massive hemoptysis, spontaneous disappearance, case report

OPEN ACCESS

Edited by:
Hsiao-Chi Chuang,
Taipei Medical University, Taiwan

Reviewed by:
Himanshu Deshwal,
New York University, United States
Mitra Rezaei,
National Research Institute of Tuberculosis and Lung Diseases (NRITLD), Iran

***Correspondence:**
Yuichiro Iwamoto
iwamoto.g@med.kawasaki-m.ac.jp

Specialty section:
This article was submitted to Pulmonary Medicine, a section of the journal Frontiers in Medicine

Received: *14 February 2022*
Accepted: *28 April 2022*
Published: *31 May 2022*

Citation:
Iwamoto Y, Takenouchi H, Koyama K, Shirai R, Kaneto H and Tomoda K (2022) Case Report: Massive Hemoptysis From a Spontaneously Regression Inflammatory Bronchial Polyp. Front. Med. 9:875311. doi: 10.3389/fmed.2022.875311

INTRODUCTION

Bronchial inflammatory polyps are non-neoplastic elevated lesions composed of inflammatory granulation tissue and are considered to be a rare disease. Causes of bronchial inflammatory polyps include infection, local chronic inflammation, chronic irritation by airflow, allergic reaction of the airway mucosa, airway foreign body, and idiopathic with no apparent cause. Bronchial inflammatory polyps are often accompanied by local hemorrhage and characterized by symptoms such as bloody sputum, hemoptysis and cough. Since they are usually found as hemorrhagic masses, it is very important to differentiate them from primary bronchial tumors in clinical practice. In general, bronchial inflammatory polyps are treated by surgical operation or with steroids and/or

antibiotics, and it is quite rare that such polys spontaneously disappear without any treatment. This report shows a rare bronchial inflammatory polyp which caused massive hemoptysis but spontaneously disappeared without any treatment in a subject with type 2 diabetes mellitus.

CASE REPORT

A 66-year-old man with type 2 diabetes mellitus and a history of cough and asthma suddenly developed massive hemoptysis of more than 1L while smoking 2 days before. After then, he was brought to an emergency room in our institution because of repeated bloody sputum. His smoking history was 60 pack years. At the time of admission, the patient was taking 50 mg of vildagliptin for diabetes mellitus. His height and body weight were 168 cm and 52.9 kg, respectively. His blood pressure, pulse rate, and respiratory rate were 120/50 mmHg, 97 beats per minute, and 18 beats per minute, respectively. In chest auscultation, there were no fine or coarse crackles, and there were no other physical findings of note. The findings of blood tests at the time of emergency transport are shown in **Table 1**. His hemoglobin level was 15.7 g/dL and there was no anemia. His coagulation functions are all in the normal range. Liver and renal functions were almost within the normal range. Serum C-reactive protein (CRP) was mildly elevated to 0.40 mg/dL. Diabetes markers were as follows: blood glucose level, 112 mg/dL; HbA1c, 7.5%. Sputum cultures did not reveal any pathologic micro-organisms. A chest radiograph on admission demonstrated reticular shadows in the right lower lung fields. Sputum cultures did not reveal any pathologic micro-organisms. A chest radiograph on admission demonstrated reticular shadows in the right lower lung fields (**Figure 1**, upper left panel). Chest computed tomography (CT) on admission showed frosted shadows in the dorsal left upper lobe and left lower lobe. The left lower lobe showed ground-glass opacity and fibrotic and cystic changes (**Figure 1**, upper right panel). In contrast-enhanced CT, however, there were no abnormal vessels or neoplastic lesions in the bronchial wall. To examine the cause of massive hemoptysis and subsequent repeated bloody sputum, bronchoscopy was performed on the day of admission. As the results, a polypoidal elevated lesion was observed in the left upper lobe bifurcation (**Figure 2**, upper left panel). There were no exposed blood vessels in the tracheal lumen, but passage of the bronchoscope revealed pulsatile bleeding from the periportal area of the polyp (**Figure 2**, upper right panel). Thrombin was applied under bronchoscopy and hemostasis was achieved. To minimize recurrence of bleeding from mechanical irritation and cough, the patient was empirically treated with anti-tussive and anti-secretory agents such as carbazochrome (90 mg/day), carbocisteine (1500 mg/day), cloperlastine (60 mg/day) with symptomatic relief. There was no sign of infection, and considering the risk of hyperglycemia, we decided not to

TABLE 1 | Laboratory data on admission.

Variable	Result	Reference range	Variable	Result	Reference range
Blood biochemistry			**Peripheral blood**		
Total protein (g/dL)	6.8	6.6–8.1	White blood cells (/μL)	6940	3300–8600
Albumin (g/dL)	4.1	4.1–5.1	Neutrophil (%)	67.5	28.0–78.0
Globulin (g/dL)	2.7	2.2–3.4	Red blood cells ($\times 10^4$/μL)	512	386–492
Total bilirubin (mg/dL)	0.5	0.4–1.5	Hemoglobin (g/dL)	15.7	11.6–14.8
AST (U/L)	12	13–30	Hematocrit (%)	46.3	35.1–44.4
ALT (U/L)	9	7–23	Platelets ($\times 10^4$/μL)	20.9	15.8–34.8
LDH (U/L)	244	124–222	**Infectious marker**		
ALP (U/L)	332	106–322	CRP (mg/dL)	0.26	<0.14
γ-GTP (U/L)	23	9–32	QFT	(–)	
BUN (mg/dL)	11	8–20	**Diabetes marker**		
Creatinine (mg/dL)	0.79	0.46–0.79	Plasma glucose (mg/dL)	112	
Cholinesterase (U/L)	207	201–421	Hemoglobin A1c (%)	7.5	4.9–6.0
Uric acid (mg/dL)	4.5	2.6–5.5	**Urinary test**		
Sodium (mmol/L)	141	138–145	Urinary pH	6.5	5.0–7.5
Potassium (mmol/L)	3.6	3.6–4.8	Urinary protein	(±)	-
Chloride (mmol/L)	104	101–108	Urinary sugar	(–)	-
Coagulation system test			Urinary ketone body	(2+)	-
PT (sec)	11.6	9.3–12.5	Urinary bilirubin	(–)	-
PT-INR	0.97	0.85–1.13	Urinary blood	(–)	-
APTT (sec)	28.5	26.9–38.1			
Fibrinogen	281	160–380			

AST, aspartate aminotransferase; ALT, alanine aminotransferase; LDH, lactate dehydrogenase; ALP, alkaline phosphatase; γ-GTP, γ-glutamyl transpeptidase; BUN, blood urea nitrogen; PT, prothrombin time; APTT, activated partial thromboplastin time; QFT, QuantiFeron test; CRP, C-reactive protein.

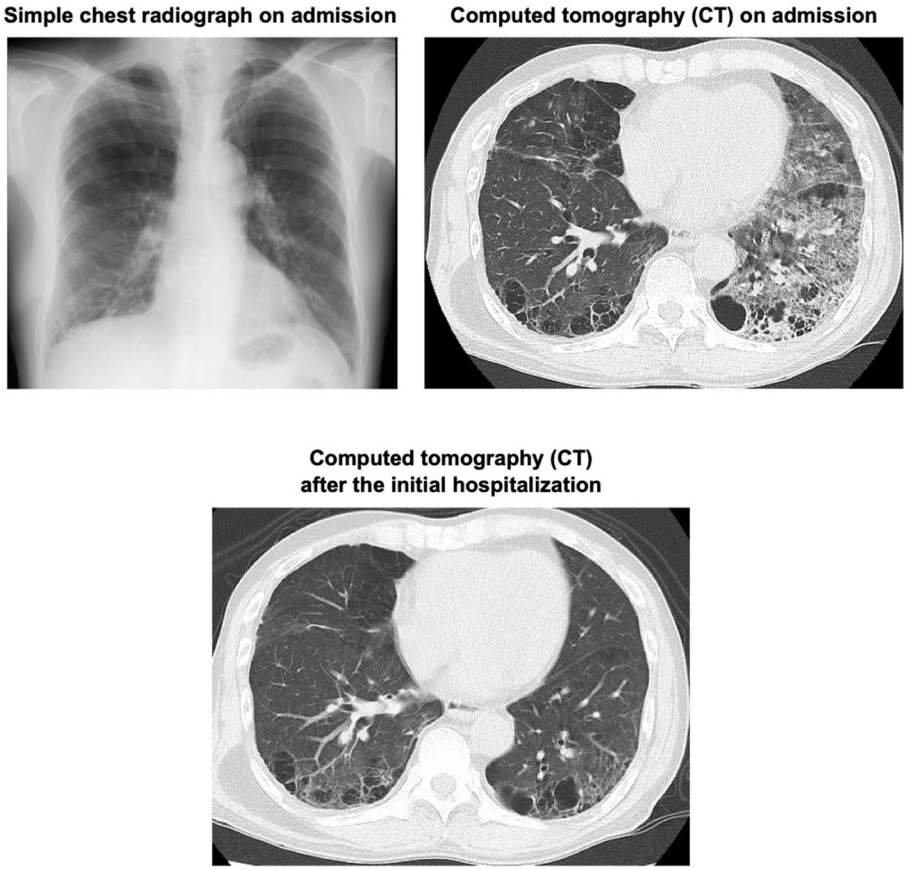

FIGURE 1 | A simple chest photograph at the time of emergency transport showed reticular shadows in the bilateral lower lung fields (upper left panel). Computed tomography (CT) at the time of emergency transport showed an infiltrative shadow with air bronchograms in the right lower lobe. There were emphysematous changes in the bilateral lungs (lower right panel). CT performed 106 days after initial discharge showed that the infiltrative shadow in the right lower lobe had disappeared (lower panel).

administer antimicrobial agents and steroids. The patient was discharged from the hospital on the 7th day after admission because hemoptysis was not observed at all after the start of medication.

The patient underwent a follow-up bronchoscopy on day 25 post discharge which showed no evidence of active bleeding. The polypoidal nodule appeared less pronounce and an endobronchial biopsy was performed. Histopathology demonstrated a foci of reactive myofibroblast growth from the bronchial mucosa to the endobronchial palace suggestive of a bronchial inflammatory polyp (**Figure 3**). The patient was instructed to quit smoking and after then he did not experience hemoptysis. To examine the alteration of the lesion, bronchoscopy was performed 106 days after the initial hospitalization. As the results, the bronchial inflammatory polyp completely disappeared although this polyp previously caused massive hemoptysis and repeated bloody sputum in this subject (**Figure 2**, lower panel). On follow-up chest imaging, the lower lobe infiltrates had resolved with residual underlying fibrotic changes that are currently being evaluated for suspected smoking-related interstitial lung disease (**Figure 1**, lower panel).

DISCUSSION

Bronchial inflammatory polyps were first reported in 1929 as a pathological diagnosis in bronchoscopic biopsies and were defined pathologically as being completely covered by normal bronchial mucosal epithelium and continuous epithelium, with submucosal connective tissue interstitium (1, 2). Causes of bronchial inflammatory polyps include airway irritation due to infection, chronic irritation by airflow, allergic reaction in the bronchial mucosa, direct mechanical irritation, and idiopathic cases in which the cause cannot be identified (3–6). In this case, the patient had a history of cough and asthma, and it seemed that repeated hemoptysis due to smoking brought about airway allergy and airway irritation by airflow.

Although neoplastic lesions such as malignant disease, bronchial tuberculosis, and bronchial papilloma can be listed

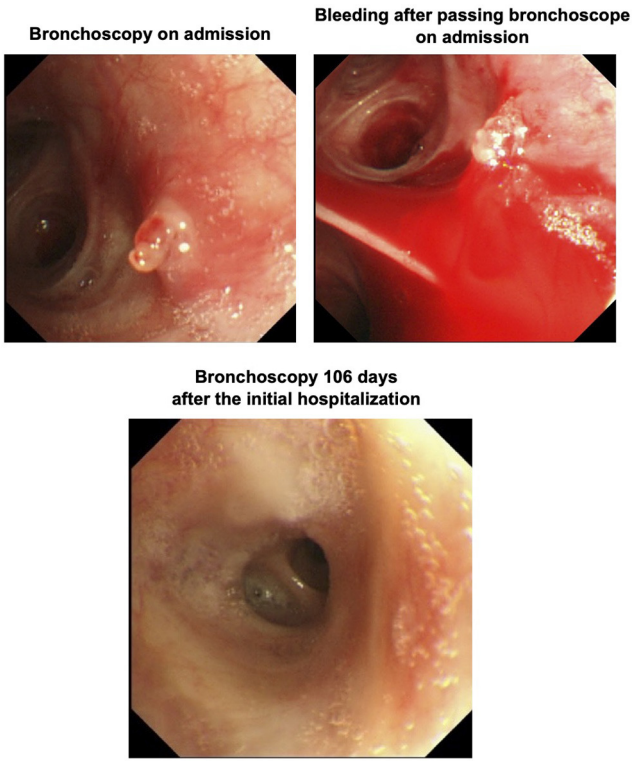

FIGURE 2 | Bronchoscopy performed on the day of admission showed a polypoid elevated lesion at the bifurcation of the left upper lobe (upper left panel). Passage of bronchoscope revealed pulsatile bleeding around the polypoid lesion (upper right panel). Bronchoscopy performed 106 days after the initial hospitalization revealed that the elevated lesion completely disappeared (lower panel).

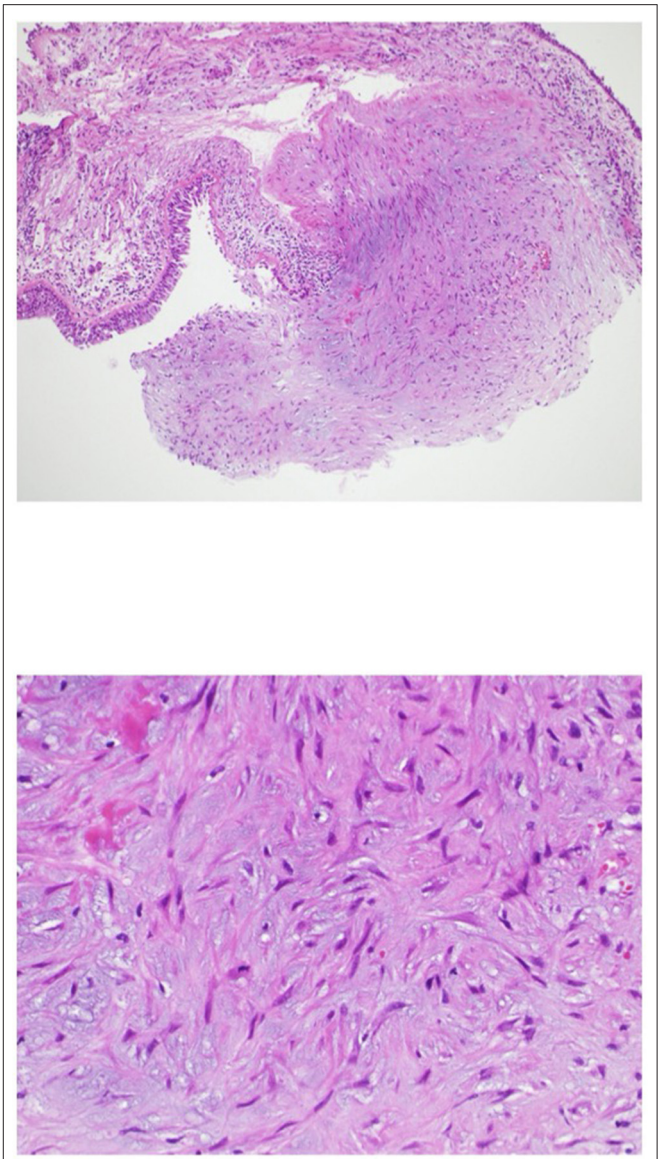

FIGURE 3 | Findings in biopsy specimen from the hemorrhagic polypoid lesion. The upper panel shows a weakly magnified image of HE staining, and the lower panel shows a strongly magnified image of HE staining. Foci of reactive myofibroblast proliferation were observed from the bronchial mucosa to the bronchial lumen.

as differential diseases for bronchial inflammatory polyps, it is difficult to diagnose bronchial inflammatory polyps based on bronchoscopic findings alone, and histopathological diagnosis by biopsy is ultimately necessary (7). It has been reported that about 8% of bronchial inflammatory polyps disappear spontaneously, while polyps themselves may cause bloody sputum, hemoptysis and cough, and thus are usually treated with some method. Treatment methods include conservative treatment, surgical resection, and endoscopic treatment such as forceps removal under a bronchoscope and cauterization with Nd-YAG laser (6, 7). In rare cases, major bleeding may occur, and it has been reported that in some cases inflammatory edema may disappear spontaneously with antibacterial agents and steroids (8). However, administration of steroids to patients with concomitant diabetes mellitus may pose a risk of secondary infection due to hyperglycemia. Furthermore, this case report clearly indicates the possibility that inflammatory polys spontaneously disappear without any surgical operation or treatment with steroids and/or antibiotics.

Taken together, although bronchial inflammatory polyps with heavy hemoptysis are usually treated by surgical operation or steroid therapy, both surgical operation and steroid therapy can induce several complications or side effects. Especially in subjects with poorly controlled diabetes mellitus, it would be better to avoid surgical operation or usage of steroid, because it is well known that both surgical operation and steroid therapy often aggravate glycemic control. Therefore, as observed in the present case, we should bear in mind the possibility of spontaneous disappearance of bronchial inflammatory polyps bringing about some serious symptoms such as massive hemoptysis and repeated bloody sputum. Finally, we should select the best therapy for bronchial inflammatory polys based on each patient's background and conditions in clinical practice.

DATA AVAILABILITY STATEMENT

The original contributions presented in the study are included in the article/supplementary material, further inquiries can be directed to the corresponding author/s.

AUTHOR CONTRIBUTIONS

YI wrote the paper. HT, KK, RS, HK, and KT were involved in teaching and revising the paper content. All authors contributed to the article and approved the submitted version.

REFERENCES

1. Yankauer S. Benign tumor of bronchus. *Laryngoscope*. (1929) 39:549. doi: 10.1288/00005537-192912000-00001
2. Peroni A. Inflammatory tumor of the bronchi experimental and pathologic consideration. *Arch Otolaryngol*. (1934). 19:1–22. doi: 10.1001/archotol.1934.03790010008001
3. Adams C, Moisan T, Chandrasekhar AJ, Warpeha R. Endobronchial polyposis secondary to thermal inhalational injury. *Chest*. (1979) 75:643–5. doi: 10.1378/chest.75.5.643
4. Gamblin TC, Farmer LA, Dean RJ, Bradley RA, Dalton ML. Tracheal polyp. *Ann Thorac Surg*. (2002) 73:1286–7. doi: 10.1016/S0003-4975(01)03115-0
5. McShane D, Nicholson AG, Goldstraw P, Ladas G, Travis WD, Ramanan R, et al. Inflammatory endobronchial polyps in childhood: clinical spectrum and possible link to mechanical ventilation. *Pediatr Pulmonol*. (2002) 34:79–84. doi: 10.1002/ppul.10120
6. Niimi A, Amitani R, Ikeda T, Kubo Y, Tanaka E, Kuze F. Inflammatory bronchial polyps associated with asthma: resolution with inhaled corticosteroid. *Eur Respir J*. (1995) 8:1237–9. doi: 10.1183/09031936.95.08071237
7. Takeuchi A, Kanemitsu Y, Takakuwa O, Ito K, Kitamura Y, Inoue Y, et al. A suspected case of inflammatory bronchial polyp induced by bronchial thermoplasty but resolved spontaneously. *J Thorac Dis*. (2018) 10:E678–81. doi: 10.21037/jtd.2018.08.144
8. Mittelman M, Fink G, Mor R, Avidor I, Spitzer S. Inflammatory bronchial polyps complicated by massive hemoptysis. *Eur J Respir Dis*. (1986) 69:63–6.

Conflict of Interest: The authors declare that the research was conducted in the absence of any commercial or financial relationships that could be construed as a potential conflict of interest.

frontiers | Frontiers in Medicine

CASE REPORT
published: 10 June 2022
doi: 10.3389/fmed.2022.916817

Pulmonary *Actinomyces graevenitzii* Infection: Case Report and Review of the Literature

*Yuan Yuan, Ziliang Hou, Dan Peng, Zhenchuan Xing, Jinxiang Wang and Shuai Zhang**

Department of Pulmonary and Critical Care Medicine, Beijing Luhe Hospital, Capital Medical University, Beijing, China

Background: Pulmonary actinomycosis (PA), a chronic indolent infection, is a diagnostic challenge. *Actinomyces graevenitzii* is a relatively rare Actinomyces species isolated from various clinical samples.

Case Presentation: A 47-year-old patient presented with a 3-month history of mucopurulent expectoration and dyspnea and a 3-day history of fever up to 39.0°C. He had dental caries and a history of alcoholism. Computed tomography (CT) images of the chest revealed a consolidation shadow in the right upper and middle lobes, with necrosis containing foci of air. *Actinomyces graevenitzii* was isolated from bronchoalveolar lavage fluid (BALF) culture and was identified by matrix-assisted laser desorption/ionization time-of-flight mass spectrometry. He received treatment with intravenous piperacillin-sulbactam for 10 days and oral amoxicillin-clavulanate for 7 months. His clinical condition had considerably improved. The consolidation shadow was gradually absorbed.

Conclusion: Early diagnosis and treatment of pulmonary actinomycosis are crucial. Bronchoscopy plays a key role in the diagnostic process, and matrix-assisted laser desorption/ionization time-of-flight mass spectrometry (MALDI-TOF/MS) is an accurate tool for *Actinomyces* identification.

Keywords: pulmonary actinomycosis (PA), *Actinomyces graevenitzii*, bronchoscopy, matrix-assisted laser desorption/ionization time-of-flight mass spectrometry, consolidation

OPEN ACCESS

Edited by:
Shu-Min Lin,
Linkou Chang Gung Memorial Hospital, Taiwan

Reviewed by:
Mohamed Yassin,
University of Pittsburgh, United States
Manuel Rodriguez-Iglesias,
Hospital Universitario Puerta del Mar, Spain

***Correspondence:**
Shuai Zhang
zhangshuai1974@ccmu.edu.cn

Specialty section:
This article was submitted to Pulmonary Medicine, a section of the journal Frontiers in Medicine

Received: *10 April 2022*
Accepted: *24 May 2022*
Published: *10 June 2022*

Citation:
Yuan Y, Hou Z, Peng D, Xing Z, Wang J and Zhang S (2022) Pulmonary Actinomyces graevenitzii Infection: Case Report and Review of the Literature. Front. Med. 9:916817. doi: 10.3389/fmed.2022.916817

INTRODUCTION

Actinomycosis is a rare chronic disease caused by the anaerobic Gram-positive bacteria *Actinomyces spp*, which normally inhabits the human oral cavity, digestive tract and genital tract (1). Due to its non-specific clinical manifestations and imaging characteristics, actinomycosis is easily misdiagnosed or missed. Pulmonary *Actinomyces graevenitzii* infection is extremely rare. The present case is the only case of pulmonary actinomycosis in our department. In this report, we describe it in detail and review the pertinent literature to improve our understanding of this disease, avoid misdiagnosis, and provide evidence for its clinical diagnosis, treatment, and prognosis.

CASE PRESENTATION

A 47-year-old man was admitted to the Department of Pulmonary and Critical Care Medicine, Beijing Luhe Hospital, Capital Medical University (Beijing, China) with a 3-month history of mucopurulent expectoration and dyspnea. He was initially diagnosed with bronchitis at a health center in the local town and did not undergo chest radiography and laboratory tests. He received intravenous antibiotics for 14 days, but his symptoms were not relieved. Three days before admission, he started having a fever with a maximum temperature of 39.0°C. He did not report chest pain, hemoptysis, headache, vomiting, and other symptoms. His past medical history was unremarkable with no exposure to chronic diseases, infectious diseases or allergy. The patient was a worker and lived in an urban setting. No data on major epidemic, family history, toxic habits, or occupational exposure was reported. He was married and denied any sexually transmitted infections or drug abuse. He had a 30-year smoking history (20 cigarettes per day on average) and a 20-year history of alcohol intake of a 150 mL daily.

At admission, the patient was febrile with a temperature of 38.9°C, tachycardiac (107 beats/min), and tachypneic (22 breaths/min). His blood pressure (110/80 mmHg) and oxygen saturation (99%, measured by pulse oximetry while breathing ambient air) were normal. Examination of the oral cavity showed poor hygiene. There were wet rales in the right lung. The auscultation of the heart revealed regular rhythm without murmur. The abdomen was tender, and there was no organomegaly. No abnormal findings were found in the neurologic examination.

The laboratory data was as follows: the peripheral blood white cell count was 8,740 cells/μl with 78.40% neutrophils, and 14.10% lymphocytes, and 6.70% monocytes; hemoglobin 110 g/L, the hematocrit 34%, the platelet count 447,000 per cubic millimeter. The C-reactive protein (71.67 mg/L), and erythrocyte sedimentation rate (100 mm/h) were significantly elevated. The PCT was mildly increased (0.13 ng/ml). Biochemical analysis of liver and renal showed normal range except slightly decreased albumin (32.1 g/L). Coagulation profile was normal and the serum tumor markers were negative. The results for possible connective tissue disease, such as antinuclear antibody, extractable nuclear antigen, and antineutrophil cytoplasmic antibody, were also negative. The serum IgM antibodies specific for respiratory pathogens, including Legionella pneumophila antibody, Mycoplasma pneumoniae antibody, Chlamydia pneumoniae antibody, influenza A virus antibody, and influenza B virus antibody, revealed no abnormality. The serum (1,3)-beta-D-glucan test (G test), the galactomannan test (GM test), and the serum TB test (T-SPOT) were all negative. The results of two blood cultures were negative. No pathological findings were detected in repeated sputum smears and cultures. A chest computed tomography (CT) scan showed a consolidation shadow in the upper and middle lobes of right lung with foci of necrosis (**Figure 1**).

Initially, We considered pneumonia as a possible diagnosis, which needed to be identified with lung cancer or pulmonary tuberculosis, and Antibiotic therapy with intravenous piperacillin-sulbactam was initiated. To make a definitive diagnosis, we performed a flexible bronchoscopy (**Figures 2A–C**), revealing purulent secretions in the medial and lateral segments of the right middle lobe (RML), drastically obstructing the lumen. After suction, the purulent secretions of the medial segment were reduced and the lateral segment was unobstructed. Then, bronchial brushing (BB), bronchial biopsy, and bronchoalveolar lavage were performed in the medial segment of the RML. Bronchial mucosal biopsy and BB specimens revealed only non-specific inflammation of the mucosa, and no pathogens were observed in the bronchoalveolar lavage fluid (BALF) through routine specimen smear and culture. On the third day after admission, the patient had no fever and continued to receive intravenous piperacillin-sulbactam therapy. To reduce secretions and search pathogens, we performed a second flexible bronchoscopy (**Figures 2D–F**), showing purulent secretions in the medial segment of the RML and the anterior segment of the right upper lobe (RUL). The BALF sample of the second time was sent for microbiological analysis. We took an appropriate amount of BALF samples for Gram staining, which is blue-purple (**Figure 3**). The BALF specimen was vortexed and shaken for 30–60 s. We used a sterile tool to spread a 10 μL calibration sample on the surface of the blood plate. The inoculated blood plate was incubated at 35°C for 48 h in a carbon dioxide incubator (5–10% CO2). The colony growing on the culture medium was smeared on a target plate. After drying, it was covered using a 1 μL Bruker matrix solution. When it was dry, the target plate was loaded into the machine: Microflex LT (Bruker Daltonics, Bremen, Germany). Matrix-assisted laser desorption/ionization time-of-flight mass spectrometry (MALDI-TOF/MS) for the identification of pathogens was performed, and *Actinomyces graevenitzii* was identified from the BALF. These results indicated that the pulmonary lesion of our patient was caused by *A. graevenitzii*. After administration of antibiotic treatment with piperacillin-sulbactam for ten days, the clinical condition of the patient improved obviously, and the CRP dropped to 29.34 mg/L, though the pulmonary lesions on the chest CT scan (**Figures 4A–D**) were not significantly absorbed. The patient was discharged with oral amoxicillin-clavulanate. A timeline with all relevant data from this clinical case is available in **Figure 5**. At the 7-month follow-up, the clinical condition of the patient was getting better and the chest CT scans (**Figure 4**) revealed that the consolidation shadow of the right lung was gradually absorbed.

DISCUSSION

Nowdays, more and more pulmonary actinomycosis is identified, through its clinical manifestations and imaging characteristics lack specificity. However, to date, there are only few reports of pulmonary *Actinomyces graevenitzii* infection. In the present study, we described a case of pulmonary *Actinomyces graevenitzii* infection diagnosed by microbiological identification through matrix-assisted laser desorption/ionization time-of-flight mass

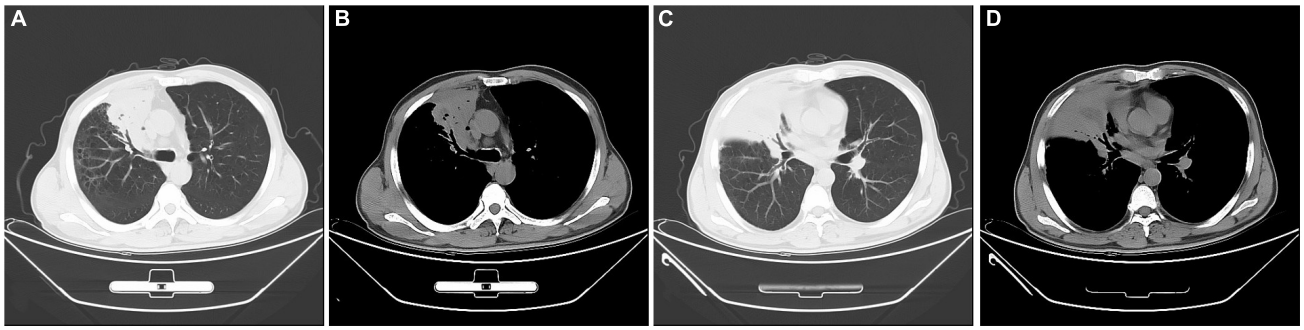

FIGURE 1 | Chest computed tomography images at admission. A consolidation shadow in the right upper and middle lobes, with necrosis containing foci of air. **(A,C)** lung window; **(B,D)** mediastinal window.

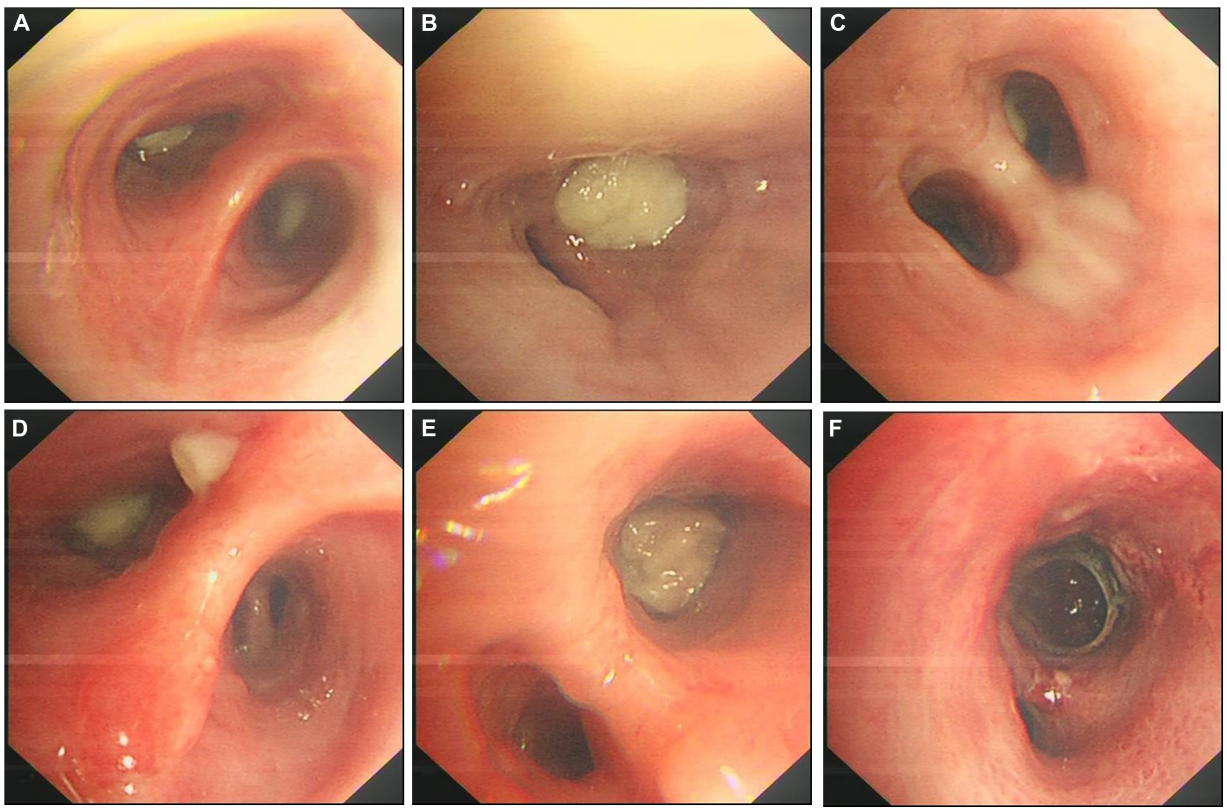

FIGURE 2 | A series of bronchoscopy images. The first bronchoscopy images **(A–C)**, the secondary bronchoscopy images **(D–F)**. **(A)** The medial and lateral segments of the RML were blocked by purulent yellow secretions. **(B)** The medial subsegment of the RML was completely obstructed by an endobronchial white necrotized mass. **(C)** The media subsegment of the RML became unobstructed after suction. **(D)** The medial and lateral segments of the RML were blocked by purulent yellow secretions. **(E)** The medial subsegment of the RML was completely obstructed by a an endobronchial white necrotized mass. **(F)** The media subsegment of the RML became unobstructed after suction. RML: Right middle lobe.

spectrometry (MALDI-TOF/MS). After treatment with targeted antibiotic, the clinical manifestations and imaging presentations of the patient gradually improved.

Actinomycosis is a slowly progressing granulomatous disease caused by *Actinomyces* species. *Actinomyces* is an anaerobic gram-positive bacterium, belonging to the human commensal flora of the oropharynx, gastrointestinal tract, and urogenital tract. Some species of *Actinomyces* have already been described, including *Actinomyces israelii* (2, 3), *Actinomyces odontolyticus* (4), *Actinomyces viscocus* (5), *Actinomyces meyeri* (6), *Actinomyces gerencseriae* (7), *Actinomyces naeslundii* (8), and *Actinomyces graevenitzii* (9–16). Among them, *A. israelii* is the most prevalent species isolated in human infections (9, 17–19). However, in our case, *A. graevenitzii* was identified

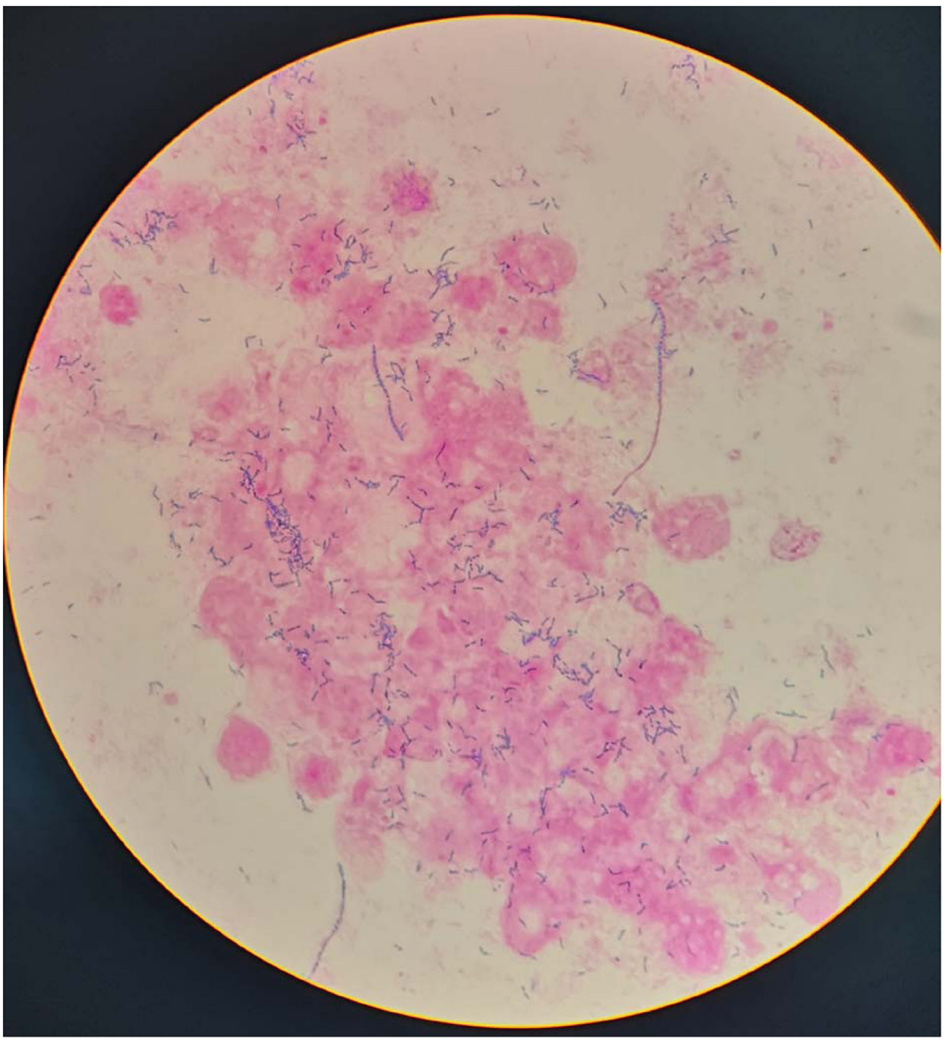

FIGURE 3 | Gram stain of the bronchoalveolar lavage fluid.

as the pathogenic bacteria isolated from bronchoalveolar lavage fluid. *A. graevenitzii* was first described in 1997 by Ramos et al. (20) in human clinical specimens (three respiratory and one bone samples). Being a catalase-negative, facultatively anaerobic, gram-positive, rod-shaped organism, *A. graevenitzii* is isolated almost exclusively from oral or respiratory sites and may have a unique ability to cause clinical actinomycosis (21). Although the clinical prevalence and pathogenic potential of *A. graevenitzii* is little known, the frequency of isolation from clinical specimens is increasing. We performed a PubMed search with the term "*Actinomyces graevenitzii*" or "pulmonary *Actinomyces graevenitzii* infection," and found that seven case reports in patients with pulmonary *Actinomyces graevenitzii* infection had been published (1, 6, 10–15). We reviewed the eight cases involving pulmonary actinomycosis in patients with *A. graevenitzii* infection, including our patient. The clinical features of the cases are shown in **Table 1**.

The pathogenesis of actinomycosis remains unclear, however some factors probably promote the disease (1). Pulmonary actinomycosis results mainly from aspiration of oropharyngeal or gastrointestinal secretions, and poor oral hygiene (22), pre-existing dental disease (4, 23), and alcohol abuse are the important predisposing factors for actinomycosis. Other risk factors include chronic lung diseases, such as emphysema, chronic bronchitis, and bronchiectasis (1). When local mucosal tissue is damaged, infection occurs in the form of continuous growth through the anatomical barrier, leading to the formation of abscesses and fistulas (17). In the eight cases, our case had dental caries, one case had periodontitis (15), and another case had septic mouth with several teeth missing (14). In our case, the patient also had a drinking habit. Actinomycosis is frequently associated with immunocompromised states. Cohen R D et al. described a case of pulmonary actinomycosis in association with infliximab treatment for Crohn's disease (16). One case of disseminated coinfection with *A. graevenitzii* and

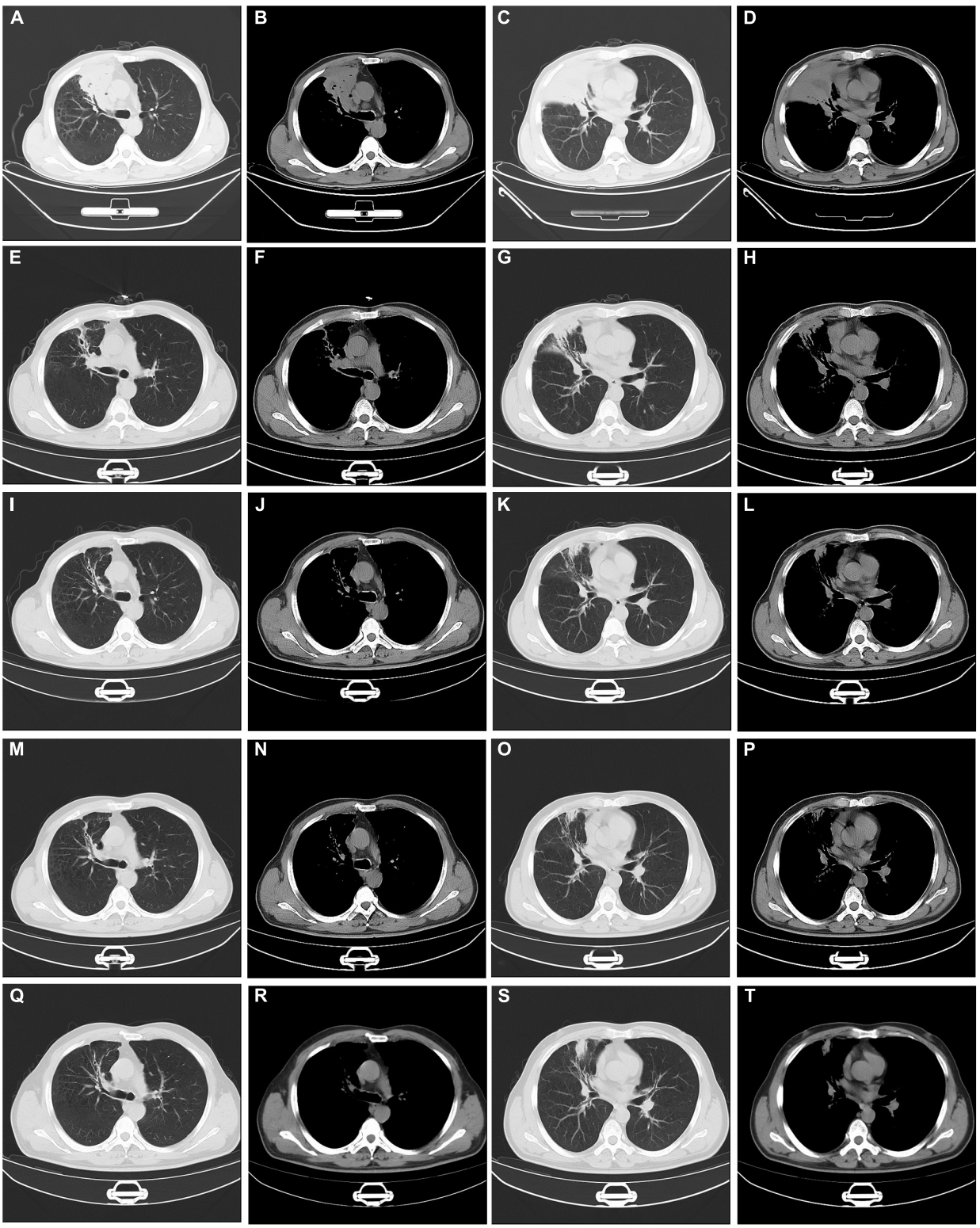

FIGURE 4 | Serial changes on chest computed tomography findings. Chest CT at discharge **(A–D)**. Chest CT at one month's follow-up **(E–H)**. Chest CT at three months' follow-up **(I–L)**. Chest CT at five months' follow-up **(M–P)**. Chest CT at seven months' follow-up **(Q–T)**. CT: computed tomography.

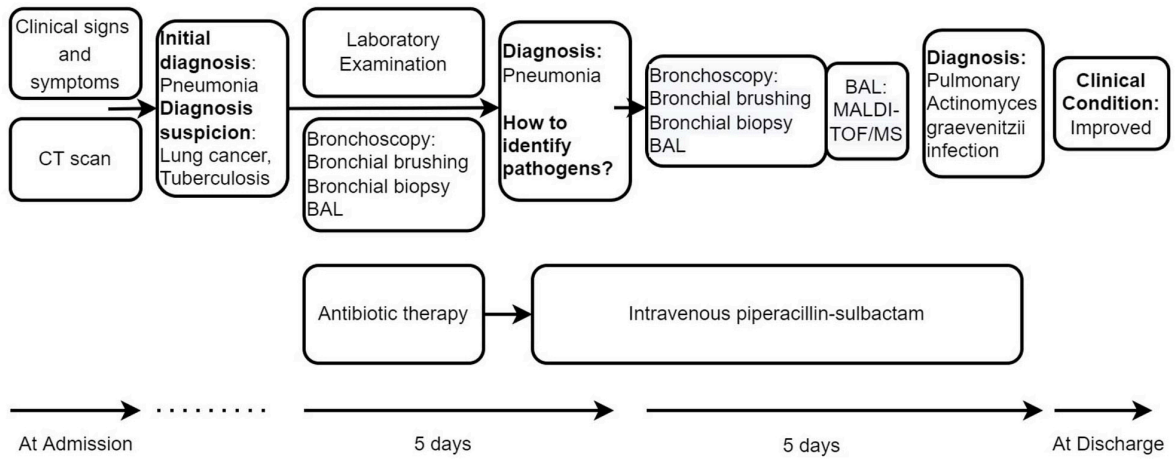

FIGURE 5 | Timeline with the most relevant data of the clinical case.

Mycobacterium tuberculosis has been reported (10). Besides those, it can also affect healthy people (4). S Gliga et al. reported a healthy young man of pulmonary *A. graevenitzii* infection (13).

The clinical symptoms of pulmonary actinomycosis are often non-specific, including fever, cough, dyspnea, or chest pain (24). Therefore, early diagnosis of the slowly progressing actinomycosis is difficult. In eight cases, patients were required be distinguished from tuberculosis, cancer, pulmonary coccidioidomycosis, or atypical pneumonia.

Radiological findings of pulmonary actinomycosis are also non-specific, including mass (23), nodules, patchy infiltrates, segmental air-space consolidation, and cavitation. It's often confused with malignancy or tuberculosis. A characteristic CT finding is a central low density within the parenchymal consolidation and adjacent pleural thickening (25, 26). Initially, the disease is present as a small, poorly defined nodule in the peripheral lung, with or without an interlobular septal thickening. Gradually, the nodule develops into a segmental air-space consolidation or mass. With the slow progression of infection, a cavity forms in central areas of low attenuation. CT enhanced images may show rim-like peripheral enhancement and multiple central low-attenuation areas. Further progression of the disease may involve the pleura, the chest wall, or the neighboring pulmonary lobes (25–28). In the eight cases, four cases showed nodules, three cases showed air-space consolidation. And five of eight cases had a cavity formation.

Bacterial cultures and histopathological features of biopsy specimens are the cornerstone of diagnosis. However, it is challenging to confirm the presence of bacterial by culture due to antibiotic treatment, concomitant organisms growth, or inadequate conditions (1). Therefore, this requires clear communication of the suspicion of actinomycosis with the microbiology laboratory. With the development of techniques, more bacterial identification methods are increasingly used, including 16S rRNA gene sequence analysis, next-generation sequencing (29) or MALDI-TOF/MS. In our case, the patient was diagnosed by bronchoalveolar lavage fluid culture using mass spectrometry, with a consolidation with central low density on chest CT. In addition, PCR analysis and 16S rRNA gene sequencing analysis are used to identify pathogens in four cases (10–12, 15). For pathology, the main non-surgical diagnostic methods are ultrasound or CT-guided percutaneous lung biopsy and transbronchial biopsy, with a high positive rate. The identification of actinomycete hyphae and sulfur particles in biopsy samples is the gold standard for diagnosis. In the eight cases, pulmonary *A. graevenitzii* infection was confirmed *via* sulfur granules or Actinomyces species detected in sputum (10), bronchoalveolar lavage (BAL) (12, 13, 15, 16), video-assisted thoracoscopic lung biopsy (11, 12), or transbronchial needle aspiration biopsy of lymph node guided by endoscopic ultrasonography (14).

A long term beta-lactam antibiotic therapy is needed for patiens with pulmonary actinomycosis. The intravenous administration of penicillin G is recommended for 2 to 6 weeks, followed by oral administration of penicillin V or amoxicillin for 6 to 12 months (1). It may be necessary to perform surgical management to drain voluminous abscesses, marsupialize chronic sinus tracts, and excise fibrotic lesions. All the eight cases were treated with antibiotics, mainly beta-lactams, and the duration of treatment varied from 5 weeks to 7 months with one case not mentioned. Of note, our case was successfully treated for 7 months and was being followed up closely. Pleasingly, his clinical status and imaging presentations were getting better.

In conclusion, our case and literature review indicated that pulmonary *A. graevenitzii* infection was a rare disease with non-specific clinical characteristics. The diagnosis is mainly based on pathogen identification and histopathology. We need to consider the possibility of pulmonary actinomycosis when investigating a consolidation shadow with necrosis or *trans*-fissural extension. Bronchoscopy plays a key role in the non-invasive diagnostic procedure, providing specimens to make the final diagnosis. In addition, matrix-

TABLE 1 | The characteristics of the eight cases of pulmonary *Actinomyces* graevenitzii infection.

Case No	Year	Age /Sex	Symptom	Comorbidity	Diagnoses initially Suspected	Chest CT Finding	Invasive Examination	Confirmatory Specimen	Identification Methods	Treatment	Treatment Duration	Outcome
1	2022	47/M	Cough, dyspnea For 3 months; Fever for 3 days	Smoking history Alcohol history Dental caries	Bacterial pneumonia TB Lung cancer	A consolidation shadow *Trans*-fissural extension With necrosis	Bronchoscopy	BALF	MALDI-TOF MS	PIP-SBT IV AMC PO	10 days 7 months	Improved
2 (15)	2018	75/M	Low-grade fever, dry cough For 10 days	GBS Periodontitis Smoking history	Lung cancer AFB infection Actinomycosis	A nodule with a cavity In the right upper lobe	Bronchoscopy EBUS-GS	BALF	MALDI-TOF MS PCR amplification 16S rRNA sequencing	SAM IV AM IV AM PO	1 week 1 week 2 months	Improved
3 (14)	2017	58/F	Fever For 6–8 weeks; Cough, dyspnea, Loss of appetite,	DVT TR Bronchial asthma	NR	Bilateral hilar, mediastinal Lymphadenopathies, Alveolar infiltrate In the right lower lobe	Bronchoscopy EBUS-TBNA	Lymph node biopsy	NR	AMC and CC	NR	Improved
4 (13)	2014	35/M	Cough for 1 year; Night sweats, Cough for 1 week	Travel to Sicily, Italy	TB	A nodule with cavitation In the right middle lobe	Bronchoscopy	BALF	NR	AMX	6 weeks	Improved
5 (12)	2012	38/F	Fever, Dry cough For 8 days	Visit Los Angeles, California For 3 days	Metastatic tumors Coccidioidomycosis	Multiple round lesions Located on both lobes, With partial cavity formation	Bronchoscopy EBUS-GS VATS	BALF	PCR amplification 16S rRNA sequencing	AMX	2 months	Improved
6 (11)	2012	69/M	Low-grade fever Night sweats For 2 months	Smoking history	CAP Malignancy	Multiple consolidation With air bronchograms In the lungs bilaterally	Bronchoscopy VATS	Lung biopsy	PCR amplification 16S rRNA sequencing	AM IV AM and CLR PO	1 month 6 months	Improved
7 (16)	2007	52/M	Fever, cough Night sweats For 12 days	CD for 9 years Infliximab IS medication Exposure to TB	TB Bacterial pneumonia Atypical pneumonia	Diffuse patchy consolidation, Ground-glass opacities, Branching centrilobular Nodular opacities	Bronchoscopy	BALF	NR	PEN and CLR PO DOX PO	5 weeks NR	Improved
8 (10)	2005	46/M	Fever, cough, Night sweats, Weight loss For 4 weeks	CAD Hypertension CHF Drug use history	CAP TB Actinomycosis	A right-upper-lobe cavity	Needle Aspiration	Sputum	PCR amplification 16S rRNA sequencing	AM PO	6 months	Improved

M, Male; F, Female; GBS, Guillain-Barre syndrome; DVT, Deep vein thrombosis; TR, Tricuspid regurgitation; CD, Crohn's disease; IS, Immunosuppressive; TB, Tuberculosis; CAD, Coronary artery disease; CHF, chronic congestive heart failure; AFB, Acid-fast bacillus; CAP, Community-acquired pneumonia; EBUS-GS, Endobronchial ultrasonography with a guide sheath; EBUS-TBNA, Endobronchial ultrasonography-transbronchial needle aspiration; VATS, Video-assisted thoracoscopic surgery; BALF, Bronchoalveolar lavage fluid; MALDI-TOF MS, Matrix-assisted laser desorption/ionization time-of-flight mass spectrometry; PCR, Polymerase chain reaction; PIP-SBT, piperacillin-sulbactam; AMC, amoxicillin-clavulanate; SAM, Ampicillin-sulbactam; AM, Ampicillin; AMX, Amoxicillin; CC, Clindamycin; CLR, Clarithromycin; PEN, Penicillin; DOX, Doxycycline; IV, Intravenously; PO, orally; NR, Not reported.

assisted laser desorption/ionization time-of-flight mass spectrometry is an accurate tool for *Actinomyces* identification.

ETHICS STATEMENT

Written informed consent was obtained from the individual(s) for the publication of any potentially identifiable images or data included in this article.

AUTHOR CONTRIBUTIONS

YY and ZH: concept and writing of the manuscript. DP: interpretation of the sources and patient acquisition. ZX: image example. JW and SZ: supervision and concept. All authors read and approved the final draft, contributed to the article, and approved the submitted version.

REFERENCES

1. Valour F, Sénéchal A, Dupieux C, Karsenty J, Lustig S, Breton P, et al. Actinomycosis: etiology, clinical features, diagnosis, treatment, and management. *Infect Drug Resist.* (2014) 7:183–97. doi: 10.2147/IDR.S39601
2. Tabarsi P, Yousefi S, Jabbehdari S, Marjani M, Baghaei P. Pulmonary actinomycosis in a patient with AIDS/HCV. *J Clin Diagn Res.* (2017) 11:OD15–7. doi: 10.7860/JCDR/2017/27593.10092
3. Kheir F, Hamdi T, Khayr W, Latta S. Nonresolving pneumonia. *Am J Ther.* (2011) 18:e177–9.
4. Crisafulli E, Bernardinello N, Alfieri V, Pellegrino F, Lazzari C, Gnetti L, et al. A pulmonary infection by Actinomyces odontolyticus and Veillonella atypica in an immunocompetent patient with dental caries. *Respirol Case Rep.* (2019) 7:e00493. doi: 10.1002/rcr2.493
5. Mosimann J, Hany A, Kayser FH. Pulmonary Actinomyces-viscosus infection. *Schweiz Med Wochenschr.* (1979) 109:720–2.
6. Shimoda M, Yoshiyama T, Okumura M, Tanaka Y, Morimoto K, Kokutou H, et al. Actinomyces meyeri pleural infection that was difficult to treat due to delayed culture: a case report and literature review of 28 cases. *Respir Med Case Rep.* (2021) 34:101530. doi: 10.1016/j.rmcr.2021.101530
7. Llamas-Velasco M, Domínguez I, Ovejero E, Pérez-Gala S, García-Diez A. Empyema necessitatis revisited. *Eur J Dermatol.* (2010) 20:115–9.
8. Supriya BG, Harisree S, Savio J, Ramachandran P. Actinomyces naeslundii causing pulmonary endobronchial Actinomycosis - A case report. *Indian J Pathol Microbiol.* (2019) 62:326–8. doi: 10.4103/IJPM.IJPM_706_17
9. Kononen E, Wade WG. Actinomyces and related organisms in human infections. *Clin Microbiol Rev.* (2015) 28:419–42. doi: 10.1128/CMR.00100-14
10. Tietz A, Aldridge KE, Figueroa JE. Disseminated coinfection with Actinomyces graevenitzii and Mycobacterium tuberculosis: case report and review of the literature. *J Clin Microbiol.* (2005) 43:3017–22. doi: 10.1128/JCM.43.6.3017-3022.2005
11. Fujita Y, Iikura M, Horio Y, Ohkusu K, Kobayashi N. Pulmonary Actinomyces graevenitzii infection presenting as organizing pneumonia diagnosed by PCR analysis. *J Med Microbiol.* (2012) 61:1156–8. doi: 10.1099/jmm.0.040394-0
12. Nagaoka K, Izumikawa K, Yamamoto Y, Yanagihara K, Ohkusu K, Kohno S. Multiple lung abscesses caused by Actinomyces graevenitzii mimicking acute pulmonary coccidioidomycosis. *J Clin Microbiol.* (2012) 50:3125–8. doi: 10.1128/JCM.00761-12
13. Gliga S, Devaux M, Gosset Woimant M, Mompoint D, Perronne C, Davido B. Actinomyces graevenitzii pulmonary abscess mimicking tuberculosis in a healthy young man. *Can Respir J.* (2014) 21:75–7. doi: 10.1155/2014/841480
14. Caballero Vázquez A, Cruz Rueda JJ, Ceballos Gutierrez JA. Diagnosis of actinomyces graevenitzii lung infection using linear EBUS. *Arch Bronconeumol.* (2017) 53:351–2. doi: 10.1016/j.arbres.2016.10.014
15. Himeji D, Hara S, Kawaguchi T, Tanaka GI. Pulmonary actinomyces graevenitzii infection diagnosed by bronchoscopy using endobronchial ultrasonography with a guide sheath. *Intern Med.* (2018) 57:2547–51. doi: 10.2169/internalmedicine.9799-17
16. Cohen RD, Bowie WR, Enns R, Flint J, Fitzgerald JM. Pulmonary actinomycosis complicating infliximab therapy for Crohn's disease. *Thorax.* (2007) 62:1013–4. doi: 10.1136/thx.2006.075150
17. Wong VK, Turmezei TD, Weston VC. Actinomycosis. *BMJ.* (2011) 343: d6099.
18. Pulverer G, Schutt-Gerowitt H, Schaal K. Human cervicofacial actinomycoses: microbiological data for 1997 cases. *Clin Infect Dis.* (2003) 37:490–7. doi: 10.1086/376621
19. Martinez-Giron R, Pantanowitz L. Pulmonary actinomycosis: cytomorphological features. *Monaldi Arch Chest Dis.* (2021) 92:1641. doi: 10.4081/monaldi.2021.1641
20. Ramos CP, Falsen E, Alvarez N, Akervall E, Sjödén B, Collins MD. Actinomyces graevenitzii sp. nov., isolated from human clinical specimens. *Int J Syst Bacteriol.* (1997) 47:885–8. doi: 10.1099/00207713-47-3-885
21. Hall V. Actinomyces–gathering evidence of human colonization and infection. *Anaerobe.* (2008) 14:1–7. doi: 10.1016/j.anaerobe.2007.12.001
22. Grzywa-Celińska A, Emeryk-Maksymiuk J, Szmygin-Milanowska K, Czekajska-Chehab E, Milanowski J. Pulmonary actinomycosis - the great imitator. *Ann Agric Environ Med.* (2017) 25:211–2. doi: 10.26444/aaem/75652
23. Ito T, Yoshida T, Sakuraba M, Tanaka A, Hamada K, Ito A. Insufficient initial treatment but good recovery after diagnosis of pulmonary actinomycosis. *Oxf Med Case Rep.* (2019) 2019:510–2. doi: 10.1093/omcr/omz123
24. Bonnefond S, Catroux M, Melenotte C, Karkowski L, Rolland L, Trouillier S, et al. Clinical features of actinomycosis: a retrospective, multicenter study of 28 cases of miscellaneous presentations. *Medicine.* (2016) 95:e3923. doi: 10.1097/MD.0000000000003923
25. Cheon JE, Im JG, Kim MY, Lee JS, Choi GM, Yeon KM. Thoracic actinomycosis: CT findings. *Radiology.* (1998) 209:229–33.
26. Han JY, Lee KN, Lee JK, Kim YH, Choi SJ, Jeong YJ, et al. An overview of thoracic actinomycosis: CT features. *Insights Imaging.* (2013) 4:245–52. doi: 10.1007/s13244-012-0205-9
27. Kim TS, Han J, Koh WJ, Choi JC, Chung MJ, Lee JH, et al. Thoracic actinomycosis: CT features with histopathologic correlation. *AJR Am J Roentgenol.* (2006) 186:225–31. doi: 10.2214/AJR.04.1749
28. Łyżwa E, Siemion-Szcześniak I, Sobiecka M, Kacprzak A, Winiarska A, Szołkowska M, et al. Pulmonary actinomycosis complicated by fistula of the chest wall. *Adv Respir Med.* (2021) 89:532–7. doi: 10.5603/ARM.a2021.0071
29. Wang W, Ren D, Xu C, Yuan Q, Zhang Q, Hu H, et al. Pulmonary actinomycosis diagnosed by radial endobronchial ultrasound coupled with metagenomic next-generation sequencing: a case report and brief literature review. *Int J Infect Dis.* (2020) 100:379–81. doi: 10.1016/j.ijid.2020.09.1418

Conflict of Interest: The authors declare that the research was conducted in the absence of any commercial or financial relationships that could be construed as a potential conflict of interest.

frontiers | Frontiers in Medicine

CASE REPORT
published: 13 June 2022
doi: 10.3389/fmed.2022.893968

Case Report: Rare Dynein Axonemal Heavy Chain 9 Mutations in a Han-Chinese Patient With Kartagener Syndrome

*Jingjing Feng[1], Junqing Li[1], Yong Du[1], Tianyun Shi[1], Lokesh Sharma[2] and Zhijun Jie[1]**

[1] Department of Pulmonary and Critical Care Medicine, Shanghai Fifth People's Hospital, Center of Community-Based Health Research, Fudan University, Shanghai, China, [2] Section of Pulmonary, Critical Care and Sleep Medicine, Yale University School of Medicine, New Haven, CT, United States

A 52-year-old woman presented with respiratory symptoms of productive cough and shortness of breath. She had suffered from repeated pneumonia. The CT scans revealed chronic sinusitis, tree bud signs in pulmonary imaging, and situs inversus. She received a primary diagnosis of Kartagener syndrome of primary ciliary dyskinesia (PCD) and a genetic examination was performed. Compound heterozygous mutations in dynein axonemal heavy chain 9 (*DNAH9*) were identified, which encoded outer dynein arms (ODAs) components. *DNAH9* mutations are relatively rare events in PCD, and this is the first report of PCD patients with *DNAH9* mutations in the Chinese population. Further, a literature review of mutations in PCD was conducted.

Keywords: kartagener syndrome, PCD, *DNAH9*, gene mutation, situs inversus

OPEN ACCESS

Edited by:
Sara Manti,
University of Catania, Italy

Reviewed by:
Daw-Yang Hwang,
National Institute of Cancer Research, National Health Research Institutes, Taiwan
Raffaele Campisi,
Azienda Ospedaliera Universitaria Policlinico G. Rodolico-San Marco, Italy

****Correspondence:***
Zhijun Jie
jiezjlxh@163.com

Specialty section:
This article was submitted to Pulmonary Medicine, a section of the journal Frontiers in Medicine

Received: *11 March 2022*
Accepted: *10 May 2022*
Published: *13 June 2022*

Citation:
Feng J, Li J, Du Y, Shi T, Sharma L and Jie Z (2022) Case Report: Rare Dynein Axonemal Heavy Chain 9 Mutations in a Han-Chinese Patient With Kartagener Syndrome. Front. Med. 9:893968. doi: 10.3389/fmed.2022.893968

INTRODUCTION

Kartagener syndrome is characterized by bronchiectasis, chronic sinusitis, and situs inversus, which is a subtype of primary ciliary dyskinesia (PCD) (1, 2). PCD is an autosomal recessive or X-linked genetic disorder in which the cilia are dysfunctional and fail to effectively transport secretions (3). The prevalence of PCD is about 1/16,000 to 1/20,000 (4). Kartagener syndrome is present in 40–50% of PCD cases. So far, around 40 cilia-related genes have been found to be associated with PCD (5, 6). Mutations in *DNAH9* are rarely reported. There is still no case reported in China. Herein we report a Kartagener syndrome case with *DNAH9* mutations in a Han-Chinese patient.

CASE REPORT

Clinical Presentation

A 52-year-old female was admitted to the hospital due to recurrent cough, expectoration, and shortness of breath for more than 10 years. In her hometown, she frequently presented to the hospital with lung infections and was treated with antibiotics. She received a pulmonary function test in September 2021 in Shanghai, which indicated obstructive ventilatory dysfunction because FEV_1/FVC was less than 70%. Consequently, she was diagnosed with chronic obstructive pulmonary disease (COPD). She was treated with long-acting beta2-receptor agonist (LABA) + long-acting cholinergic receptor antagonist (LAMA) (Olexin) inhalation for about

2 months. Two days prior to the current admission, she was presented with increased cough and yellow sputum. She had no fever, chills, fatigue, night sweats, progressive emaciation, chest pain, or other symptoms. She had a history of spontaneous pneumothorax because of ruptured bullae of the lung. However, she could not provide the X-ray and a detailed history of the previous therapies. Although clear that she had situs inversus, she was treated as a common pulmonary disease. She denied any history of PCD in any of her parents or risk factors such as inbreeding. She has a son and a daughter, both of them are healthy with no apparent signs of lung disease. There is no other person with similar symptoms in her family.

Examination

On a physical examination, her blood pressure was 140/90 mmHg, pulse rate of 107 beats/min, respiratory rate of 15 times/min, and oxygen saturation of 98% at room air. On cardiovascular examination, heartbeats were audible on the right side of the chest. There were not any coarse crackles in both lungs. An initial investigation revealed a white cell count of 3,290/μL and a C reactive protein level of less than 1 mg/L. The arterial blood gas analysis showed her PO2 level was 111 mmHg when she received an oxygen flow rate of 3 L/min. There were not significant abnormal findings in liver and kidney functions, electrolytes, ESR, procalcitonin, peripheral blood lymphocyte subsets, markers of autoimmunity, and antinuclear antibody.

In sputum smear, Gram-positive cocci, suspected to be *Streptococcus* was identified. The bronchial alveolar lavage fluid (BALF) was obtained to perform metagenomic sequencing and *Nocardia gelsenkircheni* was identified. Chest X-ray (posteroanterior view) showed a cardiac shadow on the right side (**Figure 1**). Many tree-in-buds on both sides of lung lobes were found in Chest computed tomography (CT) (**Figure 2**). Abdominal CT confirmed complete situs inversus totalis (**Figure 3**). Otitis media tympanitis with effusion was found by an otolaryngologic examination (**Figure 4**). Fiberoptic bronchoscopy showed total bronchial inversion and bronchial mucosal inflammations in both lungs (**Figure 5**).

Given the history of repeated respiratory infections and situs inversus, combined with the physical examinations, she was suspected to have PCD. Following the European Respiratory Society (ERS) guidelines for the diagnosis of PCD (6), we intended to evaluate nasal nitric oxide (nNO) levels and perform a high-speed video analysis (HSVA). Unfortunately, we were unable to conduct those tests because of our technical limitations. We then performed genetic testing of her peripheral blood to confirm the diagnosis, according to the diagnostic criteria of the Chinese Expert Consensus on the Diagnosis and Treatment of Primary Ciliary Dyskinesia (7).

Genome Sequencing

We performed whole-exome sequencing to detect the presence of any mutation(s). Two milliliters of peripheral venous blood preserved in an ethylenediamine tetraacetic acid (EDTA) coated tube was sent to the Shenzhen BGI Medical Test Laboratory. The sequencing was performed by capture high-throughput chip technology. Sanger sequencing was used to verify the mutations. The results showed that two suspected pathogenic mutations were located on chromosome 17; CHR17:11513858-11513859 and CHR17:11593470 (**Figure 6**), and detected in *DNAH9* gene associated with PCD type 40, which was partially related to the phenotype of the subjects with PCD. One of the mutations, *DNAH9* (NM_001372.3, c.760_761delTT, p.Phe254Leufs*6) is a frame-shift mutation caused by the deletion of two nucleotide TT at nucleotide positions 760-761 of the coding sequence of the gene, resulting in the

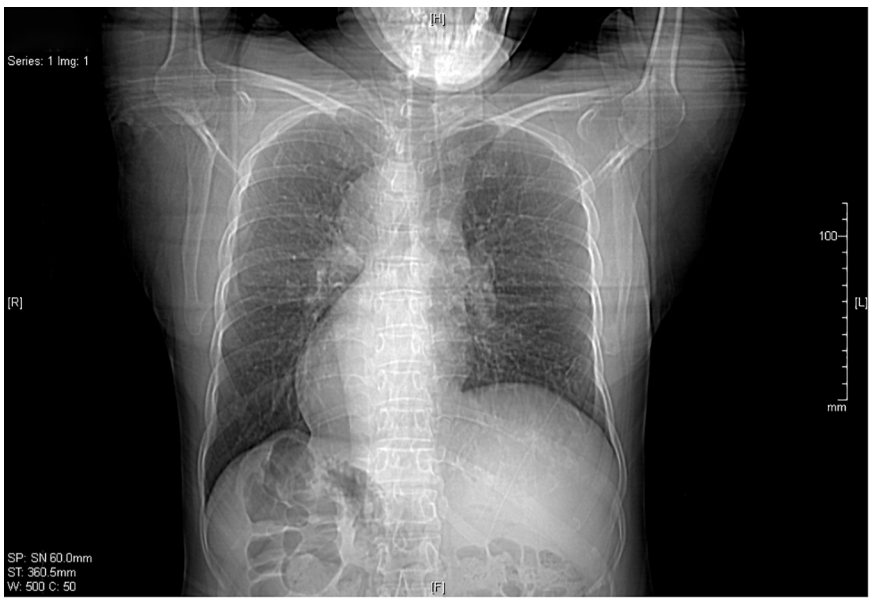

FIGURE 1 | Chest X-ray shows dextrocardia in this patient with situs inversus.

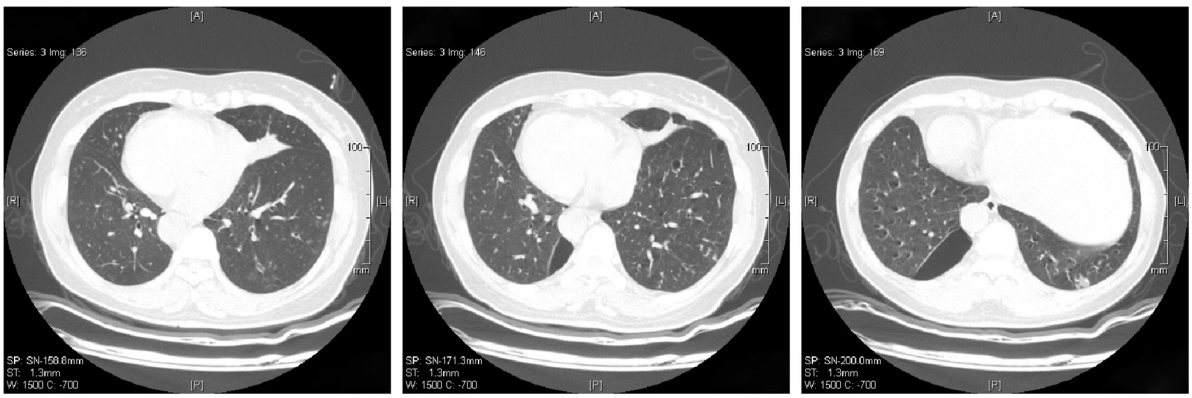

FIGURE 2 | Chest computed tomography shows inflammation in both sides of lung lobes.

phenylalanine codon at position 254 being changed to leucine, and a stop codon at position 260. The c.760_761delTT mutation is mentioned in ClinVar. Another mutation, *DNAH9* (NM_001372.3C, c.4331G > A, chr17:11593470) is a nonsense mutation caused by the substitution of nucleotide A with G, resulting in the leucine codon at position Trp being changed to a stop codon. We could not get blood samples of her parents or children for the gene analysis, but they had no clinical manifestation of PCD. This study was approved by Shanghai Ethical Review Board (2022-047).

Clinical Management

Ampicillin tazobactam was administered to treat the infection, ambroxol hydrochloride was administered to reduce sputum, albuterol, and acetylcysteine were inhaled to dilate the airways and promote sputum excretion. After treatment, the symptoms were relieved, and she was discharged. The patient was then prescribed fordostine to eliminate phlegm and urmetrium bromide and verranterol for inhalation therapy.

DISCUSSION

Due to its low prevalence, Kartagener syndrome has been rarely reported, and *DNAH9* gene mutations are even rarer. In this study, we firstly reported *DNAH9* gene mutations in a Han-Chinese subject with Kartagener syndrome. *DNAH9* is involved in the function of motile node monocilia. The loss of *DNAH9* could impair ciliary motion and subsequently alter nodal flow, result in laterality defects (8). The loss-of function mutations in

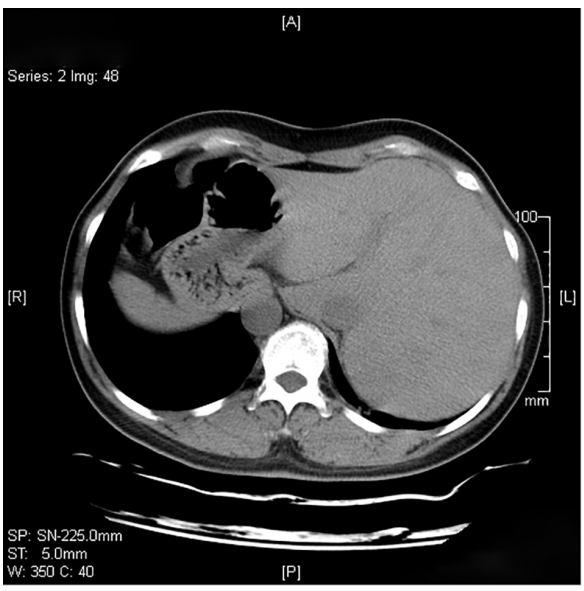

FIGURE 3 | Computed tomography scan of the abdomen showing liver on the left.

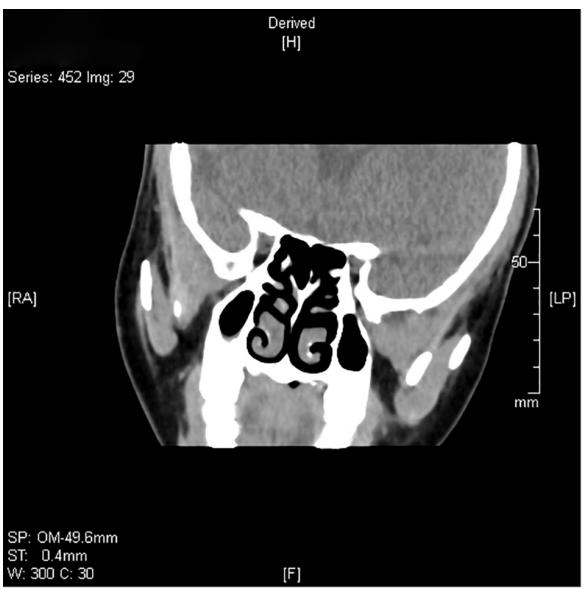

FIGURE 4 | The paranasal sinus CT scan of the proband shows non-specific thickening of the mucosa on the bilateral maxillary sinuses.

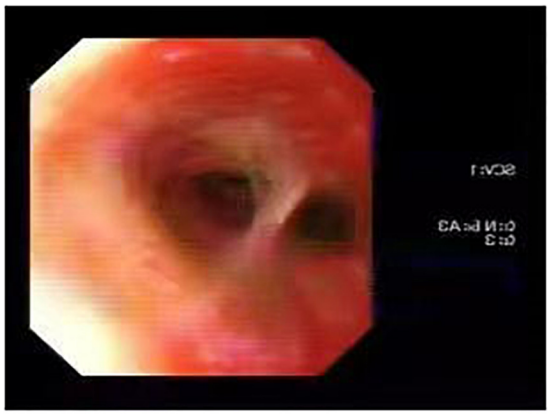

FIGURE 5 | Fiberoptic bronchoscopy showed bronchial total inversion, bronchial mucosal inflammation in both lungs.

DNAH9 cause motile cilia defects and situs inversus (9). *DNAH9* is a component of the type 2 ODA. The ODAs are responsible for the generation of ciliary motion. In the cilia of respiratory epithelium in mammals, there are at least two types of ODAs, the ODA type 1 containing *DNAH5* as well as *DNAH11* (10) and the ODA type 2 containing *DNAH5* and *DNAH9* (11). Loges et al reported eight mutations in the *DNAH9* gene among laterality defects and in patients with respiratory ciliary-beating defects (8). The mutated alleles of *DNAH9* which were previously reported are different from those presented in this study. Fassad et al analyzed three families of motile cilia defects and situs inversus, and also found five mutations in *DNAH9* genes (9). *DNAH9* gene encodes the heavy chain subunit of axonemal dynein, a large multi-subunit molecular motor. Axonemal dynein attaches to microtubules and hydrolyzes ATP to mediate the movement of cilia and flagella. The frequency of c.760_761delTT is 0.00004779 in GnomAD database and is mentioned in ClinVar. The frequency of c.4331G > A was not included in TOPMed or GnomAD database.

No case has been reported in domestic literature in China. It could also be due to a lack of genetic testing. Next generation gene sequencing and whole exome gene sequencing can not only diagnose PCD, but also find new mutations that lead to clinical manifestation of PCD. In the Chinese Expert Consensus on the Diagnosis and Treatment of Primary Ciliary Dyskinesia published in 2020, 12 literatures related to gene detection of PCD patients in China were summarized. A total of 17 cases of PCD with genetic mutations were reported, but no mutation in *DNAH9* gene was reported (7).

PCD manifests as a series of clinical presentations caused by ciliary motility disorders. Ciliary structural abnormalities in PCD patients include partial loss of ciliary motility arm, such as unilateral loss of lateral or medial ciliary motility arm, or complete loss of ciliary motility arm. The ciliary motility disorder caused by *DNAH9* gene mutation is mainly manifested as lack of ciliary tail motility, but not the total loss of ciliary motility. Loges et al reported that *DNAH9* mutations cause laterality defects with no or only mild respiratory symptoms such as recurrent airway infections instead of a classical respiratory PCD phenotype (8), which may be related to the patient's mild clinical presentation. However, severe clinical manifestations in our case might be due to novel mutations in both the alleles in *DNAH9* gene.

In this case, respiratory symptoms were the initial manifestations of the patient, including repeated cough and sputum, accompanied by shortness of breath post physical activity, and imaging revealing total visceral inversion. What was inconsistent with Kartagener syndrome diagnosis was that the patient did not have typical bronchiectasis in lung imaging but had manifestations of diffuse bronchiolitis. Wang Lifei et al. (12) summarized the imaging characteristics of lungs and sinuses of 24 Kartagener syndrome patients. They found that Digital Radiography and CT mainly showed benign multiple small nodules, linear shadow and tree bud signs. The bronchiolitis

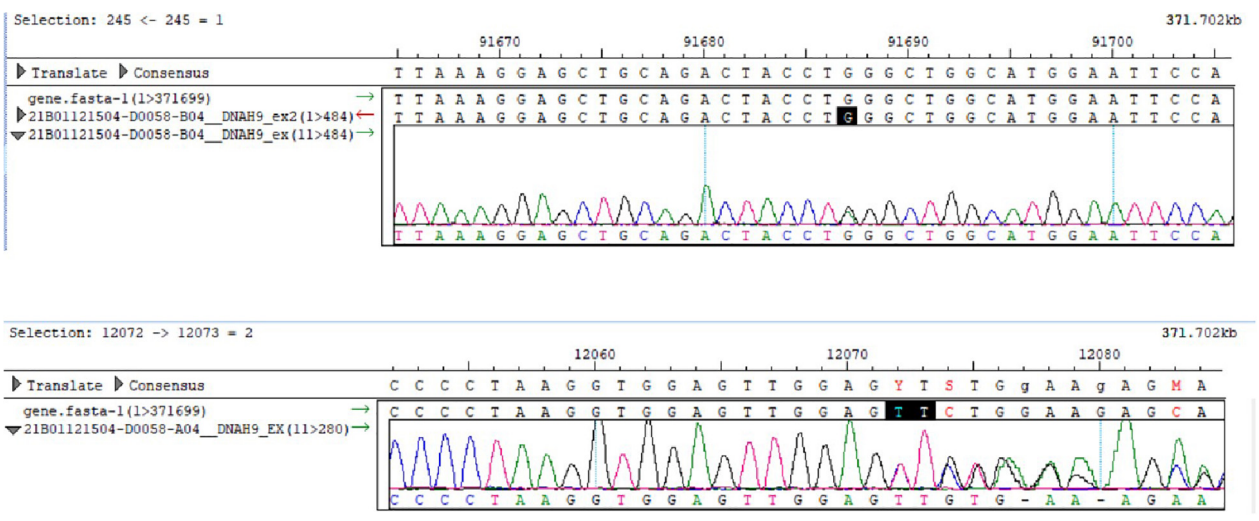

FIGURE 6 | The results of Sanger sequencing in this case. Compound heterozygous mutations in the *DNAH9* gene are shown.

changes were observed in 91.67% (22/24) patients, 58.33% (14/24) showed manifestations of diffuse panbronchiolitis (DPB). Finally, there were eight cases confirmed to be DPB. The patient's sinus CT suggested the presence of mild paranasal sinusitis, which was consistent with the common manifestations of Kartagener syndrome. The patient suffered from spontaneous pneumothorax several years ago and was admitted to hospital in her hometown in rural China. The X-ray examination was performed during hospital stay and then she learned that she had situs inversus. However, her healthcare provider did not mention PCD or Kartagener syndrome to her due to a lack of awareness of this disease, which led to a delay in appropriate diagnosis.

The diagnosis of Kartagener syndrome can also be confirmed by electron microscopy examination of nasal mucosa or bronchial mucosa epithelium to observe the ultrastructure of cilia. In addition, nNO can assist the diagnosis. Due to technical limitations, electron microscopy and nNO were not performed in the patient.

As a type of PCD, Kartagener syndrome is an inherited disease, lacking definitive cure. It is primarily managed with symptomatic treatment, including infection prevention and control. Mucolytics are used to promote sputum excretion, and drugs promoting cilia movement can be administrated to improve host immunity to prevent infections.

Appropriate antibiotics can be used according to the bacterial culture and antibiotic sensitivity tests. In this case, multiple sputum smears showed Gram-positive cocci, suspected to be *Streptococcus*, and paracillin tazobactam was given to treat the infection. Ambroxol was administered to reduce phlegm and inhaled acetyl cysteine solution was given to facilitate sputum excretion.

The patient was treated with long-term inhalation of verranterol ummeronium bromide to dilate the airways to relieve shortness of breath and delay lung function decline.

Kartagener syndrome in patients with combined chronic rhinitis, sinusitis can be treated by local use of physiological saline, antibiotics and antibiotic containing nasal douches. Surgical excision is recommended for patients with long-term repeated respiratory infection symptoms, nasal secretions, presence of drug-resistant bacteria that affect quality of life.

Kartagener syndrome is a rare genetic disease, which is not difficult to diagnose. However, due to insufficient understanding of Kartagener syndrome by clinicians, misdiagnosis and missed diagnosis result in delayed treatment. As a genetic disease, it is very important to identify the mutation site, which can assist genetic counseling, including prenatal counseling. Genetic testing can be helpful to discover new pathogenic genes and deepen the understanding of the disease.

ETHICS STATEMENT

The studies involving human participants were reviewed and approved by the Ethical Review Board. The authors declare that appropriate written informed consent was obtained for the publication of this manuscript and accompanying images. The patients/participants provided their written informed consent to participate in this study. Written informed consent was obtained from the individual(s) for the publication of any potentially identifiable images or data included in this article.

AUTHOR CONTRIBUTIONS

JF: preparation, funding acquisition, and writing—original draft. JL and LS: writing—review and editing. TS and YD: resources supply. ZJ: conceptualization and writing—review and editing. All authors contributed to the article and approved the submitted version.

FUNDING

This study was supported by the High-level professional physician training program of Minhang District (No: 2020MZYS12), Specialized Department Foundation of Minhang District (No: 2020MWTZB02), and Plan for leading talent of Minhang District (201807).

ACKNOWLEDGMENTS

We thank Yi Liu for performing the gene analysis.

REFERENCES

1. Xu X, Gong P, Wen J. Clinical and genetic analysis of a family with kartagener syndrome caused by novel DNAH5 mutations. *J Assist Reprod Genet.* (2017) 34:275–81. doi: 10.1007/s10815-016-0849-3
2. Deng H, Xia H, Deng S. Genetic basis of human left-right asymmetry disorders. *Expert Rev Mol Med.* (2015) 16:e19. doi: 10.1017/erm.2014.22
3. Lucas J, Burgess A, Mitchison H, Moya E, Williamson M, Hogg C. Diagnosis and management of primary ciliary dyskinesia. *Arch Dis Child.* (2014) 99:850–6.
4. Hjeij R, Onoufriadis A, Watson C, Slagle C, Klena N, Dougherty G, et al. CCDC151 mutations cause primary ciliary dyskinesia by disruption of the outer dynein arm docking complex formation. *Am J Hum Genet.* (2014) 95:257–74. doi: 10.1016/j.ajhg.2014.08.005
5. Guo T, Tan Z, Chen H, Zheng D, Liu L, Huang X, et al. An effective combination of whole-exome sequencing and runs of homozygosity for the diagnosis of primary ciliary dyskinesia in consanguineous families. *Sci Rep.* (2017) 7:7905. doi: 10.1038/s41598-017-08510-z
6. Lucas J, Barbato A, Collins S, Goutaki M, Behan L, Caudri D, et al. European respiratory society guidelines for the diagnosis of primary ciliary dyskinesia. *Eur Respir J.* (2017) 49:1601090.
7. Respiratory Branch of Chinese Alliance for Rare Diseases, Chinese Consensus Expert Group on diagnosis and treatment of primary ciliary dysfunction. Chinese expert consensus on diagnosis and treatment of primary ciliary dyskinesia. *Shanghai Med.* (2020) 43:193–202.
8. Loges N, Antony D, Maver A, Deardorff M, Güleç E, Gezdirici A, et al. Recessive DNAH9 loss-of-function mutations cause laterality defects and subtle respiratory ciliary-beating defects. *Am J Hum Genet.* (2018) 103:995–1008. doi: 10.1016/j.ajhg.2018.10.020

9. Fassad M, Shoemark A, Legendre M, Hirst R, Koll F, le Borgne P, et al. Mutations in outer dynein arm heavy chain DNAH9 cause motile cilia defects and situs inversus. *Am J Hum Genet.* (2018) 103:984–94. doi: 10.1016/j.ajhg.2018.10.016
10. Fliegauf M, Olbrich H, Horvath J, Wildhaber J, Zariwala M, Kennedy M, et al. Mislocalization of DNAH5 and DNAH9 in respiratory cells from patients with primary ciliary dyskinesia. *Am J Respir Crit Care Med.* (2005) 171:1343–9. doi: 10.1164/rccm.200411-1583OC
11. Dougherty G, Loges N, Klinkenbusch J, Olbrich H, Pennekamp P, Menchen T, et al. DNAH11 localization in the proximal region of respiratory cilia defines distinct outer dynein arm complexes. *Am J Respir Cell Mol Biol.* (2016) 55:213–24. doi: 10.1165/rcmb.2015-0353OC
12. Wang L, Fuan Y, Gu Y, Zheng Q, Chen L, Zhang C, et al. Kartagener's syndrome with bronchiolitis: imaging diagnosis and follow-up. *Chin Med Imaging Technol.* (2009) 25:2040–42.

Conflict of Interest: The authors declare that the research was conducted in the absence of any commercial or financial relationships that could be construed as a potential conflict of interest.

Publisher's Note: All claims expressed in this article are solely those of the authors and do not necessarily represent those of their affiliated organizations, or those of the publisher, the editors and the reviewers. Any product that may be evaluated in this article, or claim that may be made by its manufacturer, is not guaranteed or endorsed by the publisher.

frontiers | Frontiers in Medicine

TYPE Case Report
PUBLISHED 22 July 2022
DOI 10.3389/fmed.2022.904431

OPEN ACCESS

EDITED BY
Michel Gonzalez,
Centre Hospitalier Universitaire Vaudois (CHUV), Switzerland

REVIEWED BY
Jon Andri Lutz,
Fribourg Cantonal Hospital, Switzerland
Gunnar N. Hillerdal,
Karolinska University Hospital, Sweden
Ramachandra Barik,
All India Institute of Medical Sciences, Bhubaneswar, India

*CORRESPONDENCE
Xueying Yang
yangxy7412@163.com

SPECIALTY SECTION
This article was submitted to Pulmonary Medicine, a section of the journal Frontiers in Medicine

RECEIVED 25 March 2022
ACCEPTED 30 June 2022
PUBLISHED 22 July 2022

CITATION
Wu Z, Xu B, Zhou D and Yang X (2022) Anomalous systemic arterial supply to the left lower lung lobe: A case report. *Front. Med.* 9:904431. doi: 10.3389/fmed.2022.904431

Anomalous systemic arterial supply to the left lower lung lobe: A case report

Zhuo Wu, Baoning Xu, Di Zhou and Xueying Yang*

Department of Thoracic Surgery, The Fourth Affiliated Hospital of China Medical University, Shenyang, China

Background: An anomalous systemic arterial supply to the lung lobes is a rare congenital pulmonary vascular malformation. Current treatments include thoracoscopic lobectomy, anatomical segmentectomy, simple ligation and arterial embolization. However, the optimal treatment remains controversial.

Case presentation: A 29-year-old man was diagnosed with anomalous systemic arterial supply to the left lower lobe through contrast-enhanced computed tomography and three-dimensional reconstruction. He underwent coil embolization of the anomalous artery and was followed up for 1 year.

Conclusions: Blockage of the blood flow of the anomalous systemic artery alone does not improve the blood supply of the pulmonary artery to lung tissue and thus cannot restore normal gas exchange through the blood-gas barrier. Coil embolization of the anomalous arterial supply can cause early postoperative pulmonary infarction.

KEYWORDS

anomalous systemic arterial supply, coil embolization, pulmonary infarction, case report, lung segment

Introduction

An anomalous systemic arterial supply to the lung lobes is a rare congenital pulmonary vascular malformation, with that occurring to the basal segments of the left lower lobe being most common. In 1946, Pryce defined this condition as intralobar pulmonary sequestration but later realized that this disorder was significantly different from pulmonary sequestration (1, 2). Although the affected pulmonary segment is supplied by anomalous arteries, there is no lung tissue sequestration, and bronchial tree development is normal. Current treatment methods include surgery and interventional embolization. However, which method is better remains a matter of debate, and complication prevention and treatment require further observation and study. We share our experience by reporting the case of a patient who underwent embolization treatment at our hospital and presenting the results of a literature review.

Case report

A 29-year-old man with intermittent hemoptysis (10 ml/episode) after physical activity sought treatment 1 year ago at our hospital. He became tired easily after regular

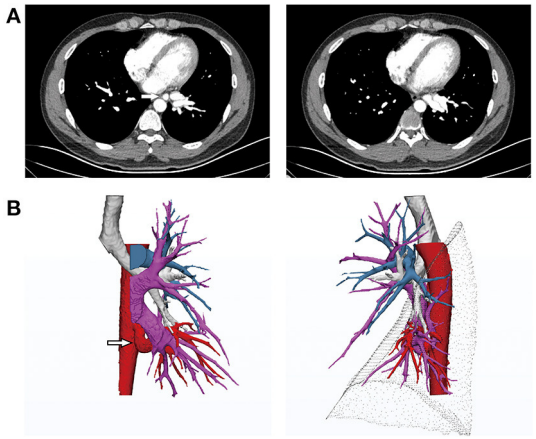

FIGURE 1
(A) Computed tomography angiography (CTA) before treatment revealing the anomalous systemic artery. **(B)** 3D reconstruction indicating normal development of the left bronchus. The anomalous systemic artery originated from the descending thoracic aorta and branched to the basal segments of the left lower lobe, parallel to the left inferior pulmonary vein. The pulmonary artery of the left lower lobe was absent from the basal segments and only present in the superior segment.

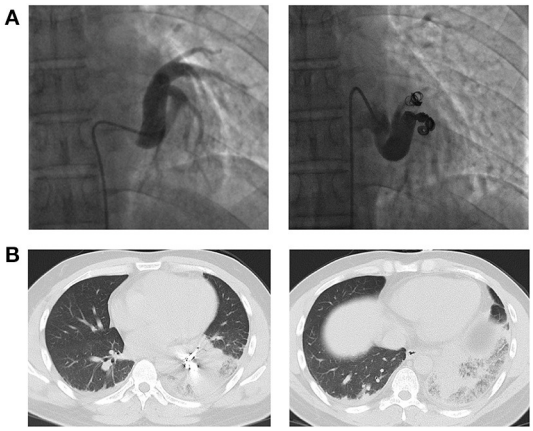

FIGURE 2
(A) Angiography and coil embolization for the anomalous systemic artery. **(B)** CT images showing pulmonary infarction at 48 h after the intervention.

physical activity. Computed tomography angiography (CTA) and three-dimensional computed tomography (3DCT) reconstruction showed a robust artery arising from the descending aorta, which was adjacent to the inferior pulmonary vein and approximately 2 cm in diameter. Branches of the artery intertwined with the inferior pulmonary vein in the basal segments. The superior segmental artery was present, whereas the basilar arterial trunk was absent. The structure of the bronchus in the left lower lobe was normal, and no lung tissue sequestration was noted (Figure 1). After consulting with the radiologist, it was determined that the superior segment was supplied by the pulmonary artery and that the basal segments were supplied by an abnormal systemic artery. The overall development of the patient was normal, and no obvious murmur was detected *via* auscultation of the heart and lungs. Ultrasonography revealed no abnormalities in the structure or function of the heart, and pulmonary function was normal.

After multidisciplinary treatment (MDT) by thoracic surgery, vascular surgery and interventional radiology, we decided to perform interventional therapy *via* coil embolization to preserve as much lung tissue as possible and protect pulmonary function and obtained the patient's consent. The procedure was uneventful (Figure 2A). However, after 24 h, the patient developed severe chest pain accompanied by labored breathing (a clinical manifestation of pulmonary infarction), and levels of serum fibrinogen and D-dimer were elevated. Forty-eight hours after the intervention, chest CT showed signs of infarction of the left lower lobe (Figure 2B). Serious symptoms of pulmonary infarction were observed at 72–96 h after the intervention and were accompanied by fever. Morphine was given for analgesia and sedation. His symptoms gradually resolved at 1 week after the intervention, and the patient was discharged at 2 weeks after the intervention.

At the 3-month follow-up, his hemoptysis had subsided completely, and his fatigue after physical activity had improved significantly. After 1 year of embolization, CTA and 3D reconstruction of the pulmonary arteries revealed that the anomalous systemic artery was completely blocked by the coils; the distal arterial branch was atrophic, and the accompanying inferior pulmonary venous branch showed no blood return. The inferior left pulmonary artery and the superior segmental vein remained unchanged (Figure 3). No coils were found to be coughed up during follow-up.

Discussion

Controversy exists regarding whether an anomalous systemic arterial supply to normal lungs is different from typical pulmonary sequestration. According to Pryce's classification, an anomalous systemic blood supply to the basal segments is considered a type of pulmonary sequestration (1). However, a normal bronchial tree is present in the abnormal lung tissue and there is no sequestration of the pulmonary parenchyma with an anomalous systemic arterial supply, unlike what occurs with pulmonary sequestration. Moreover, the pulmonary artery is absent from the lung segment in cases of anomalous arterial supply (2–4). As a result of the lack of consensus, several similar terms have been proposed, including "arterial pulmonary malinosculation" and "systemic arterialization of the lung

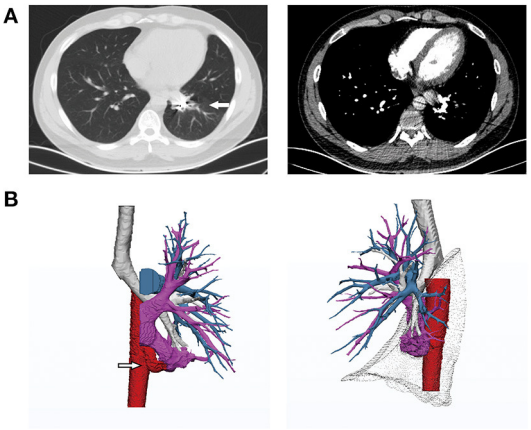

FIGURE 3
CT images at 1-year follow-up. **(A)** Lung CT showing significant alleviation of the interstitial changes in the left lower lobe. **(B)** 3D reconstruction showing blockage of the anomalous systemic artery and atrophy of the accompanying pulmonary vein in the basal segments but no change in the superior segment. The images of the pulmonary arteries were similar to those taken before the intervention. The pulmonary artery was absent from the basal segments.

without sequestration", but the most widely accepted term is "anomalous systemic arterial supply" (5, 6).

Although the cause of this disorder remains unclear, most researchers agree that it may be due to plexiform lesions of the primitive pulmonary arterial branches in the embryonic stage, which cause the primitive branches from the aorta to supply the lung buds instead of degenerating. Branches of the pulmonary artery from the lower lobe, i.e., the basal segments, are usually absent (7, 8). Different degrees of defects may lead to different degrees of variation.

Cough, expectoration and recurrent pneumonia are the most common symptoms of patients with pulmonary sequestration (9). Unlike with pulmonary sequestration, the main symptom of an anomalous systemic arterial supply to the basal segments of the left lower lobe is hemoptysis (10–12). This is because most of the anomalous systemic arteries originate from the descending aorta and are usually large in diameter, which can cause increased pressure in the pulmonary capillaries and pulmonary veins. Pulmonary capillaries and veins under excessive pressure are prone to rupture, causing intra-alveolar hemorrhage (13). Persistent pulmonary venous hypertension can lead to dilation of the left atrium, congestive heart failure, coughing, wheezing after physical activity, chest pain and even breathing difficulty, especially in people with a poor physical condition.

The current standard treatment for pulmonary sequestration is surgical resection. For symptomatic patients with extralobar or intralobar sequestration, surgical options include lobectomy, wedge resection, and anatomical segment resection (14, 15). There is controversy regarding treatment of an anomalous systemic arterial supply to the basal segments of the left lower lobe. Treatment has progressed from initial lobectomy by thoracotomy to thoracoscopic lobectomy, anatomical segment resection (16), and thoracoscopic anastomosis between anomalous systemic arteries and pulmonary arteries. However, due to the long-term high-pressure blood flow in the anomalous systemic arterial supply in adults, the blood vessel wall thickens and becomes less elastic, which results in poor blood perfusion after anastomosis. Some researchers suggest that vascular anastomosis is more suitable for children, who have been affected by this disorder for a shorter time period than adults (17, 18). Because anomalous systemic arteries provide blood to normal lung lobes with ventilation, surgeons began to attempt simple thoracoscopic ligation of anomalous systemic arteries or arterial embolization to preserve more lung tissue and reduce trauma (19–21).

The main symptom of the patient reported in this study was hemoptysis. Preoperative contrast-enhanced CT and 3D reconstruction of the pulmonary arteries showed that the patient's anomalous systemic artery originated from the descending thoracic aorta and supplied the basal segments of the left lower lobe. No obvious abnormalities in the bronchial tree were observed, though the pulmonary artery was absent from the basal segments. The pulmonary artery developed normally in the superior segment, and only one vein in the superior segment drained to the inferior pulmonary vein. Based on comprehensive analysis of the patient's medical history and imaging findings, we performed embolization of the anomalous systemic artery. The patient developed severe pulmonary infarction after the intervention; with rescue treatments, his condition gradually stabilized at 1 week. CTA and 3D reconstruction of the pulmonary arteries at 1 year after the intervention showed complete occlusion of the anomalous artery and atrophy of the accompanying inferior pulmonary vein in the basal segments. No compensatory growth of the pulmonary arteries was observed, and the basal segments of the left lower lobe were partially collapsed, with interstitial exudation.

The goal of treating hemoptysis through embolization was achieved in this patient. However, the pulmonary infarction that occurred during treatment increased his risk and caused the patient to develop scar tissue in response to the treatment, and the basal segments of the left lower lobe were left functionless. Through this case study, it can be concluded that blockage of the blood flow of an anomalous systemic artery alone does not improve the blood supply of the pulmonary artery to the lung tissue and thus cannot restore normal gas exchange through the blood-gas barrier. To confirm whether a reserved lung segment benefits patients, a study with a large sample size and long-term follow-up is needed. Overall, application of contrast-enhanced

CT and 3D reconstruction of the pulmonary arteries can aid in the diagnosis and treatment of this disorder.

Data availability statement

The original contributions presented in the study are included in the article/supplementary material, further inquiries can be directed to the corresponding author/s.

Ethics statement

The studies involving human participants were reviewed and approved by Ethics Committee of the Fourth Hospital of China Medical University (EC-2020-KS-043). The patients/participants provided their written informed consent to participate in this study. Written informed consent was obtained from the individual(s) for the publication of any potentially identifiable images or data included in this article.

Author contributions

ZW prepared the initial manuscript. XY edited and submitted the manuscript. ZW and XY drafted the article and gave final approval of the version to be published. BX and DZ were involved in the diagnosis and treatment of the patient. All authors have read and approved the final manuscript.

Funding

This work was supported by Scientific Research Projects of Education Department of Liaoning Province (#ZF2019024).

Acknowledgments

The authors would like to thank Dr. Xin Pan and Dr. Baoming Wang (Department of Interventional Radiology, The Fourth Affiliated Hospital of China Medical University, Shenyang, China) for advice and expertise.

Conflict of interest

The authors declare that the research was conducted in the absence of any commercial or financial relationships that could be construed as a potential conflict of interest.

Publisher's note

All claims expressed in this article are solely those of the authors and do not necessarily represent those of their affiliated organizations, or those of the publisher, the editors and the reviewers. Any product that may be evaluated in this article, or claim that may be made by its manufacturer, is not guaranteed or endorsed by the publisher.

References

1. Pryce DM, Sellors TH, Blair LG. Intralobar sequestration of lung associated with an abnormal pulmonary artery. *Br J Surg.* (1947) 35:18–29. doi: 10.1002/bjs.18003513704

2. Painter RL, Billig DM, Epstein I. Anomalous systemic arterialization of the lung without sequestration. *N Engl J Med.* (1968) 279:866–7. doi: 10.1056/NEJM196810172791606

3. Yamanaka A, Hirai T, Fujimoto T, Hase M, Noguchi M, Konishi F. Anomalous systemic arterial supply to normal basal segments of the left lower lobe. *Ann Thorac Surg.* (1999) 68:332–8. doi: 10.1016/S0003-4975(99)00533-0

4. Iizasa T, Haga Y, Hiroshima K, Fujisawa T. Systemic arterial supply to the left basal segment without the pulmonary artery: four consecutive cases. *Eur J Cardiothorac Surg.* (2003) 23:847–9. doi: 10.1016/S1010-7940(03)00087-3

5. Clements BS, Warner JO. Pulmonary sequestration and related congenital bronchopulmonary-vascular malformations: nomenclature and classification based on anatomical and embryological considerations. *Thorax.* (1987) 42:401–8. doi: 10.1136/thx.42.6.401

6. Hiramatsu M, Iwashita M, Inagaki T, Matsudaira H, Hirano J, Odaka M, et al. Anomalous systemic arterial supply to separate lingular and basal segments of the lung: an anatomic consideration. *Ann Thorac Surg.* (2009) 88:1358–60. doi: 10.1016/j.athoracsur.2008.11.065

7. deMello DE, Sawyer D, Galvin N, Reid LM. Early fetal development of lung vasculature. *Am J Respirat Cell Mol Biolo.* (1997) 16:568–81. doi: 10.1165/ajrcmb.16.5.9160839

8. Jefferson K, Rees S, Somerville J. Systemic arterial supply to the lungs in pulmonary atresia and its relation to pulmonary artery development. *Br Heart J.* (1972) 34:418–27. doi: 10.1136/hrt.34.4.418

9. Gezer S, Taştepe I, Sirmali M, Findik G, Türüt H, Kaya S, et al. Pulmonary sequestration: a single-institutional series composed of 27 cases. *J Thorac Cardiovasc Surg.* (2007) 133:955–9. doi: 10.1016/j.jtcvs.2006.11.003

10. Baek WK, Cho J, Kim JT, Yoon YH, Kim KH, Lim HK, et al. Systemic arterial supply to normal basal segments of the left lower lobe along with the pulmonary artery: is lung resection warranted? *J Thorac Cardiovasc Surg.* (2006) 131:742–3. doi: 10.1016/j.jtcvs.2005.10.053

11. Jiang S, Shi JY, Zhu XH, Chen C, Sun XW Yu D, et al. Endovascular embolization of the complete type of anomalous systemic arterial supply to normal basal lung segments: a report of four cases and literature review. *Chest.* (2011) 139:1506–13. doi: 10.1378/chest.10-1022

12. Abe T, Mori K, Shiigai M, Okura N, Okamoto Y, Saida T, et al. Systemic arterial supply to the normal basal segments of the left lower lobe of the lung–treatment by coil embolization–and a literature review. *Cardiovasc Intervent Radiol.* (2011) 34 Suppl 2:S117–21. doi: 10.1007/s00270-010-9798-x

13. Higuchi M, Chida M, Muto A, Fukuhara M, Suzuki H, Gotoh M. Anomalous systemic arterial supply to the basal segments of the lung. *Fukushima J Med Sci.* (2013) 59:93–6. doi: 10.5387/fms.59.93

14. Hertzenberg C, Daon E, Kramer J. Intralobar pulmonary sequestration in adults: three case reports. *J Thorac Dis.* (2012) 4:516–9. doi: 10.3978/j.issn.2072-1439.2012.06.07

15. Cooke CR. Bronchopulmonary sequestration. *Respir Care.* (2006) 51:661–4.

16. Miller JR, Lancaster TS, Abarbanell AM, Manning PB, Eghtesady P. anomalous systemic artery to the left lower lobe: literature review and a new surgical technique. *World J Pediatr Congenit Heart Surg.* (2018) 9:326–32. doi: 10.1177/2150135118755986

17. Cho S, Kim WH, Choi ES, Lee JR, Kim YJ. Surgical results of anomalous origin of one pulmonary artery branch from the ascending aorta. *Pediatr Cardiol.* (2015) 36:1532–8. doi: 10.1007/s00246-015-1197-2

18. Kim DW, Jeong IS, Kim JH, Kim YH, Cho HJ. Operation for an anomalous systemic arterial supply to the left lower lobe using an anastomosis procedure in an infant. *J Thorac Dis.* (2018) 10:E301–e3. doi: 10.21037/jtd.2018.04.05

19. Brühlmann W, Weishaupt D, Goebel N, Imhof E. Therapeutic embolization of a systemic arterialization of lung without sequestration. *Eur Radiol.* (1998) 8:355–8. doi: 10.1007/s003300050393

20. Sugihara F, Murata S, Uchiyama F, Watari J, Tanaka E, Muraishi N, et al. Transcatheter arterial embolization of anomalous systemic arterial supply to the basal segment of the lung. *Acta radiologica short reports.* (2013) 2:2047981613511363. doi: 10.1177/2047981613511363

21. Jiang S, Yu D, Jie B. Transarterial Embolization of Anomalous Systemic Arterial Supply to Normal Basal Segments of the Lung. *Cardiovasc Intervent Radiol.* (2016) 39:1256–65. doi: 10.1007/s00270-016-1361-y

frontiers | Frontiers in Medicine

TYPE Case Report
PUBLISHED 24 August 2022
DOI 10.3389/fmed.2022.936927

OPEN ACCESS

EDITED BY
John-David Aubert,
Centre Hospitalier Universitaire Vaudois (CHUV), Switzerland

REVIEWED BY
Wenjian Liao,
The First Affiliated Hospital of Nanchang University, China
Pin-Kuei Fu,
Taichung Veterans General Hospital, Taiwan

*CORRESPONDENCE
Pinhua Pan
pinhuapan668@csu.edu.cn

SPECIALTY SECTION
This article was submitted to Pulmonary Medicine, a section of the journal Frontiers in Medicine

RECEIVED 05 May 2022
ACCEPTED 29 July 2022
PUBLISHED 24 August 2022

CITATION
Peng W, Wu Y, Lu R, Zheng Y, Chen J and Pan P (2022) Successful treatment of acute respiratory distress syndrome caused by hypervirulent *Klebsiella pneumoniae* with extracorporeal membrane oxygenation and continuous renal replacement therapy: A case report and literature review. *Front. Med.* 9:936927. doi: 10.3389/fmed.2022.936927

Successful treatment of acute respiratory distress syndrome caused by hypervirulent *Klebsiella pneumoniae* with extracorporeal membrane oxygenation and continuous renal replacement therapy: A case report and literature review

Wenzhong Peng[1,2,3,4,5], Yanhao Wu[1,2,3,4,5], Rongli Lu[1,2,3,4,5], Yunpeng Zheng[1,2,3,4,5], Jie Chen[1,2,3,4,5] and Pinhua Pan[1,2,3,4,5]*

[1]Department of Respiratory Medicine, National Key Clinical Specialty, Branch of National Clinical Research Center for Respiratory Disease, Xiangya Hospital, Central South University, Changsha, China, [2]Center of Respiratory Medicine, Xiangya Hospital, Central South University, Changsha, China, [3]Clinical Research Center for Respiratory Diseases in Hunan Province, Xiangya Hospital, Central South University, Changsha, China, [4]Hunan Engineering Research Center for Intelligent Diagnosis and Treatment of Respiratory Disease, Xiangya Hospital, Central South University, Changsha, China, [5]National Clinical Research Center for Geriatric Disorders, Xiangya Hospital, Central South University, Changsha, China

Hypervirulent *Klebsiella pneumoniae* (hvKP) causes invasive infections and leads to high morbidity and mortality rates. Here, we report the case of a Chinese man with diabetes mellitus who developed acute respiratory distress syndrome and septic shock due to hvKP belonging to the K1 strain. The patient was treated with venovenous extracorporeal membrane oxygenation and continuous renal replacement therapy, in combination with antibiotics and recovered well. Clinicians should be aware of fatal infections caused by hvKP and investigate the best treatment options for patients at various stages of infection.

KEYWORDS

extracorporeal membrane oxygenation (ECMO), continuous renal replacement therapy (CRRT), hypervirulent *Klebsiella pneumoniae* (hvKP), acute respiratory distress syndrome (ARDS), septic shock

Background

The emergence of hypervirulent *Klebsiella pneumoniae* (hvKP) poses a significant challenge to public health (1). Additionally, hvKP can cause fatal systemic infections. In contrast to classical KP, hvKP displays hypervirulent phenotypic and genotypic characteristics, namely, a hypermucoviscous phenotype and the presence of different virulence genes (2).

Hypervirulent *K. pneumoniae* can cause community-acquired or nosocomial infections in both relatively healthy individuals (3) and those with underlying diseases such as diabetes mellitus (4). It may result in septic shock and multi-organ failure, which may be life-threatening.

Here, we report the case of a patient infected with hvKP belonging to serotype K1 and with virulence-associated genes *iutA* and *rmpA*. He developed septic shock, acute respiratory distress syndrome (ARDS), and acute renal failure within a short time, and was successfully treated with veno-venous extracorporeal membrane oxygenation (vv-ECMO) and continuous renal replacement therapy (CRRT) in combination with antibiotics.

Case presentation

The patient was a 52-year-old man who was admitted to the emergency room because of fever for 4 days and chest pain for 1 day. The patient had type 2 diabetes mellitus. He developed dyspnea with reduced oxygen saturation, and his blood pressure also declined the next morning; therefore, he was admitted to the respiratory intensive care unit (RICU). His temperature was 36.6°C, pulse rate 128 beats/min, respiratory rate 26 times/min, and blood pressure 113/62 mmHg (with a norepinephrine dose of 0.05 μg/kg/min). Coarse crackles were heard in both lungs. Endophthalmitis in the left eye was verified during ophthalmological consultation. Laboratory examinations revealed the following: white blood cell count, 1.7×10^9/L; neutrophil counts 1.6×10^9/L; lymphocyte counts, 0.1×10^9/L; platelets, 72×10^9/L; procalcitonin, 59.5 ng/ml; IL-6 > 1,000 pg/ml; TNF-α, 22.5 pg/ml; IL-1β, 9.31 pg/ml; IL-10, 37.9 pg/ml; and C-reactive protein, 470 mg/L. *K. pneumoniae* with a hypermucoviscous phenotype was isolated from the blood and bronchoalveolar lavage fluid (BALF) cultures. PCR and metagenomic next-generation sequencing (mNGS) of BALF identified a sequence type (ST) 23 serotype K1 strain with virulence-associated genes *iutA* (aerobactin) and *rmpA* (regulator of mucoid phenotype), the drug resistance gene *blaSH* was also positive. CT scan of the abdomen and brain revealed no abscess. Tracheal intubation and mechanical ventilation were performed promptly. Oliguria, a rapid decline in renal function (serum creatinine increase >100% within 48 h), and severe acidosis (pH 7.08–7.15) occurred; hence, CRRT was initiated on the 2nd day. Prone position and recruitment maneuver were attempted to improve oxygenation, but arterial blood gas analysis indicated continuous deterioration in the P/F ratio, pH, and hypercapnia.

On the 3rd day after admission, vv-ECMO was performed following the assessment of cardiac function by ultrasonography, and hypoxemia and hypercapnia were corrected promptly. The prone position, CRRT, and antibiotics (meropenem and levofloxacin based on antimicrobial susceptibility test findings) were continued for the next few days. The patient's condition gradually improved, and ECMO was withdrawn successfully on the 17th day. He underwent tracheostomy on the 21st day, was supported by a ventilator and high flow nasal cannula (HFNC) in turn, and subsequently moved to full HFNC support on the 29th day. He was transferred out of the RICU on the 41st day (Table 1; Figure 1). In the follow-up, his lung (Figure 1) and renal functions were gradually restored, and his serum creatinine level dropped to 143 μmol/L on 26 April 2022, but the vision of the left eye was lost.

Discussion

Here, we present the case of a diabetic patient infected with hvKP in the community. The patient developed ARDS and septic shock in a short time. After 41 days of intensive care and support, he survived with good recovery of the lung and kidney functions but lost vision in his left eye.

Hypervirulent *K. pneumoniae* was defined as the hypermucoviscosity phenotype (string test showing a positive result) (5). Other features associated with hvKP include K1 or K2 serotype, overexpression of *rmpA* (regulator of mucoid phenotype), and stealth siderophore biosynthesis (5). The hvKP strain in our case belonged to serotype K1 with virulence genes *iutA* and *rmpA*. K1 and K2 strains are the dominant strains causing community-onset infections (6). K1 is more prevalent in Asian countries whereas K2 is more prevalent in Europe (7, 8). The K1 strain is associated with a higher incidence of liver abscess (8). Numerous studies have identified virulence genes of hvKP over the past few decades (6, 9). Since not all hvKP have the hypermucoviscous phenotype, some studies have defined the hvKP based on the positivity of virulence genes, namely, the combination of *peg-344, iroB, iucA, rmpA*, and *rmpA2* (6, 9). *RmpA* is a gene that regulates the synthesis of extracellular polysaccharide capsules and is responsible for hypermucoviscosity and is found in 95.1–99.4% of hvKP (6, 10). *IutA* is a gene encoding the aerobactin system, which is crucial for growth and infection (11), and is present in 85.3–90.7% of hvKP (10, 12). Concurrence of *rmpA* and *iutA* may increase the risk of developing a severe form of infection (13). In our case, we confirmed the presence of virulence genes in BALF by NGS. In the conventional method, we should obtain a positive culture of the specimen, and PCR is needed for the identification of the serotype, sequence type, drug resistance genes, and virulence genes, which is time-consuming. NGS can be used to analyze capsular serotypes and identify virulence-associated genes and drug resistance genes simultaneously (14). Deoxyribonucleic acid extracted from clinical specimens can directly be processed for NGS analysis. Therefore, metagenomics is advantageous for the identification of the strain and virulence of the hvKP in contrast

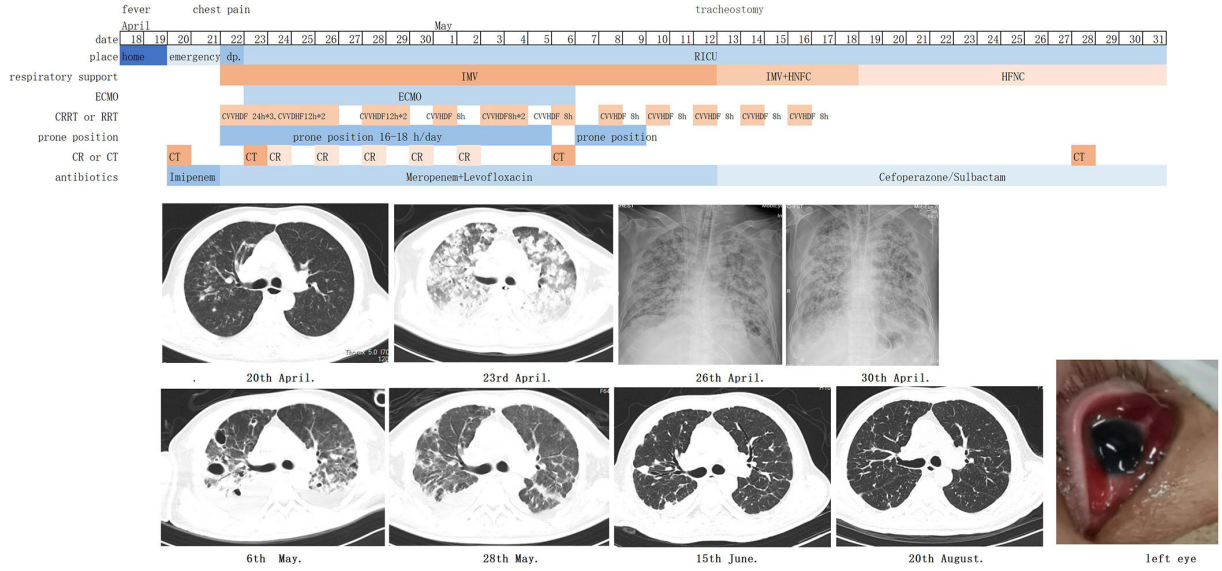

FIGURE 1
Timeline of courses and treatments. IMV, invasive mechanical ventilation; HFNC, high-flow nasal cannula oxygen therapy; ECMO, extracorporeal membrane oxygenation; CRRT, continuous renal replacement therapy; CVVHDF, continuous venovenous hemodiafiltration; CT, computerized tomography; CR, Chest radiography.

TABLE 1 ECMO, ventilator parameters, inflammatory markers, and renal function of the patient.

	D1	D2	D3	D4	D5	D6	D8	D10	D13	D17	D31
FiO_2	0.7	0.75	0.9	0.3	0.3	0.3	0.3	0.45	0.25	0.55	0.32
PEEP (mmH_2O)	12	12	12	15	15	12	10	10	10	10	HFNC
Plat pressure (mmH_2O)	15	15	–	14	–	15	–	12	–	14	–
CL	26.6	–	–	15.5	–	16.1	–	27.8	–	32.5	–
Vt (ml)	399	–	–	217	–	242	–	334	–	453	–
PaO_2 (mmHg)	63	63	61	91	89	120	86	85	82	97	123
$PaCO_2$ (mmHg)	73	55	74	45	44	40	32	43	36	45	42
pH	7.09	7.15	7.36	7.49	7.45	7.42	7.39	7.41	7.43	7.35	7.48
P/F ratio	90	84	67		–	–	–	–	–	176	384
ECMO flux (L/min)	–	–	–	4.55	4.52	4.29	4.35	4.54	4.44	–	–
ECMO FiO_2	–	–	–	1	1	1	1	1	1	–	–
NE dosage (μg/kg/min)	0.08	0.1	0.1	0.15	0.1	0.05	0.01	0	0	0	0
WBC ($*10^9$)	1.7	2.0	14.8	15.8	16.4	13.9	15.4	14.2	6.4	7.6	12.5
Platelet ($*10^9$)	72	41	20	24	44	42	23	17	84	141	212
N ($*10^9$)	1.6	1.8	14.3	15.1	15.1	13.3	14.8	13.6	5.5	6.8	10.6
L ($*10^9$)	0.1	0.2	0.3	0.4	0.7	0.4	0.4	0.4	0.4	0.4	0.8
PCT (ng/ml)	21.93	59.5	56.05	48.63	37.87	27.87	25.17	14.26	9.26	3.01	1.72
CRP (mg/L)	–		470	371	204	126	193	191	87.6	88.7	64.5
IL-6 (pg/ml)	–	–	>1000	–	–	–	275	–	–	–	–
TNF-alpha (pg/ml)	–	–	22.5	–	–	–	20.2	–	–	–	–
IL-10 (pg/ml)	–	–	37.9	–	–	–	16.9	–	–	–	–
IL-1β (pg/ml)	–	–	9.31	–	–	–	9.85	–	–	–	–
Cr (μmol/L)	126.3	204.8	150.3	242	294	273	164	194.1	348	307	351

FiO_2, fraction of inspiration O_2; PEEP, positive end-expiratory pressure; CL, Compliance of Lung; Vt, tidal volume; NE, Norepinephrine; WBC, white blood cell count; N, neutrophil; L, lymphocyte; PCT, procalcitonin; CRP, C-reactive protein; IL, interleukin; TNF-alpha, tumor necrosis factor.

TABLE 2 The case reports and studies of hvKP infections.

References	Publication year	hvKP (n)	Community acquired	Carbapenem-resistant (n)	Age	ARDS/Severe pneumonia	Septic shock	Bacteremia	Intracranial infection	Liver abscess	Mortality
Piazza et al. (16)	2022	1	1	0	75	0	0	0	1	0	0
Konagaya et al. (17)	2022	1	1	0	69	1	0	1	1	1	0
Kong et al. (18)	2022	1	1	0	24	1	1	1	0	1	0
Liu et al. (19)	2022	1	1	0	>60	0	0	1	0	1	0
Salawati et al. (20)	2021	1	1	0	58	1	1	1	0	1	1
Lin et al. (21)	2021	1	0	0	29	1	0	1	0	1	0
Kim et al. (22)	2021	1	1	0	50	0	0	1	0	1	0
Xie et al. (23)	2021	1	1	0	56	1	0	1	0	1	0
Kamau et al. (24)	2021	1	1	0	30	0	0	0	1	0	0
Marinakis et al. (25)	2021	3	3	0	51	–	–	2	3	2	3
Oh et al. (26)	2021	1	1	0	57	–	1	1	1	1	1
McHardy et al. (27)	2021	1	1	0	53	0	1	1	0	0	0
Lee et al. (28)	2021	1	1	0	63	0	0	1	0	0	0
Nakamura et al. (29)	2021	2	2	0	45, 29	0	0	2	1	1	0
JIn et al. (30)	2021	1	1	1	68	0	0	1	0	0	0
Macleod et al. (31)	2021	1	1	0	60	1	1	1	1	1	1
Horuguchi et al. (32)	2021	1	1	0	67	0	0	1	1	1	0
Hassanin et al. (33)	2021	1	1	0	55	0	0	1	0	0	0
Troché et al. (34)	2021	1	1	0	54	0	0	1	0	0	0
Chen et al. (35)	2021	1	1	0	57	1	1	1	0	0	0
Zhao et al. (36)	2021	1	0	1	68	1	1	–	–	–	1
Lan et al. (11)	2021	1	1	0	77	–	–	1	–	–	0
Khan et al. (37)	2021	1	1	0	23	0	0	1	0	0	0
Zhao et al. (38)	2021	1	1	0	80	0	0	1	0	1	0
Hosoda et al. (39)	2021	1	1	0	87	1	0	0	0	0	1
Kubota et al. (40)	2021	1	1	0	58	1	1	1	0	1	0
Himeno et al. (41)	2022	4	4	0	53 (46–72)	0	1	4	0	0	0
Anantharajah et al. (8)	2022	22	22	0	61	1	–	10	1	9	6 (27.3%)
Wei et al. (1)	2022	51	0	51	≥65	–	–	–	–	4	21 (41.2%)
Chen et al. (42)	2022	114	86	–	63 (55–73)	–	19	–	–	–	16 (14%)
Lei et al. (43)	2022	7	0	7	>60	–	–	–	–	–	5 (71.4%)
Falcone et al. (44)	2022	29	0	0	73 (65–77)	–	8	15	0	0	14 (48.3%)
Rollin et al. (45)	2021	10	10	0	58 (46–64)	–	5	–	10	–	7 (70%)
Zhou et al. (46)	2021	16	0	16	83±10	–	–	–	–	–	9 (56.2%)
Li et al. (47)	2021	9	0	9	50±13	–	–	–	–	9	5 (55.6%)
Kong et al. (48)	2021	6	0	6	29–81	–	–	–	–	–	3 (50%)

"–" means no information in the reports.

10.3389/fmed.2022.936927

to traditional cultivation (15). The use of NGS may help in the early and accurate identification of hvKP, ultimately improving patients' outcomes.

Hypervirulent *K. pneumoniae* has spread across Asian countries such as China, Japan, and South Korea, with sporadic but increasing rates reported elsewhere. We have summarized the reports on the hvKP from 1 January 2021 to 30 April 2022 in Table 2. The hvKP can cause severe community or hospital-acquired infections (49, 50). The risk factors include renal insufficiency (42, 51), diabetes (52), age ≥ 65 years (1), and chronic alcoholism (53). HvKP causes tissue invasive infection, often involving multiple sites. Septic shock and multi-organ failure are more common in patients infected with hvKP than in those infected by classical *K. pneumoniae* (cKP). The mortality rate of hvKP infection is higher in the elderly and those who are infected with carbapenem-resistant strains, but it appears to be similar in the general population between carbapenem-sensitive hvKP and cKP groups (12). In our study, the patient had type 2 diabetes without taking any hypoglycemics. He developed disseminated infections in the lungs and left eye. The patient progressed to septic shock and multi-organ failure. He also manifested a surge in inflammatory markers and prolonged thrombocytopenia.

Veno-venous extracorporeal membrane oxygenation is increasingly used in patients with severe ARDS to correct life-threatening hypoxemia and serves as a bridge for recovery. However, vv-ECMO may not always be appropriate in patients with ARDS and septic shock. In the Piotr Suwalski study (54), 7.1% of patients on vv-ECMO due to ARDS caused by COVID-19 were converted to venoarterial (va)-ECMO when septic shock developed. Han (55) reported 23 patients with refractory septic shock treated with va-ECMO, and five patients survived. Falk et al. (56) showed that patients with septic shock with or without left ventricular failure benefited from va-ECMO more than vv-ECMO, but in their study, 6 of the 10 patients with vv-ECMO survived, possibly because vv-ECMO could improve heart function by increasing cardiac oxygenation. In our case, the patient experienced ARDS and septic shock due to hvKP. His heart function was assessed using echocardiography, and the results showed no left or right ventricular dysfunction. His norepinephrine dose was <0.2 μg/kg/min. Therefore, we decided to establish vv-ECMO, and the patient improved and avoided transitioning to V-A or hybrid ECMO. Patients with refractory septic shock (high dose of vasopressin, and inability to sustain mean arterial pressure ≥65 mmHg) should be treated with va-ECMO; however, for those with a low dose of vasopressin and no heart dysfunction, vv-ECMO may also be adequate to improve the patients' outcome.

Approximately 41.4–64.4% of critically ill patients with severe sepsis or septic shock develop acute kidney injury (57, 58). Renal replacement therapy (RRT) is widely used for these patients. However, the optimal RRT modality remains controversial. A recent meta-analysis showed no significant difference in patients and kidney survival among patients receiving CRRT, sustained low-efficiency dialysis, or intermittent hemodialysis (59). Studies on early vs. late initiation of RRT revealed no benefit for patients who start early RRT (60, 61). However, for patients with complications such as obvious fluid overload, acute pulmonary edema, severe acidosis, and severe hyperkalemia, RRT may be performed urgently. Regarding CRRT, investigators had to provide treatment continuously for 24 h with a change of membranes at least every 72 h, and a minimum ultrafiltration (or dialysate) rate of 25 ml/kg/h was recommended (61, 62). For intermittent hemodialysis, the length of the session had to be 4–6 h or more, and the frequency had to be at least once every 48 h. Recommendations were to set a blood flow rate of 150–250 ml/min, and a dialysate flow rate of 300–500 ml/min (61, 62). Across the studies, RRT dependence among survivors was about 5.9–23.1% in 28 days, lowering to 2–13.4% in 90 days (61–63). In our case, the patient developed oliguria, pulmonary edema, and severe acidosis on the 1st day after admission to the RICU. The average fluid intake of the patient was >2,500 ml/day in the first week, and early initiation of CRRT could control the fluid disturbances and prevent the deterioration of lung oxygenation and heart function. We treated the patient with continuous techniques in the first 72 h and changed to intermittent hemodialysis for 8–12 h each time on the next days (Figure 1). The patient's kidney functions gradually recovered and RRT was discontinued on the 25th day. Like COVID-19 infection, inflammatory mediators play an important role in sepsis and septic shock, exacerbating organ damage and correlating with disease severity (64). Many clinical strategies have been attempted to reduce inflammatory damage. CRRT with a specific filter may successfully lower the levels of cytokines such as TNF-α, IL-6, IL-8, and IFNγ (65). In our case, hvKP led to a severe cytokine storm with IL-6 > 1,000 pg/ml, and an extended duration of continuous venovenous hemodiafiltration seemed to remove the inflammatory mediators and restore the homeostasis of the patient. Whether the combination of CRRT and ECMO can improve the outcome of patients with septic shock and ARDS, and when and which modality should be initiated requires further study.

Conclusion

This is a successful case of treating severe infection and multi-organ failure caused by hvKP, demonstrating that vv-ECMO and CRRT may improve the outcomes in this group of patients.

Data availability statement

The raw data supporting the conclusions of this article will be made available by the authors, without undue reservation.

Ethics statement

The studies involving human participants were reviewed and approved by Institutional Review Boards (IRBs) in Xiangya Hospital, Central South University. The patients/participants provided their written informed consent to participate in this study. Written informed consent was obtained from the individual(s) for the publication of any potentially identifiable images or data included in this article.

Author contributions

WP and YW reviewed the lectures and wrote the manuscript. RL and YZ collected and arranged the materials. JC and PP viewed the complete manuscript. All authors contributed to the article and approved the submitted version.

Funding

This study was supported by National Key R&D Program of China (No. 2016YFC1304204); Key Program of Hunan Province (No. 2022SK2038); the Project Program of National Clinical Research Center for Geriatric Disorders (Xiangya Hospital, Grant No. 2020LNJJ05).

Conflict of interest

The authors declare that the research was conducted in the absence of any commercial or financial relationships that could be construed as a potential conflict of interest.

Publisher's note

All claims expressed in this article are solely those of the authors and do not necessarily represent those of their affiliated organizations, or those of the publisher, the editors and the reviewers. Any product that may be evaluated in this article, or claim that may be made by its manufacturer, is not guaranteed or endorsed by the publisher.

References

1. Wei T, Zou C, Qin J, Tao J, Yan L, Wang J, et al. Emergence of hypervirulent ST11-K64 *Klebsiella pneumoniae* poses a serious clinical threat in older patients. *Front Public Health.* (2022) 10:765624. doi: 10.3389/fpubh.2022.765624

2. Arabaghian H, Salloum T, Alousi S, Panossian B, Araj GF, Tokajian S. Molecular characterization of carbapenem resistant *Klebsiella pneumoniae* and *Klebsiella quasipneumoniae* isolated from Lebanon. *Sci Rep.* (2019) 9:531. doi: 10.1038/s41598-018-36554-2

3. Shankar C, Veeraraghavan B, Nabarro LEB, Ravi R, Ragupathi NKD, Rupali P. Whole genome analysis of hypervirulent *Klebsiella pneumoniae* isolates from community and hospital acquired bloodstream infection. *BMC Microbiol.* (2018) 18:6. doi: 10.1186/s12866-017-1148-6

4. Li J, Ren J, Wang W, Wang G, Gu G, Wu X, et al. Risk factors and clinical outcomes of hypervirulent *Klebsiella pneumoniae* induced bloodstream infections. *Eur J Clin Microbiol Infect Dis.* (2018) 37:679–89. doi: 10.1007/s10096-017-3160-z

5. Mike LA, Stark AJ, Forsyth VS, Vornhagen J, Smith SN, Bachman MA, et al. A systematic analysis of hypermucoviscosity and capsule reveals distinct and overlapping genes that impact *Klebsiella pneumoniae* fitness. *PLoS Pathog.* (2021) 17:e1009376. doi: 10.1371/journal.ppat.1009376

6. Liao CH, Huang YT, Hsueh PR. Multicenter surveillance of capsular serotypes, virulence genes, and antimicrobial susceptibilities of *Klebsiella pneumoniae* causing bacteremia in Taiwan, 2017-2019. *Front Microbiol.* (2022) 13:783523. doi: 10.3389/fmicb.2022.783523

7. Talebzadeh H, Mellali H, Solgi H. Association of fluoroquinolone resistance and ESBL production in hypervirulent *Klebsiella pneumoniae* ST11 and ST893 in Iran. *Acta Microbiol Immunol Hung.* (2022). doi: 10.1556/030.2022.01638

8. Anantharajah A, Deltombe M, de Barsy M, Evrard S, Denis O, Bogaerts P, et al. Characterization of hypervirulent *Klebsiella pneumoniae* isolates in Belgium. *Eur J Clin Microbiol Infect Dis.* (2022). doi: 10.1007/s10096-022-04438-z

9. Bulger J, MacDonald U, Olson R, Beanan J, Russo TA. Metabolite transporter PEG344 is required for full virulence of hypervirulent *Klebsiella pneumoniae* strain hvKP1 after pulmonary but not subcutaneous challenge. *Infect Immun.* (2017) 85:e00093-17. doi: 10.1128/IAI.00093-17

10. Zhang S, Zhang X, Wu Q, Zheng X, Dong G, Fang R, et al. Clinical, microbiological, and molecular epidemiological characteristics of *Klebsiella pneumoniae*-induced pyogenic liver abscess in southeastern China. *Antimicrob Resist Infect Control.* (2019) 8:166. doi: 10.1186/s13756-019-0615-2

11. Lan P, Zhao D, Gu J, Shi Q, Yan R, Jiang Y, et al. Genome-based analysis of a sequence type 1049 hypervirulent *Klebsiella pneumoniae* causing bacteremic neck abscess. *Front Microbiol.* (2020) 11:617651. doi: 10.3389/fmicb.2020.617651

12. Li L, Yuan Z, Chen D, Xie X, Zhang B. Clinical and microbiological characteristics of invasive and hypervirulent *Klebsiella pneumoniae* infections in a teaching hospital in China. *Infect Drug Resist.* (2020) 13:4395–403. doi: 10.2147/IDR.S282982

13. Khaertynov KS, Anokhin VA, Davidyuk YN, Nicolaeva IV, Khalioullina SV, Semyenova DR, et al. Case of meningitis in a neonate caused by an extended-spectrum-beta-lactamase-producing strain of hypervirulent *Klebsiella pneumoniae*. *Front Microbiol.* (2017) 8:1576. doi: 10.3389/fmicb.2017.01576

14. Yang P, Wu Z, Liu C, Zheng J, Wu N, Wu Z, et al. Clinical outcomes and microbiological characteristics of sequence type 11 *Klebsiella pneumoniae* infection. *Front Med (Lausanne).* (2022) 9:889020. doi: 10.3389/fmed.2022.889020

15. Liu J, Xu Z, Li H, Chen F, Han K, Hu X, et al. Metagenomic approaches reveal strain profiling and genotyping of *Klebsiella pneumoniae* from hospitalized patients in China. *Microbiol Spectr.* (2022) 2022:e0219021. doi: 10.1128/spectrum.02190-21

16. Piazza A, Perini M, Mauri C, Comandatore F, Meroni E, Luzzaro F, et al. Antimicrobial susceptibility, virulence, and genomic features of a hypervirulent serotype K2, ST65 *Klebsiella pneumoniae* causing meningitis in Italy. *Antibiotics.* (2022) 11:261. doi: 10.3390/antibiotics11020261

17. Konagaya K, Yamamoto H, Suda T, Tsuda Y, Isogai J, Murayama H, et al. Ruptured emphysematous prostatic abscess caused by K1-ST23 hypervirulent

Klebsiella pneumoniae presenting as brain abscesses: a case report and literature review. *Front Med (Lausanne).* (2021) 8:768042. doi: 10.3389/fmed.2021.768042

18. Kong L, Wang Y, Ji H, Li Z, Sun Y, Liu Y, et al. A case of forearm soft tissue infection caused by hypervirulent *K. pneumoniae in an* otherwise healthy 24-year-old woman. *Infect Drug Resist.* (2022) 15:63–8. doi: 10.2147/IDR.S342019

19. Liu Y, Zhu H, Yin Y, Yan Z. Left eye enucleation caused by multi-systemic *Klebsiella pneumoniae* invasive syndrome. *J Int Med Res.* (2022) 50:3000605211069284. doi: 10.1177/03000605211069284

20. Salawati EM. Fatal disseminated pyogenic infection due to hypermucoviscous hypervirulent Klebsiella pneumoniae: a case report and literature review. *Clin Case Rep.* (2021) 9:e04754. doi: 10.1002/ccr3.4754

21. Lin YC, Cao X, Mo YC, Xie CP, Zhang YF Li N, et al. Successful treatment of hypervirulent *Klebsiella pneumoniae* bacteremia with combination carbapenem and rifampicin. *IDCases.* (2021) 26:e01276. doi: 10.1016/j.idcr.2021.e01276

22. Kim M, Yoo JR, Oh H, Kim YR, Lee KH, Heo ST. The first case of abdominal mycotic aneurysm caused by K1 hypervirulent *Klebsiella pneumoniae* in a healthy adult. *Acute Crit Care.* (2021) 36:390–4. doi: 10.4266/acc.2021.00010

23. Xie J, Zhu Z, A. case report of pyogenic liver abscess caused by hypervirulent *Klebsiella pneumoniae* diagnosed by metagenomic next-generation sequencing. *J Int Med Res.* (2021) 49:3000605211032793. doi: 10.1177/030006052110 32793

24. Kamau E, Allyn PR, Beaird OE, Ward KW, Kwan N, Garner OB, et al. Endogenous endophthalmitis caused by ST66-K2 hypervirulent *Klebsiella pneumoniae*, United States. *Emerg Infect Dis.* (2021) 27:2215–8. doi: 10.3201/eid2708.210234

25. Marinakis G, Kassianidis G, Kafkoula E, Stamatopoulou C, Kavallieratos F, Patrani M, et al. Community-acquired *Klebsiella* spp meningitis/invasive infection in filipino-descent patients living in Greece: a case series. *Eur J Case Rep Intern Med.* (2021) 8:002576. doi: 10.12890/2021_002576

26. Oh H, Heo ST, Kim M, Kang CH, Yoo JR. Devastating community-acquired bacterial meningitis caused by hypervirulent *Klebsiella pneumoniae* in an immunocompetent patient. *J Clin Neurol.* (2021) 17:484–6. doi: 10.3988/jcn.2021.17.3.484

27. McHardy JA, Selvaganeshapillai V, Khanna P, Whittington AM, Turton J, Gopal Rao G, et al. case of neck abscess caused by rare hypervirulent *Klebsiella pneumoniae*, capsular type K20 and sequence type 420. *Ann Clin Microbiol Antimicrob.* (2021) 20:46. doi: 10.1186/s12941-021-00453-8

28. Lee SE, Mushtaq A, Gitman M, Paniz-Mondolfi A, Chung M, Obla A, et al. Lemierre's syndrome associated with hypervirulent *Klebsiella pneumoniae*: a case report and genomic characterization of the isolate. *IDCases.* (2021) 25:e01173. doi: 10.1016/j.idcr.2021.e01173

29. Nakamura K, Nomoto H, Harada S, Suzuki M, Yomono K, Yokochi R, et al. Infection with capsular genotype K1-ST23 hypervirulent *Klebsiella pneumoniae* isolates in Japan after a stay in East Asia: two cases and a literature review. *J Infect Chemother.* (2021) 27:1508–12. doi: 10.1016/j.jiac.2021.05.011

30. Jin X, Chen Q, Shen F, Jiang Y, Wu X, Hua X, et al. Resistance evolution of hypervirulent carbapenem-resistant *Klebsiella pneumoniae* ST11 during treatment with tigecycline and polymyxin. *Emerg Microbes Infect.* (2021) 10:1129–36. doi: 10.1080/22221751.2021.1937327

31. Macleod CK, Khokhar FA, Warne B, Wick R, Butcher R, Cassimon B, et al. Rapid whole genome sequencing of serotype K1 hypervirulent *Klebsiella pneumoniae* from an undocumented Chinese Migrant. *Case Rep Infect Dis.* (2021) 2021:6638780. doi: 10.1155/2021/6638780

32. Horiguchi K, Tsurutani Y, Sasaki T, Sunouchi T, Hirose R, Watanabe S, et al. Hypervirulent *Klebsiella pneumoniae* infection in an elderly patient with diabetes mellitus. *Geriatr Gerontol Int.* (2021) 21:590–1. doi: 10.1111/ggi.14179

33. Hassanin F, Khawjah D, Elkhamary S, Al Hussain H. Renal abscesses and endogenous endophthalmitis due to hypermucoviscous hypervirulent *Klebsiella pneumoniae* (HVKP). *IDCases.* (2021) 24:e01130. doi: 10.1016/j.idcr.2021.e01130

34. Troché G, Henry A, Sarfati F, Hickel C, Amara M, Bruneel F, et al. 54-year-old healthy patient with meningitis and conjunctivitis. *J Am Coll Emerg Phys Open.* (2021) 2:e12425. doi: 10.1002/emp2.12425

35. Chen Y, Chen J, Zheng N, Chen Y. Contrast-enhanced ultrasound (CEUS) guided drainage in the treatment of a patient with lung abscess secondary to hypervirulent *Klebsiella pneumoniae* (hvKP) infection: a case report. *Respir Med Case Rep.* (2021) 32:101343. doi: 10.1016/j.rmcr.2021.101343

36. Zhao J, Zhang Y, Fan Y, Han J, Xiong Z, Liu X, et al. Characterization of an NDM-5-producing hypervirulent *Klebsiella pneumoniae* sequence type 65 clone from a lung transplant recipient. *Emerg Microbes Infect.* (2021) 10:396–9. doi: 10.1080/22221751.2021.1889932

37. Khan SF, Lacey JA, Gorrie C, Tong SYC. Genomic sequencing of hypervirulent *Klebsiella pneumoniae* with novel patterns of virulence and global epidemiological linkage. *Pathology.* (2021) 53:682–5. doi: 10.1016/j.pathol.2020.10.011

38. Zhao B, Hu R, Gong L, Wang X, Zhu Y, Wu G. Pyogenic liver abscess and endogenous endophthalmitis due to K64-ST1764 hypervirulent *Klebsiella pneumoniae:* a case report. *Infect Drug Resist.* (2021) 14:71–7. doi: 10.2147/IDR.S289088

39. Hosoda T, Harada S, Okamoto K, Ishino S, Kaneko M, Suzuki M, et al. COVID-19 and fatal sepsis caused by hypervirulent *Klebsiella pneumoniae,* Japan, 2020. *Emerg Infect Dis.* (2021) 27:556–9. doi: 10.3201/eid2702.204662

40. Kubota Y, Ishioka H, Harada S, Suzuki M, Shiotsuka J, Lefor AK, et al. Septic shock with emphysematous cholecystitis and disseminated infection caused by hypervirulent *Klebsiella pneumoniae* capsular genotype K2-ST65 in a Japanese man with diabetes mellitus: a case report. *J Infect Chemother.* (2021) 27:350–3. doi: 10.1016/j.jiac.2020.09.017

41. Himeno D, Matsuura Y, Maruo A, Ohtori S, A. novel treatment strategy using continuous local antibiotic perfusion: a case series study of a refractory infection caused by hypervirulent *Klebsiella pneumoniae*. *J Orthop Sci.* (2022) 27:272–80. doi: 10.1016/j.jos.2020.11.010

42. Chen D, Zhang Y, Wu J, Li J, Chen H, Zhang X, et al. Analysis of hypervirulent *Klebsiella pneumoniae* and classic *Klebsiella pneumoniae* infections in a Chinese hospital. *J Appl Microbiol.* (2022) 132:3883–90. doi: 10.1111/jam.15476

43. Lei J, Zhou WX, Lei K, Chen D, Zhang PQ, Xue L, et al. Analysis of molecular and clinical characteristics of carbapenem-resistant hypervirulent *Klebsiella pneumoniae* in the intensive care unit. *Zhonghua Yu Fang Yi Xue Za Zhi.* (2022) 56:63–8. doi: 10.3760/cma.j.cn112150-20210812-00781

44. Falcone M, Tiseo G, Arcari G, Leonildi A, Giordano C, Tempini S, et al. Spread of hypervirulent multidrug-resistant ST147 *Klebsiella pneumoniae* in patients with severe COVID-19: an observational study from Italy, 2020-21. *J Antimicrob Chemother.* (2022) 77:1140–5. doi: 10.1093/jac/dkab495

45. Rollin G, Rossi B, Brisse S, Decré D, Leflon-Guibout V, Bert F, et al. Spontaneous and postsurgical/traumatic *Klebsiella pneumoniae* meningitis: two distinct clinico-microbiological entities. *Int J Infect Dis.* (2021) 114:185–91. doi: 10.1016/j.ijid.2021.11.013

46. Zhou C, Wu Q, He L, Zhang H, Xu M, Yuan B, et al. Clinical and molecular characteristics of carbapenem-resistant hypervirulent *Klebsiella pneumoniae* isolates in a tertiary hospital in Shanghai, China. *Infect Drug Resist.* (2021) 14:2697–706. doi: 10.2147/IDR.S321704

47. Li Y, Hu D, Ma X, Li D, Tian D, Gong Y, et al. Convergence of carbapenem resistance and hypervirulence leads to high mortality in patients with postoperative *Klebsiella pneumoniae* meningitis. *J Glob Antimicrob Resist.* (2021) 27:95–100. doi: 10.1016/j.jgar.2021.02.035

48. Kong ZX, Karunakaran R, Abdul Jabar K, Ponnampalavanar S, Chong CW, Teh CSJ. The detection of hypermucoviscous carbapenem-resistant *Klebsiella pneumoniae* from a tertiary teaching hospital in Malaysia and assessment of Hypermucoviscous as marker of hypervirulence. *Microb Drug Resist.* (2021) 27:1319–27. doi: 10.1089/mdr.2020.0096

49. Wu H, Li D, Zhou H, Sun Y, Guo L, Shen D. Bacteremia and other body site infection caused by hypervirulent and classic *Klebsiella pneumoniae*. *Microb Pathog.* (2017) 104:254–62. doi: 10.1016/j.micpath.2017.01.049

50. Wang X, Xie Y, Li G, Liu J, Li X, Tian L, et al. Whole-genome-sequencing characterization of bloodstream infection-causing hypervirulent *Klebsiella pneumoniae* of capsular serotype K2 and ST374. *Virulence.* (2018) 9:510–21. doi: 10.1080/21505594.2017.1421894

51. Zhou S, Ren G, Liu Y, Liu X, Zhang L, Xu S, et al. Challenge of evolving *Klebsiella pneumoniae* infection in patients on hemodialysis: from the classic strain to the carbapenem-resistant hypervirulent one. *Int J Med Sci.* (2022) 19:416–24. doi: 10.7150/ijms.69577

52. Ding Z, Li Z, Tang M, Zeng Z, Song M, Yang K, et al. The molecular characteristics, clinical manifestations, and risk factors of hypervirulent *Klebsiella pneumoniae* infections in a large teaching hospital in southwest China. *Microb Pathog.* (2022) 162:105152. doi: 10.1016/j.micpath.2021.105152

53. Melot B, Brisse S, Breurec S, Passet V, Malpote E, Lamaury I, et al. Community-acquired meningitis caused by a CG86 hypervirulent *Klebsiella pneumoniae* strain: first case report in the Caribbean. *BMC Infect Dis.* (2016) 16:736. doi: 10.1186/s12879-016-2065-2

54. Suwalski P, Staromłyński J, Braczkowski J, Bartczak M, Mariani S, Drobiński D, et al. Transition from simple V-V to V-A and hybrid ECMO configurations in COVID-19 ARDS. *Membranes (Basel).* (2021) 11:e0434. doi: 10.3390/membranes11060434

55. Han L, Zhang Y, Zhang Y, Wu W, He P. Risk factors for refractory septic shock treated with VA ECMO. *Ann Transl Med.* (2019) 7:476. doi: 10.21037/atm.2019.08.07

56. Falk L, Hultman J, Broman LM. Extracorporeal membrane oxygenation for septic shock. *Crit Care Med.* (2019) 47:1097–105. doi: 10.1097/CCM.0000000000003819

57. Oppert M, Engel C, Brunkhorst FM, Bogatsch H, Reinhart K, Frei U, et al. Acute renal failure in patients with severe sepsis and septic shock—a significant independent risk factor for mortality: results from the German Prevalence Study. *Nephrol Dial Transplant.* (2008) 23:904–9. doi: 10.1093/ndt/gfm610

58. Bagshaw SM, Lapinsky S, Dial S, Arabi Y, Dodek P, Wood G, et al. Acute kidney injury in septic shock: clinical outcomes and impact of duration of hypotension prior to initiation of antimicrobial therapy. *Intensive Care Med.* (2009) 35:871–81. doi: 10.1007/s00134-008-1367-2

59. Nash DM, Przech S, Wald R, O'Reilly D. Systematic review and meta-analysis of renal replacement therapy modalities for acute kidney injury in the intensive care unit. *J Crit Care.* (2017) 41:138–44. doi: 10.1016/j.jcrc.2017.05.002

60. Bagshaw SM, Wald R, Adhikari NKJ, Bellomo R, da Costa BR, Dreyfuss D, et al. Timing of initiation of renal-replacement therapy in acute kidney injury. *N Engl J Med.* (2020) 383:240–51. doi: 10.1056/NEJMoa2000741

61. Barbar SD, Clere-Jehl R, Bourredjem A, Hernu R, Montini F, Bruyère R, et al. Timing of renal-replacement therapy in patients with acute kidney injury and sepsis. *N Engl J Med.* (2018) 379:1431–42. doi: 10.1056/NEJMoa1803213

62. Zarbock A, Kellum JA, Schmidt C, Van Aken H, Wempe C, Pavenstädt H, et al. Effect of early vs delayed initiation of renal replacement therapy on mortality in critically ill patients with acute kidney injury: the ELAIN randomized clinical trial. *JAMA.* (2016) 315:2190–9. doi: 10.1001/jama.2016.5828

63. Li X, Liu C, Mao Z, Li Q, Zhou F. Timing of renal replacement therapy initiation for acute kidney injury in critically ill patients: a systematic review of randomized clinical trials with meta-analysis and trial sequential analysis. *Crit Care.* (2021) 25:15. doi: 10.1186/s13054-020-03451-y

64. Wang X, Zhang Q, Yan Y, Yang Y, Shang X, Li Y. Clinical significance of pro-inflammatory cytokines and their correlation with disease severity and blood coagulation in septic patients with bacterial co-infection. *Shock.* (2021) 56:396–402. doi: 10.1097/SHK.0000000000001735

65. Broman ME, Hansson F, Vincent JL, Bodelsson M. Endotoxin and cytokine reducing properties of the oXiris membrane in patients with septic shock: a randomized crossover double-blind study. *PLoS ONE.* (2019) 14:e0220444. doi: 10.1371/journal.pone.0220444

frontiers | Frontiers in Medicine

TYPE Case Report
PUBLISHED 05 October 2022
DOI 10.3389/fmed.2022.956333

OPEN ACCESS

EDITED BY
Thierry Burnouf,
Taipei Medical University, Taiwan

REVIEWED BY
Levent Dalar,
Istanbul Bilim University, Turkey
Hadi Goubran Messiha,
University of Saskatchewan, Canada

*CORRESPONDENCE
Katsumasa Koyama
kkoyama@med.kawasaki-m.ac.jp

SPECIALTY SECTION
This article was submitted to Pulmonary Medicine, a section of the journal Frontiers in Medicine

RECEIVED 30 May 2022
ACCEPTED 29 August 2022
PUBLISHED 05 October 2022

CITATION
Koyama K, Minami D, Isobe H, Shirai R, Okimoto N and Tomoda K (2022) Case Report: Use of endobronchial Watanabe spigot and coagulation factor XIII supplementation in the treatment of persistent pneumothorax due to pneumocystis pneumonia with human immunodeficiency virus infection. *Front. Med.* 9:956333. doi: 10.3389/fmed.2022.956333

Case Report: Use of endobronchial Watanabe spigot and coagulation factor XIII supplementation in the treatment of persistent pneumothorax due to pneumocystis pneumonia with human immunodeficiency virus infection

Katsumasa Koyama[1]*, Daisuke Minami[2], Hayato Isobe[1], Ryo Shirai[1], Niro Okimoto[1] and Koichi Tomoda[1]

[1]Department of General Internal Medicine 1, Kawasaki Medical School, Okayama, Japan, [2]Department of Respiratory Medicine, Hosoya Hospital, Okayama, Japan

Pneumocystis jiroveceii pneumonia is one of the most common opportunistic infections associated with human immunodeficiency virus. Endobronchial Watanabe spigot has been recommended for refractory pneumothorax, even with persistant air leak despite continuous negative pressure control *via* thoracic drainage. Moreover, coagulation factor XIII is considered effective in wound healing.

KEYWORDS

endobronchial Watanabe spigot, blood coagulation factor XIII, pneumothorax, *pneumocystis jiroveceii* pneumonia, human immunodeficiency virus

Introduction

Pneumocystis jiroveceii pneumonia (PJP) is one of the most common opportunistic infections associated with human immunodeficiency virus (HIV). A high incidence of pneumothorax that may become intractable has been reported in patients with PJP with HIV infection (1). The use of endobronchial Watanabe spigot (EWS) has been proposed for refractory pneumothorax. However, air leak might persist despite continuous negative pressure control by thoracic drainage. In addition, blood coagulation factor XIII (FXIII) has been reported to be effective in promoting wound healing. Herein, we report a case of refractory pneumothorax secondary to HIV-associated PJP that responded to the use of EWS and FXIII supplementation.

Case description

A 37-year-old man visited a neighborhood hospital with a chief complaint of fever that had persisted for 3 weeks. The patient had no history of smoking or alcoholic drinking. Furthermore, his medical history was generally unremarkable. He works as a care staff and denied having a history of exposure to dust. Chest X-ray revealed pneumonia, prompting referral to our hospital.

Computed tomography (CT) scan showed diffuse ground glass opacities in both lungs (Figure 1A). He was admitted to our hospital for further diagnosis and treatment. On physical examination on admission, his height and body weight were 167.1 cm and 54.7 kg, respectively. The following vital signs were checked: body temperature, 37.3°C; blood pressure, 108/50 mmHg; and pulse rate, 66 beats per min. The patient was fully active, with an Eastern Cooperative Oncology Group performance status score of zero. The level of transcutaneous arterial oxygen saturation was 98% on room air. The bulbar conjunctiva did not exhibit significant pallor indicative of anemia. Cardiac examination revealed no abnormalities. In addition, there were no adventitious lung sounds. Abdominal and neurological findings were also normal. The patient presented with redness on the entire face. The skin of the hands was rough and covered with scales. Additionally, depression in the fingernails and toenails was observed. Interdigital scales were also noted on the left foot. Laboratory test results on admission (Table 1) showed elevated inflammatory markers: white blood cell (WBC), 4,070/μl (neutrophil, 68.0%) and C-reactive protein (CRP), 3.38 mg/dl. Liver and renal function tests were almost within normal range. The patient tested positive for the HIV antigen and his CD4 count was markedly reduced (27/μl). Transbronchial lung biopsy, bronchial brushing, and bronchoalveolar lavage were performed from the left B8a. Histological and cytological analysis (Grocott's staining) detected *Pneumocystis jirovecii* in the foamy substance from the pathological specimens. None of the findings were suggestive of malignancy or presence of cytomegalovirus.

A detailed interview aimed to identify the specific type of pneumonia revealed a history of homosexual intercourse during a 6-month period 13 years before admission. After providing informed consent, the patient tested positive for HIV. Based on this result and bronchoscopy findings, he was diagnosed with PJP complicated by HIV infection. Therefore, treatment with sulfamethoxazole-trimethoprim (nine tablets/day for 23 days) was started. Poor oxygenation was observed during the treatment course, with a level of transcutaneous arterial oxygen saturation on room air below 90%, prompting addition of prednisolone (40 mg/day for 5 days) to the treatment. The pneumonia tended to improve. However, on day 11 after disease onset, the patient reported left-sided chest pain. Repeat chest X-ray revealed grade III pneumothorax in the left lung. A single chest tube was placed and maintained under continuous negative aspiration pressure for a week. However, air leak persisted, and pleurodesis with a 50% glucose solution was not successful. CT scan of the chest showed cysts clustered on the peripheral side of the left B4 (Figure 1B). This site was identified to be the location of air leak, and bronchial occlusion with an EWS (size: M, 6 mm; Novatech, La Ciotat, France) was performed (Figure 1C). However, air leak decreased after the procedure. However, FXIII activity was reduced to 41% possibly due to the HIV infection. Therefore, intravenous infusion of FXIII (Fibrogammin® 240 IU, 4 ml/day for 5 days) was added to the treatment, enabling drain removal (Figure 1D). The patient subsequently received antiretroviral drug therapy for HIV and was discharged on day 33 after disease onset.

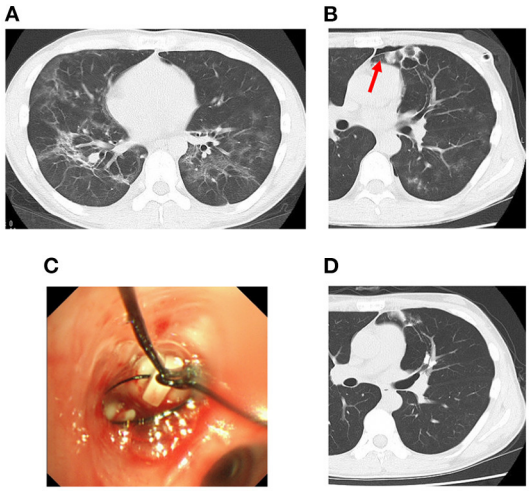

FIGURE 1
Chest computed tomography (CT) scan on admission **(A)**, at 11 days **(B)**, and after bronchial occlusion with a endobronchial Watanabe spigot (EWS) **(D)**, and EWS **(C)**. CT scan of the chest showing diffuse ground glass opacity on admission **(A)**. CT scan of the chest showing cysts clustered on the peripheral side of the left B4 at 11 days **(B)**. EWS shown being implanted in left B4b **(C)**. And, CT scan showing improvement in the pneumothorax after bronchial occlusion with EWS **(D)**.

Discussion

It has been reported that patients with HIV complicated by PJP often had symptoms similar to those of common cold, which precede disease onset by a few weeks and gradually exacerbate. A high incidence (5–10%) of pneumothorax complications have been reported in patients with PJP with HIV (1). In addition, 10–35% of these patients present with cystic changes in the lungs (2). Pneumothorax in these patients requires long-term drainage due to high recurrence and persistence of air leaks.

TABLE 1 Laboratory findings.

Variable	Result	Reference range	Variable	Result	Reference range
Hematology			**Biochemistry**		
Red blood cells ($\times 10^4/\mu l$)	407	435–555	Sodium (mmol/L)	134	138–145
Hemoglobin (g/dl)	13.0	13.7–16.8	Potassium (mmol/L)	4.0	3.6–4.8
Hematocrit (%)	39.0	40.7–50.1	Chlorine (mmol/L)	107	101–108
White blood cells (/μl)	4,070	3,300–8,600	BUN (mg/dl)	9	8–20
Nt. (%)	68.0	40.7–50.1	Creatinine (mg/dl)	0.63	0.65–1.07
Lym. (%)	21.1	15.8–34.8	Total bilirubin (mg/dl)	0.30	0.4–1.5
Eos. (%)	1.0	1.0–5.0	AST (U/L)	25	13–30
Bas. (%)	0.0	6.6–8.1	ALT (U/L)	6	10–42
Mon. (%)	9.9	4.1–5.1	LDH (U/L)	357	124–222
Mon. (%)	9.9	4.1–5.1	Albumin (g/dl)	1.9	4.1–5.1
Platelets ($\times 10^4/\mu l$)	14.3	15.8–34.8	Total protein (g/dl)	5.6	6.6–8.1
Collagen disease-related antibodies			CK	18	59–248
Anti-nuclear Ab. (IU/L)	<10	0–12	CRP (mg/dl)	3.38	34.0–46.0
Rheumatoid factor (IU/L)	<15	0–15	KL-6 (U/ml)	460	<500
Anti-CCP Ab. (IU/L)	<0.5	<4.5	CD4	3.7	
Anti-ds-DNA Ab. (IU/L)	<10	0–112	CD8	75.2	
Anti-RNP Ab. (IU/L)	<2.0	<10.0	CD4/8	0.05	
Anti-Scl-70 Ab. (IU/L)	<1.0	<10.0	C7-HARP	–	–
Anti-SS-A Ab. (IU/L)	<1.0	<10.0	β-D	108.8	0.0–20.0
Anti-ARS Ab. (IU/L)	<5.0	<25.0	QFT	–	–
PR3-ANCA	<1.0	<3.5	HIV-Ab	+	–
MPO-ANCA	<1.0	<3.5			

ALT, alanine aminotransferase; AST, aspartate aminotransferase; Bas, basophils; BUN, blood urea nitrogen; CRP, c-reactive protein; Eos, eosinophils, Hb, hemoglobin; Hct, hematocrit; HIV-Ab; human immunodeficiency virus antibodies; KL-6, Krebs von den Lungen-6; LDH, lactate dehydrogenase; Lym, lymphocytes; Mon, monocytes; RBC; Nt, neutrophils; PLT, platelets; QFT, QuantiFERON®-TB Gold; RBC, red blood cells; T-Bil, total bilirubin, WBC, white blood cells; β-D, beta-D-glucan.

This may be due to pleural necrosis caused by PJP as well necrosis spread to the pulmonary parenchyma (3). In some cases in which pneumothorax does not respond to conservative treatments, such as chest drainage and pleurodesis, surgery is performed. However, surgery is not recommended in patients positive for HIV due to delayed wound healing, possibility of postoperative complications, and potential postoperative worsening of HIV infection. In addition, elevated postoperative mortality has been reported in patients with a low CD4 count (4). Surgery was therefore contraindicated in this particular patient due to the markedly low number of $CD4^+$ T cells (27/μl) (5).

Endobronchial spigot placement is an endoscopic treatment developed by Watanabe et al. (6) with the aim of improving various conditions by bronchial occlusion through the endoscopic occlusion of segmental and subsegmental bronchi. Secondary pneumothorax without adequate lung expansion due to persistent air leak, pulmonary fistula, and empyema with bronchopleural fistula are indications for EWS placement (7). EWS placement is also appropriate in patients at high risk for surgery, such as the one described in this report. We selected and performed EWS due to possible risk of pneumonia exacerbation after valve placement in the tracheal tube. Since EWS is simple and minimally invasive treatment, it was an appropriate option in our patient. In addition, valve placement was not covered by insurance in Japan. Therefore, we could not consider valve placement according to the general clinical situation. On the other hand, since valve placement was difficult to preform, EWS, which has a high safety profile and made of medical silicone, could be often implanted for a long period of time (8). In our case, cysts that clustered on the peripheral side of the left B4 disappeared and secondary pneumothorax was improved after EWS for about 1 year. In addition, his condition regarding CPC stabilized. Therefore we considered to remove the spigots.

FXIII deficiency has been associated with failure of wound healing and fistula (9). Unlike direct occlusion of fistula, as is the case in surgery and pleurodesis, FXIII supplementation aims to promote spontaneous patient recovery.

The mechanism of action of FXIII involves enhancement of wound healing through promoting fibroblast proliferation, bridging of the gap using fibrin scaffolds, and making changes into the favored net structure. FXIII supplementation is indicated for cases of anastomotic failure and fistula in which FXIII activity is 70% or less than the normal values. FXIII supplementation has been reported to be effective in fistula and anastomotic failure after gastrointestinal surgery, as well as in 70% of patients with pulmonary fistula that persisted at least 5 days after lung lobectomy. It has also been reported to be useful after surgery for secondary pneumothorax caused by pneumocystis pneumonia. In Japan, the local application of FXIII supplementation is not covered by insurance. Howeveer, the efficacy of FXIII systemic infusion has been reported (10). Therefore, in the current case, FXIII supplementation was reduced to 41% of its normal value. Consequently, intravenous administration of FXIII might have contributed to the observed improvement in the bronchial fistula.

Conclusion

Herein, we report a case of intractable secondary pneumothorax that originated as a complication of a pneumocystis pneumonia with HIV infection. This case well responded to bronchial occlusion with EWS and treatment with FXIII.

Data availability statement

The original contributions presented in the study are included in the article/supplementary material, further inquiries can be directed to the corresponding author.

Ethics statement

Written informed consent was obtained from the individual(s) for the publication of any potentially identifiable images or data included in this article.

Author contributions

KK researched data and wrote the manuscript. DM, HI, and RS researched data and contributed to the discussion. NO and KT reviewed the manuscript. All authors contributed to the article and approved the submitted version.

Acknowledgments

We would like to thank Editage (www.editage.com) for English language editing.

Conflict of interest

The authors declare that the research was conducted in the absence of any commercial or financial relationships that could be construed as a potential conflict of interest.

Publisher's note

All claims expressed in this article are solely those of the authors and do not necessarily represent those of their affiliated organizations, or those of the publisher, the editors and the reviewers. Any product that may be evaluated in this article, or claim that may be made by its manufacturer, is not guaranteed or endorsed by the publisher.

References

1. Pastores SM, Garay SM, Naidich DP, Rom WN. Review: pneumothorax in patients with AIDS-related pneumocystis carinii pneumonia. *Am J Med Sci.* (1996) 312:229–34. doi: 10.1097/00000441-199611000-00008

2. Sandhu JS, Goodman PC. Pulmonary cysts associated with pneumocystis carinii pneumonia in patients with AIDS. *Radiology.* (1989) 173:33–5. doi: 10.1148/radiology.173.1.2789413

3. Matesanz López C, Cardona Arias AF, Río Ramírez MT, Díaz Ibero G, Rodríguez Álvarez SJ, Juretschke Moragues MA. Simultaneous bilateral pneumothorax in an immunocompromised HIV patient with *Pneumocystis jirovecii* pneumonia. *Respir Med Case Rep.* (2018) 25:147–9. doi: 10.1016/j.rmcr.2018.08.008

4. King JT Jr, Perkal MF, Rosenthal RA, Gordon AJ, Crystal S, Rodriguez-Barradas MC, et al. Thirty-day postoperative mortality among individuals with HIV infection receiving antiretroviral therapy and procedure-matched, uninfected comparators. *JAMA Surg.* (2015) 150:343–51. doi: 10.1001/jamasurg.2014.2257

5. Yii MK, Saunder A, Scott DF. Abdominal surgery in HIV/AIDS patients: indications,operative management, pathology and outcome. *Aust N Z J Surg.* (1995) 65:320–6. doi: 10.1111/j.1445-2197.1995.tb00646.x

6. Watanabe Y, Bessho A, Horiuchi T. Bronchial occlusion with EWS for pulmonary diseases. *J Jpn Soc Resp Endosc.* (2013) 35:552–5.

7. Duckert F, Jung E, Shmerling DH. A hitherto undescribed congenital haemorrhagic diathesis probably due to fibrin stabilizing factor deficiency. *Thromb Diath Haemorrh.* (1960) 5:179–86. doi: 10.1055/s-0038-1654918

8. Sakugawa R, Nishii K, Fukamatsu N, Toyota Y, Oda N, Hosokawa S, et al. EWS. *J Jpn Soc Resp Endo.* (2014) 36:538–41.

9. Inoue H, Nishiyama N, Mizuguchi S, Nagano K, Izumi N, Komatsu H, et al. Clinical value of exogenous factor XIII for prolonged air leak following pulmonary lobectomy: a case control study. *BMC Surg.* (2014) 14:109. doi: 10.1186/1471-2482-14-109

10. Yajima K, Urabe N, Asai K. A case of recurrent pneumothorax with interstitial pneumonia successfully treated by coagulation factor XII. *J Jpn Assoc Chest Surg.* (2004) 18:637–40. doi: 10.2995/jacsurg.18.5_637

frontiers | Frontiers in Medicine

TYPE Case Report
PUBLISHED 25 October 2022
DOI 10.3389/fmed.2022.1025894

OPEN ACCESS

EDITED BY
Rodrigo Torres-Castro,
University of Chile, Chile

REVIEWED BY
Michael J. Brenner,
University of Michigan, United States
Patrick Zardo,
Hannover Medical School, Germany

*CORRESPONDENCE
Lina Zuccatosta
linazuccatosta@tiscalinet.it

SPECIALTY SECTION
This article was submitted to Pulmonary Medicine, a section of the journal Frontiers in Medicine

RECEIVED 23 August 2022
ACCEPTED 27 September 2022
PUBLISHED 25 October 2022

CITATION
Zuccatosta L, Zamacona BR, Porcarelli F, Mei F, Gonnelli F, Gasparini S and Di Marco Berardino A (2022) Case Report: Tracheal stenosis due to fibrotic bridges in a post-tracheostomy COVID-19 patient. *Front. Med.* 9:1025894. doi: 10.3389/fmed.2022.1025894

Case Report: Tracheal stenosis due to fibrotic bridges in a post-tracheostomy COVID-19 patient

Lina Zuccatosta[1]*, Borja Recalde Zamacona[1,2], Francesco Porcarelli[1], Federico Mei[1,3], Francesca Gonnelli[1], Stefano Gasparini[1,3] and Alessandro Di Marco Berardino[1]

[1]S.O.D. di Pneumologia, Ospedali Riuniti Ancona, Azienda Ospedaliero Universitaria, Ancona, Italy, [2]Interventional Pulmonology Clinica Universidad de Navarra, Pamplona, Spain, [3]Department of Biomedical Sciences and Public Health, Polytechnic University of Marche, Ancona, Italy

Tracheal stenosis is a common complication of prolonged endotracheal intubation or tracheostomy, that can be classified as simple (without cartilage involvement) or complex (with cartilaginous support involvement). We report a case of a post-COVID-19 tracheal stenosis with fibrotic bridges between the tracheal walls, creating a net within the lumen and causing significant respiratory distress. The absence of cartilaginous support involvement allowed a definitive bronchoscopic treatment with complete and permanent resolution of stenosis.

KEYWORDS

case report, tracheal stenosis, COVID-19, tracheostomy, laser therapy

Introduction

It's well known that prolonged endotracheal intubation is a risk factor for tracheal stenosis or malacia and that the endotracheal cuff pressure plays a major role. Furthermore, patients who receive a tracheostomy can develop tracheal stenosis at the level of tracheal stoma.

In fact, tracheal stenosis does not always occur at the cuff level: *cuff stenosis* refers to stenosis at the site of the cuff of an endotracheal tube or tracheostomy, but also other kinds of stenoses are documented: *stomal stenosis* refers to stenosis at the site of a tracheotomy, *subglottic stenosis* is usually caused by injury of the endolaryngeal structures distal to the vocal cords within the cricoid cartilage, typically as a result of the effects of a cricothyroidostomy tube or oversized endotracheal tube; *glottic stenosis* is related to endotracheal intubation with secondary injury to the posterior vocal cords and arytenoid cartilages, anatomic regions against which the endotracheal tube rests in the supine position. These lesions can occur simultaneously or sequentially in the larynx and trachea of the postintubation patient (1).

However tracheal stenoses above the cuff are less frequent, as reported by James et al. (2).

During COVID-19 pandemic, many symptomatic patients required tracheal intubation, mechanical ventilation and tracheostomy.

Tracheostomy in patients with severe respiratory failure due to COVID-19 is matter of concern. There's still not agreement about patient selection and timing, but in cases like ours the relatively young age of the patient and the lack of severe comorbidities prompted Anesthesiologists to perform the tracheostomy. McGrath et al. (3) suggest to accurately assess risks and benefit before performing tracheostomy in a COVID-19 patient, and, when necessary, to carry out the intervention within 10 days.

Even if it can be postulated that the incidence of tracheal stenosis increases in COVID-19 patients (4), the rate of this complication in intubated/tracheostomized patients for SARS-COV2 related respiratory insufficiency still remains unknown.

We report an unusual case of post-tracheostomy tracheal stenosis (PTTS) with fibrotic bridges successfully treated with endobronchial laser therapy.

Case description

A 68-year-old woman, former smoker with a mild hypertension, required orotracheal intubation due to respiratory failure secondary to SARS-CoV2 infection, and subsequently tracheostomy. Tracheostomy was performed after 7 days from intubation and maintained for 5 weeks. Cuffometry was monitored and cuff pressure was constantly maintained below 30 cm H_2O in order to avoid tracheal ischemia. After the resolution of the pneumonia and of the respiratory failure, the tracheostomic cannula was removed and the patient was discharged.

Three months later she referred progressive dyspnea with inspiratory effort. Inspiratory wheezing was evident on pulmonary auscultation; however, oxygen saturation was stable over 95% without oxygen supplementation.

Diagnostic assessment

A chest computerized tomography revealed a marked tracheal stenosis at the proximal third level. Rigid bronchoscopy showed fibrotic net with tracts crossing the anterior-to-posterior trachea and causing a tracheal stenosis 5 cm below the vocal cords (**Figures 1A,B**, **2**). Endobronchial laser therapy (Dornier Medilas Fibertom 8100, Nd- YAG laser) was applied on the fibrotic tracts achieving a good airway patency (**Figure 1C**). After 2 months follow-up, the patient showed significant improvement of respiratory symptoms and flexible bronchoscopy confirmed the lack of significative obstruction of tracheal lumen (**Figure 1D**). This result was confirmed even 2 years after the treatment: a further flexible bronchoscopy demonstrated an optimal tracheal patency (**Figure 3**).

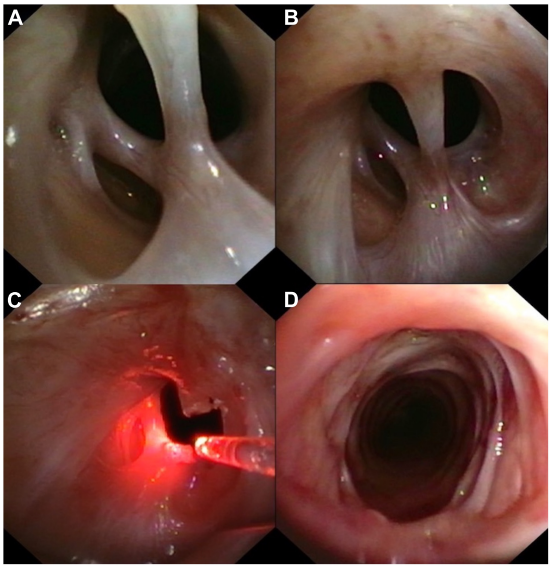

FIGURE 1
(A,B) Tracheal stenosis caused by a fibrotic net; **(C)** endobronchial laser therapy; **(D)** bronchoscopic aspect of the trachea after 30 days from treatment.

Discussion

PTTS is a well-established and relative common type of acquired benign stenosis, occurring in 0.6–22% of patients subjected to prolonged intubation and ventilation, as late complication (5). The high pressure of the cuff plays a major role inducing ischemia of the mucosa and chondritis. Recently, some other risk factors such as obesity, tube size > 6 mm, performing tracheostomy after 10 days of orotracheal intubation or high cuff pressure (>30 cm H_2O) have been described (6).

During the global coronavirus 2019 (COVID-19) pandemic, a massive increase of critically ill patients suffering from respiratory failure was observed and prolonged mechanical ventilation was required.

Ayten et al. analyzed the incidence of post-invasive mechanical ventilation tracheal stenosis in COVID-19 patients; tracheal stenosis was reported in 7% of patients, and a web-like stenosis was identified in 43% of them. All the simple tracheal stenoses were treated through rigid bronchoscopy, obtaining optimal patency, and showing that rigid bronchoscopy could be an excellent treatment even in simple tracheal stenosis due to invasive mechanical ventilation in COVID-19-related respiratory failure (7).

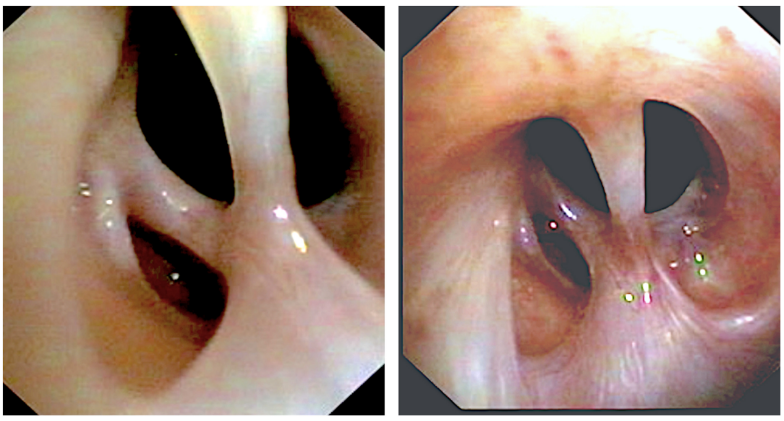

FIGURE 2
Tracheal stenosis due to fibrotic bridge.

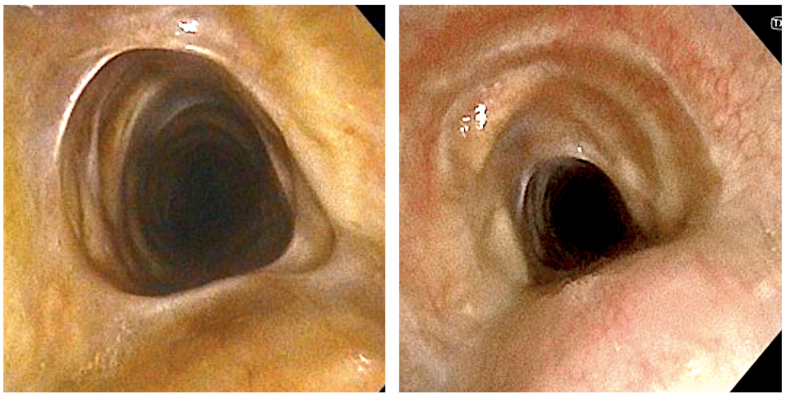

FIGURE 3
Bronchoscopic aspect of the trachea after 2 years from treatment.

Additional factors that increased the risk of tracheal stenosis in COVID patients treated with intubation and mechanical ventilation were recognized in delayed tracheostomy, critically ill state, prone position ventilation, prothrombotic and antifibrinolytic state, high viral replication in the tracheal epithelium, superimposed local infections, lower PaO_2/FiO_2 ratio with increased hypoxia of laryngo-tracheal mucosa (4, 8).

Tracheal stenosis usually appears as a concentric narrowing that obstructs normal airflow, leading to respiratory symptoms including dyspnea, inspiratory stridor, coughing and shortness of breath.

The type of obstruction, the level (subglottic, upper, middle, or lower third of trachea) and the severity of narrowing (reduction of cross-sectional area of the trachea) are well detected by bronchoscopy.

Narrowing of tracheal lumen can be due to granulation tissue (local or concentric hyper granulation), fibrosis and inflammation, fibrosis and malacia (9, 10). Tracheal stenoses are classified as simple or complex. Simple stenosis involves less than 1 cm of the trachea without evidence of cartilaginous support involvement. Complex stenosis has one or more of the following features: involvement of more than 1 cm of trachea, varying degree of cartilage involvement, circumferential contraction scarring and malacia (11).

Tracheal resection with end-to-end anastomosis is the first-line treatment for complex stenosis. However, postsurgical complications increase in patients with poor general health and comorbidities (12), which are frequent in PTTS patients. Mortality rate has been reported racing from 1.8% up to 5% (13). Endoscopic procedures, elective for granuloma or simple stenosis (mechanical dilatation, laser) can be an alternative to surgery, especially when the patency of trachea must be restored immediately or when the patient is not suitable for surgery due to several clinical conditions.

The tracheal stenosis that we observed had a very rare morphology: in fact, even if single tracheal bridges are reported

in other cases of PTTS (14), this kind of pattern, characterized by multiple bridges is quite singular. Though it can be classified as fibrotic stenosis without involvement of cartilage, the transversal bridges induced severe narrowing of the upper third of the trachea. Laser was used to cut the fibrotic bands at the site of implantation, sparing the normal mucosa. The patency was restored through a single-time therapeutic rigid bronchoscopy and rubber-like fibrin-rich plaques were not observed at follow-up with flexible bronchoscopy.

The optimal management of PTTS is still far from being fully elucidated and multidisciplinary approach involving surgeon (thoracic, ENT), anesthetists and pulmonologists is mandatory in complex cases and severe ill patients. Our case is an example that endoscopic procedures can offer good and stable results in restoring patency of the airway in selected cases without cartilage involvement. Endoscopic recanalization can be considered an adequate alternative to surgery in the treatment of PPTS in most cases (15) and interventional pulmonology plays an essential role in the management of PPTS.

Data availability statement

The raw data supporting the conclusions of this article will be made available by the authors, without undue reservation.

Ethics statement

Ethical review and approval was not required for the study on human participants in accordance with the local legislation and institutional requirements. The patients/participants provided their written informed consent to participate in this study.

Author contributions

LZ: performance of the endoscopic procedure, acquisition, analysis, and interpretation of data, and final approval of the work. BZ and FP: acquisition and interpretation of data. FM and FG: revisiting of the work. SG: conception, revisiting, and interpretation of data. AD: conception and revisiting of the work. All authors read and approved the final version of the manuscript.

Conflict of interest

The authors declare that the research was conducted in the absence of any commercial or financial relationships that could be construed as a potential conflict of interest.

Publisher's note

All claims expressed in this article are solely those of the authors and do not necessarily represent those of their affiliated organizations, or those of the publisher, the editors and the reviewers. Any product that may be evaluated in this article, or claim that may be made by its manufacturer, is not guaranteed or endorsed by the publisher.

References

1. Wain JC. Postintubation tracheal stenosis. *Chest Surg Clin N Am.* (2003) 13:231–46. doi: 10.1016/s1052-3359(03)00034-6

2. James P, Parmar S, Hussain K, Praveen P. Tracheal stenosis after tracheostomy. *Br J Oral Maxillofac Surg.* (2021) 59:82–5. doi: 10.1016/j.bjoms.2020.08.036

3. McGrath BA, Brenner MJ, Warrillow SJ, Pandian V, Arora A, Cameron TS, et al. Tracheostomy in the COVID-19 era: global and multidisciplinary guidance. *Lancet Respir Med.* (2020) 8:717–25. doi: 10.1016/S2213-2600(20)30230-7

4. Mattioli F, Marchioni A, Andreani A, Cappiello G, Fermi M, Presutti L. Post-intubation tracheal stenosis in COVID-19 patients. *Eur Arch Otorhinolaryngol.* (2021) 278:847–8. doi: 10.1007/s00405-020-06394-w

5. Sarper A, Ayten A, Eser I, Ozbudak O, Demircan A. Tracheal stenosis after tracheostomy or intubation: review with special regard to cause and management. *Tex Heart Inst J.* (2005) 32:154–8.

6. Li M, Yiu Y, Merrill T, Yildiz V, DeSilva B, Matrka L. Risk factors for post tracheostomy tracheal stenosis. *Otolaryngol Head Neck Surg.* (2018) 159:698–704. doi: 10.1177/0194599818794456

7. Ayten O, Iscanli IGE, Canoglu K, Ozdemir C, Saylan B, Caliskan T, et al. Tracheal stenosis after prolonged intubation due to COVID-19. *J Cardiothorac Vasc Anesth.* (2022) 36:2948–53. doi: 10.1053/j.jvca.2022.02.009

8. Allgood S, Peters J, Benson A, Maragos C, McIltrot K, Slater T, et al. Acquired laryngeal and subglottic stenosis following COVID-19-Preparing for the coming deluge. *J Clin Nurs.* (2021) Epub ahead of print. doi: 10.1111/jocn.15992

9. Fiacchini G, Tricò D, Ribechini A, Forfori F, Brogi E, Lucchi M, et al. Evaluation of the incidence and potential mechanisms of tracheal stenosis complications in patients with COVID-19. *JAMA Otolaryngol Head Neck Surg.* (2021) 147:70–6. doi: 10.1001/jamaoto.2020.4148

10. Ghorbani A, Dezfouli AA, Shadmehr MB, Pejhan S, Saghebi SR, Ghare-Daghi AS, et al. A proposed grading system for post-intubation tracheal stenosis. *Tanaffos.* (2012) 11:10–4.

11. Brichet A, Verkindre C, Dupont ML, Carlier J, Darras A, Wurtz A. Multidisciplinary approach to management of post-intubation tracheal stenoses. *Eur Respir J.* (1999) 13:888–93. doi: 10.1034/j.1399-3003.1999.13d32.x

12. Rea F, Callegaro D, Loy M, Zuin A, Narne S, Gobbi T, et al. Benign tracheal and laryngotracheal stenosis: surgical treatment and results. *Eur J Cardiothorac Surg.* (2002) 22:352–6. doi: 10.1016/S1010-7940(02)00342-1

13. Maassen W, Greschuchna D, Vogt-Moykopf I, Toomes H, Lulling H. Tracheal resection-state of the art. *Thorac Cardiovasc Surg.* (1985) 33:2–7. doi: 10.1055/s-2007-1014071

14. Guinde J, Laberge F, Fortin M. A "tracheal bridge": an unusual presentation of posttracheostomy tracheal stenoses. *J Bronchology Interv Pulmonol.* (2020) 27:150–2. doi: 10.1097/LBR.0000000000000652

15. Galluccio G, Lucantoni G, Battistoni P, Paone G, Batzella S, Lucifora V, et al. Interventional endoscopy in the management of benign tracheal stenoses: definitive treatment at long-term follow-up. *Eur J Cardiothorac Surg.* (2009) 35:429–33. doi: 10.1016/j.ejcts.2008.10.041

frontiers | Frontiers in Medicine

TYPE Review
PUBLISHED 24 November 2022
DOI 10.3389/fmed.2022.1040441

OPEN ACCESS

EDITED BY
Suzana Erico Tanni,
São Paulo State University, Brazil

REVIEWED BY
Ke Cao,
Nanjing Drum Tower Hospital, China
Ricardo de Souza Cavalcante,
São Paulo State University, Brazil

*CORRESPONDENCE
Yuan Gao
gaoy2@sj-hospital.org

SPECIALTY SECTION
This article was submitted to Pulmonary Medicine, a section of the journal Frontiers in Medicine

RECEIVED 09 September 2022
ACCEPTED 10 November 2022
PUBLISHED 24 November 2022

CITATION
Liu J and Gao Y (2022) Tigecycline in the treatment of severe pneumonia caused by *Chlamydia psittaci*: A case report and literature review. *Front. Med.* 9:1040441. doi: 10.3389/fmed.2022.1040441

Tigecycline in the treatment of severe pneumonia caused by *Chlamydia psittaci*: A case report and literature review

Jiaming Liu and Yuan Gao*

Department of Pulmonary and Critical Care Medicine, Shengjing Hospital of China Medical University, Shenyang, China

Psittacosis is a zoonotic disease caused by *Chlamydia psittaci*. Systemic infections are mainly transmitted through the respiratory tract. The most common related disease is human atypical pneumonia, which is a rare pathogen of community-acquired pneumonia. Due to the difficulty of diagnosis, there have been few reports of *C. psittaci* pneumonia in the past. In recent years, with the widespread application of metagenomic next-generation sequencing (mNGS), the number of reported cases of *C. psittaci* has increased year by year. However, at present, most hospitals have little understanding of *C. psittaci*, especially for severe patients, and lack experience in diagnosis and treatment. Herein, we report the case of a 71-year-old woman with severe pneumonia that caused by *C. psittaci*. This patient was diagnosed through mNGS and was treated with tigecycline successfully. The level of IL-6 in the BALF was significantly increased. We discontinued tigecycline after mNGS of the blood was negative. In this review, we analyzed 53 cases to summarize the etiology, clinical manifestations, diagnosis and treatment strategies of severe *C. psittaci* pneumonia and hope to raise clinicians' awareness of this disease.

KEYWORDS

***psittaci*, *Chlamydia psittaci* pneumonia, severe pneumonia, tigecycline, metagenomic nextgeneration sequencing (mNGS)**

Introduction

Psittacosis is a zoonotic disease caused by *Chlamydia psittaci* (1). Humans are infected through the respiratory tract, and the most common related disease is human atypical pneumonia (2). It is a rare cause of community-acquired pneumonia, accounting for approximately 1% of community-acquired pneumonia. Some patients with psittacosis progress rapidly and can die if not treated in time. Due to the difficulty of diagnosis, there have been few reports of related cases in the past. In recent years, due to the widespread use of metagenomic next-generation sequencing (mNGS),

reports of *C. psittaci* have been increasing year by year. This article reports a case of severe *C. psittaci* pneumonia who was diagnosed by mNGS and improved after treatment with tigecycline. There have been few cases of using tigecycline to treat *C. psittaci* pneumonia in the past, so it is necessary to summarize this case and review the literature.

Case presentation

The patient of a 71-year-old woman was admitted to our hospital because of fever for 10 days and dyspnea for 5 days on November 17, 2020. She presented with fever and chills 10 days before admission, and the maximum body temperature was 40°C, accompanied by fatigue and dry cough without sputum. Chest CT at the local hospital showed pneumonia in the inferior lobe of the left lung and mediastinal lymph node enlargement (**Figure 1**). Routine blood examination showed that the white blood cell count was 10.2×10^9/L and the CRP level was 139 mg/L. She went to a local clinic and applied cephalosporin antibiotics, but the above symptoms did not improve. Nausea and vomiting occurred 7 days prior, accompanied by diarrhea and watery stools, without abdominal pain. Then, she was hospitalized in the local hospital. Using ceftriaxone and moxifloxacin intravenously for 7 days showed no improvement. Dyspnea occurred 5 days prior and was aggravated after the event. One day before admission, the patient's dyspnea was significantly aggravated, and re-examination of chest CT was significantly worse than before (**Figure 1**). The patient was treated with tracheal intubation and ventilator-assisted ventilation. She was sent immediately to Shengjing Hospital of China Midical University and was hospitalized in the Department of Pulmonary and Critiacl Care Medicine.

The patient suffered from coronary atherosclerotic cardiopathy for 3 years, and she took aspirin intermittently. She had no hypertension and diabetes. She had no hepatitis and tuberculosis. She resides in Liaoning Province, northern China. She is a retired employee, has no smoking and drinking habits, and has no drug or food allergy.

When the patient was admitted to our hospital (day 1), her vital signs were as follows: body temperature 36.5°C, pulse rate 80 beats/min, respiratory rate 27 beats/min, blood pressure 117/69 mmHg, and pulse oxygen saturation 96% with a fraction of inspired oxygen (FiO_2) of 0.80. Conscious, no yellowing of skin and sclera, no paleness of eyelid conjunctiva. Breath sounds in both lungs were rough, and wet rales were heard on auscultation. There was no audible murmur on cardiac auscultation. Tenderness in the abdomen and hepatosplenomegaly were not detected. No edema of both lower limbs.

The laboratory dates after admission to our hospital were as follows: arterial blood gas analysis showed a pH of 7.513, PaO_2 of 98.6 mmHg, $PaCO_2$ of 28.2 mmHg, HCO_3- of 22.5 mmol/L and oxygenation index of 123.2. The white blood cell count was 18.5×10^9/L, with an elevated neutrophil ratio of 90.3%. The concentration of C-reactive protein (CRP) was 253.7 mg/L. The concentrations of procalcitonin (PCT, normal < 0.05 ng/ml) and interleukin-6 (IL-6, normal ≤5.4 pg/ml) were 2.91 ng/ml and 12.64 pg/ml, respectively. The D-dimer (normal 0–252 μg/L) was 2161 μg/L. Albumin level (normal 35–53 g/L) was 23.0 g/L. Alanine aminotransferase (ALT, normal 0–40 U/L) was 68 U/L, and aspartate aminotransferase (AST, normal 5–34 U/L) was 69 U/L. Bilirubin, creatinine, and electrolytes were within normal limits. The creatine kinase (CK, normal 29–200 U/L) was 75 U/L, and the creatine kinase isoenzyme (CK-MB, normal 0–24 U/L) was 17.4 U/L. The concentrations of B-type natriuretic peptide (BNP, normal 0–154.7 pg/mL) and cardiac troponin I (cTnI, normal 0–0.0116 U/L) were 300.8 pg/ml and 0.7743 μg/L, respectively. Mycoplasma pneumoniae IgM was positive, and IgG was negative. Chlamydia pneumoniae IgM was negative, and IgG was positive. The Epstein Barr virus DNA quantification was 8.15E + 03 copies/ml (normal < 1.0E + 03 copies/ml). Tests for cytomegalovirus, influenza A virus, influenza B virus, aenovirus and legionella bacteria were all negative. The β-D-glucan test and galacto Mannan test were both negative. T-SPOT-T and Tuberculin test were negative. The indicators for autoimmune diseases (anti-extractable nuclear antigen antibody, anti-nuclear antibody and anti-neutrophilic cytoplasmic antibody) were negative. The numbers of CD3 (normal 690–2,540/μl), CD8 (normal 190–1,140/μl) and CD4 (normal 410–1,590/μl) T lymphocytes in blood were 254, 41, and 165/μl, respectively. The concentrations of carcinoembryonic antigen (CEA, normal 0–5 ng/ml), cytokeratin 19 fragment (CYFRA21-1, normal 0.1–3.3 ng/ml) and neuron-specific enolase (NSE, normal 0–16.3 ng/ml) were 2.37, 6.30, and 17.32 ng/ml, respectively.

After admission, the patient continued to be treated with ventilator-assisted ventilation. Empirical anti-infective treatments, including meropenem, levofloxacin, ganciclovir, and arbidol, were used initially. After the initial treatment, the patient's peak temperature decreased, but she still had fever. On the second day of admission (November 18), the patient underwent bronchoscopic alveolar lavage examination, and bronchoalveolar lavage fluid (BALF) was sent to Nanjing Difei Medical Laboratory Co., Ltd. for mNGS examination. The concentration of interleukin-6 (IL-6) in the BALF was

Abbreviations: mNGS, metagenomic next-generation sequencing; CT, computed tomography; BALF, bronchoalveolar lavage fluid; IL-6 interleukin-6; PCT, procalcitonin; CRP, C-reactive protein; FiO_2, Fraction of inspired oxygen; pH, Pondus Hydrogenii; PaO_2, partial arterial oxygen pressure; $PaCO_2$, arterial partial pressure of carbon dioxide; PT, prothrombin time; APTT, activated partial thromboplastin time; ALT, alanine aminotransferase; CK-MB, creatine kinase isoenzyme; BNP, B-type natriuretic peptide; cTnI, cardiac troponin I; CEA, carcinoembryonic antigen; CYFRA, cytokeratin 19 fragment; NSE, neuron-specific enolase.

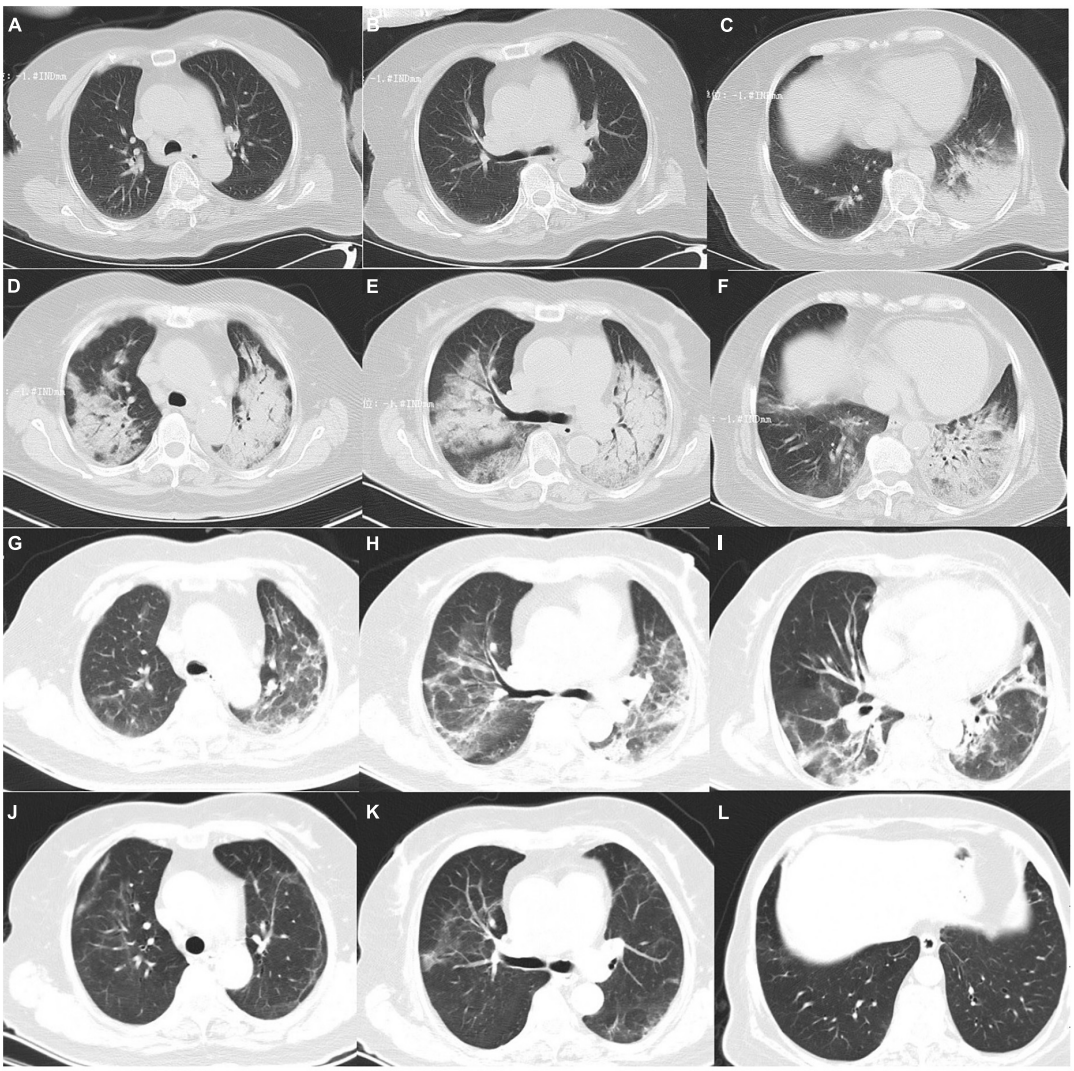

FIGURE 1
Patient's chest CT scans: panels **(A–C)** show CT scans at the time of the patient's first day of illness (November 7) in the local hospital. Panel **(D–F)** show CT scans on the 10th day of illness (November 17) in the local hospital. Panel **(G–I)** show CT scans on the 10th day after admission (November 27). Panel **(J–L)** show CT scans on the 26th day after admission (December 12).

4,519.04 pg/ml (normal range 0–5.4 pg/ml). On the 4th day of admission (November 20), the result of mNGS of the BALF was reported, and 70 sequence reads corresponding to *C. psittaci* were identified and there was no sequence read corresponding to other pathogens. The patient had no history of direct contact with birds and poultry before the illness, but there were neighbors raising pigeons in the residential area, not except for indirect contact. According to the results of mNGS of BALF suggesting *C. psittaci* infection (Table 1), antibacterial agents were switched to tigecycline (100 mg intervenous drop infusion on day 4, then 50 mg q12 h intervenous drop infusion on days 4–25) combined with levofloxacin (0.5 g qd intervenous drop infusion, days 2–7), and meropenem was discontinued. The patient's blood sample was sent to Guangzhou Weiyuan Gene Technology Co., Ltd. for mNGS testing again, and the results of the blood samples still identified 38 sequence reads corresponding to *C. psittaci* (Table 1). She was diagnosed with *C. psittaci* pneumonia. Her body temperature returned to normal on the 6th day of admission (Figures 1–4), and her dyspnea gradually eased. On the 7th day of admission (November 23), the patient's sputum culture revealed Pseudomonas aeruginosa and Candida albicans. Considering the patient had a secondary infection. According to the results of drug sensitivity, the patient was administered piperacillin tazobactam (4.5 g q8 h intervenous drop infusion, days 8–25) while strengthening oral care. The patient had sinus bradycardia, and the electrocardiogram showed a prolonged QT interval, so levofloxacin was ceased. On

TABLE 1 The patient'results of the mNGS of BALF and blood.

	The mNGS of BALF (November 19)	The NSG of blood (November 20)	The NSG of blood (December 10)
Chlamydia psittaci (reads)	70	38	–
Propionibacterium acnes (reads)	–	32	478
Moraxella osloensis (reads)	–	60	–
Staphylococcus hominis(reads)	–	6	105
Staphylococcus warneri (reads)	–	–	592
Malassezia globosa (reads)	–	–	4

the 10th day of admission (November 26), the patient's tracheal intubation was removed. Re-examination of chest CT showed that lung inflammation was significantly absorbed (Figure 1). On the 24th day of admission (December 10), blood mNGS was performed again and was negative for *C. psittaci* (Table 1). Tigecycline and piperacillin tazobactam were discontinued. Re-examination of the chest CT (December 12) showed that the inflammation was well absorbed, and only a few fiber cord shadows were left. On the 29th day of admission (December 15), the patient was discharged from the hospital, and her status was close to premorbid condition.

Other bacteria, including *Propionibacterium acnes*, *Moraxella osloensis*, *Staphylococcus hominis*, *Staphylococcus warneri*, and *Malassezia globose*, were also detected by mNGS in the patient's blood samples (Table 1). These bacteria are all skin microecological flora and not considered as pathogenic bacteria.

Literature review

We searched the PubMed database for articles on *C. psittaci* published before September 31, 2021. The search strategy was "*Chlamydia psittaci*" or "*Chlamydia psittaci* pneumonia", and a total of 870 articles were found. Among them, there were 23 articles about severe *C. psittaci* infection, and 54 severe *C. psittaci* pneumonia patients were reported; 27 cases were treated with ventilators, and 7 cases died. A summary of the detailed information is shown in Table 2. Most cases had a history of direct or indirect exposure. Contact history included raising parrots, birds and poultry, etc., or going to a bird shop, passing through a poultry market. There were also a few patients who had been infected due to contact with pets or aborted sheep. There were also reports of human-to-human transmission. Most patients had underlying diseases. There were 2 pregnant women, and 1 of them died. Chest radiography or CT showed consolidation or ground glass-like changes, and some patients had pleural effusion.

Forty-one patients (54 cases in total) were treated with quinolones, including moxifloxacin, levofloxacin, and ciprofloxacin. Among them, 6 patients were improved by quinolones alone after diagnosis, and 29 patients were initially ineffective with quinolones. A total of 9 patients had been treated with macrolides, including azithromycin, erythromycin, and spiramycin. Five patients had no effect on initial treatment with macrolides. There was no successful case of using macrolides alone in severe patients. A total of 27 patients were treated with tetracycline (alone or in combination with quinolones and macrolides) after being diagnosed with psittacosis, including doxycycline and minocycline. Among

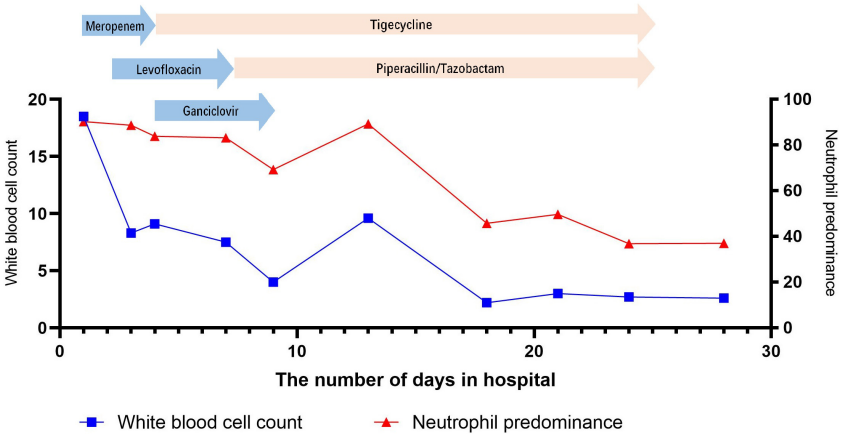

FIGURE 2
Change in white blood cell count and neutrophil predominance during hospitalization at the Shengjing Hospital of China Medical University.

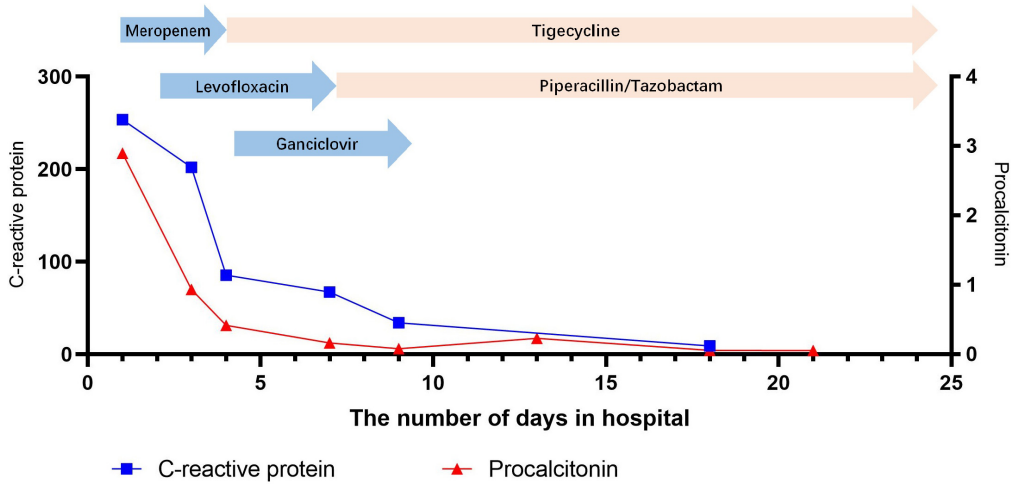

FIGURE 3
Change in C-reactive protein and procalcitonin during hospitalization at the Shengjing Hospital of China Medical University.

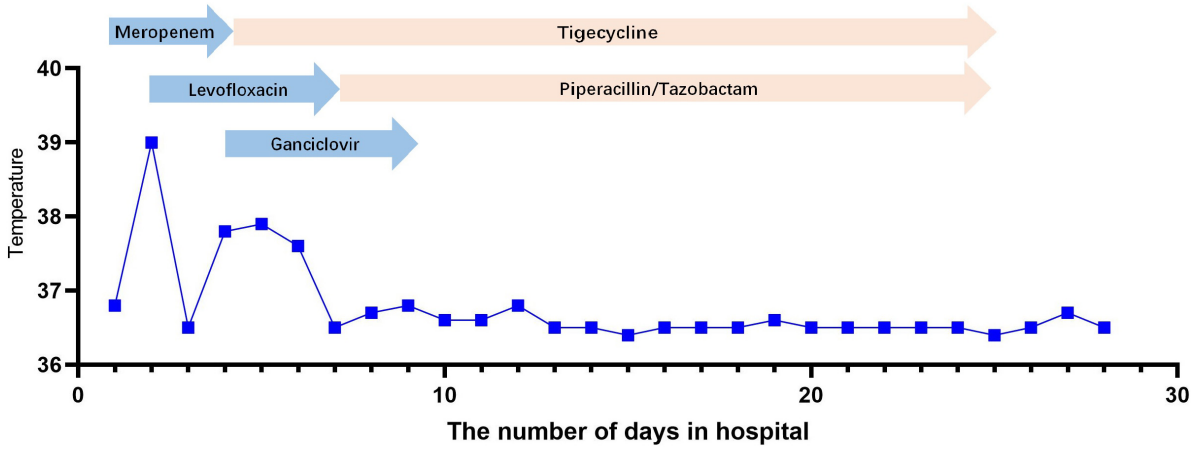

FIGURE 4
Body temperature and antimicrobial treatment during hospitalization at the Shengjing Hospital of China Medical University.

them, 5 patients died of ineffective treatment, 1 patient improved but died after being discharged from the hospital, and the rest were cured. One pregnant patient had only used meropenem during the treatment and died. In 2 patients, the initial application of quinolones was not effective but improved after changing to tigecycline.

Discussion

Chlamydia psittaci is an intracellular parasite and a gram-negative spherical pathogen that is the pathogen of epidemic avian chlamydia (1). The most common related disease is human atypical pneumonia, which is a rare cause of community-acquired pneumonia, accounting for approximately 1% of community-acquired pneumonia (2). A study on the detection rate of IgM antibodies to Mycoplasma and Chlamydia in infants and young children in Japan found that the positive rate of *C. psittaci* was approximately 2.2% (3). Spoorenberg et al. conducted PCR to detect *C. psittaci* in patients with community-acquired pneumonia in two hospitals in the Netherlands and found that the incidence of *C. psittaci* was much higher than that previously reported, approximately 4.8% (4). Among patients with severe pneumonia in the ICU, the incidence of *C. psittaci* could be as high as 8% (5). These findings suggest that the estimated incidence of *C. psittaci* in current epidemiological data may be underestimated, especially in critical patients.

The typical epidemiological data of *C. psittaci* are that humans are infected through contact with the eyes, beaks or intestinal feces of birds (1). Poultry (such as chickens, ducks,

TABLE 2 Summary of case series and case report of severe *C. psittaci* pneumonia.

Author, reported time	Reported area	Number of cases	Methods	Anti-infective drugs	History of exposure to avian or poultry	Clinical outcome
1. Chen et al. (31)	China	9	mNGS	The initial treatment of β-lactam and quinolones was ineffective. Changed to minocycline after diagnosis.	7 patients were in contact with ducks, pigeons, or poultry.	8 patients improved, 1 patient died.
2. Wang et al. (32)	China	3	mNGS	The initial treatment of carbapenems and quinolones was not effective. Changed to moxifloxacin/ceftriaxone combined with levofloxacin/moxifloxacin combined with doxycycline after diagnosis.	Bird or poultry contact	Improved
3. Zhang et al. (21)	China	1	mNSG	Doxycycline	May be related to the work environment of the wholesale market	Improved
4. Katsura et al. (33)	Japan	1	PCR	Meropenem	parrot	Died
5. Kong et al. (30)	China	2	mNGS	The initial treatment of moxifloxacin was not effective, changed to tigecycline was effective.	1 patient's workplace was located upstairs of a farmers' market (including poultry market areas). 1 patient had an exposure history of pigeon feces.	Improved
6. Shi et al. (12)	China	1	mNGS	The initial treatment of moxifloxacin was ineffective, changed to doxycycline + moxifloxacin + azithromycin after diagnosis.	No	Improved
7. Zhang et al. (34)	China	1	mNGS	The initial treatment of β-lactam and moxifloxacin was ineffective. Changed to moxifloxacin and doxycycline after diagnosis.	No	Improved
8. Yuan et al. (35)	China	1	mNGS	Meropenem + Doxycycline	Poultry	Improved, but died after discharge.
9. Meijer et al. (13)	Netherlands	1	PCR	Doxycycline, Ceftriaxone, Ciprofloxacin	Pigeons	Improved
10. Wu et al. (29)	China	13	mNGS	The initial treatment of β-lactams and quinolones was ineffective, changed to tetracyclines after the diagnosis.	Yes	11 patients improved, 2 patients died.
11. Teng et al. (36)	China	5	mNGS	1 patient received moxifloxacin; 2 patients received doxycycline; 2 patients received doxycycline combined with moxifloxacin.	3 patients had an exposure history of poultry.	4 patients improved, a pregnant woman died.
12. Wen et al. (28)	China	2	mNGS	1 patient was used ceftazidime, ofloxacin, ertapenem, micafungin, imipenem, tigecycline, moxifloxacin, and sulfamethoxazole, and changed to doxycycline combined with moxifloxacin after diagnosis. 1 patient used third-generation cephalosporin, moxifloxacin and peramivir, and changed to moxifloxacin after diagnosis.	1 patients had an exposure history of pigeons	Improved
13. Qi et al. (37)	China	1	mNGS	Piperacillin, imipenem, and moxifloxacin were ineffective. Changed to moxifloxacin and imipenem after diagnosis.	Duck	Improved
14. Arenas-Valls et al. (38)	Spain	2	PCR and MIF	Ceftriaxone, Levofloxacin, Doxycycline	Birds	Improved
15. Spoorenberg et al. (4)	Netherlands	1	PCR and MIF	Cephalosporins, Quinolones, Erythromycin	Pigeons	Improved

(Continued)

TABLE 2 (Continued)

Author, reported time	Reported area	Number of cases	Methods	Anti-infective drugs	History of exposure to avian or poultry	Clinical outcome
16. Fraeyman et al. (39)	Belgium	2	PCR	Moxifloxacin	Pigeons	Improved
17. Bourne et al. (40)	England	1	MIF	The initial treatment of ciprofloxacin was ineffective, and changed to erythromycin combined with rifampicin after diagnosis.	Budgerigar	Improved
18. Soni et al. (41)	Australian	2	CF and MIF	The initial treatment of ceftriaxone + erythromycin was ineffective, and changed to rifampicin + ciprofloxacin/ doxycycline after diagnosis.	Parrot	Improved
19. Verweij et al. (42)	Netherlands	1	PCR	The initial treatment of amoxicillin + erythromycin was ineffective, and changed to doxycycline + gentamicin after diagnosis.	Parrot	Improved
20. Lamáury et al. (10)	The United States	1	MIF	Used erythromycin, and changed to doxycycline after diagnosis.	Pigeons	Died
21. Shapiro et al. (43)	The United States	1	ulture + MIF	Used cefaclor, erythromycin, vancomycin, gentamicin, and ceftazidime. and changed to doxycycline after diagnosis.	Parrot	Improved
22. Villemonteix et al. (44)	France	1	CF and MIF	Amoxicillin + Clavulanic acid + Gentamicin + Spiramycin	Aborted sheep	Improved
23. Wang et al. (45)	China	1	mNGS	Meropenem and Doxycycline	Yes	Improved

etc.) can also be infected with *C. psittaci* and then infect humans. The transmission routes include raising poultry or frequently visiting poultry markets (6). There were also reports in the that humans were infected through mammals, such as sheep and horses, but were rare (7, 8). There have also been reports of human-to-human transmission (9). Our patient had no history of direct contact with birds and poultry before the illness, but there were neighbors who raised birds in the patient's residential area, not except for indirect contact.

The manifestations of *C. psittaci* include fever, headache, muscle aches, dry cough, dyspnea, etc., and some patients may have relative bradycardia. Severe cases may also involve other organs, including the heart, liver, skin, and central nervous system, and cause symptoms (10–14). Our patient had bradycardia, a prolonged Q-T interval, and elevated myocardial enzymological markers, which may be associated with *C. psittaci* involving the heart.

In most patients, the white blood cell counts were normal, the proportion of neutrophils was increased, the lymphocytes were decreased, C-reactive proteins (CRP) and erythrocyte sedimentation rates (ESR) were significantly increased, and the increase in procalcitonins was not obvious. In our patient, the initial white blood cell count did not increase significantly, but the CRP level increased significantly. After admission, the patient's white blood cell count, CRP and procalcitonin were all increased significantly, which might be related to secondary infection (sputum culture suggests Pseudomonas aeruginosa).

Interleukin 6 is the main mediator of physiological, hematological, and immunological reactions during the acute phase of inflammation, especially regulating the synthesis of liver proteins in the acute phase. In rodent models of experimentally induced fever, the important role of IL-6 as a circulating endogenous pyrogen has been well established (15). Prohl et al. confirmed that after inoculating *C. psittaci* into the lungs of calves, the activity of IL-6 in BALF was significantly higher than that in blood serum and revealed no apparent relation between IL-6 in blood and body temperature, but they did reveal a relation between IL-6 and other markers of inflammation in BALF and concluded that a local inflammatory response in the lungs of infected calves caused fever (16). In our patient, IL-6 was also significantly increased in the BALF and was not significantly increased in the blood. This indicates that human infection with *C. psittaci* can also cause a strong local inflammatory response in the lungs and cause fever. The inflammatory response in the blood is mild and may have no relation with fever.

Chest CT of *C. psittaci* pneumonia showed ground glass-like changes or consolidation, and the lower lobes of the lung were often involved. This was occasionally accompanied by pleural effusion and mediastinal lymph node enlargement. Large shadows on the lung lobes and extensive bilateral pneumonia may also appear in severe cases (17). Chest CT of our patient showed consolidation of the lower lobe of the left lung initially and quickly progressed to extensive bilateral pneumonia, with hilar node enlargement, without pleural effusion. After the treatment was effective, the lung inflammation was significantly absorbed, only a few fiber cords remained, and the mediastinal lymph nodes were smaller than before.

There have been few reports of *C. psittaci* pneumonia in the past, on the one hand due to its low incidence and on the other hand due to the difficulty of diagnosis. Traditional pathogen culture is time-consuming, and *C. psittaci* needs to be cultured in cells, which requires very high laboratory conditions, so clinical application is rare. Serological testing is mainly used for retrospective studies, which has little value for the early diagnosis of severe patients, and most hospitals in China do not carry out such inspection items at present. PCR tests can quickly identify *C. psittaci* (18, 19), but this test has also not been carried out in Chinese hospitals. mNGS can quickly and accurately identify pathogens and has been widely used in the diagnosis of infectious diseases, especially to detect pathogens that cannot be detected by traditional methods (20). In recent years, with the widespread use of mNGS, an increasing number of cases of psittacosis have been diagnosed. We reviewed 23 articles, including 54 cases of severe Chlamydia psitsiti pneumonia. There were 12 articles using mNGS to confirm the diagnosis, all of which were reported in China.

In our patient, only *C. psittaci* was found in mNGS of BALF, with a sequence of 70 reads and without other background pathogens. We sent blood samples to other testing institutions for mNGS, and *C. psittaci* was also detected, with a sequence of 38 reads. These results indicate that the invasion of *C. psittaci* into the human body can not only cause lung infection but can also spread in the patient's body and lead to explosive systemic disease, which may be related to the special infection mechanism of the intracellular bacteria. It has also been reported in the literature that *C. psittaci* first enters the reticuloendothelial cells of the liver and spleen to proliferate and then enters the lungs and other organs through the bloodstream (21, 22). Therefore, human psittacosis is a systemic infection, mainly respiratory infections (13, 23). Our patient was diagnosed with *C. psittaci* pneumonia. After symptomatic anti-infection treatment, the patient's fever and dyspnea improved significantly, and the inflammatory indicators returned to normal. Re-examination of lung CT indicated that the lung inflammation was significantly absorbed. On the 24th day of hospitalization, we reexamined the patient's blood mNGS, indicating that *C. psittaci*s was not detected. Then, tigecycline was discontinued, and the total course of treatment was 21 days. During the follow-up, the patient was in good condition and returned closely to her premorbid condition. Currently, the specific course of treatment for *C. psittaci* is uncertain and is generally believed to be 10–21 days. Whether a prolonged course of treatment can prevent recurrence is still controversial. Whether the negative results of mNGS in BALF and blood can be used as evidence of drug withdrawal remains to be further clinically observed.

Tetracyclines are the first choice for the treatment of *C. psittaci* pneumonia, including doxycycline, tetracycline and minocycline. In the previous articles about severe *C. psittaci* infection, 22 patients (54 cases in total) responded to tetracycline therapy in combination with or alone after diagnosis, and 5 patients did not respond to the treatment and died. The deaths were thought to be related to the subsequent infections of other resistant bacteria, but the possibility of tetracycline resistance has not been determined.

When the use of tetracycline is contraindicated, macrolides (erythromycin, azithromycin, etc.) can be used instead, but it may not be effective in patients with severe disease or pregnancy (24). In previous studies, there were successful cases of using macrolides alone, but they were all mild patients. There was no successful case of severe *C. psittaci* pneumonia treated with macrolides alone. These results indicate that macrolides have a poor effect on severe *C. psittaci* and should be combined with other drugs.

The intracellular activity of quinolones against *C. psittaci* was lower than that of tetracycline and macrolides, but they showed activity against *C. psittaci in vitro* (25, 26). In previous studies, 41 cases (54 cases in total) of severe patients had been treated with quinolones, among which 29 cases had failed to be treated with quinolones initially, and 6 cases were improved by quinolones alone. These results indicate that quinolones are effective in the treatment of *C. psittaci* and can be used for severe *C. psittaci* pneumonia, but there may be drug resistance in some patients and treatment failure. Currently, the use of antibiotics in the poultry and pet bird industries is increasing, which may have contributed to the drug resistance of *C. psittaci* (27). Our patient had been treated with cephalosporin and moxifloxacin intravenously for 7 days in the local hospital but did not improve. After being transferred to our department, the patient was given meropenem combined with levofloxacin intravenously but still had intermittent fever. *C. psittaci* in this patient was resistant to quinolones. After the diagnosis of *C. psittaci*, the patient was treated with tigecycline and improved. Tigecycline is a new tetracycline antibiotic that is mainly used for the treatment of severe abdominal infection, lung infection and bloodstream infection. There have been few reports on the treatment of Chlamydia psittacosis pneumonia with tigecycline. Wen et al. (28) reported a case of severe *C. psittaci* pneumonia in which tigecycline was used for treatment, but the treatment effect was not described in detail. Wu et al. (29) reported that three patients received carbapenems, linezolid, or tigecycline in addition to doxycycline treatment after diagnosis, but the outcomes were not stated. Kong et al. (30) reported that two patients with severe *C. psittaci* pneumonia were not effective in initial treatment with moxifloxacin and were improved after using tigecycline. This demonstrates that tigecycline can be used as an alternative treatment for severe *C. psittaci* pneumonia, especially in patients

with coexisting secondary infections, because of its broad antibacterial spectrum. Whether tigecycline is better than other tetracycline drugs in severe patients needs further large-sample clinical observation.

In conclusion, the manifestations of *C. psittaci* pneumonia are diverse and lack specificity. The overall prognosis is good, but severe patients may die if they are not treated in time. The mNGS is a promising detection method. For patients with severe infections, patients who were not efficacious with empirical anti-infection treatment, or patients who were possibly infected with special pathogens, mNGS testing should be performed as soon as possible.

Author contributions

YG contributed in diagnosing the disease, data collection, and data analysis. JL contributed to literature search and figures preparation. YG and JL were the main contributors to drafting the manuscript and performed the final manuscript review. Both authors read and approved the final manuscript.

Funding

This study was supported by grants from the National Natural Science Foundation of China (No. 82100020).

Conflict of interest

The authors declare that the research was conducted in the absence of any commercial or financial relationships that could be construed as a potential conflict of interest.

Publisher's note

All claims expressed in this article are solely those of the authors and do not necessarily represent those of their affiliated organizations, or those of the publisher, the editors and the reviewers. Any product that may be evaluated in this article, or claim that may be made by its manufacturer, is not guaranteed or endorsed by the publisher.

References

1. Balsamo G, Maxted AM, Midla JW, Murphy JM, Wohrle R, Edling TM, et al. Compendium of measures to control *Chlamydia psittaci* infection among humans (psittacosis) and pet birds (avian chlamydiosis), 2017. *J Avian Med Surg.* (2017) 31:262–82. doi: 10.1647/217-265

2. Hogerwerf L, De Gier B, Baan B, Van Der Hoek W. *Chlamydia psittaci* (psittacosis) as a cause of community-acquired pneumonia: a systematic review and meta-analysis. *Epidemiol Infect.* (2017) 145:3096–105. doi: 10.1017/S0950268817002060

3. Numazaki K, Chiba S, Umetsu M. Detection of IgM antibodies to *Chlamydia trachomatis*, *Chlamydia pneumoniae*, and *Chlamydia psittaci* from Japanese infants and children with pneumonia. *In Vivo.* (1992) 6:601–4.

4. Spoorenberg SM, Bos WJ, van Hannen EJ, Dijkstra F, Heddema ER, van Velzen-Blad H, et al. *Chlamydia psittaci*: a relevant cause of community-acquired pneumonia in two Dutch hospitals. *Neth J Med.* (2016) 74:75–81.

5. Wu X, Li Y, Zhang M, Li M, Zhang R, Lu X, et al. Etiology of severe community-acquired pneumonia in adults based on metagenomic next-generation sequencing: a prospective multicenter study. *Infect Dis Ther.* (2020) 9:1003–15. doi: 10.1007/s40121-020-00353-y

6. Hogerwerf L, Roof I, de Jong MJK, Dijkstra F, van der Hoek W. Animal sources for zoonotic transmission of psittacosis: a systematic review. *BMC Infect Dis.* (2020) 20:192. doi: 10.1186/s12879-020-4918-y

7. Janssen MJ, van de Wetering K, Arabin B. Sepsis due to gestational psittacosis: a multidisciplinary approach within a perinatological center–review of reported cases. *Int J Fertil Womens Med.* (2006) 51:17–20.

8. Johnson FW, Matheson BA, Williams H, Laing AG, Jandial V, Davidson-Lamb R, et al. Abortion due to infection with Chlamydia psittaci in a sheep farmer's wife. *Br Med J.* (1985) 290:592–4. doi: 10.1136/bmj.290.6468.592

9. Lei JH, Xu Y, Jiang YF, Shi ZH, Guo T. Clustering cases of *Chlamydia psittaci* pneumonia in coronavirus disease 2019 screening ward staff. *Clin Infect Dis.* (2021) 73:e3261–e3265. doi: 10.1093/cid/ciaa1681

10. Lamáury I, Sotto A, Le Quellec A, Perez C, Boussagol B, Ciurana AJ. *Chlamydia psittaci* as a cause of lethal bacterial endocarditis. *Clin Infect Dis.* (1993) 17:821–2. doi: 10.1093/clinids/17.4.821

11. Samra Z, Pik A, Guidetti-Sharon A, Yona E, Weisman Y. Hepatitis in a family infected by *Chlamydia psittaci*. *J R Soc Med.* (1991) 84:347–8. doi: 10.1177/014107689108400614

12. Shi Y, Chen J, Shi X, Hu JR, Li H, Li X, et al. A case of *Chlamydia psittaci* caused severe pneumonia and meningitis diagnosed by metagenome next-generation sequencing and clinical analysis: a case report and literature review. *BMC Infect Dis.* (2021) 21:621. doi: 10.1186/s12879-021-06205-5

13. Meijer R, van Biezen P, Prins G, Boiten HJ. Multi-organ failure with necrotic skin lesions due to infection with *Chlamydia psittaci*. *Int J Infect Dis.* (2021) 106:262–4. doi: 10.1016/j.ijid.2021.03.091

14. Vande Weygaerde Y, Versteele C, Thijs E, De Spiegeleer A, Boelens J, Vanrompay D, et al. An unusual presentation of a case of human psittacosis. *Respir Med Case Rep.* (2018) 23:138–42.

15. Cartmell T, Poole S, Turnbull AV, Rothwell NJ, Luheshi GN. Circulating interleukin-6 mediates the febrile response to localised inflammation in rats. *J Physiol.* (2000) 526(Pt 3.):653–61.

16. Prohl A, Ostermann CH, Rummel CD, Roth J, Reinhold P. Circulating and broncho-alveolar interleukin-6 in relation to body temperature in an experimental model of bovine *Chlamydia psittaci* infection. *PLoS One.* (2017) 12:e0189321. doi: 10.1371/journal.pone.0189321

17. Su S, Su X, Zhou L, Lin P, Chen J, Chen C, et al. Severe *Chlamydia psittaci* pneumonia: clinical characteristics and risk factors. *Ann Palliat Med.* (2021) 10:8051–60.

18. Hisada K, Hida Y, Kawabata N, Kawashima Y, Soya Y, Shimada A, et al. Development and evaluation of a novel quenching probe PCR (GENECUBE) assay for rapidly detecting and distinguishing between *Chlamydia pneumoniae* and *Chlamydia psittaci*. *J Microbiol Methods.* (2021) 184:106212. doi: 10.1016/j.mimet.2021.106212

19. McGovern OL, Kobayashi M, Shaw KA, Szablewski C, Gabel J, Holsinger C, et al. Use of real-time PCR for *Chlamydia psittaci* detection in human specimens during an outbreak of psittacosis - Georgia and Virginia, 2018. *MMWR Morb Mortal Wkly Rep.* (2021) 70:505–9. doi: 10.15585/mmwr.mm7014a1

20. Simner PJ, Miller S, Carroll KC. Understanding the promises and hurdles of metagenomic next-generation sequencing as a diagnostic tool for infectious diseases. *Clin Infect Dis.* (2018) 66:778–88. doi: 10.1093/cid/cix881

21. Zhang H, Zhan D, Chen D, Huang W, Yu M, Li Q, et al. Next-generation sequencing diagnosis of severe pneumonia from fulminant psittacosis with multiple organ failure: a case report and literature review. *Ann Transl Med.* (2020) 8:401.

22. Stewardson AJ, Grayson ML. Psittacosis. *Infect Dis Clin North Am.* (2010) 24:7–25.

23. Knittler MR, Berndt A, Böcker S, Dutow P, Hänel F, Heuer D, et al. *Chlamydia psittaci*: new insights into genomic diversity, clinical pathology, host-pathogen interaction and anti-bacterial immunity. *Int J Med Microbiol.* (2014) 304:877–93. doi: 10.1016/j.ijmm.2014.06.010

24. Binet R, Maurelli AT. Frequency of development and associated physiological cost of azithromycin resistance in *Chlamydia psittaci* 6BC and C. trachomatis L2. *Antimicrob Agents Chemother.* (2007) 51:4267–75. doi: 10.1128/AAC.00962-07

25. Miyashita N, Fukano H, Yoshida K, Niki Y, Matsushima T. In-vitro activity of moxifloxacin and other fluoroquinolones against *Chlamydia species*. *J Infect Chemother.* (2002) 8:115–7. doi: 10.1007/s101560200019

26. Prohl A, Lohr M, Ostermann C, Liebler-Tenorio E, Berndt A, Schroedl W, et al. Enrofloxacin and macrolides alone or in combination with rifampicin as antimicrobial treatment in a bovine model of acute *Chlamydia psittaci* infection. *PLoS One.* (2015) 10:e0119736. doi: 10.1371/journal.pone.0119736

27. Beeckman DS, Vanrompay DC. Zoonotic *Chlamydophila psittaci* infections from a clinical perspective. *Clin Microbiol Infect.* (2009) 15:11–7. doi: 10.1111/j.1469-0691.2008.02669.x

28. Wen W, Gu L, Zhao LW, Chen MY, Yang WQ, Liu W, et al. [Diagnosis and treatment of *Chlamydia psittaci* pneumonia: experiences of 8 cases]. *Zhonghua Jie He He Hu Xi Za Zhi.* (2021) 44:531–6.

29. Wu HH, Feng LF, Fang SY. Application of metagenomic next-generation sequencing in the diagnosis of severe pneumonia caused by *Chlamydia psittaci*. *BMC Pulm Med.* (2021) 21:300. doi: 10.1186/s12890-021-01673-6

30. Kong CY, Zhu J, Lu JJ, Xu ZH. Clinical characteristics of *Chlamydia psittaci* pneumonia. *Chin Med J.* (2021) 134:353–5.

31. Chen X, Cao K, Wei Y, Qian Y, Liang J, Dong D, et al. Metagenomic next-generation sequencing in the diagnosis of severe pneumonias caused by *Chlamydia psittaci*. *Infection.* (2020) 48:535–42. doi: 10.1007/s15010-020-01429-0

32. Wang Y, Lu H, Shao R, Wang W. [Clinical characteristics analysis of patients with pneumonia infected by *Chlamydia psittaci*]. *Zhonghua Wei Zhong Bing Ji Jiu Yi Xue.* (2020) 32:1388–90.

33. Katsura D, Tsuji S, Kimura F, Tanaka T, Eguchi Y, Murakami T. Gestational psittacosis: a case report and literature review. *J Obstet Gynaecol Res.* (2020) 46:673–7.

34. Zhang Q, Li S, Zhou W, Zheng L, Ren Y, Dong L, et al. Application of metagenomic next-generation sequencing (mNGS) combined with rapid on-site cytological evaluation (ROSCE) for the diagnosis of *Chlamydia psittaci* pneumonia. *Int J Clin Exp Pathol.* (2021) 14:389–98.

35. Yuan Y, Zhang X, Gui C. Detection of *Chlamydia psittaci* in both blood and bronchoalveolar lavage fluid using metagenomic next-generation sequencing: a case report. *Medicine.* (2021) 100:e26514. doi: 10.1097/MD.0000000000026514

36. Teng XQ, Gong WC, Qi TT, Li GH, Qu Q, Lu Q, et al. Clinical analysis of metagenomic next-generation sequencing confirmed *Chlamydia psittaci* pneumonia: a case series and literature review. *Infect Drug Resist.* (2021) 14:1481–92. doi: 10.2147/IDR.S305790

37. Qi YF, Huang JL, Chen JH, Huang CP, Li YH, Guan WJ. [*Chlamydia psittaci* pneumonia complicated with rhabdomyolysis: a case report and literature review]. *Zhonghua Jie He He Hu Xi Za Zhi.* (2021) 44:806–11.

38. Arenas-Valls N, Chacón S, Pérez A, Del Pozo R. Atypical *Chlamydia Psittaci* pneumonia. four related cases. *Arch Bronconeumol.* (2017) 53:277–9. doi: 10.1016/j.arbres.2016.10.006

39. Fraeyman A, Boel A, Van Vaerenbergh K, De Beenhouwer H. Atypical pneumonia due to *Chlamydophila psittaci*: 3 case reports and review of literature. *Acta Clin Belg.* (2010) 65:192–6. doi: 10.1179/acb.2010.040

40. Bourne D, Beck N, Summerton CB. *Chlamydia psittaci* pneumonia presenting as acute generalised peritonism. *Emerg Med J.* (2003) 20:386–7. doi: 10.1136/emj.20.4.386

41. Soni R, Seale JP, Young IH. Fulminant psittacosis requiring mechanical ventilation and demonstrating serological cross-reactivity between Legionella longbeachae and *Chlamydia psittaci*. *Respirology.* (1999) 4:203–5. doi: 10.1046/j.1440-1843.1999.00176.x

42. Verweij PE, Meis JF, Eijk R, Melchers WJ, Galama JM. Severe human psittacosis requiring artificial ventilation: case report and review. *Clin Infect Dis.* (1995) 20:440–2. doi: 10.1093/clinids/20.2.440

43. Shapiro DS, Kenney SC, Johnson M, Davis CH, Knight ST, Wyrick PB. Brief report: *Chlamydia psittaci* endocarditis diagnosed by blood culture. *N Engl J Med.* (1992) 326:1192–5. doi: 10.1056/NEJM199204303261805

44. Villemonteix P, Agius G, Ducroz B, Rouffineau J, Plocoste V, Castets M, et al. Pregnancy complicated by severe *Chlamydia psittaci* infection acquired from a goat flock: a case report. *Eur J Obstet Gynecol Reprod Biol.* (1990) 37:91–4. doi: 10.1016/0028-2243(90)90101-6

45. Wang L, Shi Z, Chen W, Du X, Zhan L. Extracorporeal membrane oxygenation in severe acute respiratory distress syndrome caused by *Chlamydia psittaci*: a case report and review of the literature. *Front Med.* (2021) 8:731047. doi: 10.3389/fmed.2021.731047

frontiers | Frontiers in Medicine

TYPE Case Report
PUBLISHED 15 December 2022
DOI 10.3389/fmed.2022.1066870

OPEN ACCESS

EDITED BY
Suzana Erico Tanni,
São Paulo State University, Brazil

REVIEWED BY
Alessandro Wasum Mariani,
Faculdade de Medicina da Universidade de São Paulo, Brazil
Patricio Maskin,
Centro de Educación Médica e Investigaciones Clínicas Norberto Quirno (CEMIC), Argentina

*CORRESPONDENCE
Lin Jiang
jianglinhapch@126.com
Rentao Wang
rtwang@126.com
Pengtao Bao
bao03@163.com

†These authors have contributed equally to this work

SPECIALTY SECTION
This article was submitted to Pulmonary Medicine, a section of the journal Frontiers in Medicine

RECEIVED 11 October 2022
ACCEPTED 28 November 2022
PUBLISHED 15 December 2022

CITATION
Gong J, Tian F, Wang Q, Mu M, Geng S, Hao P, Zhong P, Zhang R, Jiang L, Wang R and Bao P (2022) Case report: Rare epithelioid hemangioendothelioma occurs in both main bronchus and lung. *Front. Med.* 9:1066870. doi: 10.3389/fmed.2022.1066870

Case report: Rare epithelioid hemangioendothelioma occurs in both main bronchus and lung

Jiuyu Gong[1†], Fangfang Tian[2†], Qin Wang[3†], Mi Mu[2], Sijia Geng[2,4], Pengfei Hao[2,4], Pengfei Zhong[2,4], Rui Zhang[2], Lin Jiang[1*], Rentao Wang[2*] and Pengtao Bao[2*]

[1]Hubei Province Corps Hospital of CAPF, Wuhan, China, [2]The Eighth Medical Center of Chinese PLA General Hospital, College of Pulmonary and Critical Care Medicine, Chinese PLA General Hospital, Beijing, China, [3]Jinhua Municipal Central Hospital, Jinhua, China, [4]Graduate School, Hebei North University, Zhangjiakou, Hebei, China

Pulmonary epithelioid hemangioendothelioma (PEH) is a rare vascular tumor of endothelial origin with low- to intermediate-grade malignant potentials. Since there is no characteristic clinical or biological marker available for PEH, most cases require a surgical lung biopsy for diagnosis. To date, although some patients with PEH reported in the literature were diagnosed through bronchoscopic biopsy, most of the patients still underwent surgical lung biopsy for confirmation. In this case report, we present a rare case diagnosed as PEH through endobronchial biopsies due to the presence of an intraluminal mass that blocked the trachea and caused atelectasis in the right upper lobe. Moreover, since surgery was not appropriate for this patient with unresectable bilateral multiple nodules, we adopted genetic analysis using NGS to provide a guide for personalized treatment. Then, based on the NGS results, the patient was treated with anti-PD-1 mAb and sirolimus for 1 year and has been stable in a 1-year follow-up examination.

KEYWORDS

case report, pulmonary epithelioid hemangioendothelioma, bronchoscopic, genetic analysis, *POLE* (P286R) mutation

Introduction

Pulmonary epithelioid hemangioendothelioma (PEH) is known as a rare vascular neoplasm mostly arising as a primary tumor either in the lung or in the pleura (1, 2). The typical radiographic findings of PEH are multiple small bilateral perivascular lung nodules that generally measure less than 20 mm in diameter (3). PEH can also present as multiple pulmonary reticulonodular opacities or diffuse infiltrative pleural thickening (4). However, there were quite a few reports with the description of PEH with tracheal and bronchial invasion. Because of the specific clinical and imaging manifestations, the unique pathological pattern is critical for the diagnosis of PEH (5, 6). According to the distribution feature, a surgical lung biopsy but not a bronchoscopic biopsy is used for

the diagnosis. In this report, we present a rare case that not only invaded the lung but also invaded the trachea and blocked the airway are blocked, which appears to be a central type of lung cancer. We also review the literature on PEH with an emphasis on the systematic treatment that is discussed in this case report.

Case presentation

A 50-year-old male patient was referred to the hospital complaining of intermittent bloody sputum for more than a year and dyspnea for 1 week. He never smoked and had a history of left nephrectomy because of a renal malignant tumor. He has been suffering from the symptoms of paroxysmal cough and occasionally bloody sputum since April 2020. He even felt tightness in his chest and shortness of breath after a severe cough. So, he took a chest computerized tomography (CT) in a local hospital, and it showed that there was a mass in the lung. However, he did not undergo further examination and started traditional Chinese medical herbal treatment. After more than 1 year of treatment with Chinese herbs, hemoptysis aggravated and progressive dyspnea kept him in bed. He went to our hospital's emergency clinic, where a chest CT revealed an obstructed main bronchus, an atelectasis in the upper lobe of the right lung, and patchy shadows and nodules scattered throughout both lungs. The vital signs at the time of the initial assessment were stable. Initial routine laboratory results were normal. Blood gas analysis revealed a pH of 7.41, PO_2 of 71 mmHg, and a pressure of carbon dioxide of 44 mmHg.

To confirm whether there were extrapulmonary lesions, he underwent a positron emission tomography (PET) scan of the whole body, which did not reveal any increased standardized uptake value except for the neoplasm in the right lung (**Figure 1**).

Then, the patient underwent bronchoscopy with a transbronchial biopsy, which revealed neoplasia in the bronchus blocking the opening of the right main bronchus (**Figure 2A**). During the fiberoptic bronchoscopy, an unexpected decline in oxygen pressure suspended the intratracheal operation. Fortunately, we obtained enough tumor tissues for pathological analysis. The biopsy revealed that mucous epithelium is squamous metaplasia, and submucosal spindle cell proliferation was significant (partly SMA +), accompanied by mucinous degeneration and hemorrhage and necrosis. More irregular vascular spaces can be observed, and some epithelioid cell hyperplasia (CK +, TTF1-) is obvious, with mild atypia, some large nuclei, and rare mitosis, which is considered epithelioid hemangioendothelioma (borderline tumor and malignant transformation). Immunohistochemical stains showed positive staining of the tumor cells for CD10, CD31, CD34, Fli-1, CK, Vimentin, FVIII, and Ki-67 (20%). Desmin, Actin, D68, TTF-1, P53, S-100, and LCA were negative in the tumor cells (**Figure 3**).

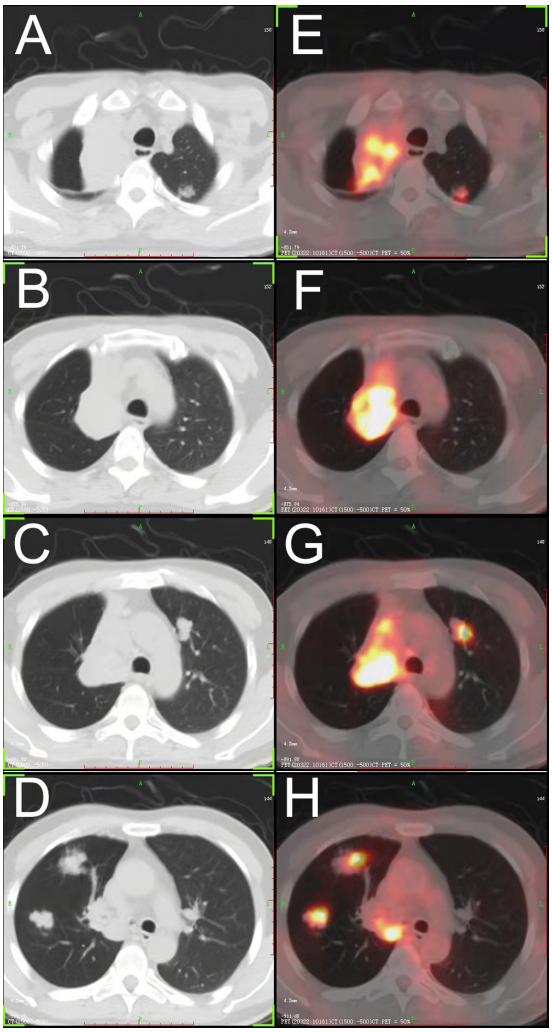

FIGURE 1
(A–D) Chest CT showing a large tumor in the hilum of the right lung, and multiple bilateral pulmonary nodules. **(E–H)** FDG-positron emission tomography/CT showing high accumulation of FDG in each lesion. FDG, fluorodeoxyglucose.

Surgery is not recommended for this patient as the tumor is bilateral diffused, and the largest tumor is distributed in the peritoneal region and invades the trachea and main bronchus. We attempted to take a rigid bronchoscopy and attempted to resect the tumor under an endoscope to liberate the right main bronchus. Unfortunately, the operation was not successfully performed because a rapid decline in oxygen saturation occurred as the process began. Then, to improve the anoxic caused by obstruction of the right main bronchus and atelectasis in the right upper lobe, the patient underwent drug-eluting bead bronchial arterial chemoembolization (DEB-BACE) for the reduction of the tumor (7). Moreover, the chemotherapy drugs including gemcitabine 1,000 mg and carboplatin 300 mg were infused into the branch.

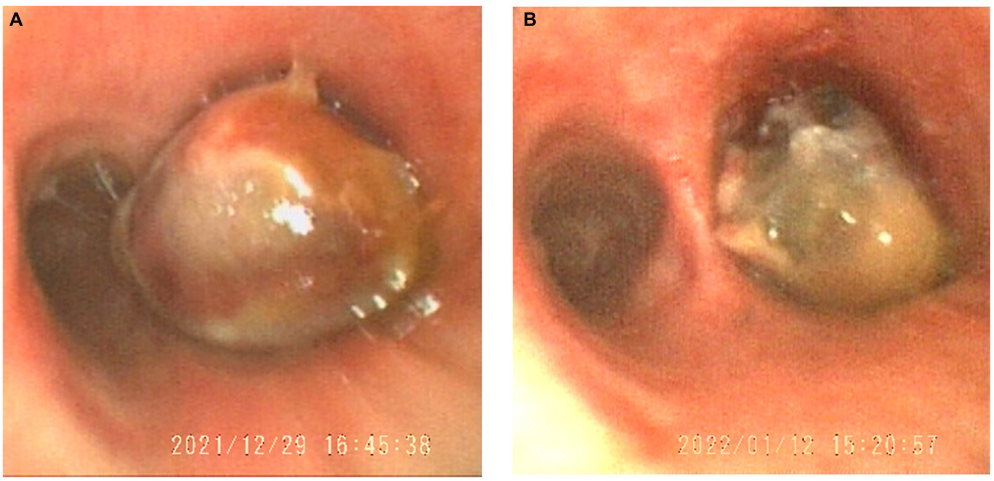

FIGURE 2
The tumor in the trachea obstructed the main right bronchial opening viewed in the bronchoscope **(A)**. After vascular thrombosis therapy, the tumor reduced **(B)**.

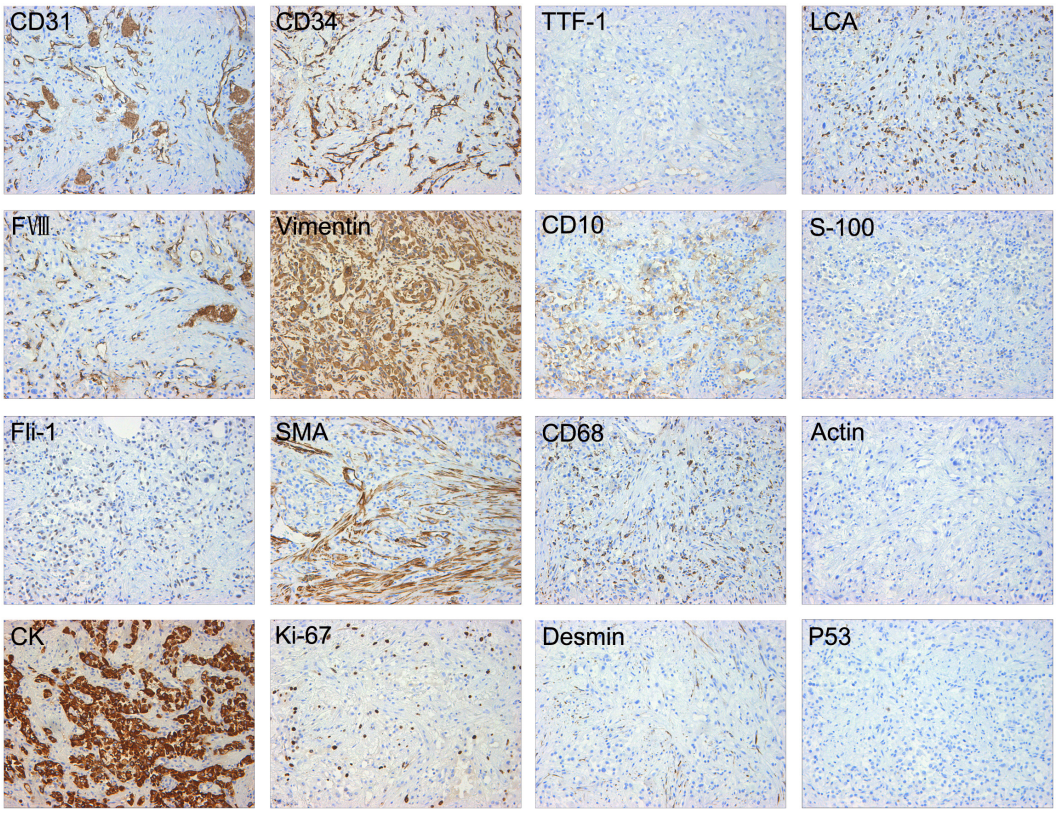

FIGURE 3
Immunohistochemical stains showed positive staining of the tumor cells for CD31, CD34, Fli-1, CK, Vimentin, FVIII, CD10, and Ki-67 (20%). Desmin, Actin, SMA, CD68, TTF-1, P53, S-100, and LCA were negative in the tumor cells.

Then, the patient underwent circulating tumor cell detection. A total of three CEP8-triploid cells and no circulating tumor microemboli were detected in circulation. For personalized medicine, full exon gene testing was performed and revealed that there were 31 somatic gene mutations, one of which has clinical consequences. The mutated gene

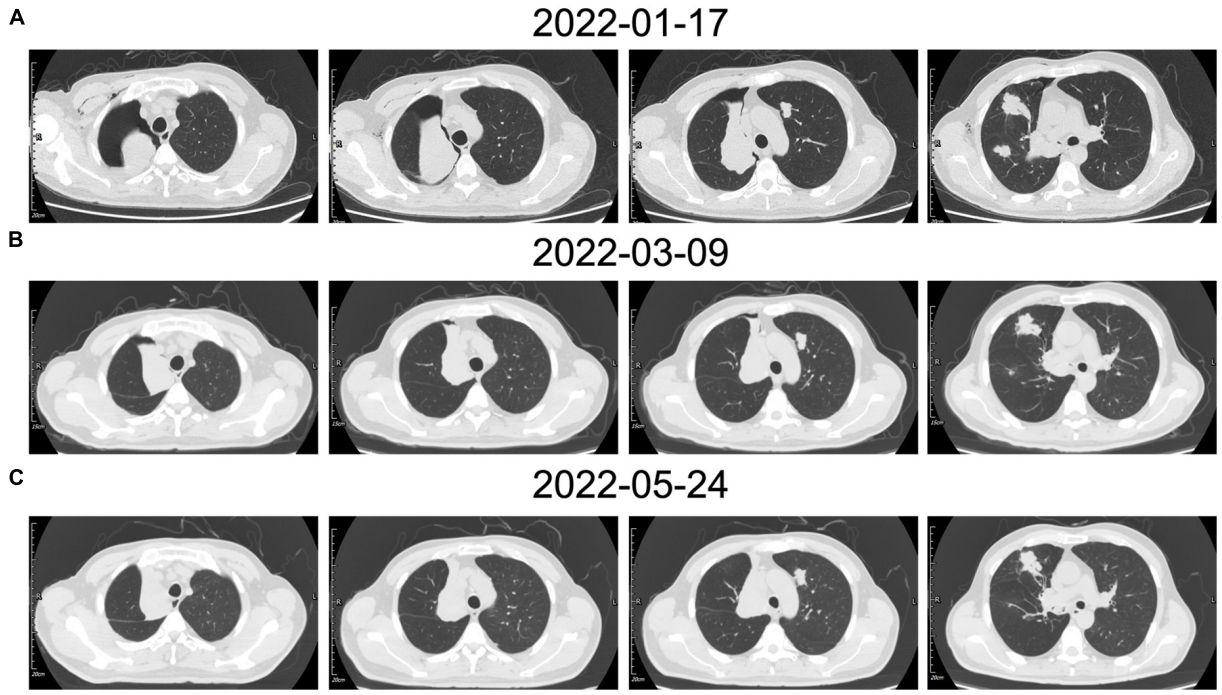

FIGURE 4
(A) The patient's chest CT examination conducted for the first time showed multiple nodules located in the bilateral lobe, the right main bronchus was obstructed which caused pulmonary atelectasis in the right upper lobe. **(B)** The chest CT examination after vascular intervention showed recruitment of the superior lobe of the right lung. **(C)** In contrast to the previous chest CT, the most recent chest CT showed a reduction in tumor size.

POLE, which has been found in colorectal and endometrial carcinomas, has been shown to correlate with cancer prognosis. According to previous studies, *POLE* mutations can potentially predict beneficial clinical outcomes in patients receiving immune checkpoint inhibitors such as anti-PD-1 therapy. On the contrary, in some cases, sirolimus proved to be effective in epithelioid hemangioendothelioma (EHE). As a result, the patient was treated individually with pembrolizumab of 200 mg once a week for 1 year, as well as sirolimus. No significant adverse effects were detected. He has since been followed for more than a year and showed stabilization of the disease (**Figure 4**).

Discussion

According to the previous reports, bilateral multiple small nodular opacities (<2 cm in diameter) are the most common presentation radiographically (8, 9). Moreover, multiple pulmonary nodules distribute in a perivascular pattern, and the perivascular nodules are usually found near medium-sized vessels and bronchi and are generally located in the middle and lower lobe (4, 10). Pleural effusion and pleural thickening were present in some cases, and the pleural involvement with malignant pleural effusion proved as a poor prognostic factor (11). In this case, there were also multiple nodules located in the bilateral lobe and each lesion possessed high fluorodeoxyglucose (FDG) accumulation according to PET/CT, which was in line with the previous report (5, 12). However, one of the biggest lesions arising centrally in the lung obstructed the right main bronchus and caused atelectasis of the right upper lobe (**Figure 1**). We observed neoplasia in the opening of the right main bronchus by fiberoptic bronchoscopy and took a biopsy of the lump. It has been reported that some cases underwent biopsy by bronchoscopy (13), but most of them obtained negative results because the lesions were always located in lung tissues and did not invade the bronchus.

There is no standard treatment for PEH. Surgical resection is the best treatment for single or multiple nodules on one side. However, this patient with bilateral multiple lung nodules was not appropriate for surgical operation, thus DEB-BACE was performed to minimize the burden of the tumor (7). Fortunately, according to the second fiberoptic bronchoscopy, we found the tumor, which obstructed the right main bronchus, significantly reduced (**Figure 2**). In addition, radiographic reexamination showed recruitment of the superior lobe of the right lung.

Moreover, the patient still required systemic therapy. Since this tumor is generally resistant to various chemotherapies, in

order to identify the most beneficial treatment option for this patient, we performed a full exon genetic test to locate the target gene. We have found 31 somatic gene mutations in 30 genes in this case. In contrast to the tumor-associated genetic variants, a genetic mutation in the *POLE* gene is associated with immune checkpoint therapy. The *POLE* mutations in colorectal and endometrial carcinoma have been reported to be a predictive factor for anti-PD1 treatment in some cases (14, 15). While we have not identified the critical gene mutation in the pathogenesis of this condition, the genetic test results provide us with a potentially effective treatment. Meanwhile, the mTOR inhibitor sirolimus has also been evaluated in treating a small cohort of patients with EHE with promising results (11, 16). Thus, we developed an individualized treatment for this case with sirolimus and pembrolizumab. After more than 1-year of follow-up, the patient remained in stable condition (**Figure 4**). It still needs further observation to evaluate the effectiveness of this personality treatment. For this rare disease, for which there is no standard treatment, we hope to find an individualized treatment protocol based on genetic analysis and pharmacodynamics tests.

Data availability statement

The raw data supporting the conclusions of this article will be made available by the authors, without undue reservation.

Ethics statement

Written informed consent was obtained from the individual(s) for the publication of any potentially identifiable images or data included in this article.

Author contributions

PB, RW, and LJ designed the entire study. MM, SG, PH, PZ, and RZ conducted patient clinical management. JG, FT, and QW analyzed the data. JG wrote the manuscript. All authors read and approved the final version of the manuscript for submission.

Funding

This study was supported by the Logistic Support Department of CMC Health Care Project (No. 21BJZ35) and Beijing Natural Science Foundation (No. 7212104).

Conflict of interest

The authors declare that the research was conducted in the absence of any commercial or financial relationships that could be construed as a potential conflict of interest.

Publisher's note

All claims expressed in this article are solely those of the authors and do not necessarily represent those of their affiliated organizations, or those of the publisher, the editors and the reviewers. Any product that may be evaluated in this article, or claim that may be made by its manufacturer, is not guaranteed or endorsed by the publisher.

References

1. Kitaichi M, Nagai S, Nishimura K, Itoh H, Asamoto H, Izumi T, et al. Pulmonary epithelioid haemangioendothelioma in 21 patients, including three with partial spontaneous regression. *Eur Respir J.* (1998) 12:89–96. doi: 10.1183/09031936.98.12010089

2. PáLföldi R, Radács M, Csada E, Molnár Z, Pintér S, Tiszlavicz L, et al. Pulmonary epithelioid haemangioendothelioma studies in vitro and in vivo: new diagnostic and treatment methods. *In Vivo.* (2013) 27:221–5.

3. Liu H, Wang J, Lang J, Zhang X. Pulmonary epithelioid hemangioendothelioma: imaging and clinical features. *J Compu Assist Tomogr.* (2021) 45:788–94.

4. Xiong W, Wang Y, Ma X, Ding X. Multiple bilateral pulmonary epithelioid hemangioendothelioma mimicking metastatic lung cancer: case report and literature review. *J Int Med Res.* (2020) 48:300060520913148. doi: 10.1177/0300060520913148

5. Oda N, Maeda Y, Kiura K, Miyahara N. Pulmonary epithelioid haemangioendothelioma mimicking lung cancer. *BMJ Case Rep.* (2021) 14:e240152.

6. Aung T, Chu A, Kondapi D, Markabawi D, Mirchia K, Kaul PA. Case of pulmonary epithelioid hemangioendothelioma with literature review. *Case Rep Oncol Med.* (2020) 2020:8048056.

7. Lin H, Wang Q, Tian F, Zhang R, Mu M, Zhao W, et al. Drug-eluting beads bronchial arterial chemoembolization in treating relapsed/ refractory small cell lung cancer patients: results from a pilot study. *Cancer Manag Res.* (2021) 13:6239–48. doi: 10.2147/CMAR.S310115

8. Onishi Y, Kusumoto M, Goto Y, Kaku S, Motoi N. Epithelioid hemangioendothelioma of the lung: CT findings and clinical course of 35 cases. *Jpn J Clin Oncol.* (2020) 50:1195–200. doi: 10.1093/jjco/hyaa106

9. Epelboym Y, Engelkemier D, Thomas-Chausse F, Alomari A, Al-Ibraheemi A, Trenor C, et al. Imaging findings in epithelioid hemangioendothelioma. *Clin Imaging.* (2019) 58:59–65.

10. Onishi Y, Kusumoto M, Motoi N, Hiraoka N, Sugawara S, Itou C, et al. Natural history of epithelioid hemangioendothelioma of the liver: CT findings of 15 cases. *Acad Radiol.* (2021) 28:778–82. doi: 10.1016/j.acra.2020.04.015

11. Zhang W, Liu Y, Chai Y, Shi K, Chen J, Shi D, et al. Case report: rare pulmonary sclerosing pneumocytoma: large, multiple, metastatic, and fatal. *Front Med.* (2021) 8:661032. doi: 10.3389/fmed.2021.661032

12. Calabrese C, Gilli M, De Rosa N, Di Crescenzo V, Zeppa P, Vitale C, et al. Role of FDG-PET scan in staging of pulmonary epithelioid hemangioendothelioma. *Open Med.* (2016) 11:158–62. doi: 10.1515/med-2016-0025

13. Sakata K, Gotway M, Smith M, Parish J, Agrwal N, Karlin N, et al. Pulmonary epithelioid hemangioendothelioma diagnosed with endobronchial biopsies: a case report and literature review. *J Bronchol Interv Pulmonol.* (2016) 23:168–73. doi: 10.1097/LBR.0000000000000230

14. Wen L, Chen Z, Ji X, Fong W, Shao Q, Ren C, et al. Pathological complete response to immune checkpoint inhibitor in patients with colorectal cancer liver metastases harboring POLE exonuclease domain mutation. *J Immunother Cancer.* (2022) 10:e004487. doi: 10.1136/jitc-2022-004487

15. Garmezy B, Gheeya J, Lin H, Huang Y, Kim T, Jiang X, et al. Clinical and molecular characterization of POLE mutations as predictive biomarkers of response to immune checkpoint inhibitors in advanced cancers. *JCO Precis Oncol.* (2022) 1:e2100267. doi: 10.1200/PO.21.00267

16. Engel E, Cournoyer E, Adams D, Stapleton SA. Retrospective review of the use of sirolimus for pediatric patients with epithelioid hemangioendothelioma. *J Pediatr Hematol.* (2020) 42:e826–9. doi: 10.1097/MPH.0000000000001643

frontiers | Frontiers in Medicine

TYPE Case Report
PUBLISHED 16 December 2022
DOI 10.3389/fmed.2022.1075745

OPEN ACCESS

EDITED BY
Yousef Shahin,
The University of Sheffield,
United Kingdom

REVIEWED BY
Sanjay Chandnani,
Topiwala National Medical College and BYL Nair Charitable Hospital, India
Patrick Zardo,
Hannover Medical School, Germany

*CORRESPONDENCE
Luís Maurício Batalin Júnior
luisbatalin@gmail.com
Suzana Erico Tanni
suzanapneumo@gmail.com

SPECIALTY SECTION
This article was submitted to Pulmonary Medicine, a section of the journal Frontiers in Medicine

RECEIVED 20 October 2022
ACCEPTED 23 November 2022
PUBLISHED 16 December 2022

CITATION
Batalin Júnior LM, Zandoná MCeSS, Vargas TA, Oliveira JCd, Chiappetto JRS, Oliveira CV, Romeiro FG and Tanni SE (2022) Case report: Biliobronchial fistula after biliary tract stenosis.
Front. Med. 9:1075745.
doi: 10.3389/fmed.2022.1075745

Case report: Biliobronchial fistula after biliary tract stenosis

Luís Maurício Batalin Júnior[1,2]*, Mariana Conceição e Silva Seleme Zandoná[1,2], Thomaz Almeida Vargas[1,2], Julio Cesar de Oliveira[1,2], Juliana Rocha Souza Chiappetto[1,2], Cassio Vieira Oliveira[1,2], Fernando Gomes Romeiro[1,2] and Suzana Erico Tanni[1,2]*

[1]Pulmonary Division of Internal Medicine, Botucatu School of Medicine—UNESP, São Paulo, Brazil, [2]Gastroenterology Division of Internal Medicine, Botucatu School of Medicine—UNESP, São Paulo, Brazil

Biliobronchial fistula (BBF) is a rare abnormality resulting from congenital or acquired communication between the bile ducts and the bronchial tree. Patients often suffer from chronic cough, dyspnea, and bilioptysis, a pathognomonic symptom of this condition. Conservative methods such as less-invasive procedures are gradually consolidating. Nonetheless, surgery remains the primary treatment, especially in more complex cases. We present the case of a 44-year-old woman with a chronic cough, no verified periods of fever, cyclic jaundice, and episodes of yellowish sputum. She had undergone cholecystectomy in 2018 and had been hospitalized several times since for pneumonia treatment. All consequent investigations for mycobacteriosis were negative. When referred to our hospital, she had cyclic jaundice and parenchymal consolidation in the right lower lobe. Suspected bilioptysis motivated the search for a biliobronchial fistula. Magnetic resonance cholangiography (MRC) confirmed stenosis of the biliary tract and fistulous path, and sputum analysis indicated high bilirubin levels. External biliary bypass was performed as an initial conservative and definitive therapy due to the presence of liver cirrhosis. Although BBF is a rare condition when bilioptysis is suspected, a diagnostic investigation should be initiated. Our case study proposes two criteria for diagnosis: an imaging exam demonstrating the fistulous path and confirmation of bilirubin in the sputum or bronchoalveolar lavage (BAL). When diagnosed, surgical correction should be performed.

KEYWORDS

biliobronchial fistula, biliary tract stenosis, bilioptysis, cyclic jaundice, pneumonia

Introduction

Peacock first described biliobronchial fistula (BBF) in 1850 as a rare abnormality resulting from the pathological communication between the bile ducts and the bronchial tree (1). Its underlying cause can be congenital or acquired, related to trauma, liver infection, neoplasia, or biliary obstruction (2–7).

Patients with BBF usually present bile expectoration as a cardinal symptom. Other clinical signs include cough, dyspnea, and abdominal or thoracic pain. The diagnosis is based on clinical symptoms and confirmation of bile in the sputum or bronchoalveolar lavage. Less-invasive procedures can be attempted, but conservative surgery is still the primary treatment, especially for more complex cases. However, there is no established guideline for the optimal management of this rare condition, and treatment must be individualized.

Case report

We report the clinical scenario of a 44-year-old woman who presented to our hospital with a 4-year history of cough, no verified periods of fever, cyclic jaundice, and expectoration of yellowish sputum. The patient had undergone cholecystectomy in 2018 and was hospitalized several times for the treatment of bacterial pneumonia as she started complaining of cyclic jaundice and frequent cough with dyspnea after surgery.

Her chronic cough during those hospitalizations led to several sputum culture analyses, including mycobacteriosis, which was negative. Concomitantly, cirrhosis diagnosis was performed due to bile duct stenosis using magnetic resonance cholangiography (MRC) and she was classified with a MELD (model for end-stage liver disease) score of 17 and a Child–Pugh score of 7.

In a previous hospital admission, the general examination identified a regular general condition with severe jaundice. Systemic examination showed thoracic auscultation with a decreased vesicular murmur, mainly at the lower right hemithorax, associated with crackling noises. The liver was palpable at 2 cm below the right costal margin with a blunt edge and a previous cholecystectomy scar.

During the current hospital admission, the patient presented with a cough with yellowish expectorant (Figure 1), dyspnea, and fever and was started on antibiotics for pneumonia. Initial laboratory tests showed compromised liver function (total bilirubin = 8.6 mg/dL, conjugate bilirubin = 7.2 mg/dL) with signs of acute liver injury (AST = 218 U/L, ALT = 131 U/L, GGT = 533 U/L, AP = 1,301 U/L). Blood count presented with hemoglobin = 14.2 g/dL, hematocrit = 42.8%, white blood cells = $10.9 \times 10^3/mm^3$, and platelets $343 \times 10^3/mm^3$, without abnormalities in the coagulogram.

Chest and abdominal computed tomography (CT) showed a right lower lobe alveolar consolidation with air bronchograms, surrounded by opacities with ground-glass attenuation compatible with an inflammatory or infectious process (Figure 2). Moreover, the liver showed an enlarged right lobe, with chronic disease characteristics and marked dilation of the intrahepatic bile ducts, without an obstructive factor or dilatation of the hepatocholedochal duct. A biochemical analysis of the sputum showed increased conjugated bilirubin (14.4 mg/dL).

FIGURE 1
Sample of yellowish expectoration.

Magnetic resonance cholangiography confirmed that bile duct stenosis and the interconnection of the bile duct between the posterior region of the liver and the right lower bronchi originated after the sequelae of cholecystectomy (Figure 3).

The surgical team performed an external biliary bypass, and the patient presented clinical improvement and was discharged 3 days after the procedure. At this time, laboratory tests showed decreased levels of total bilirubin = 3.1 mg/dL, conjugated bilirubin = 2.7 mg/dL, AST = 40 U/L, ALT = 46 U/L, GGT = 503 U/L and AP = 593 U/L.

She was re-evaluated 1 month later by the surgical team who decided to continue with the external biliary bypass regarding the liver cirrhosis. We performed a new chest CT scan 4 months after surgery, which demonstrated partial resolution of the inflammatory process. However, it presented a sequelae bronchiectasis with parenchymal fibrosis (Figure 4). At this time, the patient did not present respiratory symptoms or expectoration.

Abbreviations: BBF, Bronchobiliary fistula; MRC, magnetic resonance cholangiography; CT, Computed tomography; BAL, bronchoalveolar lavage; GGT, Gamma-glutamyl Transferase; AP, alkaline phosphatase; AST, aspartate aminotransferase; ALT, alanine aminotransferase.

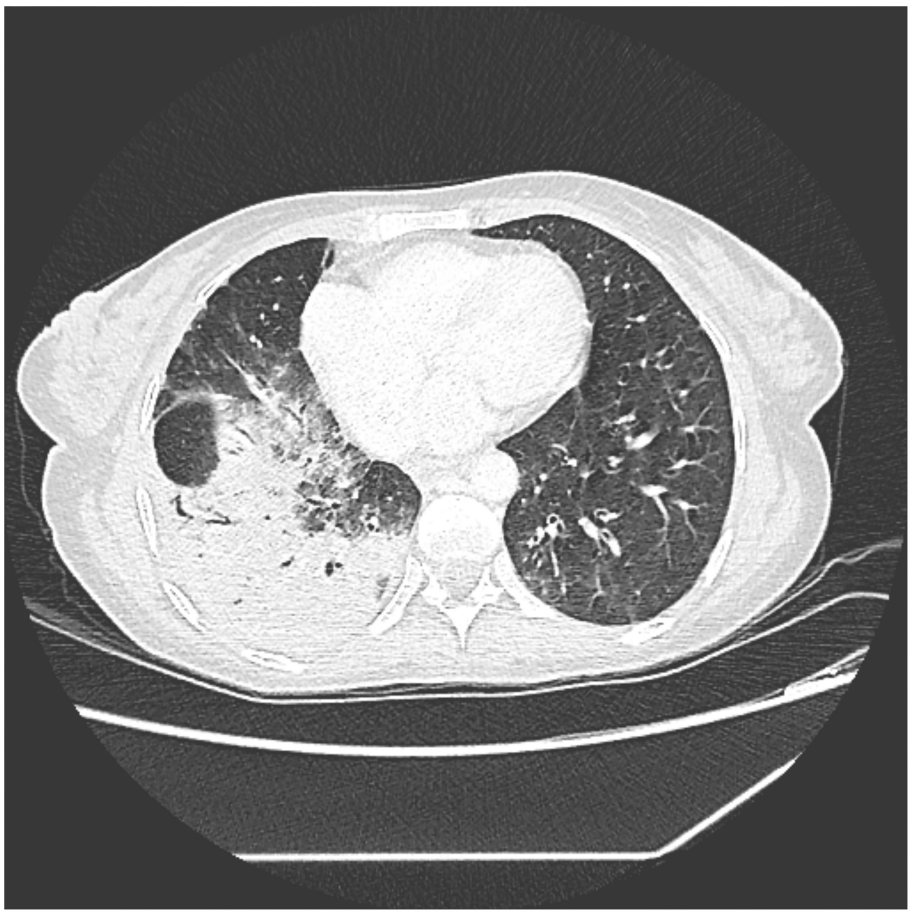

FIGURE 2
Slice of CT scan showing parenchymal consolidation of the right lower lobe.

Discussion

The physiopathology of BBF is related to injury of the adjacent lung or pleural space by erosion of the diaphragm. Consequently, the expansion of a subphrenic infected biloma with a concomitant liver and a direct diaphragmatic injury are described in cases of tumors, or in postoperative or post-ablation cases (biliary stenosis/lithiasis). In postoperative iatrogenic stenosis, such as reported in this case, the bile duct obstruction may lead to cholangitis, intrahepatic abscess, and rupture of abscess into the pleural space or bronchi when the complication is associated with adhesions. This fact explains the preferential location of bronchobiliary fistulas on the right side of the chest. However, some exceptional cases of bronchobiliary fistulas located on the left side have also been described in literature due to invasive liver disease, tumor metastases, or infectious diseases with direct involvement of the diaphragm and pleural space (8–10).

A systematic review of 68 cases published between January 1980 and August 2010 showed that the main clinical manifestation was bilioptysis, which was present in all 68 reports. The volume of biliary sputum ranged from 200 to 600 ml and reached a maximum of 1.2 L daily. More than half the patients presented with fever; other clinical features were jaundice and respiratory symptoms, such as irritating cough and dyspnea (2). Chest and right upper quadrant abdominal pain can occur (11). Some patients with a chronic course may develop potentially debilitating and life-threatening conditions such as bronchiectasis, hepatic lung disease, portal hypertension, and anemia (7, 11). Our patient developed a chronic cough, dyspnea, and bilioptysis, associated with unexpected cyclic jaundice.

One diagnostic criterion proposed is imaging methods proving BBF or bile accumulations in the pleura (3, 7, 12). The most sensitive diagnostic methods are endoscopic retrograde cholangiopancreatography, percutaneous transhepatic-cholangiography, and a fistulogram of the biliocutaneus fistula (13). Correspondingly, a CT scan can be helpful for detecting air

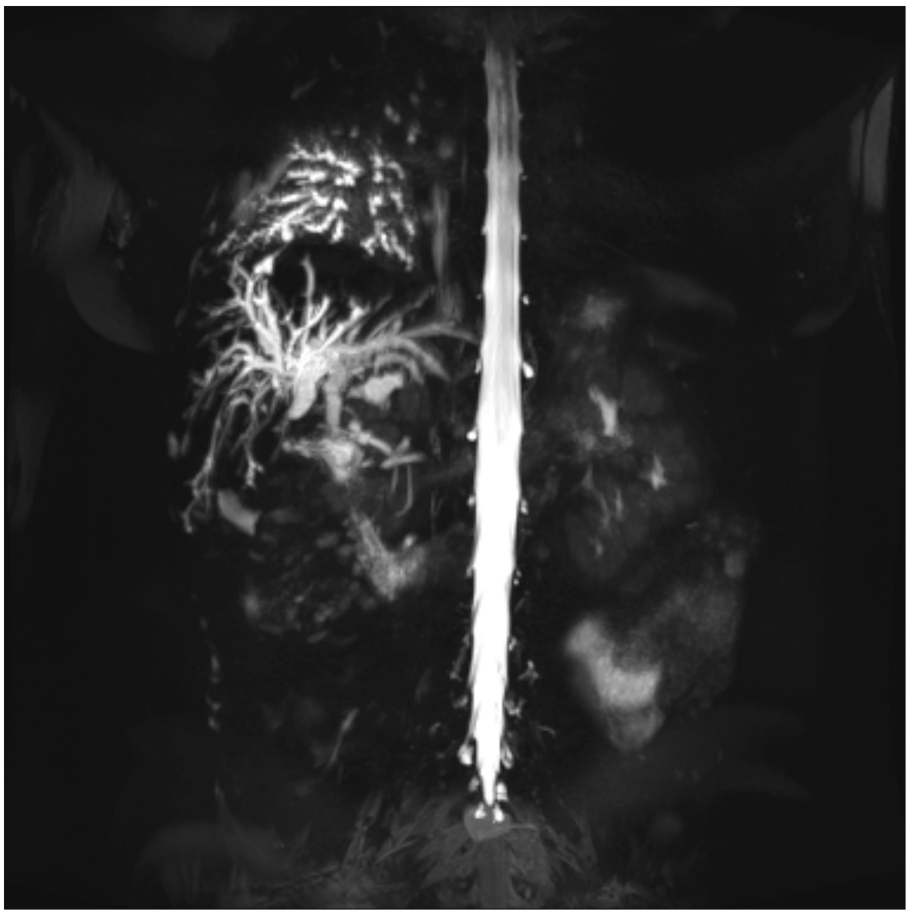

FIGURE 3
Cholangiography—MRI showing the fistulous path.

in the biliary tree, underlying hepatic abscess or hepatic biloma, pleural effusion, or pulmonary consolidation, but it might fail to demonstrate a fistula tract (11, 13). Contrast-enhanced cholangiography-MRI can identify fistulous tracts.

The other criterion is the documentation of bilirubin in sputum or BAL. However, false biliary ptyalism has been described in patients with sickle cell disease and hemolytic crisis and should be considered a confounding factor. In patients without such conditions, the presence of bile in the sputum is defined as pathognomonic BBF (14). There is no standardized method of analyzing sputum for bilirubin since it is not a routine lab test. During a bronchoscopy exam, bile in the lavage fluid may not be located. Even so, biliary pneumonia and BBF diagnosis can be made when brown bilious crystals surrounded by neutrophils are found in the transbronchial biopsy (13, 15). Bilirubin crystallization in bronchoalveolar lavage fluid can also be proof of bilirubin in the airway (16, 17). Similarly, finding bilirubin in the pleural fluid can also be used to diagnose biliopleural fistula (3, 13).

Both criteria were fulfilled in our case: bilirubin was identified in the sputum by indirect methods, and a fistulous path between the biliary tract and the bronchial tree was detected in imaging.

The BBF treatment is controversial in the literature. The use of somatostatin and its analogs has been proposed to reduce gastrointestinal secretion, but this has not been effective as a monotherapy (13). Surgical intervention is the most common treatment.

Surgical treatment is a conservative method for chronic fistulas associated with respiratory failure or sepsis, or when BBF is secondary to tumors, biliary obstruction, and trauma. Literature shows that most patients (41.7%) are treated by surgical procedures, including pulmonary lobectomy, resection, and correction of the fistula tract in the diaphragm; hepatolobectomy; hepatic enterostomy; and abscess drainage alone or in combination (3, 13).

The first stage is to perform external biliary drainage by percutaneous or surgical drainage of subphrenic abscess and/or

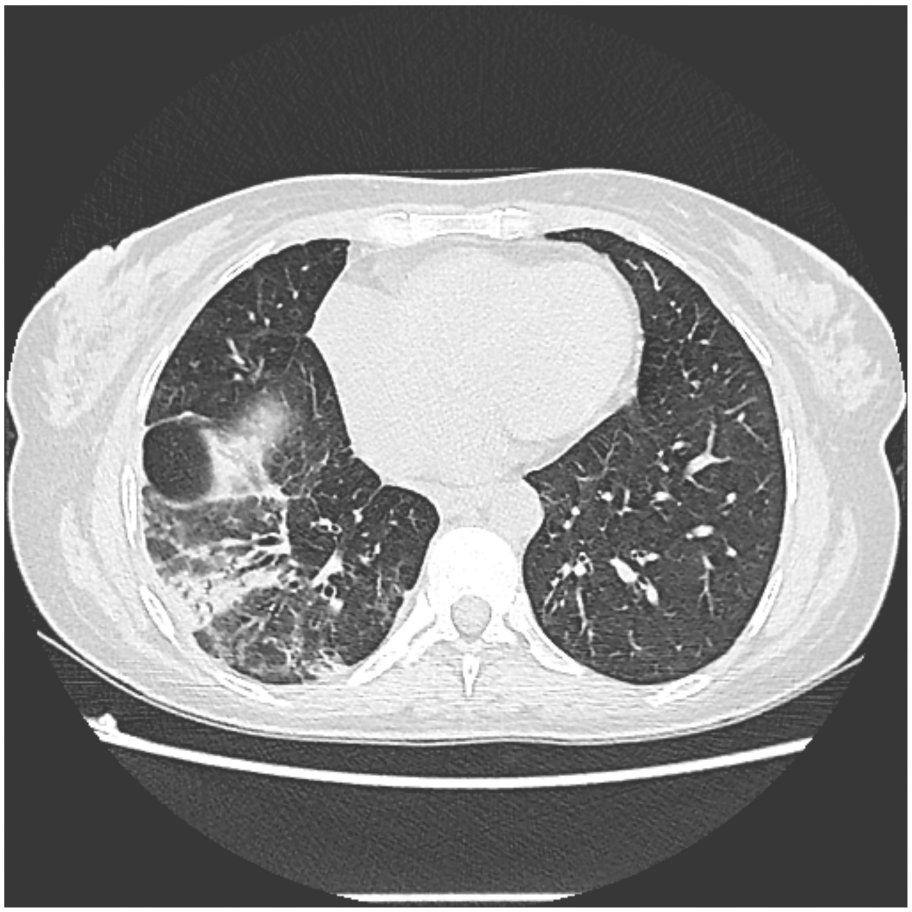

FIGURE 4
Slice of CT scan showing parenchymal fibrosis and bronchiectasis in the right lower lobe.

direct percutaneous drainage of the intrahepatic biliary tract. The second stage is to perform treatment of the underlying cause. In patients with biliary obstruction, the priority is to treat the biliary disease (8).

Less-invasive procedures tended to be employed in treating BBF, and these include endoscopic retrograde biliary drainage, endoscopic nasobiliary drainage, and endoscopic stone extraction. External biliary drainage by percutaneous ultrasound or CT scan can drain the subdiaphragmatic or intrahepatic abscess. Bronchoscopy can lead to fistula embolization. However, control of the inflammatory process can contribute to the success or failure of these methods (7, 13). External biliary drainage was performed in our case as a bridge for later definitive surgical intervention. After the procedure, cough and fever symptoms were immediately relieved, demonstrating satisfactory lung parenchyma recovery at that moment.

A transthoracic approach should be considered for rare situations in which patients maintain irreversible pulmonary and bronchial impairment or for those with traumatic bronchobiliary fistula without biliary obstruction. In this situation, pleural decortication and diaphragmatic disruption repair are recommended (8, 13).

In conclusion, although BBF is a rare condition when bilioptysis is suspected, a diagnostic investigation should be initiated. Our case study proposes two criteria for diagnosis: an imaging exam demonstrating the fistula path and a proof of bilirubin in sputum or BAL. Once diagnosed and the mechanism clarified, surgical correction is indicated. Less invasive methods are preferred over conservative methods, which are reserved for more complex cases or when treatment fails. However, individualized treatment should be emphasized for a successful outcome.

Data availability statement

The original contributions presented in the study are included in the article/supplementary material, further inquiries can be directed to the corresponding author/s.

Ethics statement

The studies involving human participants were reviewed and approved by Hospital das Clínicas of Botucatu Medical School. The patients/participants provided their written informed consent to participate in this study. Written informed consent was obtained from the individual(s) for the publication of any potentially identifiable images or data included in this article.

Author contributions

All authors listed have made a substantial, direct, and intellectual contribution to the work and approved it for publication.

Conflict of interest

The authors declare that the research was conducted in the absence of any commercial or financial relationships that could be construed as a potential conflict of interest.

Publisher's note

All claims expressed in this article are solely those of the authors and do not necessarily represent those of their affiliated organizations, or those of the publisher, the editors and the reviewers. Any product that may be evaluated in this article, or claim that may be made by its manufacturer, is not guaranteed or endorsed by the publisher.

References

1. Peacock TB. Case in which hydatids were expectorated and one of suppuration of hydatid cyst of the liver communicating with the lungs. *sl: Edinburgh Med J.* (1850) 74:33–46.

2. Liao GQ, Wang H, Zhu GY, Zhu KB, Lv FX, Tai S. Management of acquired bronchobiliary fistula: A systematic literature review of 68 cases published in 30 years. *World J Gastroenterol.* (2011) 17:3842–9. doi: 10.3748/wjg.v17.i33.3842

3. Lee MT, His SC, Hu P, et al. Biliopleural fistula: a rare complication of percutaneous transhepatic gallbladder drainage. *World J Gastroenterol.* (2007) 13:3268–70. doi: 10.3748/wjg.v13.i23.3268

4. Ghritlaharey RK. Posttraumatic bilothorax in a child: a case report. *J Clin Diagnost Res.* (2008) 2:760–3.

5. Lewis JR, Te HS, Gehlbach B, et al. A case of biliopleural fistula in a patient with hepatocellular carcinoma. *Nat Rev Gastroenterol Hepatol.* (2009) 6:248–51. doi: 10.1038/nrgastro.2009.34

6. Shimizu A, Otani Y, Ishitate M, Shimotakahara A, Miyakawa T. Congenital bronchobiliary fistula with bright yellow serous sputum. *J Pediatr.* (2022) 243:235–6. doi: 10.1016/j.jpeds.2021.12.002

7. Huang ZM, Zuo MX, Gu YK, Lai CX, Pan QX Yi XC, Zhang TQ, et al. Bronchobiliary fistula after ablation of hepatocellular carcinoma adjacent to the diaphragm: case report and literature review. *Thorac Cancer.* (2020) 11:1233–8. doi: 10.1111/1759-7714.13380

8. Gugenheim J, Ciardullo M, Traynor O, Bismuth H. Bronchobiliary fistulas in adults. *Ann Surg.* (1988) 207:90–4. doi: 10.1097/00000658-198801000-00017

9. Vu LT et al. Congenital bronchobiliary fistula: a case report and literature review. *Respirol Case Rep.* (2021) 9:e00731. doi: 10.1002/rcr2.731

10. Banerjee N, Rattan A, Priyadarshini P, Kumar S. Post-traumatic bronchobiliary fistula. *BMJ Case Rep.* (2019) 12:e228294. doi: 10.1136/bcr-2018-228294

11. Mandal A, Sen S, Baig SJ. Bronchobiliary fistula. *J Minim Access Surg.* (2008) 4:111–3. doi: 10.4103/0972-9941.45208

12. Queirós T, Castro B, Ferreira A, Amado A, Louro H, Lucas MC, Santos J, Cardoso JM, Oliveira M. Bronchobiliary fistula after stenting of biliary duct as the management of iatrogenic bile duct injury during elective cholecystectomy. *Acta Chir Belg.* (2022) 11:1–6. doi: 10.1080/00015458.2022.2049071

13. Acquasanta M, Spadarella G, Civelli EM. Spontaneous bronchobiliary fistula: Case report. *J Radiol Case Rep.* (2020) 14:10–5. doi: 10.3941/jrcr.v14i10.3743

14. Sutherland RD, Reynolds J, Sugg WL. Bile ptyalism associated with chest trauma and sickle cell crisis simulating bronchobiliary fistula. *Ann Thorac Surg.* (1972) 13:537–42. doi: 10.1016/S0003-4975(10)65170-3

15. Matsumoto T, Otsuka K, Kaihara S, Tomii K. Biliary Pneumonia due to the Presence of a Bronchobiliary Fistula. *Intern Med.* (2017) 56:1451–2. doi: 10.2169/internalmedicine.56.8066

16. Zhang N, Chen Y, Tang L, Zhou D, Hou T. Diagnosis of bronchobiliary fistula by bilirubin crystallization in the alveolar lavage fluid: case reports and literature review. *Ann Palliat Med.* (2021) 10:7121–5. doi: 10.21037/apm-21-1040

17. Cheng AC, Chen HW, Chen PJ, Huang TY, Lin JC. Bronchobiliary Fistula. *Intern Emerg Med.* (2021) 16:1093–4. doi: 10.1007/s11739-020-02572-0

frontiers | Frontiers in Medicine

TYPE Case Report
PUBLISHED 10 January 2023
DOI 10.3389/fmed.2022.1007160

OPEN ACCESS

EDITED BY
Rodrigo Torres-Castro,
University of Chile, Chile

REVIEWED BY
Catia Cilloniz,
Hospital Clinic of Barcelona, Spain
Yonghong Yang,
Beijing Children's Hospital, Capital Medical University, China

*CORRESPONDENCE
Long Li
✉ 781596710@qq.com

†These authors have contributed equally to this work

SPECIALTY SECTION
This article was submitted to Pulmonary Medicine, a section of the journal Frontiers in Medicine

RECEIVED 30 July 2022
ACCEPTED 20 December 2022
PUBLISHED 10 January 2023

CITATION
Zhang F, Qin S, Xia F, Mao C and Li L (2023) Case report: *Streptococcus pneumoniae* pneumonia characterized by diffuse centrilobular nodules in both lungs. *Front. Med.* 9:1007160. doi: 10.3389/fmed.2022.1007160

Case report: *Streptococcus pneumoniae* pneumonia characterized by diffuse centrilobular nodules in both lungs

Fangqi Zhang†, Shaowen Qin†, Fei Xia, Congzheng Mao and Long Li*

Department of Pulmonary and Critical Care Medicine, General Hospital of Central Theater Command of the People's Liberation Army, Wuhan, Hubei, China

Background: *Streptococcus pneumoniae* (*S. pneumoniae*) is the most common pathogen in community-acquired pneumonia (CAP) and takes the form of lobar pneumonia as typical computed tomography (CT) findings. Various patterns of radiological manifestation have also been reported in patients with *S. pneumoniae* pneumonia; however, the appearance of diffuse centrilobular nodules in both lungs is rarely reported.

Case presentation: We report the case of a patient with a history of chronic lymphocytic leukemia (CLL) for 9 years who presented with new-onset fever, cough, excess sputum, and shortness of breath for 1 week. He was given intravenous antibacterial (cephalosporin) treatment for 4 days, but his condition did not improve and dyspnea became more serious. The chest CT indicated diffuse centrilobular nodules in both lungs at admission. Patient's bronchoalveolar (BAL) fluid was sent for metagenomic next-generation sequencing, which only supported a diagnosis of *S. pneumoniae* infection. His condition improved gradually after antimicrobial treatment (moxifloxacin) and a follow-up CT showed that the diffuse centrilobular nodules in both lungs were absorbed completely.

Conclusion: This case highlights a rare CT presentation of *S. pneumoniae* pneumonia that should alert clinicians, so as to avoid taking unnecessary treatment measures.

KEYWORDS

***Streptococcus pneumoniae*, pneumonia, chest computed tomography, centrilobular nodules, case report**

Introduction

Streptococcus pneumoniae (*S. pneumoniae*) remains one of the most common causes of bacterial community-acquired pneumonia (CAP), encompassing infections mild enough to be treated on an outpatient basis, as well as those requiring hospital care, or even intensive care unit admission (1). Pneumolysin is the major protein virulence factor of the *S. pneumoniae* and possesses both cytotoxic and proinflammatory properties (2). The toxin is located in the cytoplasm of the *S. pneumoniae*, as well as on the cell wall, and is released extracellularly following the autolysis of the pathogen during the later stages of growth, which resulted in the development of pneumonia restricted to the lobe (2, 3). Therefore, *S. pneumoniae* pneumonia takes the form of lobar pneumonia as typical computed tomography (CT) findings (4). Various patterns and distributions of radiological manifestation have also been reported in patients with *S. pneumoniae* pneumonia owing to the widespread use of antibiotics (5). Bronchopneumonia and associated centrilobular nodules were also not uncommon in CT findings of *S. pneumoniae* pneumonia cases (6, 7). However, these nodules were usually at the periphery of consolidation, or the lesions were localized to lung segment or lobe.

Herein, we report a rare case of *S. pneumoniae* pneumonia characterized by diffuse centrilobular nodules in both lungs, which adds to the body of knowledge about *S. pneumoniae*.

Case presentation

A 66-year-old man presented with fever, cough, excess sputum, and shortness of breath for 1 week. He was given intravenous antibacterial (cephalosporin) treatment for 4 days, but his condition did not improve and dyspnea became more serious. Therefore, the patient came to our hospital where chest CT showed diffuse centrilobular nodules in both lungs, some with a "tree-in-bud" appearance (**Figure 1**), and multiple enlarged lymph nodes in mediastinum and bilateral axilla (**Figure 2**). He was then admitted to the hospital.

The patient had a history of CLL for 9 years and had received several chemotherapies in the past. His condition was stable in the past year. He has a history of smoking for 30 years. Other medical history was denied. He had no bird exposure and no history of travel outside Wuhan, Hubei, where he lived.

At admission, physical examination revealed that temperature was 37.8°C, peripheral blood oxygen saturation (SpO2) was 87% on room air, respiratory rate was 31 breaths/min, and wet rales could be heard on auscultation of both lungs. Multiple soy-sized enlarged lymph nodes could be palpable on both sides of the neck and armpits. Laboratory tests revealed that arterial blood gases at 29% fraction of inspiration O2 (FiO2) showed partial pressure of oxygen (PaO2) 65.6 mmHg, partial arterial pressure of carbon dioxide (PaCO2) 22.8 mmHg, pH 7.43, and oxygenation index (OI; PaO2/FiO2) 226 mmHg. Blood cell analyses, C-reactive protein (CRP), and erythrocyte sedimentation rate (ESR) were examined (**Table 1**). T-cell spots of tuberculosis infection (T-SPOT.TB) were positive. The detection of mycobacterium tuberculosis in bronchoalveolar (BAL) fluid by polymerase chain reaction (PCR) was negative. Sputum and BAL fluid acid-fast staining were negative. Procalcitonin, immunoglobulin (Ig) E, *Mycoplasma pneumoniae* IgM, *Chlamydia pneumoniae* IgM, and 1, 3-beta-D glucan/galactomannan tests were normal. No pathogenic bacteria or fungi were detected in blood, sputum, and BAF fluid cultures. Lymphocyte typing were noted as follows: total T cell 6% (normal, 50–87%), total T-cell number 803/μl (normal, 955–2,860/μl), CD4 + Th-cell proportion 1% (normal, 21–51%), CD4 + Th-cell number 151/μl (normal, 550–1,440/μl), total B-cell 89% (normal, 3–19%), and total B-cell number 12,603/μl (normal, 90–560/μl).

The patient was diagnosed with severe pneumonia and type 1 respiratory failure. BAL fluid was collected and sent to the Shenzhen BGI Medical Test Laboratory for metagenomic next-generation sequencing (mNGS), which only supported a diagnosis of *S. pneumoniae* infection.

After admission, the patient's condition improved gradually by giving antimicrobial treatment (moxifloxacin injection, 0.4 g, qd) and other comprehensive treatment measures, including airway clearance and oxygen support. Before discharge, SpO2, blood cell analyses, and related inflammatory markers were reexamined (**Table 1**), in which SpO2, CRP, and ESR were normal finally, and reexamination of the chest CT showed visible absorption of diffuse centrilobular nodules in both lungs (**Figure 1**). Three weeks after discharge, a follow-up CT showed that the diffuse centrilobular nodules in both lungs absorbed completely (**Figure 1**).

Discussion

The differential diagnosis of diffuse centrilobular nodules is extensive but small airway diseases are by far the most likely cause, including infectious bronchiolitis, aspiration, hypersensitivity pneumonitis, respiratory bronchiolitis (RB), and follicular bronchiolitis (8). "Tree-in-bud" indicates the presence of dilated centrilobular bronchioles with lumen impacted by mucus, fluid, or pus and is associated with peribronchiolar inflammation (9). Centrilobular nodules showing "tree-in-bud" appearance are associated with airway infection in majority of patients, and the common pathogens include mycobacterium tuberculosis, non-tubercular mycobacteria (typically MAC), *Haemophilus influenzae*, *M. pneumoniae*, *Chlamydia*, and viral and airway invasive aspergillus. In this case, however, the patient's BAL fluid was detected by mNGS, which only supported a diagnosis of *S. pneumoniae* infection. Although pathogens

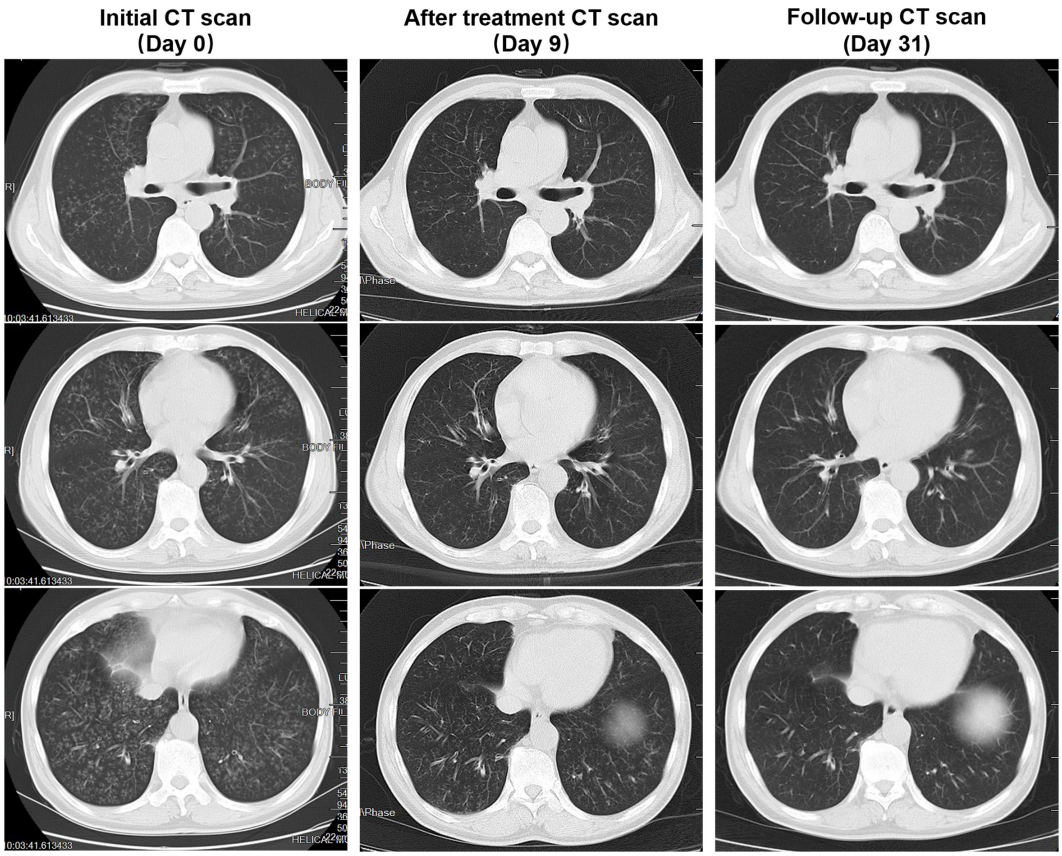

FIGURE 1
Patient's computed tomography (CT) scan images at three time points. Initial CT scan (Day 0) showed that bilateral diffuse nodules separated by the fissures and pleura. Some of the nodules have a "tree-in-bud" appearance. After treatment, CT scan (Day 9) showed visible absorption of diffuse nodules in both lungs. Follow-up CT scan (Day 31) showed that the bilateral diffuse nodules absorbed completely.

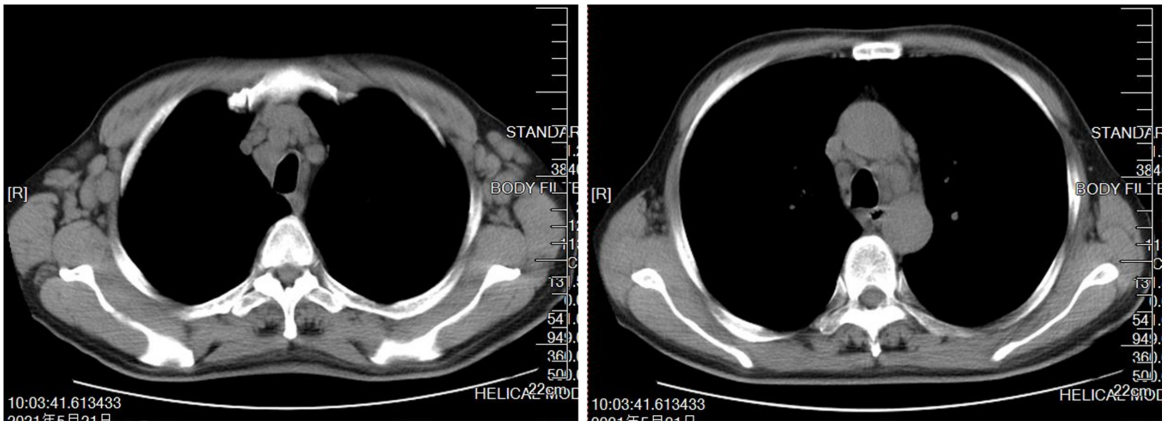

FIGURE 2
Mediastinal window of patient's initial computed tomography (CT) scan showed multiple enlarged lymph nodes in mediastinum and bilateral axilla.

mNGS can detect bacteria, viruses, fungi, and parasites without bias, there may be some omissions in RNA virus due to sample storage and transportation problems. The possibility of co-infection with virus cannot be ruled out. However, in the absence of antiviral treatment, the rapid improvement in symptoms and CT imaging in patients with an

TABLE 1 Laboratory parameters of patients at admission and before discharge.

Laboratory parameters	At admission	Before discharge
SpO2 (on room air)	87%	96%
WBC	17.1×10^9/L	12.1×10^9/L
EOS (EOS%)	0.10×10^9/L (0.6%)	0.12×10^9/L (1.0%)
NEU (NEU%)	4.98×10^9/L (29.0%)	2.02×10^9/L (16.7%)
LYM (LYM%)	11.59×10^9/L (67.7%)	9.63×10^9/L (79.7%)
CRP	89.69 mg/L	<0.449 mg/L
ESR	55 mm/h	1 mm/h

SpO2, peripheral blood oxygen saturation; WBC, white blood cell; EOS, eosinophil; NEU, neutrophil; LYM, lymphocyte; CRP, C-reactive protein; ESR, erythrocyte sedimentation rate.

impaired immune system suggests that the possibility of virus infection is unlikely.

Streptococcus pneumoniae pneumonia typically presents the form of homogeneous airspace consolidation, whereby alveolar lumens are filled with exudates containing leukocytes and alveolar walls are thickened by capillary congestion and edema (4, 5). Associated centrilobular nodules were not uncommon. Previous reports have found that 27–48% of patients with *S. pneumoniae* pneumonia exhibited centrilobular nodules on CT scans (6, 7); however, centrilobular nodules were usually at the periphery of consolidation or the lesions were localized to lung segment or lobe. To the best of our knowledge, no cases presenting diffuse centrilobular nodules in both lungs of patients with *S. pneumoniae* pneumonia have been published.

The patient had a history of CLL for 9 years and smoking for 30 years. CLL is characterized by the clonal proliferation and accumulation of mature and typically CD5 + B-cells within the blood, bone marrow, lymph nodes, and spleen (10). With an impaired immune system, patients with CLL often develop infectious complication, in which *S. pneumoniae* pneumonia is not uncommon. Unfortunately, the information of imaging patterns available about *S. pneumoniae* infection in a patient with CLL is limited. Cigarette smoking is also a common risk factor for *S. pneumoniae* pneumonia (1). The mechanisms of this association possibly include altered ciliary motility, increased nasopharyngeal carriage of organisms, altered alveolar macrophage function, and increased epithelial permeability (11). Meanwhile, there is strong evidence supporting a causal role of cigarette smoking in the development of RB and RB-associated interstitial lung disease (RB-ILD), which are also characterized by diffuse centrilobular nodules (12, 13). However, it is unknown whether these comorbid conditions contribute to this rare imaging appearance in a patient with *S. pneumoniae* infection. We hypothesize that this may have been implicated in this patient, and further studies are warranted.

This case highlights a rare CT presentation of *S. pneumoniae* pneumonia that should alert clinicians, so as to avoid taking unnecessary treatment measures.

Data availability statement

The original contributions presented in this study are included in the article/supplementary material, further inquiries can be directed to the corresponding author.

Ethics statement

Written informed consent was obtained from the individual(s) for the publication of any potentially identifiable images or data included in this article.

Author contributions

FZ and LL generated the concept. FZ and SQ drafted the manuscript. FZ was the consultant in charge of the patient. FX, CM, and LL revised the original draft critically for important intellectual content. All authors contributed to the article and approved the submitted version.

Acknowledgments

We would like to thank the patient for the consent to participate in this study and the nurses and clinical staff who provided care for the patient.

Conflict of interest

The authors declare that the research was conducted in the absence of any commercial or financial relationships that could be construed as a potential conflict of interest.

Publisher's note

References

1. Feldman C, Anderson R. The role of *Streptococcus pneumoniae* in community-acquired pneumonia. *Semin Respir Crit Care Med.* (2020) 41:455–69. doi: 10.1055/s-0040-1702193

2. Mitchell T, Dalziel C. The biology of pneumolysin. *Subcell Biochem.* (2014) 80:145–60. doi: 10.1007/978-94-017-8881-6_8

3. Feldman C, Munro N, Jeffery P, Mitchell T, Andrew P, Boulnois G, et al. Pneumolysin induces the salient histologic features of pneumococcal infection in the rat lung in vivo. *Am J Respir Cell Mol Biol.* (1991) 5:416–23. doi: 10.1165/ajrcmb/5.5.416

4. Ono A, Okada F, Takata S, Hiramatsu K, Ando Y, Nakayama T, et al. A comparative study of thin-section CT findings between seasonal influenza virus pneumonia and *Streptococcus pneumoniae* pneumonia. *Br J Radiol.* (2014) 87:20140051. doi: 10.1259/bjr.20140051

5. Haroon A, Higa F, Fujita J, Watanabe A, Aoki N, Niki Y, et al. Pulmonary computed tomography findings in 39 cases of *Streptococcus pneumoniae* pneumonia. *Intern Med.* (2012) 51:3343–9. doi: 10.2169/internalmedicine.51.7326

6. Nambu A, Saito A, Araki T, Ozawa K, Hiejima Y, Akao M, et al. *Chlamydia pneumoniae*: comparison with findings of *Mycoplasma pneumoniae* and *Streptococcus pneumoniae* at thin-section CT. *Radiology.* (2006) 238:330–8. doi: 10.1148/radiol.2381040088

7. Yagihashi K, Kurihara Y, Fujikawa A, Matsuoka S, Nakajima Y. Correlations between computed tomography findings and clinical manifestations of *Streptococcus pneumoniae* pneumonia. *Jpn J Radiol.* (2011) 29:423–8. doi: 10.1007/s11604-011-0574-x

8. Henry T, Naeger D, Looney M, Elicker B. Dyspnea and pulmonary hypertension with diffuse centrilobular nodules. *Ann Am Thorac Soc.* (2016) 13:1858–60. doi: 10.1513/AnnalsATS.201605-388CC

9. Rajagopala S, Kancherla R, Ganesan N, Balalakshmoji D, Karuppannasamy D, Ramanathan R, et al. An unusual cause of breathlessness and profuse micronodules. *Lung India.* (2018) 35:431–6. doi: 10.4103/lungindia.lungindia_452_17

10. Hallek M, Shanafelt T, Eichhorst B. Chronic lymphocytic leukaemia. *Lancet.* (2018) 391:1524–37. doi: 10.1016/S0140-6736(18)30422-7

11. Bhalla D, Hirata F, Rishi A, Gairola C. Cigarette smoke, inflammation, and lung injury: a mechanistic perspective. *J Toxicol Environ Health B Crit Rev.* (2009) 12:45–64. doi: 10.1080/10937400802545094

12. Richards J, Lynch D, Chung J. Cystic and nodular lung disease. *Clin Chest Med.* (2015) 36:299–312. doi: 10.1016/j.ccm.2015.02.011

13. Attili A, Kazerooni E, Gross B, Flaherty K, Myers J, Martinez F. Smoking-related interstitial lung disease: radiologic-clinical-pathologic correlation. *Radiographics.* (2008) 28:1383–98. doi: 10.1148/rg.285075223

frontiers | Frontiers in Medicine

TYPE Case Report
PUBLISHED 14 February 2023
DOI 10.3389/fmed.2023.1085716

OPEN ACCESS

EDITED BY
Rodrigo Torres-Castro,
University of Chile, Chile

REVIEWED BY
Nilay Etiler,
University of Nevada, Reno, United States
Ulrich Costabel,
Universitätsklinikum Essen, Germany

*CORRESPONDENCE
Qiao Ye
✉ yeqiao_chaoyang@sina.com

†These authors share first authorship

SPECIALTY SECTION
This article was submitted to Pulmonary Medicine, a section of the journal Frontiers in Medicine

RECEIVED 31 October 2022
ACCEPTED 23 January 2023
PUBLISHED 14 February 2023

CITATION
Du X, Song L, Feng R and Ye Q (2023) Pulmonary sarcoid-like granulomatosis induced by aluminum dust: A case report and literature review. *Front. Med.* 10:1085716. doi: 10.3389/fmed.2023.1085716

Pulmonary sarcoid-like granulomatosis induced by aluminum dust: A case report and literature review

Xuqin Du[1,2†], Lihong Song[3†], Ruie Feng[4] and Qiao Ye[1,2*]

[1]Department of Occupational Medicine and Toxicology, Beijing Chaoyang Hospital, Capital Medical University, Beijing, China, [2]Clinical Center for Interstitial Lung Diseases, Beijing Institute of Respiratory Medicine, Beijing, China, [3]Department of Occupational Diseases, The Affiliated Weihai Second Municipal Hospital of Qingdao University, Weihai, China, [4]Department of Pathology, Peking Union Medical College Hospital (CAMS), Beijing, China

Case report: We present a case of a 48-year-old woman with 27 months of exposure to aluminum dust and silica owing to polishing processing. The patient was admitted to our hospital with intermittent cough and expectoration. Chest high-resolution computed tomography showed diffuse ill-defined centrilobular nodules and patchy ground-glass opacities in bilateral lungs. A video-assisted thoracoscopic surgery biopsy demonstrated multiple isolated and confluent granulomas in an otherwise normal parenchyma without malignancy or signs of infection. Elemental analysis was performed on the grinding wheel powder in the workplace using an X-ray fluorescence spectrometric analyzer, showing 72.7% of Al_2O_3 and 22.8% of SiO_2 as raw materials. She was diagnosed with aluminum-associated sarcoid-like granulomatous lung disease, rather than sarcoidosis, according to occupational exposure by a multidisciplinary panel.

Conclusion: Occupational aluminum dust exposure may induce pulmonary sarcoid-like granulomatosis recognized by a multidisciplinary diagnostic panel.

KEYWORDS

granulomatosis, sarcoidosis, lung disease, case report, aluminum dust

Introduction

Exposure to aluminum dust may induce a wide range of pulmonary lesions in humans, including granulomatous pneumonia (1), pulmonary granulomatosis, pulmonary fibrosis (2), pulmonary alveolar proteinosis (3), and desquamative interstitial pneumonia (DIP) (4). In most reported patients, the main histological pictures were the presence of diffuse and extensive interstitial pulmonary fibrosis with variable degrees of emphysema. Despite these, aluminum-induced diffuse parenchymal disease has remained controversial owing to the relatively uncommon occurrence of interstitial lung diseases in aluminum-exposed workers (5, 6). Various environmental and occupational exposures have been related to sarcoidosis and sarcoid-like granulomatous lung diseases, which showed epithelioid granulomas that are pathologically and clinically indistinguishable from pulmonary sarcoidosis (7–9). To the best of our knowledge, granulomatous lung disease induced by aluminum dust is rare. The patients with aluminum-induced pulmonary inflammation, with lung biopsies showing granulomas, were similar to those found in sarcoidosis and chronic beryllium disease (9).

Understanding the potential role of aluminum in the development of lung granulomas in humans is limited to patient reports. Our research in medical literature led us to find 10 patients with granulomas secondary to aluminum or multiple exposures including aluminum, and the results are presented in Table 1. Two and eight patients exposed to aluminum and multiple metal exposures including aluminum, respectively, were reported. Nine of these patients had sarcoid-like granulomatosis patterns on their lung biopsies, and one patient had DIP associated with pulmonary granulomatosis.

The first patient with pulmonary granulomatosis associated with aluminum-containing welding fumes was reported in 1978 (1). Histological examination showed extensive interstitial granulomas composed of macrophages, foreign body giant cells, and many birefringent crystalline structures. Later, De Vuyst et al. (10) reported a patient (a chemist by profession) whose histological examination showed sarcoid-like epithelioid granulomatosis with Langhans-type giant cells. These granulomas contained dust identified by mineralogic analyses as consisting of aluminum, iron, silica, aluminosilicates, and rare occurrences of Ni, Sn, Cr, stainless steel (FeCrNi), and titanium oxides. No corticosteroids were administered, and 16 months later, chest radiograph and lung function showed no significant changes. Brancaleone et al. (11) reported a case of a dental technician who presented with non-caseating foreign body granulomas at histological examination. The bronchoalveolar lavage (BAL) lymphocytic transformation test (LTT) to beryllium nitrate detected a beryllium sensitization. Mineralogic studies showed the presence of aluminum, silica, and silicates. This patient developed lung granulomatosis most likely related to beryllium and aluminum. Cai et al. (12) reported a patient with sarcoid-like granulomatosis related to aluminum dust. High-resolution computed tomography (HRCT) showed bilateral ground-glass attenuation, patchy consolidation, extensive reticular hyperattenuating areas, and traction bronchiectasis. After 1 month of treatment with prednisone, the ground-glass attenuation decreased; the symptoms of cough, sputum, and dyspnea improved; and diffusing capacity of carbon monoxide (DLco) improved. From 2014 to 2019, five patients with granulomatosis lung disease exposed to multiple metal dust (all including aluminum) and silica were reported (13–16). Two patients were not treated with corticosteroids, while the therapy undertaken by the other three patients was not mentioned. In 2020, the first patient with DIP and pulmonary granulomatosis secondary to multiple metal exposure was reported (17). The authors concluded that DIP was associated with pulmonary granulomatosis linked to aluminum and zirconium exposure. The clinical, functional, and radiological evolution were favorable after 1 year of systemic corticosteroid treatment.

Abbreviations: GGOs, patchy ground-glass opacities; Al: aluminum; HRCT, high resolution computed tomography; FVC, forced vital capacity; TLC, total lung capacity; FEV_1, forced expiratory volume in 1 s; DLco, diffusing capacity of carbon monoxide; PaO_2, arterial oxygen tension; BAL, bronchoalveolar lavage; TBLB, transbronchial lung biopsy; VATS, video-assisted thoracoscopic surgery; ICP-MS, inductively-coupled plasma mass spectrometry; ICP-AES, inductively-coupled plasma emission spectrometer; LTT, lymphocytic transformation test; C_{TWA}, time-weighted average; C_{STEL}, short-term; occupational exposure limits (OELs); RCT, randomized control trial.

In this report, we describe a patient with pulmonary sarcoid-like granulomatosis in an aluminum polisher with clinical history, radiographic and histopathological findings, and mineralogical analyses performed on lung tissue obtained by surgical lung biopsy.

Case description

A 48-year-old woman presented with intermittent cough and expectoration, which she had been experiencing since May 2018. In early October 2018, the aforementioned symptoms significantly progressed with dyspnea on exertion. A chest radiograph recorded at a local clinic showed increased and disordered lung markings and scattered small patchy shadows in bilateral lungs. She was diagnosed with bronchopneumonia and was administered antibiotics; however, there was no improvement in dyspnea. On 8 October 2018, her chest radiograph of regular occupational medical check-ups at the local occupational disease hospital showed diffuse punctate and nodular shadows in the bilateral lungs (Figure 1B), while the initial chest radiograph taken on June 2016 (before work) was normal (Figure 1A). Chest CT scans revealed diffuse ill-defined centrilobular nodules, as well as patchy ground-glass opacities (GGOs) in bilateral lungs, and no pleural effusion was present (Figures 2A, B). The patient quit work and was admitted to a local occupational hospital for further evaluation.

On admission, arterial oxygen tension (PaO_2) was 88 mmHg at rest in room air. Her routine hematological and biochemical blood tests were normal. Autoantibodies such as an antinuclear antibody, rheumatoid factor, anti-single stranded DNA antibody, anti-double stranded DNA antibody, anti-extractable nuclear antigen antibodies, and anti-neutrophil cytoplasmic antibodies were negative. At initial presentation, pulmonary function revealed a mild obstructive pattern, with forced vital capacity (FVC) of 3.02 L (101% predicted), total lung capacity (TLC) of 5.24 L (110% predicted), forced expiratory volume in 1 s (FEV1) of 2.28 L (89% predicted), FEV1/FVC ratio of 0.75, and a reduction of diffusing capacity of carbon monoxide (DLco) of 66% predicted (Figure 2). The histological findings of transbronchial lung biopsy (TBLB) revealed sarcoid-like granulomas with multinucleated giant cells, while birefringent particles were observed in the granulomas under a polarizing microscope.

The patient worked as an accountant in a restaurant when she was 19 years old for 8 years, as a bottler in a mineral water company for 4 years, and as a housewife for the next 4 years. Then she was engaged in attaching labels to fishing rods in a factory from 2007 to 2016. She had no occupational dust or fume exposure during these three early careers. From 6th July 2016 to 8th Oct 2018, the patient was engaged in polishing snowboards at a sporting products company. She worked 5–6 days per week and 8–12 h per day, using white corundum electric grinding wheels to polish the polyethylene baseplate of snowboards. It was a wet process with water-soluble cutting fluid spraying on the electric grinding wheels. The chief constituents of water-soluble cutting fluid were polyether, lauric acid, amine, and 1H-benzotriazole. She wore dust respirators during the operation. The workplace was ~2,000 m^2 with 12 production assembly lines. There were four grinding machines with eight electric grinding wheels in every assembly line. The patient and four colleagues worked together on the same assembly line, using 30 grinding wheels each month, each weighing 10 kg. None of her 106 colleagues in the same

TABLE 1 Literature review.

No. of patients	Age (yr)	Sex	Occupation	Tissue sample	Reference	Location (country)	Histology	Elemental analysis	Corticosteroids (Y/N/NA)	Prognosis
1	31	M	Welder in the aircraft industry for 5 years	Open lung biopsy	Chen et al. (1)	USA	Diffuse pulmonary granulomatosis	Aluminum	NA	NA
2	32	M	Chemist in a catalyst fabrication plant for 8 years	TBLB	De Vuyst et al. (10)	Belgium	Sarcoid-like epithelioid granulomas with Langhans-type giant cells	Aluminum, iron, silicon, aluminosilicates, rare nickel, tin, chromium, and titanium	N	16 months later, chest radiograph and lung function show no significant changes
3	37	M	Dental laboratory technician for 20 years	VATS biopsy	Brancaleone et al. (11)	Belgium	Non-caseating epitheloid granulomas	Aluminum, silicon, silicates, beryllium	Inhaled corticosteroid	2 years later, exertional dyspnea and a little cough persist. Lung function and arterial blood gas remain unchanged
4	50	F	A worker in a metal reclamation factory for 15 years	Open lung biopsy	Cai et al. (12)	China	Non-necrotizing granulomas with multinucleated giant cells	Aluminum	Oral corticosteroid	Clinical, functional, and radiological improvement
5	64	F	To polish wood furniture with sandpaper and wire brush without protection for 40 years	Lymph node biopsy	Catinon et al. (13)	France	Non-necrotizing granulomas with epithelioid cells and multinucleated giant cells	Aluminum; silicates; steel (iron, chromium, and nickel); silica; iron; calcite; titanium	NA	NA
6	33	M	A worker in the battery manufacturing industry for 7 years	VATS biopsy	Tomioka et al. (14)	Japan	Epithelioid cell granuloma	Aluminum; silicon; iron; and titanium	N	4 years later, his VC is reduced by 12.5% and DLco is induced by 12.8%. His chest HRCT shows no changes
7	46	M	A worker in an aluminum-processing factory for 6 years	VATS biopsy	Tomioka et al. (14)	Japan	Epithelioid cell granuloma	Aluminum, silicon, iron, and titanium	N	6 years later, his chest HRCT shows no changes and no respiratory symptoms
8	44	M	To brush and polish surgical instruments without any protection for 7 years	VATS biopsy	Catinon et al. (15)	France	Granuloma with multinucleated giant cells	Aluminum, silicates, silicon, iron, steel, and titanium	NA	NA
9	59	M	A worker in a company that produced refractory material for 28 years	Lung biopsy	Baur et al. (16)	Germany	Necrotizing/focally infarcted granulomas and chronic lymphoplasmacytic inflammation	Aluminum, silicon, titanium, zirconium, niobium, vanadium, and steel	NA	NA
10	57	M	As a plumber exposed to asbestos, then a worker exposed to multiple metals (not detailed the exposure time)	VATS biopsy	Blin et al. (17)	France	DIP + non-necrotizing granulomas	Aluminum, zirconium, steel	Y	1-year evaluation: clinical, functional, and radiological improvement

Video-assisted thoracoscopic surgery (VATS) biopsy; TBLB, transbronchial lung biopsy; NA, not known or not done.

10.3389/fmed.2023.1085716

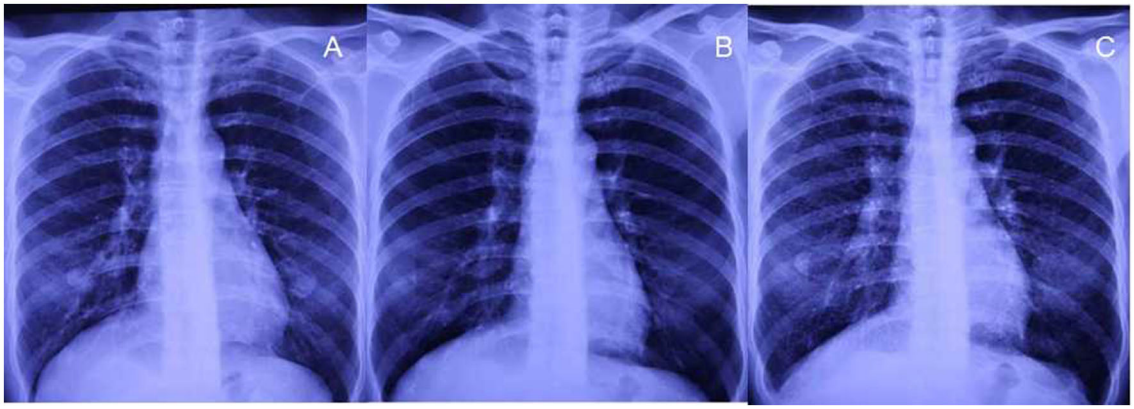

FIGURE 1
Chest radiographs before exposure and after 27 months of exposure. **(A, B)** No small nodules are observed on chest radiographs before exposure and after exposure for 15 months. **(C)** Diffuse small nodules are demonstrated on the radiograph after 27 months of exposure during work.

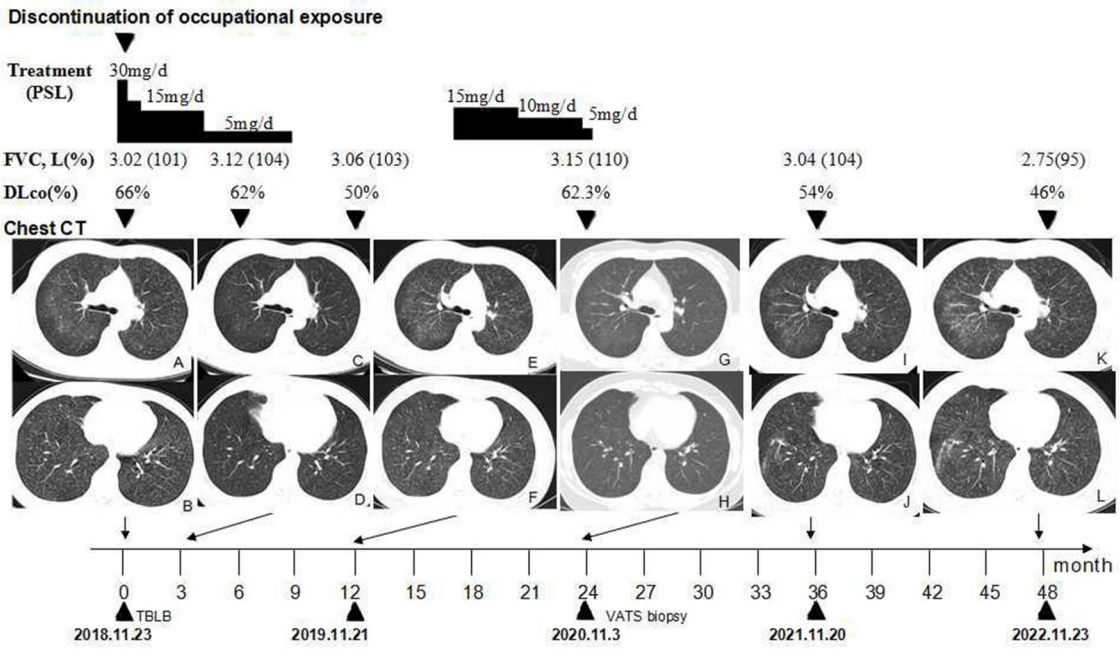

FIGURE 2
Timeline of the clinical course. **(A, B)** Chest CT showing scattered GGOs on bilateral lobular areas of ground glass attenuation and centrilobular nodules throughout the lung parenchyma before treatment. **(C, D)** GGOs are significantly reduced after the cessation of occupational exposure and using oral prednisone for 3 months. **(E, F)** GGOs and centrilobular nodules recurred after the cessation of prednisone for 3 months. **(G, H)** GGOs and centrilobular nodules significantly reduced after the second course of using oral prednisone for approximately 28 weeks. **(I–L)** Follow-up after the cessation of occupational exposure for 3 years **(I, J)** and 4 years **(K, L)**, the number of ground glass nodules in her lungs is slightly increased when compared, and fiber streak shadows are observed in the lower lobe of her right lung. CT, high-resolution computed tomography; GGOs, ground-glass opacities; PSL, prednisolone.

workplace reported similar symptoms and their chest radiographs of regular occupational medical check-ups were all normal.

The level of air dust in the workplace from 2016 to 2018 was detected. Exposure concentration of time-weighted average (C_{TWA}) and short-term (C_{STEL}) of mixed dust in a different spot of the workplace was 1.05–8 times the occupational exposure limits (OELs) in 2016 and 2017, while the concentration of polyethylene dust was within the OELs. The maximum C_{TWA} and C_{STEL} of mixed dust were 57.5 and 55.7 mg/m^3, respectively, exceeding the permissible concentration-time weighted average (8 mg/m^3) by seven times. Elemental analysis was performed on the grinding wheel powder in the workplace by an X-ray fluorescence spectrometric analyzer. The assay showed that 72.7% of Al_2O_3 and 22.8% of SiO_2 were raw materials. The water-soluble cutting fluid was detected. Microorganism stains and cultures, such as bacteria, acid-fast bacilli, and fungi, were negative.

The patient resigned from her job. She was diagnosed with pneumoconiosis at a local occupational hospital and received oral

prednisone with a dosage of 0.5 mg/kg/day for 2 weeks. The dosage was gradually tapered to 5 mg/day for a total of 36 weeks (Figure 2). The discontinuation of occupational exposure and the first course of using corticosteroids resulted in an improvement of symptoms and a slight reduction of the multiple nodules in lung fields (Figures 2C, D). In November 2019, after the cessation of oral prednisone for 3 months, the symptoms worsened, her lung function value of DLco (Figure 2) was significantly reduced to 50%, and findings on the chest CT (Figures 2E, F) were more severe than before. She received oral prednisone again with an initial dosage of 15 mg/day from 23 April 2020. The dosage was gradually tapered to 5 mg/day (Figure 2). The respiratory symptoms were improved. She was then admitted to our hospital for further medical evaluation on 3 Nov 2020. The patient had no history of other diseases. She was a non-smoker and denied having tuberculosis, night sweats, fever, chills, or weight loss previously.

Physical examination revealed chest roughness on auscultation. The remaining clinical examination was without particularity, and no extrathoracic signs or symptoms such as arthralgia, myalgia, dry eye, or dry mouth syndrome were found. The patient had no history of asthma, allergies, or any family history of respiratory disorders. Her lung function was almost improved to the initial level, with FVC of 3.15 L (110% predicted) and DLco of 62.3% predicted (Figure 2) after the second course of using prednisone in the local hospital. HRCT revealed multiple ill-defined centrilobular nodules and patchy GGOs gradually reduced with oral prednisone therapy (Figures 2G, H). Neither evidence of pleural fluid nor cardiac enlargement was noted. A video-assisted thoracoscopic surgery (VATS) biopsy of the right lower lobe was performed for further examination. The histological appearance under the microscope showed many well-formed non-necrotizing granulomas composed of epithelioid and multinucleated giant cells, mainly around the bronchi and vessels, with fibrous hyperplasia and lymphocytic inflammation (Figures 3A, B); a Schaumann body was also observed (arrows) (Figure 3C). Lightly pigmented dust macules within the interstitium were observed with adjacent focal emphysema. No classic silicotic nodules were detected. Microorganism stains and cultures, including acid-fast bacilli and fungi, were negative. In addition, 122.55 μg/g of aluminum and 455.23 μg/g of silicon were detected in the lung tissue by inductively coupled plasma mass spectrometry (ICP-MS) and inductively coupled plasma emission spectrometer (ICP-AES). No tungsten, cobalt, or beryllium was detected in both grinding wheel powder or biopsy samples.

Based on occupational dust exposure combined with clinical, radiological, and histological findings of sarcoid-like granulomatosis, the patient was diagnosed with aluminum-associated sarcoid-like granulomatous lung disease by a multidisciplinary panel, rather than sarcoidosis. Upon admission to our hospital in November 2020, the respiratory symptoms, chest HRCT scans, and lung function of DLco improved; therefore, the second course of prednisone therapy lasted for a total of ∼ 28 weeks. She was administered oral N-acetylcysteine and inhalational corticosteroids. After discharge from our hospital, she was followed up regularly in a local occupational hospital. During the 36-month follow-up observational period, her chest CT (Figures 2I, J) revealed that GGOs slightly increased, and fiber streak shadows were observed in the lower lobe of the right lung, as well as the value of DLco reduced to 54%; however, her respiratory symptoms were stable. A 48-month follow-up revealed that her symptoms of dyspnea on exertion gradually worsened, while GGOs (Figures 2K, L) gradually increased and DLco reduced to 46%. The patient gained weight significantly after oral glucocorticoid treatment. After stopping the glucocorticoid, the shortness of breath was not obvious in the resting state, so she resisted the use of glucocorticoid therapy again.

This study was approved by the Medical Ethical Committee and the patient provided informed consent for the publication of the case.

Discussion

The differential diagnosis of sarcoid-like granulomatosis induced by aluminum is challenging. First, the disease is not well-established and easy to be misdiagnosed. Second, it may be difficult to distinguish from sarcoidosis, especially by the pathological manifestations. Third, a multidisciplinary panel including occupational specialists may be essential for enhancing the accuracy of the diagnosis. A variety of infectious, occupational, and environmental factors have been implicated in sarcoid-like granulomatous lung disease (7, 8, 18). As infection is a common cause of pulmonary granulomas, infectious lung diseases must be excluded. Infectious diseases may reasonably be excluded for the absence of serologic and bacteriologic abnormalities.

Silicon was detected in both grinding wheel powder and biopsy samples. Under a polarizing microscope, several birefringence particles can be observed in the granulomas of TBLB tissues. Silicosis is common in workers who produce corundum grinding wheels and has an exposure–response relationship. The cumulative dose of silica exposure, which is respirable dust concentration multiplied by crystalline silica content and exposure duration, is considered the most important factor in the development of silicosis (19, 20). This patient was a grinder and the radiograph showed bilateral diffuse small nodules after working for only 2 years and 3 months. The elemental analysis showed a relatively low content of free silica (22.8% of SiO_2) in the raw grinding wheel powder. The surgical biopsy demonstrated that multiple sarcoid-like granulomas were composed of clustered epithelioid and multinucleated giant cells, while the silica nodules were mainly composed of dust-laden hyalinized collagen, and pathologic findings of aluminous showed diffuse interstitial fibrosis with emphysema. Recent case reports have postulated that sarcoid-like granulomatous lung disease can also be induced by silicates (21, 22). Different epidemiological studies have demonstrated a higher risk of sarcoidosis among persons occupationally exposed to silica (23). Regarding the role of aluminum combined with silicon or silicates in sarcoid-like granulomatous lung disease pathogenesis, no randomized control trial (RCT) studies other than case reports exist. However, in the present case report, the content of Al_2O_3 was much higher than that of SiO_2 in the raw material; therefore, we diagnosed the patient with aluminous-associated sarcoid-like granulomatous lung disease.

The diagnosis of sarcoidosis is based on the exclusion of other granulomatous lung diseases (24, 25). Recent epidemiologic studies have revealed a potential correlation between occupational exposure and the disease (26). Based on occupational dust exposure and initial transbronchial lung biopsy pathology, we suspected that exposure to "grinding wheel powder" resulting from her occupational history might be implicated in the development of granulomatous pulmonary disease. With elemental analysis, the X-ray fluorescence spectrum of the grinding wheel powder yielded discrete peaks for

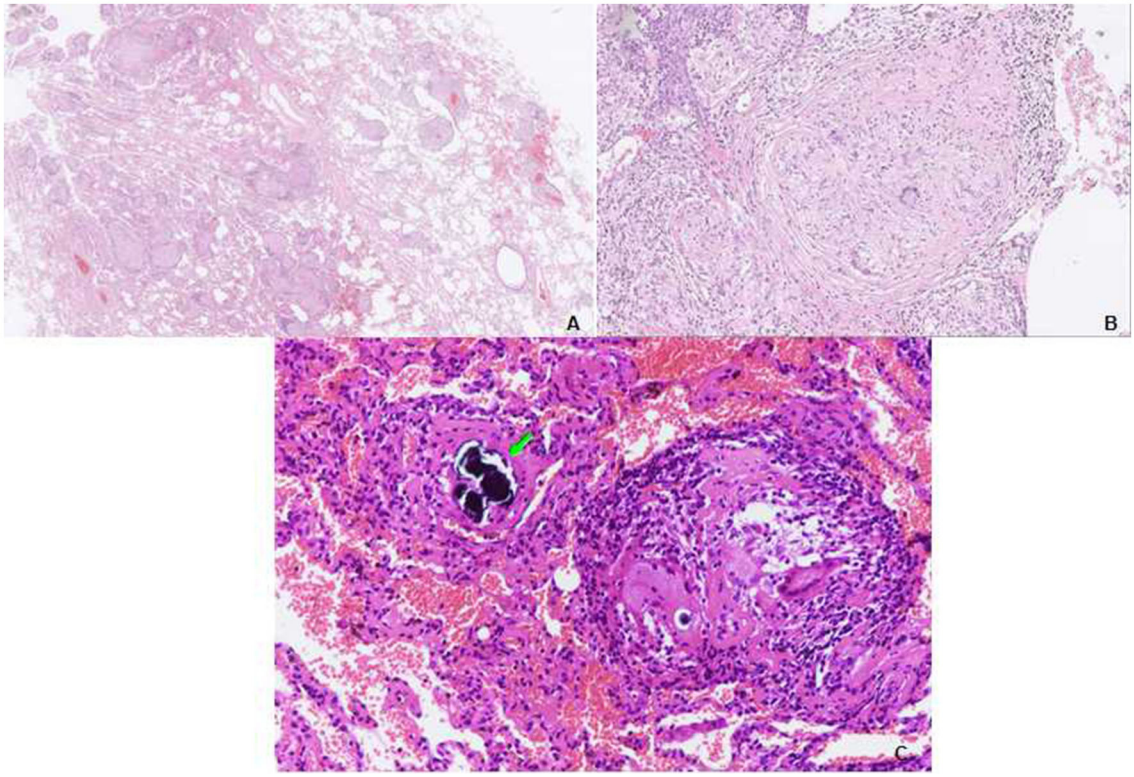

FIGURE 3
Transbronchial lung biopsy (TBLB) of the right lower lobe. **(A)** Lower power view showing the granulomas distributed in the interstitium, not in the airspace. Some of them have a centrilobular distribution, while some are distributed in the interlobular septum. A video-assisted thoracoscopic surgery (VATS) biopsy of the right lower lobe. **(B)** Many well-formed non-necrotizing granulomas are composed of epithelioid and multinucleated giant cells, with fibrous hyperplasia (hematoxylin and eosin [HE], ×40). **(C)** Multiple sarcoid-like granulomas composed of clustered epithelioid and multinucleated giant cells, a Schaumann body is observed (arrows) (HE, ×100).

aluminum. Meanwhile, high amounts of aluminum were detected in lung tissue using ICP-MS.

The exact mechanism that leads aluminum to induce these sarcoid-like granulomas is unclear. The metal elements may directly act as antigens to stimulate the immune system to cause sarcoidosis. The antigens may interact with the immune system to cause its dysregulation, which was involved in the formation of sarcoid (8). Immunoreactivity to metal elements had been found only in patients with sarcoidosis using a lymphoid proliferation test, suggesting that in addition to beryllium, aluminum may also be a possible stimulated antigen triggering an immune response. Even if the patient stopped exposure, the aluminum deposited in the lung may be a persistent stimulated antigen triggering an immune response. We reviewed the medical literature works and found 10 patients with granulomas secondary to aluminum or multiple exposures including aluminum. Six cases were followed up and the follow-up time spanned 1 year to 6 years. Among these cases, one patient's VC was reduced by 12.5% and DLco was induced by 12.8%, while his chest HRCT showed no changes after stopping exposure for 4 years (14). Four cases had no information of follow-up.

Pulmonary granulomatosis caused by aluminum dust or multiple other dust types (including aluminum) is an individual heterogeneous disease. The susceptible individuals may develop this disease even in a short time and on a relatively small amount of aluminum exposure. For workers exposed to aluminum dust, if the onset, symptoms, and imaging are not consistent with the characteristics of aluminum pneumoconiosis, a lung biopsy should be performed. When the pathology of lung biopsy shows sarcoid-like granulomas, oral glucocorticoid may be beneficial. The dosage and duration of glucocorticoids are still controversial. It may depend on the willingness of the patient and response to the medications. This patient took prednisone for a total of 15 months. Pulmonary symptoms, CT scans, and lung function values were improved after prednisone therapy; however, the disease recurred after the cessation of prednisone. Further insights concerning the relationship of aluminum exposure to the development of granulomatous lung disease may have a major impact on the prevention and treatment of this enigmatic disease.

Conclusion

Aluminum-associated sarcoid-like granulomatous lung disease is rarely diagnosed. This report described the case of a patient who had suffered from extensive occupational inhalation of aluminum dust. The diagnosis was based on occupational dust exposure combined with clinical-radiological-histological findings. The findings of the present case support the association between aluminum exposure and sarcoid-like granulomatous lung disease, and the emergence of these diseases should be taken into account in the clinical course of aluminum dust exposure.

Data availability statement

The original contributions presented in the study are included in the article/supplementary material, further inquiries can be directed to the corresponding author.

Ethics statement

Written informed consent was obtained from the individual(s) for the publication of any potentially identifiable images or data included in this article.

Author contributions

QY designed the study. XD and LS collected and analyzed the patient data and play an equally important role in this manuscript. LS followed up on the patient data and XD wrote the manuscript. RF performed the histological examination of the lung tissue. All authors contributed to the article and approved the submitted version.

Funding

The work was supported by Reform and Development Program of Beijing Institute of Respiratory Medicine (ysrh2022013).

Conflict of interest

The authors declare that the research was conducted in the absence of any commercial or financial relationships that could be construed as a potential conflict of interest.

Publisher's note

All claims expressed in this article are solely those of the authors and do not necessarily represent those of their affiliated organizations, or those of the publisher, the editors and the reviewers. Any product that may be evaluated in this article, or claim that may be made by its manufacturer, is not guaranteed or endorsed by the publisher.

References

1. Chen WJ, Monnat RJ Jr, Chen M, Mottet K. Aluminium induced pulmonary granulomatosis. *Hum Pathol.* (1978) 9:705–11. doi: 10.1016/s0046-8177(78)80053-7

2. Herbert A, Sterling G, Abraham J, Corrin B. Desquamative interstitial pneumonia in an aluminium welder. *Hum Pathol.* (1982) 13:694–9. doi: 10.1016/s0046-8177(82)80291-8

3. Miller RR, Churg AM, Hutcheon M, Lam Stephen. Pulmonary aveolar proteinosis and aluminium dust exposure. *Am Rev Respir Dis.* (1984) 130:312–5. doi: 10.1164/arrd.1984.130.2.312

4. Iijima Y, Bando M, Yamasawa H, Moriyama H, Takemura T, Niki T, et al. A patient of mixed dust pneumoconiosis with desquamative interstitial-like reaction in an aluminium welder. *Respir Med Patient Rep.* (2017) 20:150–3. doi: 10.1016/j.rmcr.2017.02.002

5. Taiwo OA. Diffuse parenchymal diseases associated with aluminium use and primary aluminium production. *Occup Environ Med.* (2014) 56:S71–2. doi: 10.1097/JOM.0000000000000054

6. Igbokwe IO, Igwenagu E, Igbokwe NA. Aluminium toxicosis: a review of toxic actions and effects. *Interdiscip Toxicol.* (2019) 12:45–70. doi: 10.2478/intox-2019-0007

7. Newman KL, Newman LS. Occupational causes of sarcoidosis. *Curr Opin Allergy Clin Immunol.* (2012) 12:145–50. doi: 10.1097/ACI.0b013e3283515173

8. Judson MA. Environmental risk factors for sarcoidosis. *Front Immunol.* (2020) 11:1340. doi: 10.3389/fimmu.2020.01340

9. Mayer AS, Hamzeh N, Maier LA. Sarcoidosis and chronic beryllium disease: similarities and differences. *Semin Respir Crit Care Med.* (2014) 35:316–29. doi: 10.1055/s-0034-1377059

10. De Vuyst P, Dumortier P, Schandené L, Estenne M, Verhest A, Yernault JC. Sarcoidlike lung granulomatosis induced by aluminium dusts. *Am Rev Respir Des.* (1987) 135:493–7. doi: 10.1164/arrd.1987.135.2.493

11. Brancaleone P, Weynand B, De Vuyst P, Stanescu D, Pieters T. Lung granulomatosis in a dental technician. *Am J Ind Med.* (1998) 34:628–31. doi: 10.1002/(sici)1097-0274(199812)34:6<628::aid-ajim12>3.0.co;2-9

12. Cai HR, Cao M, Meng FQ, Wei JY. Pulmonary sarcoid-like granulomatosis induced by aluminium dust: report of a patient and literature review. *Clin Med J.* (2007) 120:1556–60.

13. Catinon M, Chemarin C, Assaad S, Vuillermoz-Blas S, Roux E, Traverse-Glehen A. et al. Wire brushing wood furniture, granulomatosis and microscopic mineralogical analysis. *Sarcoidosis Vasc and Diffuse Lung Dis.* (2014) 31:262–4.

14. Tomioka H, Kaneda T, Katsuyama E, Kitaichi M, Moriyama H, Suzuki E. Elemental analysis of occupational granulomatous lung disease by electron probe microanalyzer with wavelength dispersive spectrometer: two patient reports. *Respir Med Patient Rep.* (2016) 18:66–72. doi: 10.1016/j.rmcr.2016.04.009

15. Catinon M, Chemarin C, Roux E, Cavalin C, Rosental PA, Thivolet-Bejui F, et al. Polishing surgical metal pieces, granulomatosis and mineralogical analysis. *Sarcoidosis Vasc and Diffuse Lung Dis.* (2016) 33:166–70.

16. Baur X, Sanyal S, Abraham J. Mixed-dust pneumoconiosis: review of diagnostic and classification problems with presentation of a work-related patient. *Sci Total Environ.* (2019) 652:413–21. doi: 10.1016/j.scitotenv.2018.10.083

17. Blin T, Muret AD, Teulier M, Ferreira M, Vincent M, Catinon M, et al. Desquamative interstitial pneumonia induced by metal exposure. A patient report and literature review. *Sarcoidosis Vasc Diffuse Lung Dis.* (2020) 37:79–84. doi: 10.36141/svdld.v37i1.9103

18. Blanc PD, Annesi-Maesano I, Balmes JR, Cummings K, Fishwick D, Miedinger D, et al. The occupational burden of nonmalignant respiratory diseases. An official American thoracic society and European respiratory society statement. *Am J Respir Crit Care Med.* (2019) 199:1312–34. doi: 10.1164/rccm.201904-0717ST

19. Barnes H, Goh NSL, Leong TL, Hoy R. Silica-associated lung disease: an old-world exposure in modern industries. *Respirology.* (2019) 24:1165–75. doi: 10.1111/resp.13695

20. Leung CC, Yu IT, Chen W. Silicosis. *Lancet.* (2012) 379:2008–18. doi: 10.1016/S0140-6736(12)60235-9

21. Mochizuka Y, Kono M, Katsumata M, Hirama R, Watamuki M, Oshima Y, et al. Sarcoid-like granulomatous lung disease with subacute progression in silicosis. *Intermal Medicine.* (2022) 61:395–400. doi: 10.2169/internalmedicine.7533-21

22. Vihlborg P, Bryngelsson IL, Andersson L, Graff P. Risk of sarcoidosis and seropositive rheumatoid arthritis from occupational silica exposure in Swedish iron foundries: a retrospective cohort study. *BMJ Open.* (2017) 7:e016839. doi: 10.1136/bmjopen-2017-016839

23. Beijer E, Meek B, Bossuyt X, Peters S, Vermeulen RCH, Kromhout H, et al. Immunoreactivity to metal and silica associates with sarcoidosis in Dutch patients. *Respir Res.* (2020) 21:141. doi: 10.1186/s12931-020-01409-w

24. Ohshimo S, Guzman J, Costabel U, Bonella F. Differential diagnosis of granulomatous lung disease: clues and pitfalls. *Eur Resp Rev.* (2017) 26:170012. doi: 10.1183/16000617.0012-2017

25. Vico G, Nuova S. What is sarcoiddosis? *Resp Med.* (2013) 107:1285–6. doi: 10.1016/j.rmed.2013.07.004

26. Oliver LC, Zarnke AM. Sarcoidosis: an occupational disease? *Chest.* (2021) 160:1360–7. doi: 10.1016/j.chest.2021.06.003

frontiers | Frontiers in Medicine

TYPE Case Report
PUBLISHED 02 March 2023
DOI 10.3389/fmed.2022.1108637

OPEN ACCESS

EDITED BY
Rodrigo Torres-Castro,
University of Chile, Chile

REVIEWED BY
Zhanqi Zhao,
Furtwangen University, Germany
Richard Bayford,
Middlesex University, United Kingdom

*CORRESPONDENCE
Changjun Gao
✉ gaocj74@163.com
Xude Sun
✉ sunxude@fmmu.edu.cn;
✉ sunxudes@163.com

†These authors have contributed equally to this work

SPECIALTY SECTION
This article was submitted to Pulmonary Medicine, a section of the journal Frontiers in Medicine

RECEIVED 26 November 2022
ACCEPTED 27 December 2022
PUBLISHED 02 March 2023

CITATION
Xiao Z, Zhang N, Zhang X, Lu W, Gao C and Sun X (2023) Case report: Post-thoracoscopy pendelluft monitoring. *Front. Med.* 9:1108637. doi: 10.3389/fmed.2022.1108637

Case report: Post-thoracoscopy pendelluft monitoring

Zhibin Xiao[1,3†], Na Zhang[2†], Xiajing Zhang[4†], Wenjun Lu[1], Changjun Gao[1*] and Xude Sun[1*]

[1]Department of Anesthesiology, The Second Affiliated Hospital of Air Force Medical University, Xi'an, Shaanxi, China, [2]Department of Thoracic Surgery, The Second Affiliated Hospital of Air Force Medical University, Xi'an, Shaanxi, China, [3]Department of Anesthesiology, The 986th Air Force Hospital, Xijing Hospital, The Air Force Medical University, Xi'an, Shaanxi, China, [4]Institute of Medical Research, Northwestern Polytechnical University, Xi'an, Shaanxi, China

Asynchronous alveolar ventilation is called pendelluft, which may induce lung injury in spontaneously breathing patients. We report a case that electrical impedance tomography (EIT) was used to assess the pendelluft in a post-thoracoscopy patient. The pendelluft amplitude was as high as 77.5% of the tidal variation. The average regional time shift was 0.5 s. The patient was instructed to adjust the breathing method, symptomatic treatment was performed, and the symptoms were improved. This is the first case reporting pendelluft in a post-thoracoscopy patient. Our case demonstrated that (1) pendelluft may occur in post-thoracoscopy patients and it effects lung function, and (2) early identification of affected patients and implementation of corresponding treatments could improve patient outcomes.

KEYWORDS

electrical impedance tomography, pendelluft, post-thoracoscopy, lung injury, pulmonary ventilation

Introduction

In recent years, lung protective ventilation strategies during the perioperative period have been widely used. However, post-operative pulmonary complications can occur from time to time (1, 2). Post-operative pulmonary function recovery can also be time-consuming. Additionally, individualized pulmonary rehabilitation training has not been popularized, one important reason being the current lack of effective clinical methods to assess intrapulmonary ventilation in different regions (2). Pulmonary function defect may occur after minimal invasive surgery, which was not systematically assessed (3). Once the patient recovers spontaneously breathing after surgery, non-uniform transmission of pleural pressure generated by diaphragmatic contraction may cause a phenomenon called pendelluft (4). In the extreme cases such as flail chest, pendelluft volume can be as high as 12.5% of the total volume passing through an airway (5). Although pendelluft could be potentially harmful by introducing local overstretch, tidal recruitment and inflammation, up to now, no traditional technique can track the pendelluft level.

Electrical impedance tomography (EIT) is a novel bedside imaging modality that provides continuous images of pulmonary ventilation and shows regional ventilation changes (6). EIT has been proposed to assess the pulmonary rehabilitation program and inspiratory muscle activities (7, 8), as well as capture the amplitude of pendelluft (9).

We present a case in which significant pendelluft was captured in a patient after thoracoscopy detected by EIT. Pulmonary rehabilitation was conducted for the patient who otherwise would have been discharged. Improvement in pulmonary function was observed after the early intervention.

Case description

A 49-year-old male patient with 10 years history of diabetes was admitted to our hospital. Ground-glass opaque nodules and dense nodular shadows were found in the posterior segment of the upper right lobe of the lung during computed tomography examination. A single-port thoracoscopy resection of S2b + lymph node sampling of the right upper lobe was performed under general anesthesia. The surgery lasted 1 h 55 min and was conducted successfully.

During the follow-up on the day after surgery, the patient had rapid, shallow breathing and was irritable. EIT measurement was conducted (VenTom-100, MidasMED Biomedical technology, Suzhou, China). A belt with 16 equidistantly fixed electrodes was placed around the chest in one transverse plane at the level of the 4th intercostal space at the parasternal line. Raw EIT data were acquired with at a scan rate of 20 images/s using excitation currents of 1 mArms applied through opposite electrodes. Image reconstruction was accomplished by the GREIT algorithm (10). In brief, inspiration and expiration were identified for global and regional impedance-time curves. The impedance differences between the sum of all regional tidal impedance variation (TIV) and the global TIV represented the pendelluft volume. The time shift between the regional and global inspiration start denoted as the pendelluft-induced time differences. EIT revealed asynchronous breathing in the right and left lungs with obvious pendelluft breathing pattern (Figure 1). The pendelluft amplitude was as high as 77.5% of the tidal variation. The average regional time shift was 0.5 s. We suspected that the airways were partially blocked by the sputum, which significantly increased the airway resistance heterogeneously.

To further clarify the patient's lung status, he was then scheduled for a computed tomography examination, the results of which suggested: subcutaneous emphysema in the right thoracolumbar region, right hydropneumothorax and a small amount of fluid in the left pleural cavity, and a patchy high-density shadow in the surgical area of the right lung. The patient was advised to cough up more sputum and practice deep breathing exercises more frequently. After three days of anti-infection, expectorant, and analgesic symptomatic treatment, the patient had a respiratory rate of 24 bpm with no symptoms of chest tightness or dyspnoea, though he still felt shortness of breath after physical activities. The patient was discharged after the removal of the chest drainage tube.

Timeline: Figure 2 showed information about the treatment process.

Diagnostic assessment

Telephone follow-up one month after the operation: the patient felt good, but he had shortness of breath after fast walking. Unfortunately, due to the COVID-19 epidemic, it was inconvenient for the patient to come for re-examination.

Discussion

The pendelluft is a phenomenon of gas redistribution in the lungs due to asynchronous alveolar ventilation. It was found that for patients with acute respiratory failure or intrapulmonary injury who are mechanically ventilated in the ICU, preserving moderate spontaneous breathing can help improve ventilation in the gravity-dependent zone, increase oxygenation, and prevent diaphragmatic atrophy. However, excessive inspiratory efforts have the potential to exacerbate lung injury through the pendelluft mechanism (11, 12). Since the pendelluft phenomenon involves only intrapulmonary gas redistribution and does not change the tidal volume *per se*, it means that in critically ill patients with lung injury, even if a small tidal volume lung-protective ventilation strategy has been adopted, the pendelluft phenomenon may still cause local regional lung hyperinflation and become a hidden source of lung injury exacerbation (13). During thoracoscopy, one-lung ventilation with positive pressure combined with the extended resection of the S2b in the upper lobe of the right lung may result in a non-uniform transfer of pleural pressure from diaphragmatic contraction. Such non-uniform pleural pressure may cause pendelluft. Due to the limitation of currently well-established techniques, the presence of pendelluft was not reported so far in patients after thoracoscopy (14). Follow-up treatment for the post-thoracoscopy patients could not be provided accordingly. As the first report of its kind, we took advantage of EIT as a bedside tool to detect the pendelluft in timely manner, helping with early treatment and intervention. The patient was instructed to adjust the breathing method, symptomatic treatment was performed, and the abnormal breathing phenomenon disappeared.

The EIT imaging technique has its known limitations: EIT image does not provide the precise anatomical localization of lung tissue and the spatial resolution is relatively low compared to computed tomography or magnetic resonance

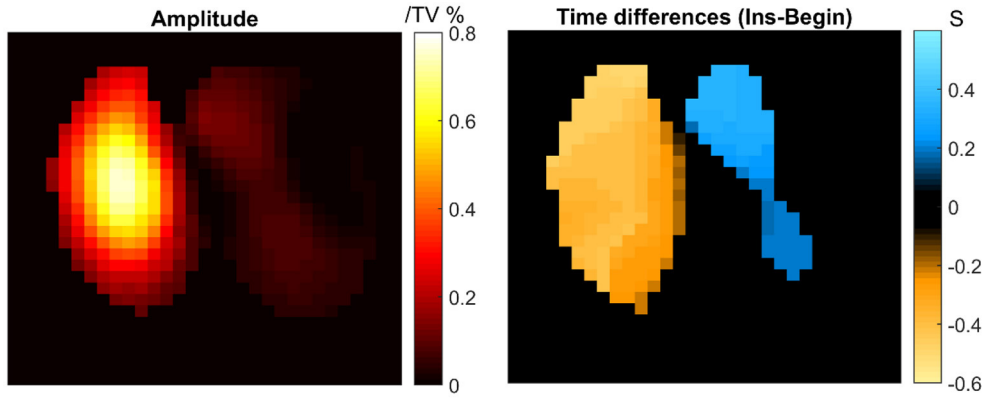

FIGURE 1
Pendelluft amplitude and time differences calculated according to a previous study (9). TV, tidal variation.

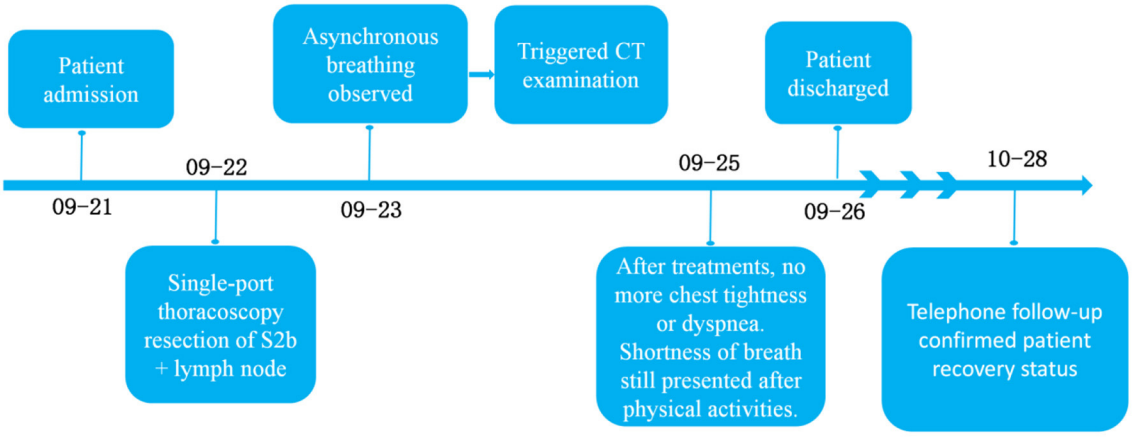

FIGURE 2
Timeline of patient treatment.

imaging. Electrode belt cannot be attached to the thorax for EIT measurement when the patients' wounds are around 4th intercostal space after surgery. As a limitation of the study, quantitative assessment of the treatment outcomes was not recorded. Nevertheless, our case demonstrated that (1) pendelluft may occur in post-thoracoscopy patients and it effects lung function, and (2) early identification of affected patients and implementation of corresponding treatments could improve patient outcomes. Further studies are warranted to explore the incidence of pendelluft in such patient group. Randomized controlled trial could be conducted to compare the post-operation recovery with and without EIT-based pendelluft assessment. *But EIT does have a very high temporal resolution, which makes the functional imaging possible. In fact, the calculation utilizes the high temporal resolution to estimate the pendelluft phase shift and thereby the corresponding amplitude.*

Conclusion

EIT can be used to detect the pendelluft phenomenon in post-thoracoscopy patients at the bedside, which provides important evidence for symptomatic diagnosis and treatment.

Data availability statement

The original contributions presented in the study are included in the article/supplementary material, further inquiries can be directed to the corresponding authors.

Ethics statement

The studies involving human participants were reviewed and approved by Ethics Committee of Tangdu

Hospital of Air Force Military Medical University. The patients/participants provided their written informed consent to participate in this study. Written informed consent was obtained from the individual(s) for the publication of any potentially identifiable images or data included in this article.

Author contributions

XS and CG conceived and designed the study. ZX and NZ performed of the experiments and drafted the manuscript. XZ edited the manuscript. WL analyzed the data. All authors have read and approved the final version of the manuscript.

Conflict of interest

The authors declare that the research was conducted in the absence of any commercial or financial relationships that could be construed as a potential conflict of interest.

Publisher's note

All claims expressed in this article are solely those of the authors and do not necessarily represent those of their affiliated organizations, or those of the publisher, the editors and the reviewers. Any product that may be evaluated in this article, or claim that may be made by its manufacturer, is not guaranteed or endorsed by the publisher.

References

1. Gómez-Hernández MT, Forcada C, Varela G, Jiménez MF, Embún R, de Antonio DG, et al. Operating time: an independent and modifiable risk factor for short-term complications after video-thoracoscopic pulmonary lobectomy. *Eur J Cardio-Thoracic Surgery*. (2022) 62:ezac503. doi: 10.1093/ejcts/ezac503

2. Miskovic A, Lumb AB. Postoperative pulmonary complications. *Br J Anaesth.* (2017) 118:317–34. doi: 10.1093/bja/aex002

3. Hashem MD, Nelliot A, Needham DM. Early mobilization and rehabilitation in the ICU: moving back to the future. *Respir Care.* (2016) 61:971–9. doi: 10.4187/respcare.04741

4. Zhao Z, Yuan TM, Chuang YH, Wang YW, Chang HT, Bien MY, et al. Lung ventilation distribution in patients after traditional full sternotomy and minimally invasive thoracotomy: An observational study. *Acta Anaesthesiol Scandinavica.* (2021) 65:877–85. doi: 10.1111/aas.13759

5. Vyshedskiy A, Murphy R. Pendelluft in chronic obstructive lung disease measured with lung sounds. *Pulm Med.* (2012) 2012:139395. doi: 10.1155/2012/139395

6. Harada K, Saoyama N, Izumi K, Hamaguchi N, Sasaki M, Inoue K. Experimental pendulum air in the flail chest. *Jpn J Surg.* (1983) 13:219–26. doi: 10.1007/BF02469481

7. Gong B, Krueger-Ziolek S, Moeller K, Schullcke B, Zhao Z. Electrical impedance tomography: functional lung imaging on its way to clinical practice? *Expert Rev Respir Med.* (2015) 9:721–37. doi: 10.1586/17476348.2015.1103650

8. Yuan S, Chi Y, Long Y, He H, Zhao Z. Effect of position change from the bed to a wheelchair on the regional ventilation distribution assessed by electrical impedance tomography in patients with respiratory failure. *Front Med.* (2021) 8:744958. doi: 10.3389/fmed.2021.744958

9. Zhao Z, Frerichs I, Chang MY, Moller K. Inspiratory muscle training can be monitored by electrical impedance tomography. *Aust Crit Care.* (2019) 32:79–80. doi: 10.1016/j.aucc.2018.10.004

10. Sang L, Zhao Z, Yun PJ, Frerichs I, Möller K, Fu F, et al. Qualitative and quantitative assessment of pendelluft: a simple method based on electrical impedance tomography. *Ann Transl Med.* (2020) 8:1216. doi: 10.21037/atm-20-4182

11. Adler A, Arnold JH, Bayford R, Borsic A, Brown B, Dixon P, et al. GREIT: a unified approach to 2D linear EIT reconstruction of lung images. *Physiol Meas.* (2009) 30:S35–55. doi: 10.1088/0967-3334/30/6/S03

12. Yoshida T, Nakahashi S, Nakamura MAM, Koyama Y, Roldan R, Torsani V, et al. Volume-controlled ventilation does not prevent injurious inflation during spontaneous effort. *Am J Respirat Crit Med.* (2017) 196:590–601. doi: 10.1164/rccm.201610-1972OC

13. Yoshida T, Roldan R, Beraldo MA, Torsani V, Gomes S, De Santis RR, et al. Spontaneous effort during mechanical ventilation: maximal injury with less positive end-expiratory pressure. *Crit Care Med.* (2016) 44:e678–688. doi: 10.1097/CCM.0000000000001649

14. Yoshida T, Torsani V, Gomes S, De Santis RR, Beraldo MA, Costa EL, et al. Spontaneous effort causes occult pendelluft during mechanical ventilation. *Am J Respir Crit Care Med.* (2013) 188:1420–7. doi: 10.1164/rccm.201303-0539OC

frontiers | Frontiers in Medicine

TYPE Case Report
PUBLISHED 20 March 2023
DOI 10.3389/fmed.2023.1088815

OPEN ACCESS

EDITED BY
Suzana Erico Tanni,
São Paulo State University, Brazil

REVIEWED BY
Erica Hasimoto,
São Paulo State University, Brazil
Sarhang Sarwat Gul,
University of Sulaymaniyah, Iraq

*CORRESPONDENCE
Yingshuo Wang
✉ wangyingshuo@zju.edu.cn

†These authors have contributed equally to this work

SPECIALTY SECTION
This article was submitted to Pulmonary Medicine, a section of the journal Frontiers in Medicine

RECEIVED 03 November 2022
ACCEPTED 20 February 2023
PUBLISHED 20 March 2023

CITATION
Tao X, Wu L, Li S, Wu Y, Lai C, Chen E, Chen Z, Jin G and Wang Y (2023) Successful management of tracheal lobular capillary hemangioma with arterial embolization followed by electrosurgical snaring *via* flexible bronchoscopy in an 11-year-old boy: A case report and literature review. *Front. Med.* 10:1088815. doi: 10.3389/fmed.2023.1088815

Successful management of tracheal lobular capillary hemangioma with arterial embolization followed by electrosurgical snaring *via* flexible bronchoscopy in an 11-year-old boy: A case report and literature review

Xiaofen Tao[1,2†], Lei Wu[1,2†], Shuxian Li[1,2], Yuxin Wu[3], Can Lai[4], Enguo Chen[5], Zhenjie Chen[6], Guoping Jin[2] and Yingshuo Wang[1*]

[1]Department of Pulmonology, Children's Hospital, Zhejiang University School of Medicine, National Clinical Research Center for Child Health, Hangzhou, Zhejiang, China, [2]Department of Endoscopy Center, Children's Hospital, Zhejiang University School of Medicine, National Clinical Research Center for Child Health, Hangzhou, Zhejiang, China, [3]Zhongshan School of Medicine, Sun Yat-sen University, Guangzhou, Guangdong, China, [4]Department of Radiology, Children's Hospital, Zhejiang University School of Medicine, National Clinical Research Center for Child Health, Hangzhou, Zhejiang, China, [5]Department of Respiratory Medicine, Sir Run Run Shaw Hospital, Zhejiang University School of Medicine, Hangzhou, Zhejiang, China, [6]Department of Pediatric Intensive Care Unit, Children's Hospital, Zhejiang University School of Medicine, National Clinical Research Center for Child Health, Hangzhou, Zhejiang, China

Lobular capillary hemangioma (LCH), previously known as pyogenic granuloma, is a benign vascular lesion commonly found within the oral and nasal cavities. However, it is rarely encountered within the trachea, especially in pediatric patients, where it manifests as hemoptysis, cough, and wheeze, and is frequently misdiagnosed as bronchitis or asthma. There is limited literature on the presentation, behavior, and management of tracheal LCH. Herein, we describe a rare case of tracheal LCH in an 11-year-old boy with a history of hemoptysis, which was successfully managed with arterial embolization followed by electrocautery loop snaring *via* flexible bronchoscopy. No complications occurred during and after the procedure. A review of the relevant literature is also provided. Our case is unique, given the therapeutic strategy utilized for pediatric tracheal LCH, and reminds physicians to be aware of tracheal LCH in the differential diagnosis for hemoptysis.

KEYWORDS

lobular capillary hemangioma, tracheal, arterial embolization, electrocautery loop snaring, flexible bronchoscopy, case report

Introduction

Primary tracheal tumors are rare, with an estimated annual incidence of 2.7 new cases per million population (1). As a benign tumor, lobular capillary hemangioma (LCH) was previously known as pyogenic granuloma and most commonly appears on the lip, nose, oral cavity, or tongue (2, 3). The etiology of this lesion remains elusive. There are many theories on pathogenesis revolving around LCH, such as a sequela of local irritation and minor trauma, neovascular response to an angiogenic stimulus with an imbalance of promoters and inhibitors, and bacterial and viral infections (3–6). As the clinical presentations are various and non-specific, LCH is often confused with true hemangiomas and granulation tissue (7, 8). Definitive diagnosis relies on histopathologic examination, which demonstrates a distinctive lobular arrangement of variably sized capillaries embedded in a fibromyxoid matrix without atypical mitoses (2, 9–11). Despite their benign nature, localized recurrence is common, and thus, surgical debulking or excision remains the mainstay of treatment if symptomatic (6, 12–14). Although there are a few studies of LCH on mucous membranes (2, 3, 6, 11, 15–17), tracheal origin for LCH is extremely rare among all primary tracheal tumors, with only four cases of children reported in the literature (9, 10, 18, 19). Thus, there is limited knowledge about the presentation, behavior, and management of tracheal LCH, which represents a diagnostic and therapeutic challenge in pediatric patients. Herein, we report a rare case of an 11-year-old boy with a tracheal LCH managed by arterial embolization, followed by electrosurgical snaring *via* flexible bronchoscopy.

Case presentation

An 11-year-old otherwise healthy boy presented to our hospital with hemoptysis for 5 days on 20 July 2022. He had more than 10 episodes of hemoptysis per day, with 5–30 ml of bright red blood mixed with clots each time, over the preceding 5 days. Associated fatigue, dizziness, shortness of breath, chest pain, dysphagia, nasal congestion, runny nose, hematuresis, hematochezia, fever, and rigors were denied. There was no history of foreign body aspiration, trauma, hoarseness, airway intubation, or endoscopy. Initially, he was treated at a local hospital for 5 days, but he was not responding well to medical treatment with antibiotics.

On admission, he was in good condition, and the physical examination showed no abnormalities. Thoracic non-contrast-enhanced computed tomography (CT) imaging revealed a cauliflower-like lesion of 4.9*4.6*4.6 mm in size affixed to the right wall of the lower trachea (Figure 1A), with an average density of 29 Hounsfield unit (HU). Contrast-enhanced CT imaging showed an inhomogeneous enhancement in the lesion with an average density of 200 HU (Figure 1B). Flexible bronchoscopy revealed a hyperemic, broad pedunculated tracheal neoplasm, arising from the right wall of the trachea in the lower one-third and projecting into its lumen, approximately 1 cm above the main carina with blood on the surface (Figure 1C). Glomus tumor was highly suspected. To avoid potential massive tumor bleeding during the biopsy, a multidisciplinary consultation was scheduled; the boy's parents were also in favor of less invasive surgery, rather than thoracotomy. The multidisciplinary consensus was to proceed with bronchial artery embolization (BAE) for the tracheal neoplasm by interventional radiologists, and then the mass was removed with an electrocautery snare *via* flexible bronchoscopy by a pulmonologist. Surgical resection (e.g., thoracotomy) was considered as an alternative option by thoracic surgeons if procedures mentioned above failed, and the extracorporeal membrane oxygenation (ECMO) team was also on standby.

In order to minimize the possibility of bleeding during lesion resection, the feeding artery was attempted to be embolized through the right common femoral artery. Digital subtraction angiography (DSA) confirmed the presence of a feeding artery (Figure 2A). Under fluoroscopic guidance, endovascular embolization was performed using a 5-Fr catheter and polyvinyl alcohol particles of 300–500 microns and 500–700 microns for distant and proximal branches, respectively. Embolization of the main bronchial artery with gelatin sponge particles was performed simultaneously. Post-embolization DSA revealed a marked reduction of the abnormal vascular blush and occlusion of the feeding artery and its branches (Figure 2B).

Then, the tumor was debulked by electrosurgical snaring with a flexible bronchoscope under general anesthesia. In detail, the electrocautery snare was used in a blend mode at 40 W to cut and coagulate the base of the mass (Figure 2C), which was resected without significant bleeding, and tracheal patency was achieved (Figure 2D). Histological examination revealed numerous capillaries arranged in a lobular pattern, separated by an edematous fibrous stroma, accompanied by mild inflammatory changes (Figure 3A) with fungal hyphae inside it (Figure 3B), which was suggestive of polypoid LCH. Immunohistochemistry revealed SMA(+), LYVB1(partial +), D2-40(-), CD34(+), WT1(+), Glut1(-), and CD31(+), further supporting the diagnosis. Although pathology suggested fungal infection, the patient did not have any typical symptoms of fungal infection throughout the course of the disease. Thus, antifungal therapy was not given during the hospitalization. The patient's postoperative recovery was uneventful, and he was discharged on the third postoperative day.

Discussion

In the present case, the lesion was discovered while searching for causes of non-specific clinical symptoms, such as hemoptysis. It is known that primary tracheal tumors account for <2% of all upper respiratory tract tumors (20), which are usually malignant in the adult population. The most common benign tumors in the trachea include papilloma, chondroma, and fibroma, with <10% being vascular in origin (21), and LCH commonly appears on the lip, nose, oral cavity, and tongue (2, 3). These data indicate that the occurrence of LCH within the tracheobronchial tree is extremely rare and infrequently described in medical literature, especially in children. Based on CT findings, bronchoscopy was indicated and led us to the final diagnosis of tracheal LCH. To the best of our knowledge, only four pediatric cases of tracheal LCH have been reported in the literature (9, 10, 18, 19), further implying the rarity of tracheal LCH in the pediatric population. However, it should be kept in mind for the differential diagnosis of causes of hemoptysis.

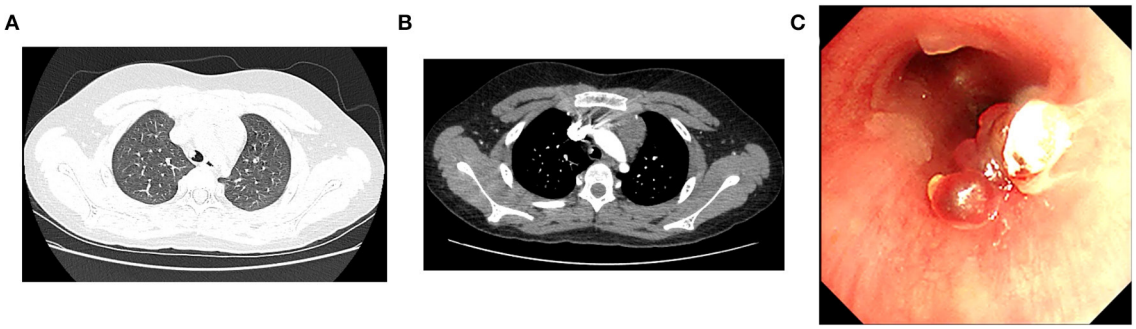

FIGURE 1
Both lung views of plain chest computed tomography (CT) scan **(A)** and mediastinal view of contrast-enhanced CT scan **(B)** demonstrate the tracheal mass. **(C)** Initial bronchoscopic view of the mass occluding the lower trachea.

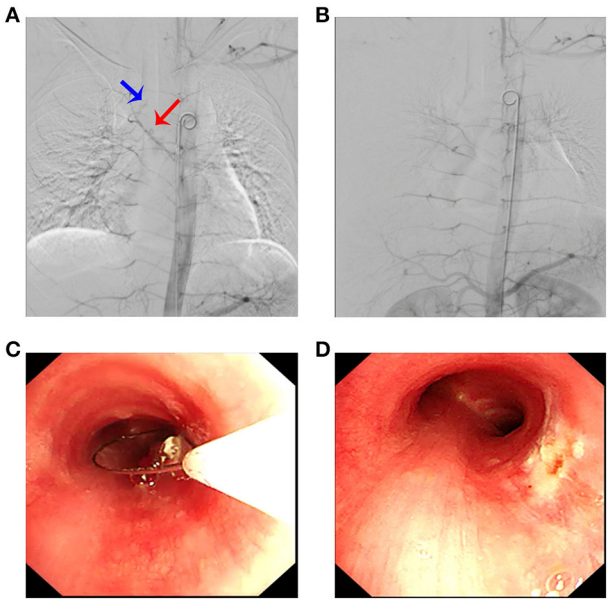

FIGURE 2
Arteriography revealed a pathological artery originating from the bronchial artery **(A)** (blue arrow: tumor; red arrow: bronchial artery branch) that was selectively embolized **(B)**. **(C)** Electrocautery loop snaring *via* flexible bronchoscopy; **(D)** posttreatment view of the same area.

Lobular capillary hemangioma (LCH), as benign vascular tumors characterized microscopically by a distinctive lobular arrangement of capillaries (2, 9, 22), was previously known as "pyogenic granulomas" or "granulomatous hemangiomas." The traditional term "pyogenic granuloma" is inaccurate since the tumor neither contains purulent material nor is a true granuloma (11). However, the mechanism triggering the evolution of LCH is unknown, prior trauma, hormonal imbalances, infection, drug adverse effects, and genetic abnormalities associated with the nitric oxide pathway, angiogenesis and vascular injury have been proposed as predisposing factors (3–5). The possible explanation for fungal infection showed by pathology is that BAE caused local tumor tissue necrosis, and then, the necrotic material combined with the previous bleeding on the tumor surface led to the attachment of fungal hyphae to the tumor surface. Our patient had no prior history of foreign body aspiration, severe respiratory infection, signs of fungal infection, significant abnormalities, or traumatic surgery, thus, the most likely cause of our case was underlying microscopic arteriovenous malformations.

The most common clinical symptoms of tracheal LCH are cough, hemoptysis ranging from minor to massive, and expectoration. Giant masses may narrow the airway, causing dyspnea and breathlessness. The most frequent causes of hemoptysis are infectious diseases, tuberculosis, malignant tumors, cardiovascular disorders, and other inflammatory diseases. Only one of the five kids with tracheal LCH presented without hemoptysis (18) or a chronic cough. Qiu et al. summarized 12 tracheal LCH cases in the adult population and found that all of them had hemoptysis (12). Altogether, tracheal LCH should be considered a possible benign cause of hemoptysis and cough despite its rarity. Although it is a benign disease, tracheal LCH has a tremendous bleeding tendency even life-threatening. Therefore, tracheal LCH should be managed in a well-prepared manner.

The diagnosis of tracheal LCH relies on chest CT and bronchoscopy, while X-ray may show no abnormality. In detail, chest CT, especially contrast-enhanced CT, identifies the occupying lesions and reveals the nature of the mass with a plentiful blood supply, while bronchoscopy with biopsy plays a key role in achieving the final diagnosis of tracheal LCH and provides additional opportunities for therapeutic intervention. Endoscopic appearances are non-specific and sometimes may be confused with granulation tissue, carcinoid tumor, Kaposi sarcoma, angioendothelioma, paraganglioma, adenoma, angiosarcoma, intravascular angiomatosis, and carcinoma (7, 8). Hence, histopathological findings are crucial for a definite diagnosis of tracheal LCHs.

Due to the limited number of tracheal LCH cases, the preferred treatment for it has not yet been established, and therapy methods vary considerably among different studies (12, 13). Generally speaking, tracheal LCH can be treated with interventional bronchoscopy or surgical excision. Endoscopic excision, laser therapy, cryoprobe, electrocautery, brachytherapy, surgical debulking, argon plasma coagulation (APC), and cryotherapy were performed in a separate or combined way in adult tracheal LCH cases (12). The treatment experience is relatively limited in children when compared with adults because only four cases reported in the literature. The previously reported interventions for

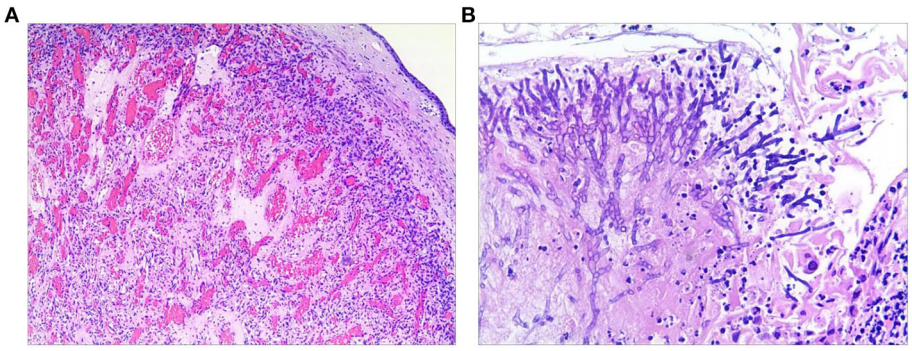

FIGURE 3
Histological examination of the resected specimen revealed capillary hemangioma **(A)** covered by the squamous epithelium and with fungal hyphae inside it **(B)**.

pediatric tracheal LCH include electrocauterization, cryoablation, potassium-titanyl-phosphate laser ablation, and cylindrical resection (9, 10, 18, 19), while a tracheal LCH utilizing DSA/BAE followed by electrosurgical snaring *via* flexible bronchoscopy in an 11-year-old boy was successfully removed in the present case. Collectively, although no adequate guidelines were provided and tracheal LCH is amenable to various techniques, the extent and size of the lesion, as well as patient age and comorbidities require consideration prior to any therapeutic intervention for tracheal LCH.

Although our department has rich experience in removing transbronchial tracheal tumors (23, 24), there is a substantial risk of intraoperative hemorrhage dealing with the tracheal LCH. We confront the following challenges: (1) the large size of the tumor and the rich blood supply did not allow the resection with biopsy forceps; (2) the lesion was attached to the trachea wall, and the resection with laser or cryotherapy may be associated with a high risk of perforation [6]. In the present case, DSA/BAE was employed to prevent massive intra-procedural bleeding. Of note, bronchial artery embolization ahead of tracheal LCH removal is of great importance for our case. For instance, without scheduling BAE before surgery, Dabó et al. described significant hemorrhage during tracheal LCH removal by rigid forceps *via* rigid bronchoscopy, and the instillation of cold saline and epinephrine failed to control the massive bleeding was described [20]. Inversely, in another case of BAE followed by lumpectomy under bronchoscopy, the amount of intraoperative blood loss was dramatically decreased [17]. This evidence further emphasizes that BAE was the procedure of choice in order to achieve better control of bleeding.

Meanwhile, electrocautery loop snaring was used in our case due to its ability to cut and cauterize simultaneously. The specimens obtained by electrosurgical loop snaring for diagnostic purposes are much larger and of excellent tissue quality compared with specimens extracted with forceps. Moreover, alternative surgical options are available. If a flexible bronchoscope fails to remove the tumor, a rigid bronchoscope will be employed. The endotracheal intubation should adjust the depth of endotracheal intubation if the patient loses a substantial amount of blood during the procedure, and balloon compression should be used to try to stop the bleeding. In the event that the endobronchial treatment cannot be performed as intended, the thoracic surgeon will perform a thoracotomy. If vital signs become unstable, the extracorporeal membrane oxygenation team is prepared to provide emergency care. In other words, the ECMO team and thoracic surgeons were on standby as a precautionary measure to ensure the removal of the lesion successfully. This information demonstrates the safe, successful, effective, and less invasive removal of the challenging tracheal LCH without discernible bleeding depends on close interdisciplinary cooperation and elaborate preparation.

Since the degree of tumor infiltration into the tracheal wall cannot be evaluated during bronchoscopy, individuals who have undergone bronchoscopy for tumor resection may have residual and incomplete tumor removal, and some patients may experience tumor recurrence. Future monitoring of this patient is required. In other words, it might be necessary to use bronchoscopy during the follow-up period because there is a risk of local recurrence (1).

Conclusion

Our case is unique as it highlights the successful use of DSA/BAE followed by electrosurgical loop snaring *via* flexible bronchoscopy for the diagnosis and treatment of pediatric tracheal LCH with an abundant blood supply. Although exceeding rare, tracheal LCH should be considered a cause of recurrent hemoptysis in children. However, our experience should be validated in further large studies and further rigorous follow-up is needed for the possibility of local recurrence.

Data availability statement

The original contributions presented in the study are included in the article/supplementary material, further inquiries can be directed to the corresponding author.

Ethics statement

Written informed consent was obtained from the minor(s)' legal guardian/next of kin for the publication of any potentially identifiable images or data included in this article.

Author contributions

XT and LW collected the data and drafted and edited the manuscript. SL, YWu, CL, EC, ZC, and GJ revised the manuscript. YWa supervised this study. All authors critically reviewed, revised, and approved the final manuscript and agreed to be responsible for all aspects of the study.

Funding

This study was supported by a grant from the Zhejiang Provincial Natural Science Foundation (LQ20H190006).

Acknowledgments

The authors appreciate the support from the boy enrolled in this study and his guardians. Moreover, the authors gratefully thank all the doctors and nurses who were involved in the treatment.

Conflict of interest

The authors declare that the research was conducted in the absence of any commercial or financial relationships that could be construed as a potential conflict of interest.

Publisher's note

References

1. Prakash S, Bihari S, Wiersema U. A rare case of rapidly enlarging tracheal lobular capillary hemangioma presenting as difficult to ventilate acute asthma during pregnancy. *BMC Pulm Med.* (2014) 14:41. doi: 10.1186/1471-2466-14-41

2. Irani S, Brack T, Pfaltz M, Russi EW. Tracheal lobular capillary hemangioma: a rare cause of recurrent hemoptysis. *Chest.* (2003) 123:2148–9. doi: 10.1378/chest.123.6.2148

3. Amy FT, Enrique DG. Lobular capillary hemangioma in the posterior trachea: a rare cause of hemoptysis. *Case Rep Pulmonol.* (2012) 2012:592524. doi: 10.1155/2012/592524

4. Marla V, Shrestha A, Goel K, Shrestha S. The histopathological spectrum of pyogenic granuloma: a case series. *Case Rep Dent.* (2016) 2016:1323798. doi: 10.1155/2016/1323798

5. Godfraind C, Calicchio ML, Kozakewich H. Pyogenic granuloma, an impaired wound healing process, linked to vascular growth driven by FLT4 and the nitric oxide pathway. *Mod Pathol.* (2013) 26:247–55. doi: 10.1038/modpathol.2012.148

6. Giblin AV, Clover AJ, Athanassopoulos A, Budny PG. Pyogenic granuloma - the quest for optimum treatment: audit of treatment of 408 cases. *J Plast Reconstr Aesthet Surg.* (2007) 60:1030–5. doi: 10.1016/j.bjps.2006.10.018

7. Spinelli C, Di Giacomo M, Bertocchini A, Loggini B, Pingitore R. Multiple pyogenic granuloma of the penis in a four-year-old child: a case report. *Cases J.* (2009) 2:7831. doi: 10.4076/1757-1626-2-7831

8. Onofrio AR, Kwon J, Kang LH, Wang J. Endobronchial paraganglioma: AIRP best cases in radiologic-pathologic correlation. *Radiographics.* (2018) 38:581–5. doi: 10.1148/rg.2018170184

9. Porfyridis I, Zisis C, Glinos K, Stavrakaki K, Rontogianni D, Zakynthinos S, et al. Recurrent cough and hemoptysis associated with tracheal capillary hemangioma in an adolescent boy: a case report. *J Thorac Cardiovasc Surg.* (2007) 134:1366–7. doi: 10.1016/j.jtcvs.2007.07.014

10. Chen E, Yu X, Zhang R, Wang P, Ying K. A large tracheal capillary hemangioma treated with interventional bronchoscopy. *Respir Med CME.* (2011) 4:60–1. doi: 10.1016/j.rmedc.2010.10.002

11. Mills SE, Cooper PH, Fechner RE. Lobular capillary hemangioma: the underlying lesion of pyogenic granuloma. A study of 73 cases from the oral and nasal mucous membranes. *Am J Surg Pathol.* (1980) 4:470–9. doi: 10.1097/00000478-198010000-00007

12. Qiu X, Dong Z, Zhang J, Yu J. Lobular capillary hemangioma of the tracheobronchial tree: a case report and literature review. *Medicine.* (2016) 95:e5499. doi: 10.1097/MD.0000000000005499

13. Fiorelli A, Accardo M, Venetucci P, Cascone R, Carlucci A, Noro A, et al. Endoscopic resection of tracheal lobular capillary haemangioma with ultrasonically activated device. *Gen Thorac Cardiovasc Surg.* (2021) 69:379–82. doi: 10.1007/s11748-020-01451-x

14. Lee J, Sinno H, Tahiri Y, Gilardino MS. Treatment options for cutaneous pyogenic granulomas: a review. *J Plast Reconstr Aesthet Surg.* (2011) 64:1216–20. doi: 10.1016/j.bjps.2010.12.021

15. Ikeda K, Ichiba T, Seo K, Okazaki Y. Intravenous lobular capillary haemangioma presenting as neck discomfort associated with neck anteflexion. *BMJ Case Rep.* (2021) 14:e237529. doi: 10.1136/bcr-2020-237529

16. Magaz Martinez M, Martinez Porras JL, Barrios C, Abreu L. Capsule endoscopy: Diagnosis of lobular capillary haemangioma. *Gastroenterol Hepatol.* (2017) 40:403–4. doi: 10.1016/j.gastre.2017.05.004

17. Suman S, Kumar A. Intraoperative mitomycin C and cryotherapy as adjunct therapy for recurrent lobular capillary haemangioma of conjunctiva. *BMJ Case Rep.* (2020) 13:e233438. doi: 10.1136/bcr-2019-233438

18. Wang RY, Quintanilla NM, Chumpitazi BP, Gitomer S, Chiou EH, Ongkasuwan J. Pediatric tracheal lobular capillary hemangioma: a case report and review of the literature. *Laryngoscope.* (2021) 131:1729–31. doi: 10.1002/lary.29091

19. Luo J, He YQ. Tracheal lobular capillary hemangioma. *Am J Respir Crit Care Med.* (2022) 206:1035–6. doi: 10.1164/rccm.202202-0297IM

20. Howard DJ, Haribhakti VV. Primary tumours of the trachea: analysis of clinical features and treatment results. *J Laryngol Otol.* (1994) 108:230–2. doi: 10.1017/S0022215100126362

21. Sie KC, Tampakopoulou DA. Hemangiomas and vascular malformations of the airway. *Otolaryngol Clin North Am.* (2000) 33:209–20. doi: 10.1016/S0030-6665(05)70216-4

22. Madhumita K, Sreekumar KP, Malini H, Indudharan R. Tracheal haemangioma: case report. *J Laryngol Otol.* (2004) 118:655–8. doi: 10.1258/0022215041917871

23. Wu L, Sha MC, Wu XL, Bi J, Chen ZM, Wang YS. Primary intratracheal neurilemmoma in a 10-year-old girl: a case report. *World J Clin Cases.* (2021) 9:8888–93. doi: 10.12998/wjcc.v9.i29.8888

24. Wu L, Chen W, Li P, Li S, Chen Z. Case report: resection of giant endotracheal hamartoma by electrosurgical snaring via fiberoptic bronchoscopy in a 9-year-old boy. *Front Pediatr.* (2021) 9:528966. doi: 10.3389/fped.2021.528966

frontiers | Frontiers in Medicine

TYPE Case Report
PUBLISHED 24 May 2023
DOI 10.3389/fmed.2023.1157922

OPEN ACCESS

EDITED BY
Suzana Erico Tanni,
São Paulo State University, Brazil

REVIEWED BY
Mansoor C. Abdulla,
Sultan Qaboos Hospital, Oman
Serena Vettori,
Monaldi Hospital, Italy
Fabio Arimura,
University of São Paulo, Brazil

*CORRESPONDENCE
Hui Huang
✉ pumchhh@126.com

RECEIVED 03 February 2023
ACCEPTED 03 May 2023
PUBLISHED 24 May 2023

CITATION
Shao C, Chen RX, Huang H, Zhao Y, Chen KQ and Xu K (2023) Microscopic polyangiitis initially presenting with idiopathic pulmonary fibrosis: a case report. *Front. Med.* 10:1157922. doi: 10.3389/fmed.2023.1157922

Microscopic polyangiitis initially presenting with idiopathic pulmonary fibrosis: a case report

Chi Shao[1], Ruxuan Chen[1], Hui Huang[1]*, Yang Zhao[1], Keqi Chen[1] and Kai Xu[2]

[1]Department of Pulmonary and Critical Care Medicine, Peking Union Medical College Hospital, Chinese Academy of Medical Sciences and Peking Union Medical College, Beijing, China, [2]Department of Radiological, Peking Union Medical College Hospital, Chinese Academy of Medical Sciences and Peking Union Medical College, Beijing, China

Usual interstitial pneumonia is the most common type of microscopic polyangiitis (MPA)-associated interstitial lung disease, and patients may initially present with isolated pulmonary fibrosis, which often leads to a misdiagnosis of idiopathic pulmonary fibrosis (IPF). Here, we describe a patient who developed fever of unknown origin, microscopic hematuria and renal insufficiency, who then tested positive for antineutrophil cytoplasmic antibody (ANCA) and was diagnosed with MPA after receiving antifibrotic medication for IPF (original diagnosis) for almost 10 years. The patient's symptoms were ameliorated after administration of additional glucocorticoids and immunosuppressants.

KEYWORDS

usual interstitial pneumonia pattern, ANCA antibody, microscopic polyangiitis, antifibrotic therapy, idiopathic pulmonary fibrosis

Introduction

Pulmonary fibrosis and diffuse alveolar hemorrhage were the main respiratory involvement of microscopic polyangiitis (MPA) (1), and usual interstitial pneumonia (UIP) pattern is the most common radiological manifestation (2). Interstitial lung disease (ILD) might be the first clinical manifestation in one fifth antineutrophil cytoplasmic antibodies (ANCA)-associated vasculitis (AAV), however, ILD might be diagnosed earlier than AAV in more than 80% p-ANCA positive patients (2). Patients with MPA may initially present with isolated pulmonary fibrosis, which often leads to a misdiagnosis of idiopathic pulmonary fibrosis (IPF).

Case presentation

A 69-year-old male patient visited our hospital on December 1, 2021, due to dry cough and shortness of breath after activity for the past 10 years and intermittent fever for the past 3 months. In early November 2011, the patient suffered from a processive cough after catching a cold and was given antibiotics and cough suppressants, but no marked effect was observed. He also had shortness of breath after intense activities, which affected his daily work but did not affect his daily life. Therefore, he did not seek further medical consultation. In early January 2012, the above symptoms were aggravated by a cold, accompanied by a small amount of white sputum, without fever and hemoptysis. The cough was relieved after treatment with antibiotics and cough suppressants at a local hospital. However, shortness of breath was aggravated during intense activities. He presented to the local hospital again, and chest computed tomography (CT) showed pulmonary fibrosis.

On May 8, 2012, the patient presented to our interstitial lung disease clinic. The 17-item antinuclear antibody (ANA) profile, antineutrophil cytoplasmic antibody (ANCA) profile and rheumatoid arthritis (RA)-related antibody profile [including rheumatoid factor, antikeratin antibody (AKA), antiperinuclear factor antibody (APF) and anticyclic citrullinated peptide (CCP)] were all negative. The results of complete blood count testing, urine sediment and routine urine testing and biochemical analysis were all normal. The chest high-resolution CT (HRCT) manifestations were consistent with usual interstitial pneumonia (UIP) (Figure 1). The pulmonary function tests showed mild restrictive ventilation dysfunction and moderate diffusion impairment: forced expiratory volume in one second (FEV1)/forced vital capacity (FVC), 78%; FVC/FVC% predicted, 2.81 L/74.9%; total lung capacity (TLC)/TLC% predicted, 5.09 L/86.3%; diffusing capacity for carbon monoxide (DLCO)/DLCO% predicted, 3.66 mmol/min/kpa/52.9%. Bronchoalveolar lavage fluid tests showed the following: cell count, 8.6×10^6/L; phagocytes, 64%; neutrophils, 11%; lymphocytes, 24%; eosinophils, 1%. After a global multidisciplinary discussion (MDD), he was diagnosed with idiopathic pulmonary fibrosis (IPF) and enrolled in the INPULSIS clinical trial (3). The patient took nintedanib (after unblinding, the patient was in the nintedanib group) from May 21, 2012, to June 15, 2017, i.e., in the INPULSIS and INPULSIS ON trials. During this period, he was complained with intermittent diarrhea, which was relieved with smectite and berberine. The series reports of PFTs were listed in Table 1.

When the INPULSIS ON trial concluded, nintedanib was no longer free of charge. He therefore started pirfenidone (0.6 g tid) on January 13, 2018. No significant adverse effects were reported. However, since September 2019, he experienced worse exertional shortness of breath than before and was unable to perform physical labor. He complained of fatigue in early September 2021 and had a fever on September 12, with a maximum temperature that ranged from 37.8 to 38.7°C. Dry cough was aggravated, and tests for COVID-19 were negative. Repeated chest CT revealed pulmonary fibrosis progression but no significant exudative shadows (Figure 2). The microbiological analysis for induced sputum, 1,3-β-D-glucan test, Widal test, Weil-Felix test, mycoplasma pneumoniae antibodies, chlamydia antibody and Legionella antibodies were all negative. Empirical antibiotics (i.e., meropenem, ceftriaxone, moxifloxacin and azithromycin) were ineffective. Then, he came to our outpatient department on December 1, 2021. He had no arthralgia, no dry mouth and dry eyes. He was healthy before 2012 but had a history of smoking (10 cigarettes/day for 20 years) and had quit smoking in 2008. He was a farmer and had no history of occupational dust exposure. Physical examinations revealed the following: pulse oxygen saturation of 95% while breathing air, no palpable superficial cervical lymph nodes and no clubbing of the fingers, Velcro-like crackles in both lower lungs and no swelling in either inferior limb. Routine blood test: white blood cell count, 10.4×10^9/L ($N < 9.5$); neutrophil percentage, 84.3% ($N < 75\%$); hemoglobin, 107 g/L (N: 120–160). Urine sediment and urine routine testing: red blood cell count, 80/μL; 100% abnormal morphology. The 24 h urine protein was 0.3 g. Biochemical tests: serum creatine, 147 μmol/L; blood urea nitrogen (BUN), 9.34 mmol/L; erythrocyte sedimentation rate (ESR), 82 mm/h ($N < 15$); C-reactive protein (CRP), 25.6 mg/L ($N < 8$). The serum complement analysis and quantitative analysis of IgG, IgM and IgA were normal. The ANA profile: ANA 1:320 (AC-4), other indicators were negative; ANCA (P-type) 1:20, and myeloperoxidase (MPO): 148 RU/mL ($N < 20$). The rheumatoid arthritis (RA) antibody profile showed that the rheumatoid factor (RF) level was 169 IU/mL ($N < 20$). The anti-extractable nuclear antigen (ENA), CCP, AKA and APF were all negative. Repeated pulmonary function tests indicated an FVC/FVC% predicted of 2.31 L/69%, a TLC/TLC% predicted of 4.47 L/72% and a DLCO/DLCO% predicted of 2.89 mmol/min/kpa/36%, which were worse than the findings from 2012 at our hospital.

Concomitant with malignancies were common for IPF patients. So, common cancer screening tests had been arranged annually for him during the follow-up, series cancer antigen (CA) serum biomarkers, fecal occult blood, annual abdominal and urinary ultrasonography, and annual chest CT scan. There were no significant abnormal of these test and examinations before December 2021.

According to his medical history, laboratory analysis and chest HRCT, he was diagnosed with microscopic polyangiitis (MPA) after repeated MDD, which included experts in ILD, rheumatology,

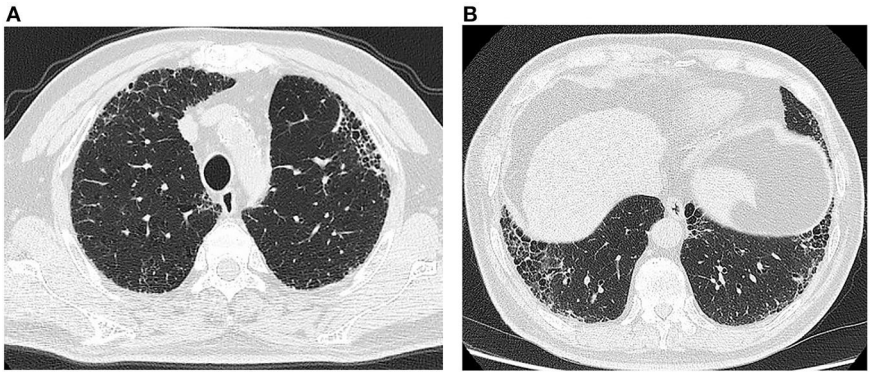

FIGURE 1
Chest HRCT: (May 8, 2012, **A, B**): Reticular and scattered honeycomb opacities predominantly in the proximal pleural parts of both lungs without significant exudative opacities.

TABLE 1 Series reports of pulmonary function tests.

Characters	FEV1/FVC (%)	FVC (L)	FVC% predicted	TLC (L)	TLC% predicted	DLCO (mmol/min/kpa)	DLCO% predicted
May 2012	78	2.81	74.9	5.09	86.3	3.66	52.9
May 2013	78.9	2.98	79.4	5.28	89.8	2.92	42.6
June 2017	75.6	2.71	73.1	4.98	79.8	3.02	42.8
December 2021	76.9	2.31	69	4.47	72	2.89	36

FEV1, forced expiratory volume in one second; FVC, forced vital capacity; TLC, total lung capacity; DLCO, diffusing capacity for carbon monoxide.

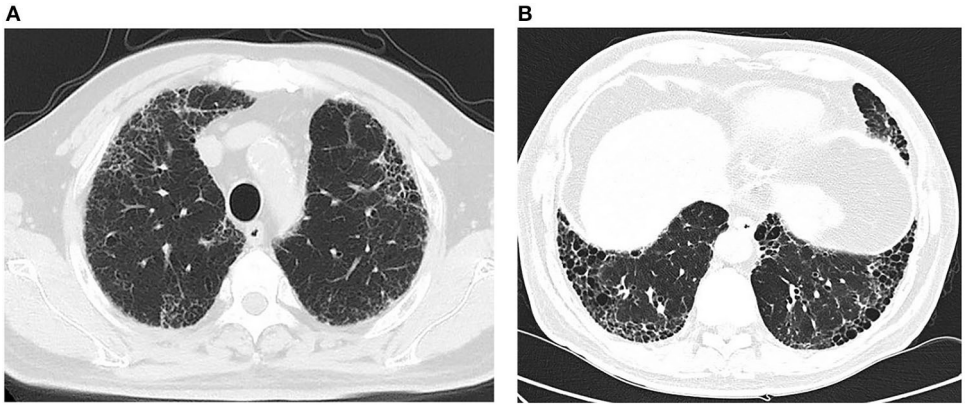

FIGURE 2
Chest HRCT: (September 27, 2021, **A, B**): Progressive Reticular and honeycomb opacities in the proximal pleural parts of both lungs compared with previous observations.

nephrology and radiology. When he breathed deeply and held his breath, he suffered from severe dry cough. Renal biopsy was recommended but refused by the patient and his family. Then, the patient was given oral prednisone on December 20, 2021 (50 mg qd; the dose was reduced 3 weeks later) plus cyclophosphamide (100 mg qd) on the basis of pirfenidone. His temperature was normalized since Day 3 after administration, his fatigue was significantly relieved 2 weeks later, and his shortness of breath after activity was also alleviated. One month later (on February 2, 2022), repeated tests in local hospital showed an ESR of 28 mm/h, and his renal function and CRP had returned to normal. On April 19, 2022, he came to our clinic. His exertional shortness of breath relieved and repeated MPO was 34.5 RU/mL. The regimen of prednisone (10 mg qd), cyclophosphamide (50 mg qd) and pirfenidone (0.6 g tid) was maintained. The timeline was shown in Figure 3.

Discussion

MPA, one type of systemic small-vessel vasculitis, frequently occurs in men aged 60–65 years and has been increasingly reported in the last two decades with the widespread use of the serum ANCA profile in clinical practice (4). In recent years, MPO-ANCA is considered to be possibly related to the occurrence and development of MPA, which has characteristic pathological manifestations of necrotizing small-vessel vasculitis and no or rare immune complex deposition in the vessel wall at the site of involvement. However, the specific etiology and pathogenesis of MPA remain unclear. Additionally, 95% of MPA patients have been reported to be positive for ANCA, approximately 70% of whom are positive for MPO-ANCA (5, 6). In MPA patients, the kidney is the most commonly involved organ, followed by the lungs. Pulmonary involvement in MPA mainly manifests as interstitial lung disease (ILD) and diffuse alveolar hemorrhage (7), and UIP-ILD is the most common chest HRCT phenotype of MPA-ILD. Patients with MPA-UIP often initially present with IPF and are diagnosed with MPA due to other manifestations associated with ANCA and MPA during subsequent visits. As reported by Fernandez et al. (7) patients with MPA-UIP can present with UIP 6–108 months earlier than other manifestations of MPA (7). Some patients with UIP-ILD are positive only for MPO-ANCA without other manifestations of organ involvement or systemic disease, and some authors believe that MPA cannot yet be diagnosed at this stage, but a close follow-up of urine sediment and routine urine testing is needed to identify early renal involvement and promptly prevent progression to acute/rapidly progressive renal insufficiency. Thompson et al. (8) concluded that ~25% of MPA-UIP cases may progress to MPA and therefore suggested that patients with MPA-UIP who do not meet the diagnostic criteria for MPA should be monitored monthly for urinary occult blood to improve their prognosis through early detection of renal involvement and update their diagnosis and treatment (8).

Here, we reported a rare case in which the patient developed fever of unknown origin, microscopic glomerular hematuria and elevated inflammatory indicators, including elevated ESR and CRP,

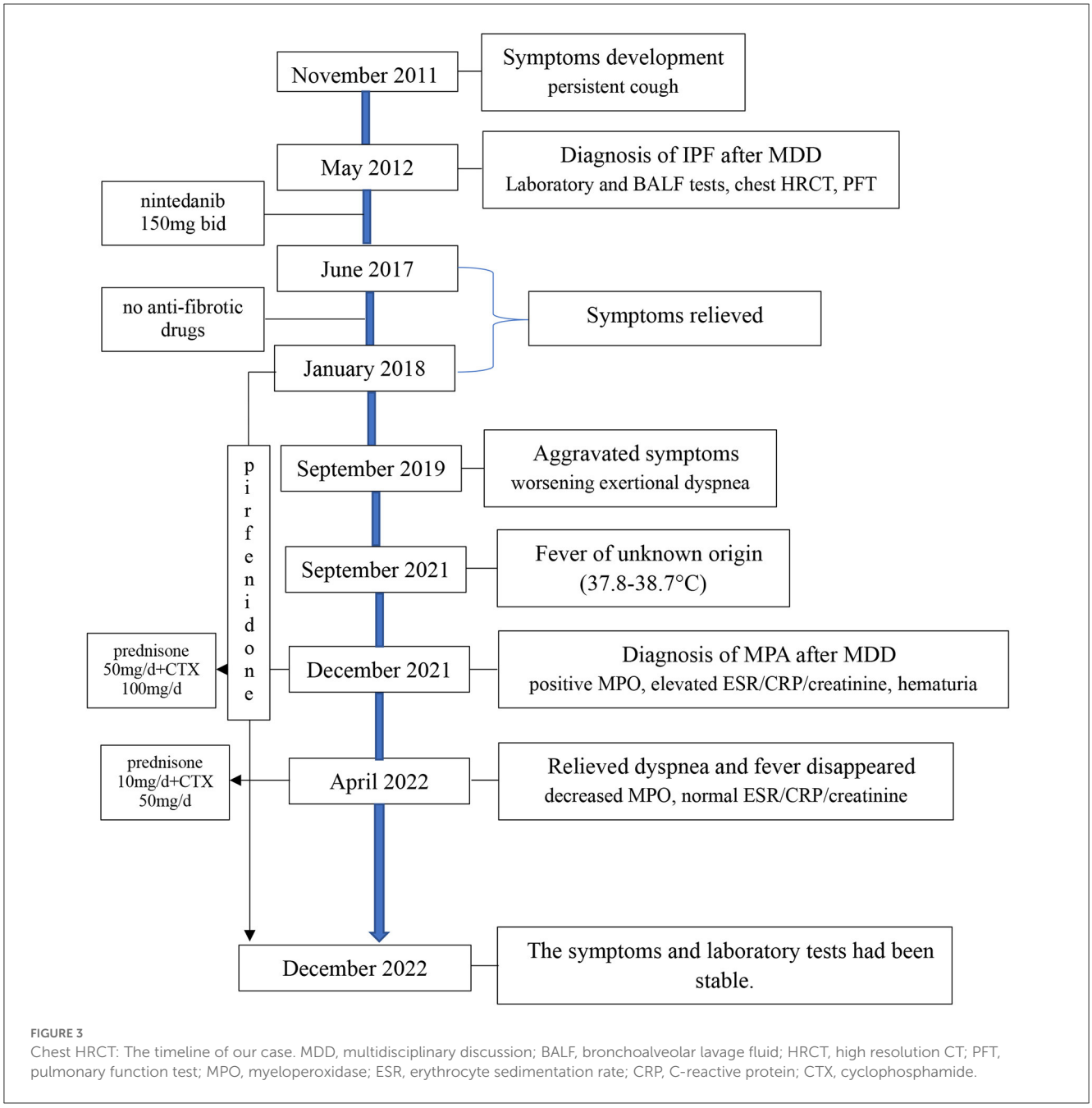

FIGURE 3
Chest HRCT: The timeline of our case. MDD, multidisciplinary discussion; BALF, bronchoalveolar lavage fluid; HRCT, high resolution CT; PFT, pulmonary function test; MPO, myeloperoxidase; ESR, erythrocyte sedimentation rate; CRP, C-reactive protein; CTX, cyclophosphamide.

followed by renal insufficiency and high-titer MPO-ANCA 2–3 months later. According to the 2022 Rheumatology classification criteria for microscopic polyangiitis (9), he could be diagnosed with MPA. However, he had been diagnosed with IPF and administrated with antifibrotic medications for almost 10 years. In the IPF cohort of Ando et al. (10) although only 4.9% of patients were positive for MPO-ANCA at the time of initial diagnosis, the positive rate of MPO-ANCA reached 14.8% during subsequent visits (10). So, in addition to ANCA screening at the time of initial diagnosis of IPF patients, the possibility of MPA rather than infectious diseases and acute exacerbation of IPF should be considered in the presence of fever and significant ESR and CRP elevations during follow-up. The serum ANCA profile, urine test and renal function should be screened promptly for early diagnosis.

No uniform recommendations are available for the treatment of MPA-UIP. Thompson et al. (8) at the Mayo Clinic proposed that glucocorticoids and immunosuppressants are not recommended for isolated MPO-ANCA-positive UIP without extrapulmonary involvements, but antifibrotic meidications can be used as appropriate. However, active glucocorticoids and immunosuppressants are suggested for MPA-UIP (8). French scholars Maillet et al. (11) also considered that immunosuppressive agents cannot improve the prognosis of MPA-UIP, but antifibrotic drugs may benefit these patients (11). In this case report, the patient was administered antifibrotic drugs until MPA was diagnosed, and no acute exacerbation of IPF was reported for up to 10 years despite progression indicated by chest CT and pulmonary function parameters, also verifying to some extent that

nintedanib and pirfenidone can delay progression and improve the prognosis of MPA-UIP. After the patient developed fever, elevated inflammatory indicators and positivity for anti-MPO-ANCA, the updated diagnosis of MPA was made. His condition improved with glucocorticoids and immunosuppressive agents. Therefore, antifibrotic medications are also recommended for MPA-UIP without extrapulmonary involvement and systemic inflammation. Glucocorticoids plus immunosuppressants are suggested for these patients once MPA-related systemic manifestations emerge.

Conclusions

Regular follow-up is important for all IPF patients. If they suffered from fever of unknown origin, microscopic hematuria, and/or abnormal ESR or CRP, MPA should be considered for the differential diagnosis. Except for antifibrotic drugs, add-on glucocorticoids and immunosuppressants were suggested for them with the updated diagnosis of MPA.

Data availability statement

The raw data supporting the conclusions of this article will be made available by the authors, without undue reservation.

Ethics statement

The studies involving human participants were reviewed and approved by the Institutional Review Board (IRB) of Peking Union Medical College Hospital (K2238). The patients/participants provided their written informed consent to participate in this study. Written informed consent was obtained from the individual(s) for the publication of any potentially identifiable images or data included in this article.

Author contributions

HH is the guarantor of the content of the manuscript including the data and analysis. HH, CS, and RXC conceived and designed the study. CS, RXC, KX, and YZ performed the study. CS and KQC analyzed the data. HH and CS wrote the paper. All authors have read and agreed to the published version of the manuscript.

Funding

This research was funded by the National High Level Hospital Clinical Research Funding (grant numbers 2022-PUMCH-A-009 and 2022-PUMCH-C-069).

Acknowledgments

We would like to thank the American Journal Experts Language Editing Services for its linguistic assistance during the preparation of this manuscript.

Conflict of interest

The authors declare that the research was conducted in the absence of any commercial or financial relationships that could be construed as a potential conflict of interest.

Publisher's note

References

1. Karras A. Microscopic polyangiitis: new insights into pathogenesis, clinical features and therapy. *Semin Respir Crit Care Med.* (2018) 39:459–64. doi: 10.1055/s-0038-1673387

2. Manfredi A, Cassone G, Izzo R, Dallagiacoma G, Felicetti M, Cariddi A, et al. Interstitial lung disease in microscopic polyangiitis and granulomatosis with polyangiitis: demographic, clinical, serological and radiological features of an Italian cohort from the Italian Society for Rheumatology. *Clin Exp Rheumatol.* (2022) 6:1. doi: 10.55563/clinexprheumatol/xu4hmh

3. Richeldi L, Du Bois RM, Raghu G, Azuma A, Brown KK. Efficacy and safety of nintedanib in idiopathic pulmonary fibrosis. *N Engl J Med.* (2014) 370:2071–82. doi: 10.1056/NEJMoa1402584

4. Jennette JC, Falk RJ, Bacon PA. 2012 Revised International Chapel Hill consensus conference nomenclature of vasculitides. *Arthritis Rheum.* (2013) 65:1–11. doi: 10.1002/art.37715

5. Greco A, De Virgilio A, Rizzo MI, Gallo A, Magliulo G, Fusconi M. Microscopic polyangiitis: advances in diagnostic and therapeutic approaches. *Autoimmun Rev.* (2015) 14:837–44. doi: 10.1016/j.autrev.2015.05.005

6. Kallenberg CGM. The diagnosis and classification of microscopic polyangiitis. *J Autoimmun.* (2014) 49: 90–3. doi: 10.1016/j.jaut.2014.01.023

7. Fernandez Casares M, Gonzalez A, Fielli M, Caputo F, Bottinelli Y, Zamboni M. Microscopic polyangiitis associated with pulmonary fibrosis. *Clin Rheumatol.* (2015) 34:1273–7. doi: 10.1007/s10067-014-2676-1

8. Thompson GE, Specks U. Update on the management of respiratory manifestations of the antineutrophil cytoplasmic antibodies-associated vasculitides. *Clin Chest Med.* (2019) 40:573–82. doi: 10.1016/j.ccm.2019.05.012

9. Ando M, Miyazaki E, Ishii T, Mukai Y, Yamasue M, Fujisaki H, et al. Incidence of myeloperoxidase anti-neutrophil cytoplasmic antibody positivity and microscopic polyangitis in the course of idiopathic pulmonary fibrosis. *Respir Med.* (2013) 107:608–15. doi: 10.1016/j.rmed.2013.01.006

10. Suppiah R, Robson JC, Grayson PC, Ponte C, Craven A, Khalid S. 2022 American College of Rheumatology/European Alliance of Associations for Rheumatology classification criteria for microscopic polyangiitis. *Ann Rheum Dis.* (2022) 81:321–6. doi: 10.1136/annrheumdis-2021-221796

11. Maillet T, Goletto T, Beltramo G, Dupuy H, Jouneau S, Borie R. Usual interstitial pneumonia in ANCA-associated vasculitis: a poor prognostic factor. *J Autoimmun.* (2020) 106:102338. doi: 10.1016/j.jaut.2019.102338

frontiers | Frontiers in Medicine

TYPE Case Report
PUBLISHED 25 May 2023
DOI 10.3389/fmed.2023.1099040

OPEN ACCESS

EDITED BY
Rodrigo Torres-Castro,
University of Chile, Chile

REVIEWED BY
Hope M. Amm,
University of Alabama at Birmingham, United States
Mehmet Oğuzhan Özyurtkan,
Medicana International İstanbul Hospital, Türkiye

*CORRESPONDENCE
Lingling Wang
✉ hongtao7@163.com

RECEIVED 15 November 2022
ACCEPTED 08 May 2023
PUBLISHED 25 May 2023

CITATION
Sun Y, Dong H, Zhang N, Zhao P, Qi Y, Yang X and Wang L (2023) Empyema caused by *Fusobacterium nucleatum* with squamous cell carcinoma of the lung: a case report and literature review. *Front. Med.* 10:1099040. doi: 10.3389/fmed.2023.1099040

Empyema caused by *Fusobacterium nucleatum* with squamous cell carcinoma of the lung: a case report and literature review

Yue Sun, Han Dong, Na Zhang, Peng Zhao, Yuan Qi, Xin Yang and Lingling Wang*

Department of Respiratory and Critical Care Medicine, The Fourth People's Hospital of Shenyang, Shenyang, China

Background: *Fusobacterium nucleatum* is a common oral symbiotic flora that can cause respiratory tract, oral nervous system, obstetric and skin infections. *Fusobacterium nucleatum* infections are mostly caused by aspiration. The clinical manifestations of pulmonary infections with *Fusobacterium nucleatum* can include simple pneumonia, lung abscesses, empyema, etc.

Case presentation: We described the case of a 49-year-old man with a 1-year history of intermittent cough and sputum production who had worsened over the last 4 days with fever and right chest pain. After thoracentesis and catheter drainage were performed, *Fusobacterium nucleatum* was detected in the pleural effusion by using next-generation sequencing. Meanwhile, a diagnosis of squamous cell carcinoma of the right lung was made by fiberoptic bronchoscopy. The patient's condition improved significantly after percutaneous drainage and long-term intravenous antibiotic treatment.

Conclusions: This is the first case reported of empyema due to *Fusobacterium nucleatum* infection in a patient with squamous cell carcinoma.

KEYWORDS

***Fusobacterium nucleatum*, empyema, next-generation sequencing, squamous cell carcinoma, lung cancer**

Introduction

Empyema is a suppurative infection caused by pathogenic bacteria invading the pleural cavity and produces purulent exudate that accumulates in the pleural cavity. Risk factors associated with empyema include bacterial pneumonia, pulmonary abscess, mediastinal infection, damage to the chest wall or esophagus, bacteremia or sepsis, pleural puncture, iatrogenic infection, etc. (1). A study evaluated 198 patients with pleural empyema, 74.2% of whom tested positive for anaerobic bacteria. *Fusobacterium nucleatum* was detected in 27.2% of the samples that grew anaerobes (2). Due to the difficulty in the isolation and cultivation of anaerobic bacteria in clinical work, the actual detection rate of anaerobic bacteria is low. *Fusobacterium nucleatum* is a common oral symbiotic flora that is also found in the digestive and genitourinary tracts. *Fusobacterium nucleatum* has also been linked to the reactivation of colorectal adenocarcinoma and inflammatory bowel disease. In fact, the reported incidence of Fusobacterium infections is between 0.6 and 3.5 cases per 1 million population (3).

Here, we report a case of squamous cell carcinoma of the right lung with empyema that was diagnosed by fiberoptic bronchoscopy, and next-generation sequencing was used (NGS) for the detection of a Fusobacterium infection in the pleural effusion.

Case report

We described the case of a 49-year-old man with a 1-year history of intermittent cough and sputum production who had worsened over the last 4 days with fever and right chest pain. The patient recently had a history of unexplained weight loss of 5 kg. He has smoked 20 cigarettes per day since the age of 19. The patient had periodontitis and tooth loss. The patient had no history of travel or tuberculosis exposure and no food or drug allergies.

On admission, his temperature was 37.9°C, pulse rate 81 beats/min, respiratory rate 22 breaths/min, blood pressure 132/80 mmHg, and oxygen saturation 95% on room air.

Pulmonary percussion found dullness in the right lower lung, and pulmonary auscultation revealed decreased breath sounds in the right lower lung. The remaining physical examination was normal.

The laboratory findings were as follows: white blood cell (WBC) count 22.98 $\times$ 10^9/L with 85.5% segmented neutrophils, 7.6% lymphocytes, neutrophil count 19.9 $\times$ 10^9/L, and lymphocyte count 1.76 $\times$ 10^9/L, and his ultrasensitive C-reactive protein (hs-CRP) was 248.56 mg/L (normal range 0–5 mg/L). Serum tumor marker screening showed a slightly elevated neuron-specific enolase (NSE) of 17.05 ng/ml (normal range <16.3 ng/ml). The squamous cell carcinoma antigen (SCCA), cytokeratin-19-fragment (CYFRA21-1) and carcinoembryonic antigen (CEA) levels were normal. The other laboratory test results were normal. Chest computed tomography (CT) revealed an irregular mass in the right middle lobe of the lung near the interlobar fissure with right atelectasis and thickening of the right pleura with encapsulated effusion and pneumatosis (Figure 1A). Thoracentesis and catheter drainage were performed immediately after chest ultrasound confirmed pleural effusion. Analysis of the drained purulent fluid suggested an exudative process [fluid protein 54.9 g/L, serum protein 69.8 g/L (normal: 65–85 g/L), fluid lactate dehydrogenase 3,014 U/L, serum lactate dehydrogenase 220 U/L (normal 120.0–250.0 U/L)]. Other pleural fluid analysis showed WBC 3,800/μL with 80% neutrophils, fluid glucose 0 mmol/L, and fluid adenosine deaminase 81.8 U/L. Pleural fluid smear, Gram staining, bacterial culture, acid-fast bacilli culture and smear, and cytology were all negative. A blood culture was also negative. Empyema was diagnosed. He received intravenous imipenem/cilastatin 1.0 g once every 8 h. After repeated pleural effusion drainage and anti-infective treatment for 3 weeks, re-examination of lung CT showed no significant change in the amount of pleural effusion (Figure 1B).

The patient requested to be discharged after his fever improved. Half a month after discharge, he was admitted to our hospital due to progressive worsening of cough and shortness of breath. On April 1, a contrast-enhanced CT scan showed uneven enhancement of the mass in the lateral segment of the right middle lobe, mediastinal lymphadenopathy with visible enhancement, and a right hydropneumothorax (Figure 1C). In addition, the laboratory test results included WBC 11.56 $\times$ 10^9/L, neutrophil ratio 71.84%, and CRP 219.35 mg/L. Ultrasound re-examination showed that there was a localized anechoic area of 5.3 cm $\times$ 7.7 cm $\times$ 3.4 cm in the right thoracic cavity, and he underwent pleural puncture and drainage again. The pleural drainage fluid was sent for NGS. The NGS results only detected *Fusobacterium nucleatum*. Subsequently, the patient underwent bronchoscopy. Fiberoptic bronchoscopy showed complete airway obstruction due to whitish endobronchial membranous lesions in the lateral segment of the right middle lobe (Figure 2A). A cauliflower-like mass was seen and biopsied after clamping the whitish endobronchial membranous lesions (Figure 2B). Histological examination of the biopsy specimens demonstrated a highly differentiated squamous cell carcinoma in the right lung (Figure 2C). He was finally diagnosed with empyema caused by *Fusobacterium nucleatum* and squamous cell carcinoma of the lung. The patient's cough and shortness of breath were improved after draining 1,800 ml pleural effusion for 3 days, and cefoperazone sodium/sulbactam sodium 3 g was given intravenously twice a day for 2 weeks. Repeat chest CT revealed absorption of the fluid and gas in the right pleural cavity (Figure 1D). Meanwhile, blood biochemical examination showed that infection indexes, such as white blood cells and CRP, had returned to normal. Regrettably, the patient refused antitumor therapy.

Discussion

Fusobacterium nucleatum is a human anaerobic Gram-negative bacterium that colonizes the oral cavity and was originally isolated from dental plaque, and it is often closely related to the development of periodontal disease and other oral diseases (4). There are 13 species in the Fusobacteriaceae family, among which *Fusobacterium nucleatum* and Fusobacterium necrophorum are the most common invasive pathogens in humans. Lipopolysaccharide endotoxins in the outer membrane of this bacterium, which help bacteria to accumulate and invade tissues, are common pathogenic factors. In addition to the oral cavity, *Fusobacterium nucleatum* can be isolated from the human blood, genitourinary system, brain, lung, liver and other organs where abscesses can form (5). Pleuropulmonary infections caused by *Fusobacterium nucleatum* could present as simple aspiration pneumonia, necrotizing pneumonia, lung abscess (6), and empyema (7, 8), and these infections are often due to oropharyngeal aspiration in patients with periodontal disease (9). In this case, the patient had extremely poor oral hygiene with periodontitis and tooth loss, which increased the risk of aspiration of *Fusobacterium nucleatum* into the oral cavity and into the pleural cavity, resulting in empyema.

In addition, squamous cell carcinoma obstructing the right middle lobe plays an important role in pleuropulmonary infection. Lung CT (Figure 1C) showed a mass of 3.2*5.4 cm in the right middle lobe, which had atelectasis. A cauliflower tumor obstructing the airway could be seen after removing the white necrotic tissue. The abundant blood supply of the tumor allowed for the proliferation of *Fusobacterium nucleatum*, which could then be inhaled into the airways. *Fusobacterium nucleatum* has been shown to invade the intracellular compartments of tumor cells (10). CT examination could not determine whether the tumor in the right middle lobe was benign or

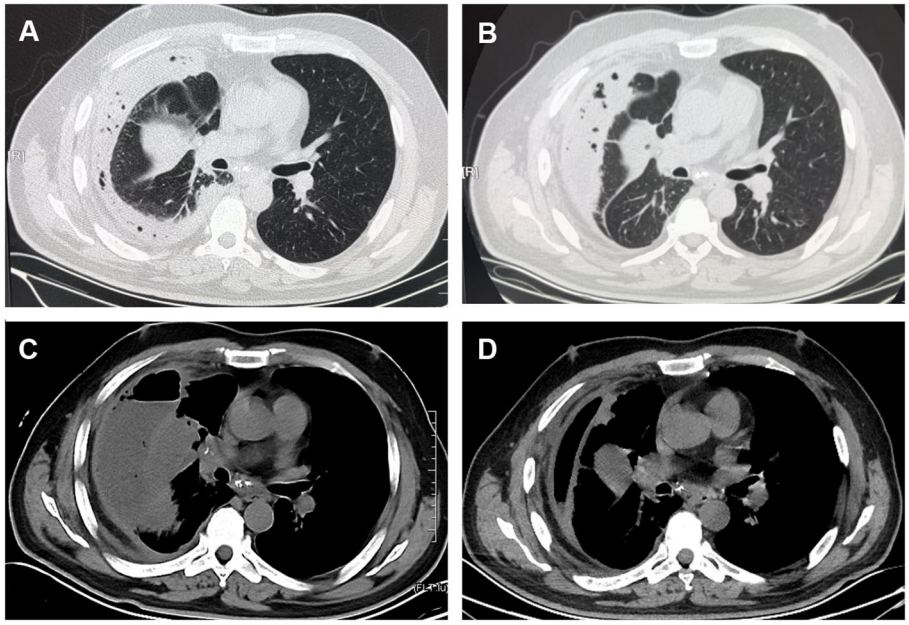

FIGURE 1
CT scan images. **(A)** Chest CT showed an irregular mass at the right middle lobe of the lung near the interlobar fissure with right atelectasis and encapsulated effusion and pneumatosis. **(B)** Chest CT showed no significant changes in the amount of right-sided pleural effusion after thorough pleural drainage and anti-infective treatment for 3 weeks. **(C)** Contrast-enhanced CT scan showed uneven enhancement of the mass in the lateral segment of right middle lobe, mediastinal lymphadenopathy with visible enhancement, and a right hydropneumothorax on April 1. **(D)** Two weeks after readmission, chest CT showed that the right-sided pleural effusion and gas were significantly reduced.

malignant, but timely bronchoscopy and bronchoscopic biopsy confirmed the diagnosis. The etiology of cancer increasingly recognizes chronic infection and inflammation as components in carcinogenic feedback loops including the local microbiota. The cancer-promoting features of *Fusobacterium nucleatum* include bacterial invasion and inflammation (e.g., flagellar assembly and bacterial chemotaxis) (11–13), metabolic pathways (e.g., homolactic fermentation) (14), creation of DNA-damaging substances (15), and encouragement of cell proliferation (e.g., E-cadherin/β-catenin signaling through unique FadA adhesion) (16), suggesting the potential role of *Fusobacterium nucleatum* in the early stages of tumorigenesis. Interestingly, a comprehensive analysis found that *Fusobacterium nucleatum* enrichment in head and neck squamous cell carcinoma tissues was strongly associated with non-smokers, lower tumor stage, lower recurrence rates, and better cancer-specific survival (10), which in contrast to low survival and poor prognosis for *Fusobacterium nucleatum* infection in colorectal and esophageal cancers (17–19). The association between *Fusobacterium nucleatum* and lung cancer has not been reported. Therefore, more research is needed to explore the underlying mechanism of *Fusobacterium nucleatum* in the development of lung malignancies. In addition, This patient may develop recurrent lung infections due to poor oral health (20–22) and obstructive pneumonia complicated with lung cancer (23, 24), resulting in clinical decline and poor prognosis.

This is the first reported case of empyema secondary to a *Fusobacterium nucleatum* infection detected by NGS. The traditional detection method is bacterial culture, and the recommended medium is Brucella-based or fastidious anaerobe agar, which can improve the detection rate (25). The detection rate of anaerobic bacteria can be up to 70% by next-generation sequencing (NGS), which is better than the 20% by traditional bacterial culture technology (7). NGS combined with semiquantitative PCR was reported to be more helpful in the diagnosis of the pathogenic bacteria of pleural empyema and parapulmonary effusion (26). Compared to the difficulty of traditional culture, NGS was able to amplify and detect cell-free DNA and DNA fragments in dead cells to determine the type and number of pathogens (27). Negative results for all pleural fluid cultures, partly due to the nature of anaerobic bacteria that are difficult to culture, or partly due to limited microbiological testing techniques in hospitals (only blood agar plates can be performed). Therefore, with the patient's consent, we tested the patient's pleural fluid with NGS. This case highlights the application of NGS in the etiological diagnosis and guidance for the treatment of empyema.

Conclusion

In conclusion, this case reported a patient with squamous cell cancer with empyema due to an infection by *Fusobacterium nucleatum*, and NGS and bronchoscopy helped to quickly identify the pathogens and pathology. Early pleural effusion drainage and a full treatment course with effective antibiotics are imperative.

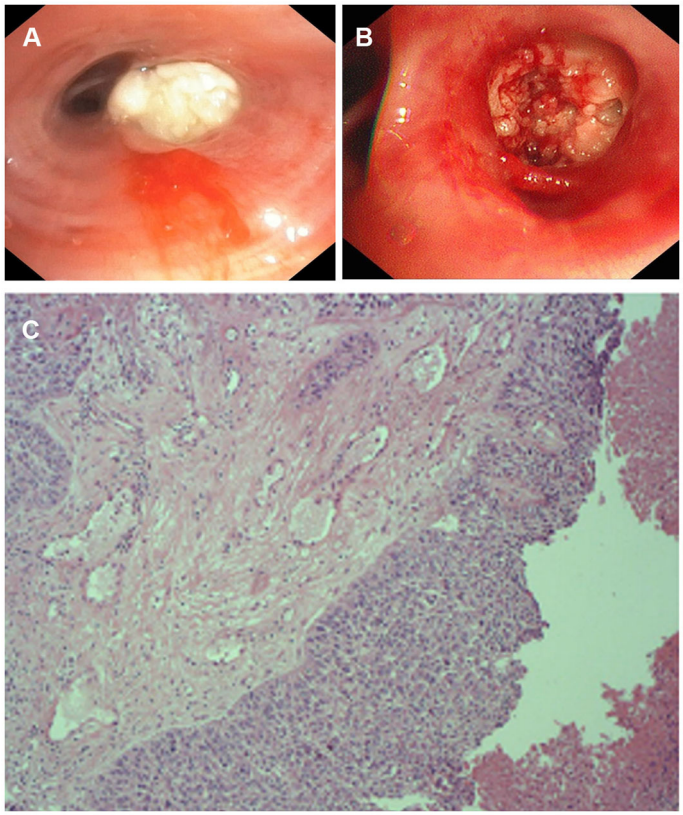

FIGURE 2
The appearance of fiberoptic bronchoscopy and Pathological examination. **(A)** Complete stenosis of the airway in the lateral segment of the right middle lobe due to white endobronchial lesions. **(B)** A cauliflower-like mass was seen and biopsied. **(C)** Pathological examination of bronchial tissue in the middle lobe of the right lung shows a high-differentiated squamous cell carcinoma.

Data availability statement

The original contributions presented in the study are included in the article/supplementary material, further inquiries can be directed to the corresponding author.

Ethics statement

Written informed consent was obtained from the patient for the publication of this case report.

Author contributions

YS wrote the first draft. LW revised the manuscript. HD and NZ recorded the medical information. YQ, PZ, and XY contributed to the treatment of the patient. All authors contributed to the critical revision and provided final approval of the submitted version of this article.

Funding

This study was supported by Shenyang Science and Technology Program (22-321-33-60).

Conflict of interest

The authors declare that the research was conducted in the absence of any commercial or financial relationships that could be construed as a potential conflict of interest.

Publisher's note

All claims expressed in this article are solely those of the authors and do not necessarily represent those of their affiliated organizations, or those of the publisher, the editors and the reviewers. Any product that may be evaluated in this article, or claim that may be made by its manufacturer, is not guaranteed or endorsed by the publisher.

References

1. Dyrhovden R, Nygaard RM, Patel R, Ulvestad E, Kommedal Ø. The bacterial aetiology of pleural empyema. A descriptive and comparative metagenomic study. *Clin Microbiol Infect*. (2019) 25:981–6. doi: 10.1016/j.cmi.2018.11.030

2. Boyanova L, Vladimir D, Gergova G, Dragomir I, Petrov D, Osmanliev D, et al. Anaerobic microbiology in 198 cases of pleural empyema: a Bulgarian study. *Anaerobe*. (2004) 10:261–7. doi: 10.1016/j.anaerobe.2004.06.001

3. Ahmed Z, Bansal SK, Dhillon S. Pyogenic liver abscess caused by Fusobacterium in a 21-year-old immunocompetent male. *World J Gastroenterol*. (2015) 21:3731–5. doi: 10.3748/wjg.v21.i12.3731

4. Brennan CA, Garrett WS. *Fusobacterium nucleatum* - symbiont, opportunist and oncobacterium. *Nat Rev Microbiol*. (2019) 17:156–66. doi: 10.1038/s41579-018-0129-6

5. Han YW. *Fusobacterium nucleatum*: a commensal-turned pathogen. *Curr Opin Microbiol*. (2015) 23:141–7. doi: 10.1016/j.mib.2014.11.013

6. Gedik AH, Cakir E, Soysal O, Umutoglu T. Endobronchial lesion due to pulmonary *Fusobacterium nucleatum* infection in a child. *Pediatr Pulmonol*. (2014) 49:E63–5. doi: 10.1002/ppul.22834

7. Tang W, Liu ZY, Abreu C. *Fusobacterium nucleatum* pleural empyema in a patient with progressive rheumatoid arthritis and immunosuppression. *Case Rep Infect Dis*. (2021) 2021:5212401. doi: 10.1155/2021/5212401

8. Barrera-López L, Macía-Rodríguez C, Ferreiro-Fernández L, Díaz-Peromingo JA. *Fusobacterium nucleatum* empyema: an atypical presentation. *Eur J Case Rep Intern Med*. (2020) 7:001631. doi: 10.12890/2020_001631

9. Civen R, Jousimies-Somer H, Marina M, Borenstein L, Shah H, Finegold SM. A retrospective review of cases of anaerobic empyema and update of bacteriology. *Clin Infect Dis*. (1995) 20(Suppl. 2):S224–9. doi: 10.1093/clinids/20.Supplement_2.S224

10. Chen Z, Wong PY, Ng CWK, Lan L, Fung S, Li JW, et al. The intersection between oral microbiota, host gene methylation and patient outcomes in head and neck squamous cell carcinoma. *Cancers*. (2020) 12:3425. doi: 10.3390/cancers12113425

11. Edgar RC. UPARSE: highly accurate OTU sequences from microbial amplicon reads. *Nat Methods*. (2013) 10:996–8. doi: 10.1038/nmeth.2604

12. Chen Z, Hui PC, Hui M, Yeoh YK, Wong PY, Chan MCW, et al. Impact of preservation method and 16S rRNA hypervariable region on gut microbiota profiling. *mSystems*. (2019) 4:e00271-18. doi: 10.1128/mSystems.00271-18

13. Bolyen E, Rideout JR, Dillon MR, Bokulich NA, Abnet CC, Al-Ghalith GA, et al. Reproducible, interactive, scalable and extensible microbiome data science using QIIME 2. *Nat Biotechnol*. (2019) 37:852–7. doi: 10.1038/s41587-019-0209-9

14. Gilbert JA, Jansson JK, Knight R. The earth microbiome project: successes and aspirations. *BMC Biol*. (2014) 12:69. doi: 10.1186/s12915-014-0069-1

15. Geng F, Zhang Y, Lu Z, Zhang S, Pan Y. *Fusobacterium nucleatum* caused DNA damage and promoted cell proliferation by the Ku70/p53 pathway in oral cancer cells. *DNA Cell Biol*. (2020) 39:144–51. doi: 10.1089/dna.2019.5064

16. Rubinstein MR, Wang X, Liu W, Hao Y, Cai G, Han YW. *Fusobacterium nucleatum* promotes colorectal carcinogenesis by modulating E-cadherin/beta-catenin signaling via its FadA adhesin. *Cell Host Microbe*. (2013) 14:195–206. doi: 10.1016/j.chom.2013.07.012

17. Yin H, Zhang J, Zhang H, Li Q, Qiu H, Hong K, et al. *Fusobacterium nucleatum* promotes proliferation in oesophageal squamous cell carcinoma via AHR/CYP1A1 signalling. *FEBS J*. (2023) 290:837–54. doi: 10.1111/febs.16619

18. Nomoto D, Baba Y, Liu Y, Tsutsuki H, Okadome K, Harada K, et al. *Fusobacterium nucleatum* promotes esophageal squamous cell carcinoma progression via the NOD1/RIPK2/NF-kappaB pathway. *Cancer Lett*. (2022) 530:59–67. doi: 10.1016/j.canlet.2022.01.014

19. Hsieh YY, Kuo WL, Hsu WT, Tung SY, Li C. *Fusobacterium nucleatum*-induced tumor mutation burden predicts poor survival of gastric cancer patients. *Cancers*. (2022) 15:269. doi: 10.3390/cancers15010269

20. Yoneyama T, Yoshida M, Matsui T, Sasaki H. Oral care and pneumonia. Oral Care Working Group. *Lancet*. (1999) 354:515. doi: 10.1016/S0140-6736(05)75550-1

21. El-Solh AA. Association between pneumonia and oral care in nursing home residents. *Lung*. (2011) 189:173–80. doi: 10.1007/s00408-011-9297-0

22. Dorfer C, Benz C, Aida J, Campard G. The relationship of oral health with general health and NCDs: a brief review. *Int Dent J*. (2017) 67(Suppl. 2):14–8. doi: 10.1111/idj.12360

23. Penman C, Dixon G, Daly R, Low A. When is a lung abscess not a lung abscess? Recurrent pneumonia and empyema associated with intrapulmonary cystic teratoma. *Thorax*. (2023) 78:526–7. doi: 10.1136/thorax-2022-219617

24. Valvani A, Martin A, Devarajan A, Chandy D. Postobstructive pneumonia in lung cancer. *Ann Transl Med*. (2019) 7:357. doi: 10.21037/atm.2019.05.26

25. Nagaoka K, Yanagihara K, Morinaga Y, Kohno S. Detection of *Fusobacterium nucleatum* in two cases of empyema and lung abscess using paromomycin-vancomycin supplemented Brucella HK agar. *Anaerobe*. (2017) 43:99–101. doi: 10.1016/j.anaerobe.2016.12.011

26. Shiraishi Y, Kryukov K, Tomomatsu K, Sakamaki F, Inoue S, Nakagawa S, et al. Diagnosis of pleural empyema/parapneumonic effusion by next-generation sequencing. *Infect Dis*. (2021) 53:450–9. doi: 10.1080/23744235.2021.1892178

27. Xia J, Xia L, Zhou H, Lin X, Xu F. Empyema caused by Streptococcus constellatus: a case report and literature review. *BMC Infect Dis*. (2021) 21:1267. doi: 10.1186/s12879-021-06955-2

Frontiers in Medicine

Translating medical research and innovation into improved patient care

A multidisciplinary journal which advances our medical knowledge. It supports the translation of scientific advances into new therapies and diagnostic tools that will improve patient care.

Discover the latest Research Topics

See more →

Frontiers

Avenue du Tribunal-Fédéral 34
1005 Lausanne, Switzerland
frontiersin.org

Contact us

+41 (0)21 510 17 00
frontiersin.org/about/contact